UNIVERSITY OF LIVERPOOL

Characterization of the cross-interactions between Deformed Wing Virus (DWV), honey bee, and ectoparasitic mite, *Tropilaelaps mercedesae*

Thesis submitted in accordance with the requirements of the University of Liverpool for the degree of
Doctor in Biological Sciences

by

Yunfei Wu

June 2020

Declaration

I hereby declare that this Ph.D. dissertation entitled **"Characterization of the cross-interactions between Deformed Wing Virus (DWV), honey bee, and ectoparasitic mite, *Tropilaelaps mercedesae***" I have submitted to Biological Sciences, Xi'an Jiaotong Liverpool University and University of Liverpool, is entirely my original work with the supervision of my supervisors, Prof. Tatsuhiko Kadowaki and Prof. Gregory D. Hurst.

I have understood the University's policy on plagiarism, and no part of this dissertation has been or is being submitted for any other qualification at any other universities.

Signature: 

Date: 2020-06-12

Abstract

Recently, honey bee colony losses have been reported to be associated with both presence of the pathogen Deformed Wing Virus (DWV) and ectoparasitic mites. The DWV vectoring role of *Varroa destructor* is well established while the role of *Tropilaelaps mercedesae* in viral transmission has not been fully investigated. In this project, I examined the effects of both mite species infestation on honey bee by comparing the DWV copy number and alteration of DWV variants of individual pupae and their infesting mites. Infestation with either mite species causes increased DWV copy number in honey bee pupae, which proves the vector role of *V. destructor* on honey bee and as well as suggesting a similar viral vectoring role for *T. mercedesae*. Through artificial infestation and wound induction experiments, a biological and mechanical vector role for *T. mercedesae* has been established. I also identified a positive correlation between DWV copy number in pupae and copy number in infesting mites, which forms two clusters with either high or low copy number in both honey bee pupae and infesting mites. The same DWV type A variant was present in either low or high copy number in both honey bee pupae and infesting *V. destructor* or *T. mercedesae*. These data suggest a previously proposed hypothesis that DWV suppressed the honey bee immune system when DWV copy number reaches a specific threshold, promoting greater replication. *Tropilaelaps mercedesae* infestation induces Hymenoptaecin and Defensin-1 expression in honey bee pupae; however, they are associated with two independent events, mite feeding activity and DWV replication, respectively. DWV can be transmitted from honey bee to mite via intake of fat body or other tissues through feeding activity, which is supported by the observation of accumulated DWV in the mite's intestinal region. During feeding activity, induced Hymenoptaecin is ingested by mite as well and it has a negative role, down-regulating vitellogenin synthesis, which further influences mite's reproductive capability. Hymenoptaecin expression induced by mite feeding exerts the negative feedback on the mite reproduction, and may help establishing an equilibrium between host (honey bee) and parasite (mite). I also explore the critical factors for DWV infection/replication, including 1) the host with A/T-rich genome and a skewed codon usage; 2) an intact accessible VP1-P domain on the viral virion; and 3) certain factors critical for viral replication and at least exclusively present in honey bee rather than *V. destructor*, *T. mercedesae* nor *C. sonorensis*.

关于残翅病毒（DWV），蜜蜂和体外寄生螨梅式热厉螨（*Tropilaelaps mercedesae*）三者间交互作用及相互关系的研究

摘要

最近有报道称蜜蜂蜂群损失与病原体残翅病毒（DWV）和体外寄生螨的存在有关。狄斯瓦螨（*Varroa destructor*）作为残翅病毒的载体作用已被确定，然而梅式热厉螨（*Tropilaelaps mercedesae*）在病毒传播中的作用尚未得到充分研究。在这个项目中，我通过比较单独的蜂蛹及感染蜂蛹的螨虫中的 DWV 拷贝数和病毒变体的改变，来检验两种螨虫感染对蜜蜂的影响。两种螨虫的感染均可导致蜂蛹中 DWV 拷贝数的增加，这证明了狄斯瓦螨对于蜜蜂病毒的载体作用，也表明了梅式热厉螨有可能具有类似的病毒媒介作用。通过人工感染和创伤诱导实验，梅式热厉螨的生物性和机械性媒介作用得到证明。我还发现蜂蛹的 DWV 拷贝数和感染螨的拷贝数之间存在正相关关系，且该关系形成高拷贝数或低拷贝数的两个集群。在低拷贝数或者高拷贝数感染的蜜蜂蜂蛹和感染螨狄斯瓦螨或者梅式热厉螨中，DWV 的同一种 A 型变体均存在。这些数据提议了一个之前提出的假设：当 DWV 拷贝数达到一个特定的阈值时，DWV 将抑制蜜蜂免疫系统，从而促进更多的复制。梅式热厉螨感染诱导了蜂蛹中蜜蜂抗菌肽（Hymenoptaecin）和防御素-1（Defensin-1）的表达；但它们分别与螨虫摄食活动和 DWV 复制两个独立事件相关。DWV 可以通过摄食活动中摄取脂肪体或者其他组织从蜜蜂传递给螨虫，DWV 积聚在螨虫的肠道区域内的观察也支持这一观点。在摄食活动中，诱导的蜜蜂抗菌肽也被螨虫吸收并对螨虫健康具有副作用，它下调卵黄生成素的合成进而影响螨虫的繁殖能力。螨虫摄食诱导的蜜蜂抗菌肽对螨虫的繁殖具有负反馈作用，可能有助于建立宿主（蜜蜂）和寄生物（螨虫）之间的平衡。我还探讨了 DWV 感染/复制的关键因素，包括 1）宿主具有多 A/T 的基因组及倾斜密码子使用；2）病毒粒子上完整且可接近的 VP1-P 结构域；3）特定存在于蜜蜂中的对病毒复制至关重要的因素且该因素不存在于狄斯瓦螨，梅式热厉螨和叮咬库蚊（*C. sonorensis*）中。

Acknowledgements

I would like to express my sincere gratitude to my supervisors, Prof. Tatsuhiko Kadowaki and Prof. Gregory D. Hurst for providing their invaluable guidance and suggestions throughout my project. I would also show my appreciation to my assessors Dr. Jian Liu, Dr. Alistair Darby, and Dr. Ruiz-Carrillo for their useful comments. I also appreciate Prof. Lesley Bell-Sakyi for providing the *LLE/LULS 40* and KC cell lines, and Benjamin Weiss for ectoparasitic mites' thin-sectioning.

Also I would like to thank Dr. Xiaofeng Dong, Dr. Qiushi Liu, Technician Xuye Yuan, Technician Jing Li, Jing Lei, Gongjie Wu, and Xinyi Li for their help on this project. Thanks to all staff, teachers and PhD students in my department of Xi'an Jiaotong Liverpool University and University of Liverpool, for their support during my project.

Finally, I show my gratitude to my parents for their help and understanding during my PhD study.

List of abbreviations

3C: 3C-protease

ABPV: Acute bee paralysis virus

AMP: Antimicrobial peptides

AP: Alkaline Phosphatase

BQCV: Black queen cell virus

CCD: Colony Collapse Disorder

CBPV: Chronic bee paralysis virus

CoCoPUTs: Codon/Codon Pair Usage Tables

CrPV: Cricket paralysis virus (CrPV)

Cryo-EM: Cryo-electron microscopy

DCV: Drosophila C virus

DEG: Differentially expressed gene

DWV: Deformed wing virus

EBV: Egypt bee virus

FBS: Foetal bovine serum

FC: Fold Change

FISH: Fluorescence *in situ* hybridization

HRM: High resolution melt

IAPV: Israeli acute paralysis virus

IPTG: Isopropyl-thio-galactoside

IRES: Internal ribosomal entry site

KBV: Kashmir bee virus

LB: Lysogeny broth

LP: Leader polypeptide

LSV: Lake Sinai virus

MJRP: Major Jelly Royal Protein

MS: Mass Spectrometry

ORF: Open reading frame

PBS: Phosphate buffered saline

PBST: Phosphate buffered saline with Tween 20

PFA: Paraformaldehyde

PVDF: Polyvinylidene difluoride

RdRP: RNA-dependent RNA polymerase

RT: Reverse transcription

SBV: Sacbrood virus

SBPV: Slow bee paralysis virus

UTR: Untranslated region

VDV-1: *Varroa destructor* virus-1

Vg: Vitellogenin

VPG: Genome-linked viral protein

VRC: Viral replication complexes

Table of Contents

Declaration ii
Abstract iii
Acknowledgements v
List of abbreviations vi
Table of Contents viii
Chapter 1 General introduction and the aims of research project 11

Section 1.1 Honey bee colony decline 11
Section 1.2 Deformed Wing Virus 12
Section 1.3 Ectoparasitic mites 16

Section 1.3.1 *Varroa destructor* 16
Section 1.3.2 *Tropilaelaps mercedesae* 20

Section 1.4 Aims of research project 23

Chapter 2 *Tropilaelaps* mite vectors DWV transmission to honey bee 25

Section 2.1 Brief introduction 25
Section 2.2 Materials and Methods 26

Section 2.2.1 Sample collection 26
Section 2.2.2 RT-PCR analysis of DWV 27
Section 2.2.3 qPCR analysis of DWV copy number 27
Section 2.2.4 Sequencing of RT-PCR product 28
Section 2.2.5 Artificially *T. mercedesae* infestation to honey bee pupae 28
Section 2.2.6 Construction of phylogenetic tree 28
Section 2.2.7 DWV virus isolation 29
Section 2.2.8 Artificially wound induction and DWV infection to honey bee pupae 29
Section 2.2.9 Western blot 29
Section 2.2.10 qPCR analysis of *Hymenoptaecin* and *Defernsin-1 mRNAs* 30
Section 2.2.11 Statistical analysis 30

Section 2.3 1Results 30

Section 2.3.1 *V. destructor*'s infestation increases DWV prevalence in honey bee colony 30
Section 2.3.2 *V. destructor*'s infestation increases DWV titer and prevalence in the individual honey bee pupae and a linear correlation of DWV copy number between pupae and the infesting mites 31
Section 2.3.3 DWV strains and variants identified in the honey bee pupae and *V. destructor* 33
Section 2.3.4 *T. mercedesae*'s infestation increases DWV prevalence and titer within individual honey bee pupae and a linear correlation of DWV copy number between pupae and infesting mites 37
Section 2.3.5 DWV strains and variants identified in the honey bee pupae and *T. mercedesae* 39
Section 2.3.6 Artificial infestation of *T. mercedesae* increases DWV copy number in honey bee pupae 42
Section 2.3.7 DWV variants identified in artificially infested-honey bee pupae and the infesting *T. mercedesae*, suggesting the vectorial role of *T. mercedesae* for DWV transmission 43
Section 2.3.8 Association between DWV variant and copy number in honey bee pupae and the infesting mites 45
Section 2.3.9 *T. mercedesae* acts as a mechanical vector for DWV 46
Section 2.3.10 *Hymenoptaecin* and *Defensin-1 mRNAs* were induced in honey bee pupae by *T. mercedesae* infestation 47

Section 2.4 Discussion 50

Section 2.4.1 *V. destructor* and *T. mercedesae* infestation increase DWV copy number in honey bee pupae 50
Section 2.4.2 *T. mercedesae* acts as a biological and mechanical vector for DWV transmission 51
Section 2.4.3 *V. destructor* and *T. mercedesae* mediated stimulation of DWV replication in honey bee pupa 52

Chapter 3 Raising the antibodies to detect DWV 54

Section 3.1 Brief introduction 54
Section 3.2 Materials and Methods 55

Section 3.2.1 Construction of VP1 and RdRP expression vectors 55
Section 3.2.2 Protein expression and purification 56
Section 3.2.3 Dialysis, condensation and protein concentration measurement 57
Section 3.2.4 Raise antibody 57
Section 3.2.5 SDS-PAGE 58
Section 3.2.6 RT-PCR analysis of DWV 58
Section 3.2.7 Western blot 58
Section 3.2.8 Transfection 59
Section 3.2.9 Immunofluorescence 59
Section 3.2.10 Microscopy observation and data analysis 60

Section 3.3 Results 60

Section 3.3.1 Raising the antibodies to detect DWV 60
Section 3.3.2 Anti-VP1P antibody can be used for immunofluorescence 66

Section 3.4 Discussion 67

Chapter 4 Effects of DWV on *T. mercedesae* 69

Section 4.1 Introduction 69
Section 4.2 Materials and Methods 70

Section 4.2.1 Sample collection 70
Section 4.2.2 RNA isolation, RT-PCR and qRT-PCR 70
Section 4.2.3 RNA-seq 71
Section 4.2.4 Analysis of RNA-seq data 71
Section 4.2.5 Detection of viral replication by western blot 71
Section 4.2.6 Reproduction experiment 72
Section 4.2.7 Thin-section of ectoparasitic mites 72
Section 4.2.8 Immunofluorescence 72
Section 4.2.9 Confocal microscopy observation 73
Section 4.2.10 qPCR analysis of *Vitellogenin (Vg)*, *Hymenoptaecin* and *Defernsin-1* mRNAs 73
Section 4.2.11 Statistical analysis 73

Section 4.3 Results 73

Section 4.3.1 Identification of Differentially Expressed Genes (DEGs) in *T. mercedesae* with high or low DWV copy number 73
Section 4.3.2 RdRP was not detected in *V. destructor* and *T. mercedesae* with high DWV, suggesting DWV does not replicate 81
Section 4.3.3 Negative correlation between reproductive capability of *T. mercedesae* and the DWV copy number 82
Section 4.3.4 The localization of DWV in *V. destructor* and *T. mercedesae* 82

Section 4.3.5 Correlation between honey bee immune effectors and *T. mercedesae Vitellogenin (Vg)* gene 97
Section 4.4 Discussion 98
Section 4.4.1 Ectoparasitic mites contain high DWV load without the active replication 98
Section 4.4.2 DWV negatively affects reproduction of *T. mercedesae* 99
Section 4.4.3 Suppressed reproduction of *T. mercedesae* is associated with honey bee immune effector, Hymenoptaecin 99
Chapter 5 Essential factors for DWV infection and replication 101
Section 5.1 Brief introduction 101
Section 5.2 Materials and Methods 103
Section 5.2.1 Cell culture medium and supplements 103
Section 5.2.2 Honey bee primary culture 104
Section 5.2.3 Artificial DWV infection in *Sf9*, *S2*, *LLE/LULS40* and *KC* cell lines 104
Section 5.2.4 RdRP detection in honey bee primary cells and the *KC* cells with DWV infection 105
Section 5.2.5 Detection of DWV replication in pupal cells infected by antibody-DWV 105
Section 5.2.6 Detection of DWV replication in pupal cells with pre-incubation of VP1-P protein 106
Section 5.2.7 DWV Binding assay 106
Section 5.2.8 Detection of DWV replication in pupae with different developmental stages 106
Section 5.2.9 RT-PCR and qRT-PCR 107
Section 5.2.10 Detection of negative-strand DWV RNA 107
Section 5.2.11 RNA-seq 107
Section 5.2.12 Transcriptome analysis and GO enrichment analysis 108
Section 5.2.13 Western blot 108
Section 5.2.14 Immunoprecipitation 108
Section 5.2.15 Sliver staining 109
Section 5.2.16 Mass Spectrometry 109
Section 5.2.17 Codon usage analysis 109
Section 5.2.18 Statistical analysis 109
Section 5.3 Results 110
Section 5.3.1 Testing DWV replication/ infection in the established insect cell lines 110
Section 5.3.2 Comparison of DWV infection/replication between honey bee primary cells and *KC* cell line 113
Section 5.3.3 Explore DWV replication/infection in honey bee primary cells 114
Section 5.3.4 Identification of potential honey bee genes critical for DWV replication via RNA-seq 119
Section 5.3.5 Interactions between DWV structural protein and honey bee proteins 125
Section 5.4 Discussion 127
Section 5.4.1 DWV contains a skewed codon usage and adapts to the host with A/T-rich genome 127
Section 5.4.2 A catalytic role of P-domain for DWV entry and replication 130
Section 5.4.3 Honey bee contains critical factors for DWV infection/replication 130
Chapter 6 Conclusion 132
Supplementary Materials 134
References 136

Chapter 1 General introduction and the aims of research project

Section 1.1 Honey bee colony decline

Apis mellifera, the most commonly managed bee in the world (vanEngelsdorp and Meixner, 2010), plays essential roles for agriculture and apiculture (Chanpanitkitchote et al., 2017). It provides honey and the estimated international production was 1.07 million metric ton in 2007, which was worth of US$1.25 billion (vanEngelsdorp and Meixner, 2010). Many agricultural crops and wild plants are pollinated by *A. mellifera*. Honey bee also provides 90% of commercial pollination services and the yield of such crops would reduce to 10% without pollination (Klein et al., 2007, Aizen et al., 2008, Müller, 2019). The pollinator-dependent crops are worth of US$235-577 billion annually (Smith et al., 2013, IPBES, 2016). Decline of pollinators not only negatively affects fruit quality and quantity (Klein et al., 2007) but also reduces quality and variety of human diet since numerous plants depending on insect pollination provide vitamins, minerals and proteins (Steffan-Dewenter et al., 2005). Pollination by honey bee for numerous wild flowering plants also supports biodiversity and ecosystem (J. C. Biesmeijer, 2006, Allsopp et al., 2008). Therefore, honey bee is a critical component of global biodiversity and ecosystem and providing vital pollination services for human living.

However, decline of honey bee colonies has been reported in the United States (Ellis et al., 2010, van Engelsdorp et al., 2008, Vanengelsdorp et al., 2011), Europe (Crailsheim et al., 2009, Potts et al., 2010b), the Middle East (Haddad et al., 2009, Soroker et al., 2009), and Japan (Gutierrez, 2009, Neumann and Carreck, 2010) over recent decades. In the United States, 33% of honey bee colonies on average collapse annually, and some of these losses are attributed to Colony Collapse Disorder (CCD), a large-scale enigmatic sudden death of honey bee workers (Evans et al., 2009, Brutscher et al., 2015, van Engelsdorp et al., 2008, Steinhauer et al., 2014, vanEngelsdorp et al., 2012). Generally colony decline is not caused by a single factor, but rather an interaction of multiple abiotic and biotic factors (Zeil et al., 2013, Brunner et al., 2014, Brown et al., 2016, Goulson et al., 2015, Renzi et al., 2016, Sanchez-Bayo et al., 2016). Abiotic factors include climate change (Jeremy T. Kerr et al., 2015), pesticide (Godfray et al., 2015), and habitat loss and homogenization (Kennedy et al., 2013, Potts et al., 2010a). Biotic factors include invasive species like predators and pests (Stout and Morales, 2009, Morse and Flottum, 1997), pathogens and parasites (Fig.1.1) (McMahon et al., 2015, Fürst et al., 2014, Wilfert et al., 2016). Interactions between these factors are usually complicated and worrisome since one factor with sub-lethal effect could make another one lethal, consequently leading to colony collapse. One example is a combination of pesticides and pathogens (Neumann and Carreck, 2010). Understanding the most influential factors for the decline of honey bee population and the potential synergistic interactions with other factors is critical to develop strategies to maintain honey bee colony health (Gallant et al., 2014). Among the above causes, pathogens and parasites are considered as the major threats for *A. mellifera* (vanEngelsdorp and Meixner, 2010, Williams et al., 2010).

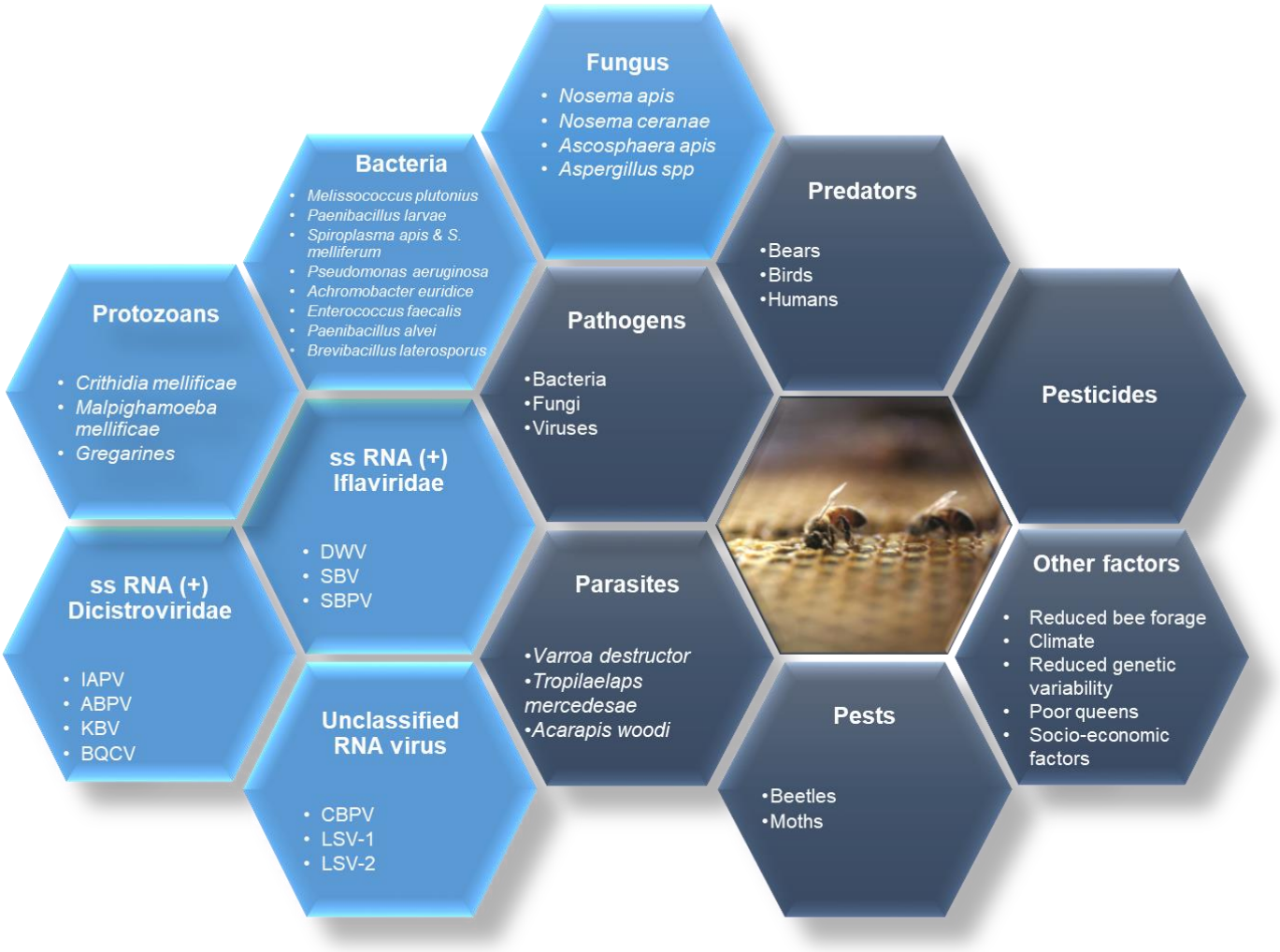

Figure 1.1 Overview of threats for honey bee health.

The diagram indicates biotic and abiotic factors negatively affecting global honey bee health. The major honey bee pathogens are listed in detail with ice blue. Abbreviations: DWV, Deformed wing virus; SBV, Sacbrood virus; SBPV, Slow bee paralysis virus; IAPV, Israeli acute paralysis virus; ABPV, Acute bee paralysis virus; KBV, Kashmir bee virus; BQCV, Black queen cell virus; CBPV, Chronic bee paralysis virus; LSV, Lake Sinai virus (Adapted from (Evans and Schwarz, 2011)).

Section 1.2 Deformed Wing Virus

Honey bee viruses are now prevalent globally. Since 1963, when Acute bee paralysis virus (ABPV) and Chronic bee paralysis virus (CBPV) were initially isolated, 22 further viruses have been identified and characterized (Tantillo et al., 2015). Most of these viruses individually exist or co-exist with others in honey bee colonies with or without apparent symptoms (L. BAILEY et al., 1981, Chen et al., 2005a, Forgach et al., 2008, Gisder et al., 2009, Tentcheva et al., 2004b). The seven most prevalent viruses are ABPV, Black queen cell virus (BQCV), Kashmir bee virus (KBV), Sacbrood virus (SBV), CBPV, Israeli acute paralysis virus (IAPV), and Deformed wing virus (DWV) (Chanpanitkitchote et al., 2017).

In 1977, DWV was first isolated from asymptomatic adult honey bees in Egypt and known as Egypt bee virus (EBV) (Bailey et al., 1979). Subsequently, a virus, named Japanese isolate of EBV, was isolated in

the deformed adult bees sampled from Japan in 1982 (Ribière et al., 2008, de Miranda and Genersch, 2010, Bailey and Ball, 1991). Ball associated this virus with deformed adult bees, and in 1989 re-named the virus DWV following its pathology and symptoms (Ball, 1983, Ball, 1989, Ball, 1993, Genersch and Aubert, 2010). With the following arrival of the parasitic mite, *Varroa destructor* and its global distribution, this virus has become the major cause of honey bee colony collapse (Ribière et al., 2008, de Miranda and Genersch, 2010).

DWV belongs to the order *Picornavirales* and family *Iflaviridae* (Lanzi et al., 2006). Like many picorna-like insect viruses, DWV produces a 30 nm diameter nonenveloped icosahedral virion consisting of a 10,000-nucleotide single positive-stranded RNA genome and three major structural proteins including VP1 (44 kDa), VP2 (32 kDa), and VP3 (28 kDa) (Le Gall et al., 2008, Lanzi et al., 2006, de Miranda and Genersch, 2010, Moore and Eley, 2017). The short VP4 (2.3 kDa) is generated adjacent the N-terminal of VP1 region (Lanzi et al., 2006). During viral infection, the capsid undergoes a conformational change to entry host cells while VP4 may be inserted directly into cell membranes prior to viral insertion (Martin and Brettell, 2019). The polyadenylated viral RNA genome contains a single open reading frame (ORF), which is flanked by a long 5'-untranslated region (UTR) and a short conserved 3'-UTR, including the elements to control replication and translation (J. E. Wilson et al., 2000, Isawa H et al., 1998, Wu et al., 2002, Wang, 2004, Lanzi et al., 2006). The RNA genome encodes a polyprotein of 2,894 amino acids, which is translated through an internal ribosomal entry site (IRES) (Lamp et al., 2016). The polyprotein is cleaved into the structural and non-structural proteins by the viral protease (Lanzi et al., 2006). The capsid proteins locate at the N-terminal part of the polyprotein in the order of VP2, VP4, VP1, and VP3; while its C-terminal part contains the non-structural proteins including the RNA helicase, genome-linked viral protein (VPG), a-chymotrypsin-like 3C protease (3C), and RNA-dependent RNA polymerase (RdRP) (Lanzi et al., 2006, Skubnik et al., 2017) (Fig.1.2).

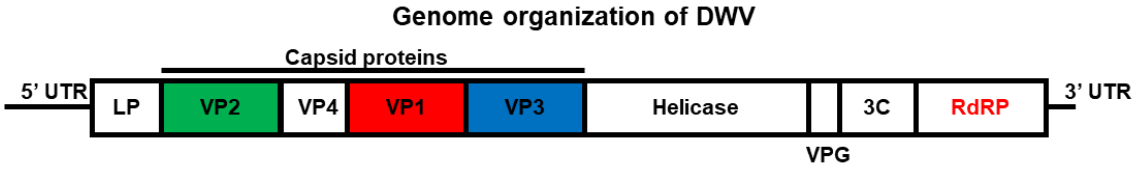

Figure 1.2 The genome organization of DWV.

The DWV genome is polyadenylated and contains a single open reading frame (ORF), flanked by a long 5'-untranslated region (UTR) and a short conserved 3'-UTR. The identified domains from N-terminal to C-terminal are the leader polypeptide (LP), four capsid proteins (VP2, VP4, VP1, and VP3), the helicase, the genome-linked viral protein (VPG), the 3C-protease (3C), and the RNA-dependent RNA polymerase (RdRP).

Similarly, to other RNA viruses, DWV exists as quasispecies. Viral quasispecies are generated by a replication process lacking proof reading and repair (Holland et al., 1992, Steinhauer et al., 1992) as well as RNA recombination (Lai, 1992). Replication of the RNA genome is an error-prone process with high mutation rate, and thus mutations accumulate in the viral progeny (Holland et al., 1992, Domingo and Holland, 1997). Viral quasispecies form dynamic mutant clouds, which are characterized by predominant

master variants, surrounded by abundant low frequency mutants (Domingo and Holland, 1997, Holland et al., 1992, Domingo, 2002, Lauring and Andino, 2010). Three major master DWV variants (type A, type B, and type C) have been identified to date (Ryabov et al., 2014, Ongus et al., 2004, Mordecai et al., 2016c). The International Committee on Taxonomy of Viruses designated two variants, DWV and Kakugo virus as type A master strain (Lanzi et al., 2006, Fujiyuki et al., 2004), which is the most prevalent and frequently associated with honey bee colony decline (Martin et al., 2012, Schroeder and Martin, 2012, Francis et al., 2013). The type B is a different strain which shares approximately 84% nucleotide identity with the type A and *Varroa destructor* virus-1 (VDV-1) is designated as the type B strain (Martin et al., 2012, Mordecai et al., 2016a). The type B DWV strain was found to protect a honey bee colony against the type A infection mediated by the mites in the UK (Mordecai et al., 2016a); however, it was pathogenic at the level of individual honey bee (McMahon et al., 2016). The type B variant was found to replicate in *V. destructor* by detection of negative-strand RNA (Ongus et al., 2004); nevertheless, the negative-strand RNA of the type A genome was exclusively detected in *V. destructor* infesting honey bee pupae with high DWV titer. Thus, *V. destructor* is likely to acquire the negative-strand RNA from the honey bee cells containing DWV replication complexes (Posada-Florez et al., 2019). The type C has been recently identified and its characteristics are still unknown (Mordecai et al., 2016c). Furthermore, co-infection by the multiple master strains in the same host leads to the formation of viral recombinants (Mordecai et al., 2016c, Moore et al., 2011, Dalmon et al., 2017). Recombinants of DWV type A and type B were identified as the major variants in some locations in the UK, France and Israel (Moore et al., 2011, Zioni et al., 2011, Dalmon et al., 2017). The virulence, pathogenicity and relationship with *V. destructor* of the three master variants are still controversial.

Virus infection can be categorized into overt and covert infection in the insect. Overt infection is characterized by obvious disease symptoms with high viral titer. It is sub-categorized into acute and chronic infection. Acute overt infection is characterized by highly productive infection with severe symptoms or even death in a short period, while chronic overt infection is characterized by long-term viral production with disease symptoms persisting over the lifetime of the infected host for some insect viruses. Covert infection is characterized as the following: 1) virus persists beyond the current host's life stage which allows the vertical transmission over numerous generations (Burden et al., 2002, Kukan, 1999, de Miranda and Genersch, 2010); 2) the virus-infected host does not show clear disease symptoms; 3) there is potential to induce the overt infection under certain circumstances (Burden et al., 2003, de Miranda and Genersch, 2010). Covert infection is sub-categorized into latent and persistent infection (Dimmock and Primrose, 1994). For latent infection, the viral genome is either integrated into the host cell genome or persists as the extrachromosomal episome (de Miranda and Genersch, 2010, Dimmock and Primrose, 1994). Persistent covert infection is characterized by constantly low level of viral production which requires to evade from the host's immune-surveillance system. Expression of both host and viral genes should be regulated to allow the continuous viral production inside the infected cell (Dimmock and Primrose, 1994). Therefore, there must be a balance between the host immune system and viral infection for the persistent infection. DWV can be detected in honey bee at all development stages without clear symptoms (Chen et al., 2005b, Tentcheva et al., 2006, Yue and Genersch, 2005). However, *V. destructor* infestation induces

the viral outbreak with visible symptoms, including crippled wings, malformed appendages, bloated and shortened abdomens, miscolouring, and even death (Ball and Allen, 1988, Bowen-Walker et al., 1999, Martin, 2001, Tentcheva et al., 2006, Yue and Genersch, 2005, Stephen Martin et al., 1998). These results suggest that DWV can shift from covert to overt infection. Especially, the replicating genome of DWV was detected in the head of healthy-looking honey bee, indicating a chronic overt infection (Zioni et al., 2011). DWV chronic infection is associated with cognitive impairment (Navajas et al., 2008) or learning deficit (Iqbal and Mueller, 2007) (Table.1.1).

Table 1.1 Summary of the different types of DWV infection and transmission pathways.

Infection type	Sub-type	Duration	Symptoms	Impact on host fitness	Vertical transmission	Horizontal transmission (direct)	Horizontal transmission (vectorial)
Overt	Acute	Short	Short lifespan, crippled wings, malformed appendages, bloated and shortened abdomens, miscolouring	High	No	No	Yes
	Chronic	Long	Learning deficits, cognitive impairment, reduced lifespan	Medium		Yes	Yes
Covert	Persistent	Long	None	Low	Yes	Yes	Yes

This table is adapted from (de Miranda and Genersch, 2010).

Honey bee virus is transmitted via horizontal and/or vertical transmission routes. For horizontal transmission, virus is transmitted between infected and susceptible individuals, i.e. among worker bees or between the queen and her offspring via food-borne or air-borne transmission (de Miranda and Genersch, 2010). Virus transmission from parent to the offspring through egg or/and sperm during reproduction also exists and represents vertical transmission. DWV can be transmitted both vertically and horizontally. DWV viral sequence could be detected in the queen's ovary, spermatheca, the drone's reproductive tract, seminal fluid, and in eggs, indicating the multiple routes for vertical transmission (Chen et al., 2006b, Chen et al., 2005a, Fievet et al., 2006, Yue et al., 2006). A virgin queen from a mite-infested colony could lay unfertilized eggs with or without DWV infection. DWV-positive unfertilized eggs develop to DWV-infected drones, and artificial insemination of DWV-negative unfertilized egg with DWV-positive sperm results in 100% DWV-positive fertilized egg, which further develops to DWV-infected worker bees. These prove the vertical transmission of virus from queen and drone to the offspring (Yue et al., 2007). Detection of DWV in larval food also indicates the direct horizontal transmission in which DWV is transmitted to honey bee via feeding and trophallaxis (Yue and Genersch, 2005). This is also established by the development of DWV-positive workers from DWV-negative eggs following feeding on contaminated food (Nordström, 2003, Yue et al., 2007). The vectorial transmission of DWV by *V. destructor*, in which virus is injected into pupae,

is an additional horizontal transmission route, one which usually results in overt infections (Gisder et al., 2018) (Table.1.1).

Previous research indicates that DWV overt infection is intimately associated with 1) *V. destructor* infesting the developing pupae (Ball, 1983, Ball, 1989, Ball, 1993, Hung et al., 1995, Carreck et al., 2010, Bowen-Walker et al., 1999); 2) *V. destructor* directly injecting the virus to developing pupae (Bowen-Walker et al., 1999, Yue and Genersch, 2005, Gisder et al., 2009, Martin, 2001, Mockel et al., 2011, Schoning et al., 2012, Wilfert et al., 2016); 3) DWV replicating in *V. destructor* prior to transmitting to pupae (Yue and Genersch, 2005, Gisder et al., 2009, Schoning et al., 2012, Ryabov et al., 2014, Campbell et al., 2016); 4) transmission of more virulent DWV variants (Gisder et al., 2009, Ryabov et al., 2014, McMahon et al., 2016, Natsopoulou et al., 2017).

Section 1.3 Ectoparasitic mites

Section 1.3.1 *Varroa destructor*

Varroa destructor is currently the most common and detrimental ectoparasitic mite of honey bee worldwide (Rosenkranz et al., 2010). With the importation of European honey bee, *A. mellifera* to Asia, *V. destructor* shifted from the original host Asian honey bee, *Apis cerana* to *A. mellifera* and the mite has spread all continents where *A. mellifera* is present, except Australia (Stephen Martin et al., 1998, vanEngelsdorp and Meixner, 2010, Rosenkranz et al., 2010). *V. destructor* was first recorded at the eastern coastal region of the Union of Soviet Socialist Republics in 1952, Pakistan in 1955, Japan in 1958, China in 1959, Bulgaria in 1967, South America in1971, Germany in 1977, and United State in 1987 (Ruttner, 1980, de Guzman et al., 1998).

Varroa destructor has distinct sexual dimorphism (Ifantidis, 1983). For both sexes of mite, bodies are divided into two parts, the idiosoma and the gnathosoma. The idiosoma consists of one dorsal shield and different ventral shields. The female mite contains a flattened, ellipsoidal idiosoma with greater width than length, and is highly sclerotised with reddish-brown colour (Rosenkranz et al., 2010) (Fig.1.3A-B). The male mite is pear-shaped with weaker sclerotization and lighter reddish-brown colour. Males are smaller in size than female mites during all development stages (Rosenkranz et al., 2010) (Fig.1.4).

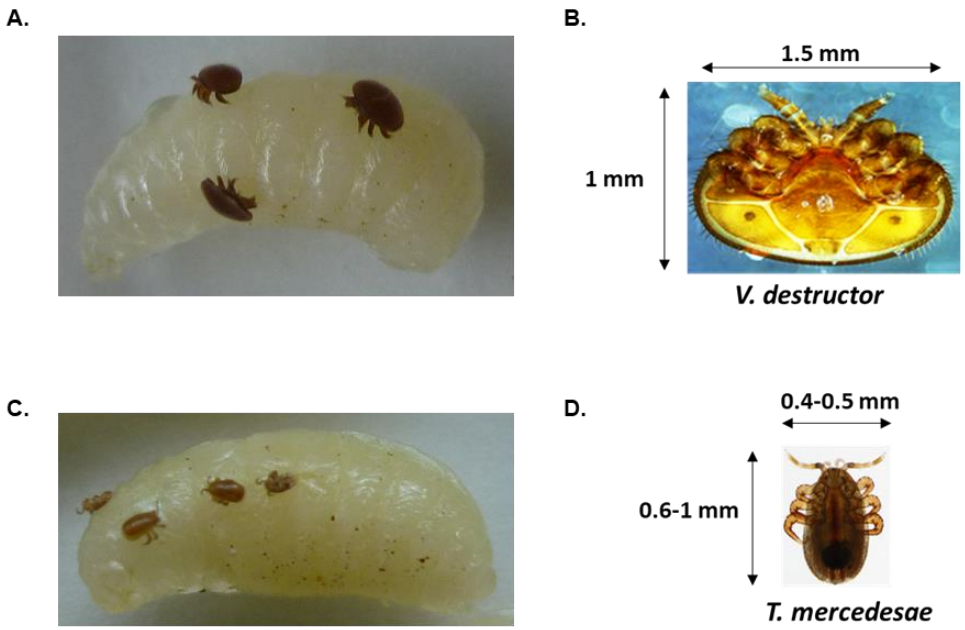

Figure 1.3 Comparison between *Varroa destructor* and *Tropilaelaps mercedesae*.
The honey bee larva is infested by (A) *V. destructor* and (C) *T. mercedesae*. (B) *V. destructor* and (D) *T. mercedesae* have the different sizes and morphologies.

The life cycle of *V. destructor* consists of two distinct phases: a phoretic phase on adult honey bee and a reproductive phase on pupa (Rosenkranz et al., 2010). Both male and nymphal mites live inside capped brood cells for a short period during the reproductive phase. Female mites propagate during the reproductive phase and transport between brood cells or spreading to other colonies via adult bees during the phoretic phase (Kuenen and Calderone, 1997, Rosenkranz et al., 2010). For the reproductive phase, the matured female mite first enters to a brood cell with the 5th instar bee larva and consumes the larval food inside the cell. Approximately 5 hours after cell capping, the mite sucks haemolymph and fat body from the larva (Rosenkranz et al., 2010, Ifantidis et al., 1988, Ramsey et al., 2019). After oogenesis and vitellogenesis within few hours, (Garrido et al., 2000, Steiner et al., 1995, Steiner et al., 1994), the first mite egg is laid around 70 hours after cell capping (Ifantidis, 1983, Steiner et al., 1994). The first egg is usually unfertilized and developed to a haploid male mite. Subsequent female eggs are fertilized and laid with the interval of 30 hours (Ifantidis, 1990, Martin, 1994, Rehm and Ritter, 1989). For worker and drone brood cells, the maximum number of eggs laid are five and six, respectively (Martin, 1994, Martin and acarology, 1995, Garrido and Rosenkranz, 2003). Mite development usually takes around one hour in the egg phase (Nannelli, 1985). After hatching, the mite develops to protonymph, deutonymph and adult stages successively. The nymphal periods are approximately 5.8 and 6.6 days for female and male mites, respectively (Ifantidis, 1990, Martin, 1994, Rehm and Ritter, 1989, Donzé et al., 1994). Male mites, sexually maturing earlier than female, locate at the fecal accumulation site inside the brood cell and start mating once the female mite arrives (Rosenkranz et al., 2010, Donze et al., 1996) (Fig.1.4).

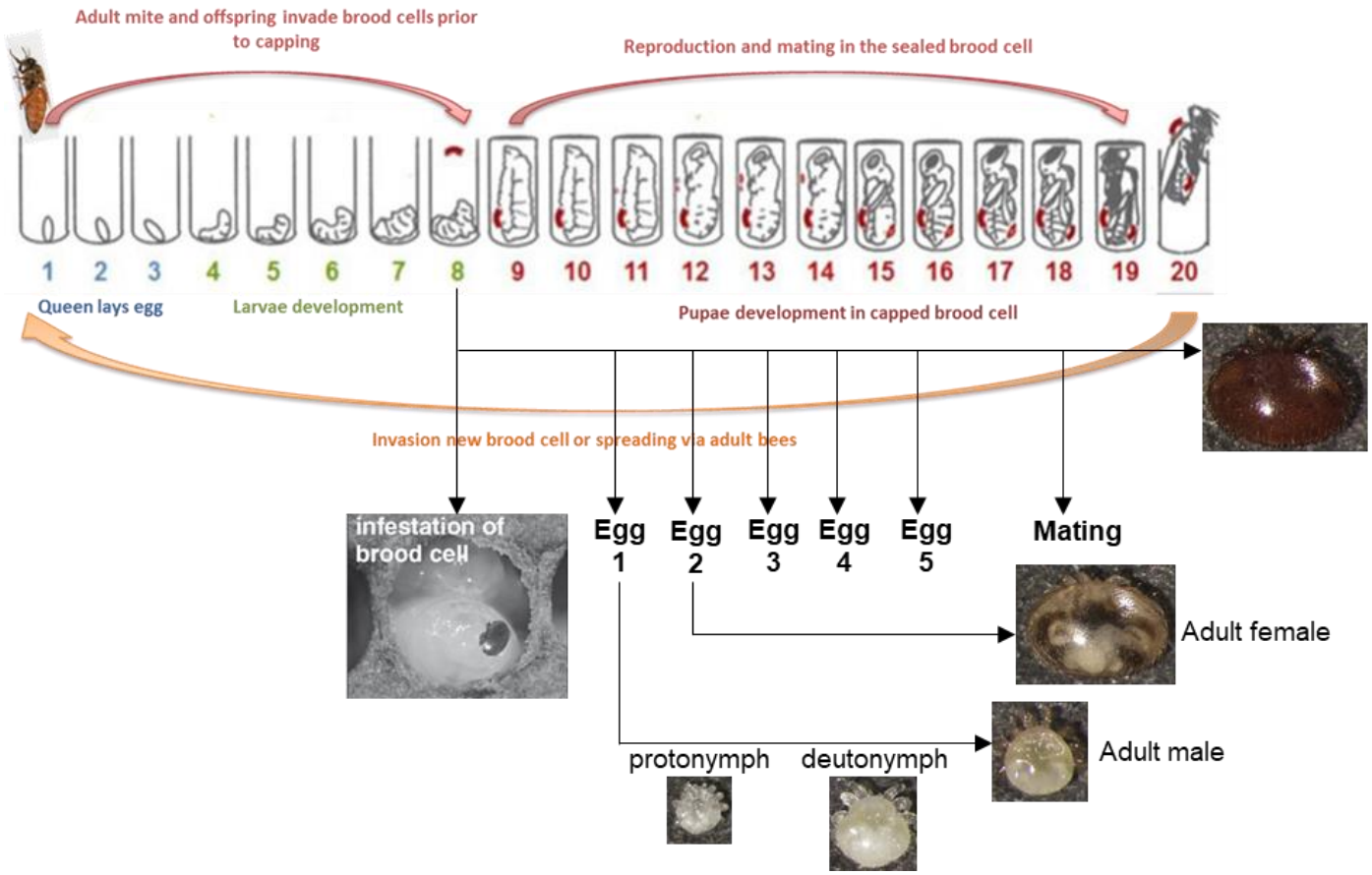

Figure 1.4 The phoretic and reproductive phases of *V. destructor* with honey bee development.

During the reproductive phase, a female *V. destructor* enters into a 5th instar brood cell shortly before capping and laid the first unfertilized male egg approximately 70 hours later after capping, subsequently laid four fertilized female eggs with the interval of 30 hours. Mite egg develops into adult through protonymph and deutonymph stages, and takes approximately 5.8 and 6.6 days for female and male mites, respectively. Sexually mature male mite mates with females inside brood cells. Mother mite and mature daughter mite will leave the brood cell via adhering on the hatching bee to start the phoretic phase (adapted from (Rosenkranz et al., 2010, de Miranda et al., 2015)).

Varroa destructor is able to vector various honey bee viruses, including KBV, SBV, ABPV, IAPV and DWV. Among these viruses, DWV is the most significant transmitted by *V. destructor* (de Miranda and Genersch, 2010). The initial phase for the evolution of tripartition relationship 'Honey bee-DWV-*Varroa* mite' was revealed via studying honey bees among the Hawaiian archipelago after the arrival and spread of *V. destructor*, which sharply increased DWV prevalence, from around 10% to 100% within the honey populations, with a 10^6 increase of viral titer and significant reduction of strain diversity (Martin et al., 2012). In fact, the prevalence, biodiversity and virulence of DWV appear to be dependent on its transmission by *V. destructor*: Historically DWV was unknown and understudied prior to *V. destructor*'s arrival (Bailey et al., 1979) and currently it is almost undetectable in the mite-free areas (Mondet et al., 2014). With effective miticide treatment, DWV level can be gradually reduced and even cured. In regions with well-established *V. destructor*, DWV is usually the major cause for honey bee colony collapse infested by *V. destructor* (Neumann and Carreck, 2010, Dahle, 2010, Le Conte et al., 2010, Mondet et al., 2014).

Varroa destructor infestation of honey bee is one of the inducers of DWV overt infection (Shen et al., 2005), but the underlying mechanisms of the transition of DWV from a relatively benign virus to a pathogenic one with the mite infestation remain unclear. Three hypothesises have been proposed: 1) *V. destructor* suppresses the immune system of honey bee and promotes the replication and proliferation of DWV (Yang and Cox-Foster, 2005, Gregory et al., 2005); 2) *V. destructor* selects more virulent DWV strain by the replication inside mite prior to the transmission (Moore et al., 2011, Martin et al., 2012, Neumann et al., 2012); 3) DWV replicates in *V. destructor* and directly transmits to honey bee through feeding activity (Neumann et al., 2012, Yue and Genersch, 2005, Gisder et al., 2009, Schoning et al., 2012, Ryabov et al., 2014, Campbell et al., 2016).

Through transcriptome (RNA-seq) analysis of adult honey bees with both high *V. destructor* infestation and DWV titer, it was observed that 19 immune-related genes encoding dorsal-1A, components of the immune signalling pathways (*hem*, *socs*, and *tak1*), and pathogen recognition receptors (*Am SCR*, *B5* and *B7 scavenger receptors*, and *C-type lectin 8*) are down-regulated, whereas 6 genes involved in both pathogen recognition (*NimC2*, *PGRP-S2*, and *Eater-like*) and signalling molecules (serine proteases) are up-regulated . In particular, *dorsal-1A* which is a NF-kB family member, was the most down-regulated gene (Nazzi et al., 2012). However, the generality of these 19 down- or up-regulated immune-regulated genes is questionable (Gerth and Hurst, 2017). The reduced expression of *dorsal-1A* in honey bees infected with DWV together with the mite infestation but not the mite infestation alone was further confirmed. Significantly higher DWV titer was also detected with larvae in which *dorsal-1A* was knocked down by the RNAi. These observations demonstrate that *V. destructor* de-stabilizes the dynamics of DWV in honey bee by suppressing the transcription factor dorsal-1A (NF-kB), promoting DWV replication (Nazzi et al., 2012). For antimicrobial peptides, the reduced Defensin transcription was reported in honey bee infested by *V. destructor* (Yang et al., 2004, Gregory et al., 2005), nevertheless, Abaecin and Defensin were non-linearly correlated with the number of infesting *V. destructor*. Their expression levels were lower in bees exposed to low or moderate number of *V. destructor*, than in bees with heavily infestation or without infestation (Gregory et al., 2005). Aggregation of haemocytes was observed in the centres of the wound sites on honey bee pupae caused by *V. destructor* feeding activity, and this observation suggests the cellular immune response of honey bee against mite infestation (Kanbar and Engels, 2003). The mother mite creates a feeding hole on the abdominal sternites of honey bee pupa and the offspring continues to use the same feeding hole to suck the fat body and other tissues of pupa (Donzé et al., 1994, Ramsey et al., 2019). Di Prisco *et al.* found mutualistic symbiosis between DWV and *V. destructor*, in which DWV associated with the pupa positively influences the mite's feeding and reproduction. Meanwhile, the mite's feeding strongly affects DWV replication in the pupa, induces the negative impacts on honey bee immunity, and finally leads to the honey bee colony decline (Di Prisco et al., 2016, Yang and Cox-Foster, 2005).

Contrary to the previous view that *V. destructor* feeds on haemolymph (Sadov, 1976, Dinda et al., 1977, Smirnov, 1978), recent study has indicated that the mites primarily exploit the fat body from honey bee pupa (Ramsey et al., 2019). The fat body is a nutrient rich and vital organ with essential functions for immune system, pesticide detoxification, and overwinter survival for both adult and developing honey bees

(Arrese and Soulages, 2010). *Varroa destructor* not only acts as a mechanical vector to transmit DWV, but also as a biological vector through supporting DWV replication prior to transmission (Yue and Genersch, 2005). Currently, all evidence of DWV replication in *V. destructor* have been based on detection of the negative-strand RNA (Ryabov et al., 2014, Yue and Genersch, 2005, Gisder et al., 2009), and it is still controversial whether DWV really replicates in *V. destructor* (Wilfert et al., 2016). Recently, it has been shown that the negative-strand RNA of DWV type A strain is exclusively detected in *V. destructor* collected from honey bee pupae with high DWV titer. It indicated that *V. destructor* acquires the negative-strand RNA from honey bee cells containing DWV replication complexes, suggesting a non-propagative transmission manner for DWV type A (Posada-Florez et al., 2019).

The underlying mechanisms of 'Honey bee-DWV-*Varroa* mite' interactions are still not fully understood. In order to maintain healthy honey bee colony, further investigations are required.

Section 1.3.2 *Tropilaelaps mercedesae*

Tropilaelaps mercedesae, another major honey bee ectoparasitic mite, has coexisted with *Varroa* mites in Asia for more than 50 years (Delfinado, 1963). In 2007, through molecular marker analysis, *T. mercedesae* was characterized alongside with three other *Tropilaelaps* species (*Tropilaelaps clareae*, *Tropilaelaps koenigerum*, and *Tropilaelaps thaii*) (Anderson et al., 2007). Among these species, *T. mercedesae* and *T. clareae* can cause the most serious impacts on *A. mellifera* (de Guzman et al., 2017). *T. mercedesae* has a wider geographic distribution compared to *T. clareae*, which infests *A. mellifera* only in Philippines (Anderson et al., 2007). *T. mercedesae* was originally identified to infest *Apis dorsata* in mainland Asia as well as Indonesia and *Apis laboriosa* in Himalayas. Through introduction of *A. mellifera* to Asia, *T. mercedesae* switched host to *A. mellifera*; nevertheless, the mite remains confined inside Asia and bordering areas (Anderson and Roberts, 2013, Burgett et al., 1983, Woyke, 1985, Anderson et al., 2007, Dainat et al., 2009, Chantawannakul et al., 2018).

Compared to *V. destructor*, *T. mercedesae* is smaller (< 1 mm long), with idiosoma of greater length than width. For the adult female collected from *A. mellifera*, the average length and width are 956.1 ± 27.6 μm and 533.2 ± 21.1 μm, respectively, while for the adult male, they are 907.4 ± 9.2 μm and 514.1 ± 18.3 μm, respectively (Anderson et al., 2007) (Fig.1.3C-D). The adult mite has red-brown colour, and its first pair of legs are long and upright-holding to resemble insect antennae. Compared to female *T. mercedesae*, male mites consist of two distinct morphological difference: 1) a shorter and sharply pointed epigynial thoracic plates (highlighted by red star in Fig.1.5A); and 2) a longer chela spermatodactyl with a spirally coiled apex (Fig.1.5B).The nymphal mite shares a similar body structure with adult mites, but with partially transparent white colour (Anderson and Roberts, 2013, Anderson et al., 2007, de Guzman et al., 2017) (Fig.1.5C).

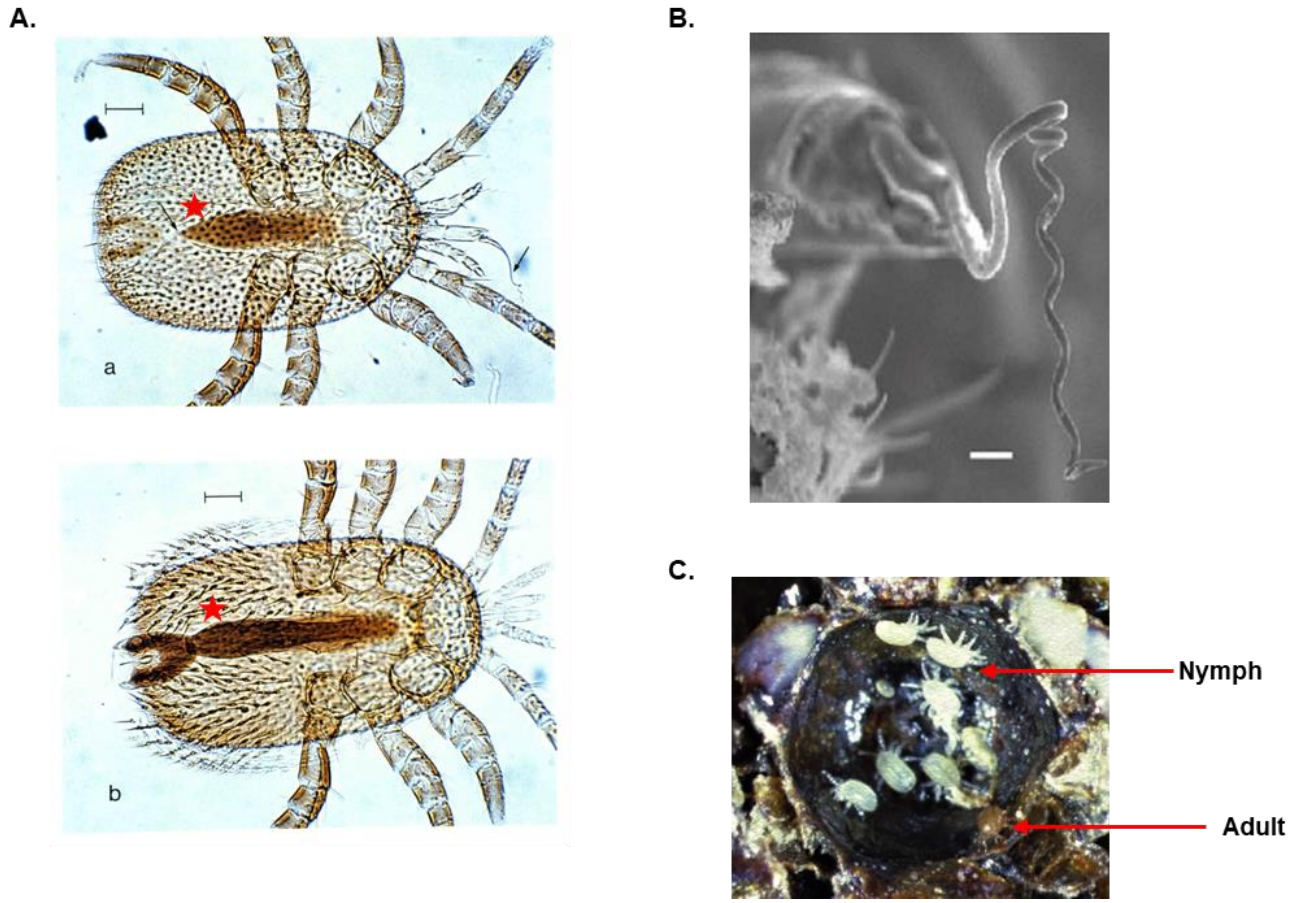

Figure 1.5 Different sexes and developmental stages of *T. mercedesae*.

(A) Comparison of mounted specimens of male (top, a) and female (bottom, b) adult *T. mercedesae*. The epigynial thoracic plates (highlighted by red star) of male mite is shorter and sharply pointed toward the posterior end. Bars = 0.1 mm. (B) Scanning electron micrograph of chela spermatodactyl of male mite, which is longer with a spirally coiled apex. Bar = 10 µm. (C) The partially transparent white nymphs and brown adult mites inside a brood cell. (adapted from (Anderson and Roberts, 2013)).

The life cycle of *T. mercedesae* is similar to that of *V. destructor*. The mature mated adult female enters to an uncapped brood cell with the 5th instar larva followed by ovipositing 1-4 offspring inside the sealed brood cell. The interval of egg laying is approximately one day and the development to adult mite takes about one week. Multiple female mites may enter a single cell in severely infested colony (Ritter et al., 1988). Mother mite and mature offspring will emerge with adult honey bee from the cell and immediately search for a new host (Woyke, 1987b, Woyke and acarology, 1994) (Fig.1.6). Unlike *V. destructor*, *T. mercedesae* can only feed on haemolymph of honeybee larva or pupa, as their mouthparts and body shape do not allow them to feed on adult honeybees (Needham et al., 1988). Therefore, compared to *V. destructor*, *T. mercedesae* has very short phoretic phase, only 1-2 days (Woyke, 1987a). Unmated *T. mercedesae* females are able to reproduce both female and male offspring after the eclosion, which is probably caused by endosymbiotic bacteria or deuterotokous parthenogenesis (de Guzman et al., 2018, Phokasem et al., 2019). Both daughter and foundress mites collected from capped brood cells with tan-bodied pupae reproduce successfully, suggesting *T. mercedesae* is able to reproduce without the phoretic phase (de Guzman et al., 2018). As a result, *T. mercedesae* has relatively quicker reproduction cycle and its population increases inside honey bee colony faster than *V. destructor* (Koeniger and Muzaffar, 1988,

Rinderer et al., 1994, Woyke, 1984, Anderson and Roberts, 2013, de Guzman et al., 2017, Chantawannakul et al., 2018). Previous studies indicated that *T. mercedesae* could be far more prevalent than *V. destructor* in several Asian countries such as Thailand (Chantawannakul et al., 2018), and it imposes more severe impact on honey bee colonies than *V. destructor* based on the Chinese beekeeper's report (Buawangpong et al., 2015). Therefore, *T. mercedesae* is a potentially greater threat on honey bee colony and health with the risk of global spread (Buawangpong et al., 2015, Burgett et al., 1983).

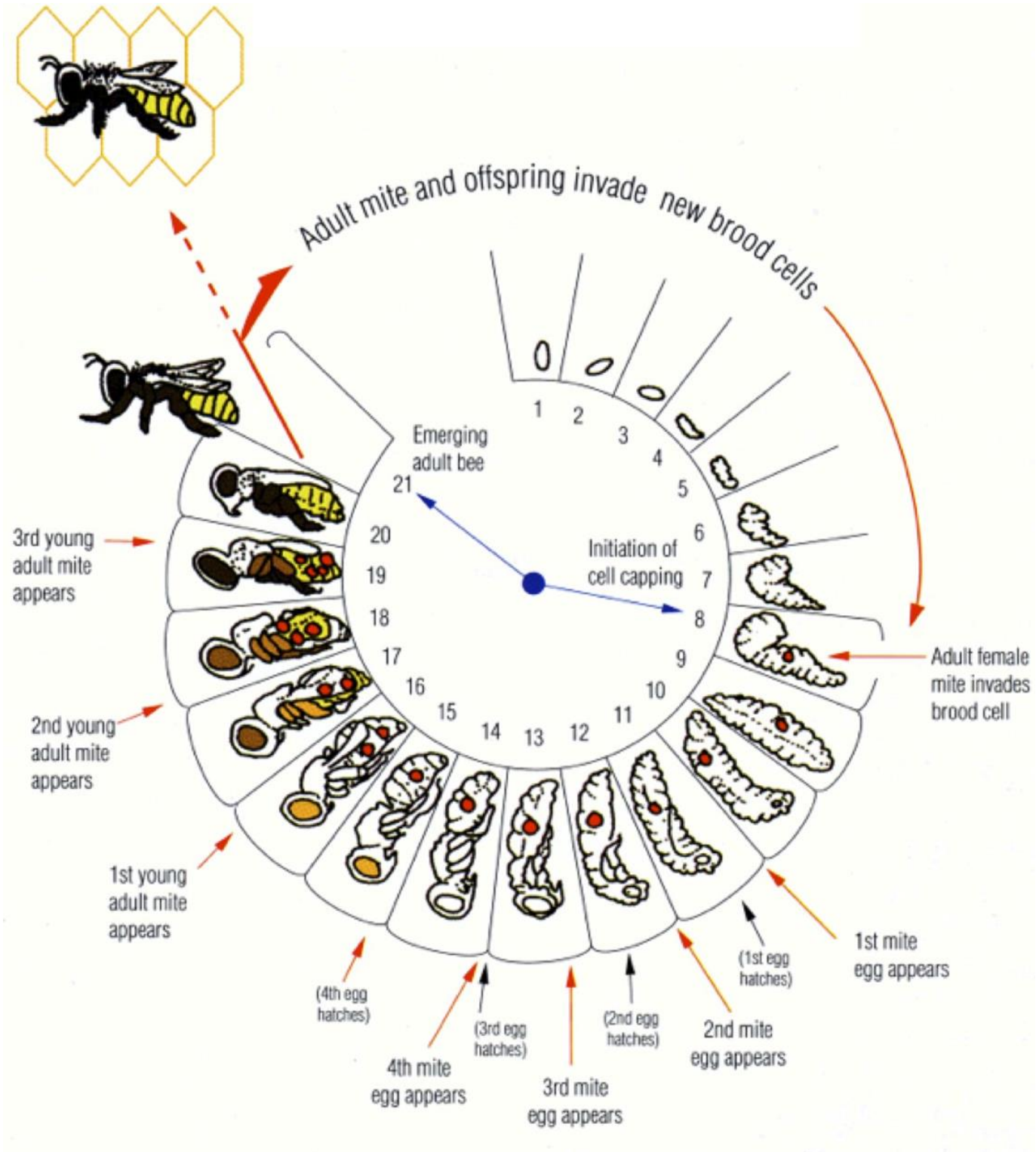

Figure 1.6. Life cycle of *T. mercedesae* on honey bee.

Diagram was adapted from (Anderson and Roberts, 2013).

Since *Tropilaelaps* mites have similar life cycle and food requirement as *Varroa* mites, they also cause detrimental effects to individual honey bee and the colony by weakening or killing brood (Laigo and Morse, 1968, Morse and Laigo, 1969, Burgett et al., 1983, Kitprasert, 1984), suppressing bee immune responses and promoting viral infection (Khongphinitbunjong et al., 2015), reducing the weight and longevity of adult bees (Khongphinitbunjong et al., 2016), malformed or dead callow bees (Akratanakul, 1987), and reducing the total protein concentration of pupae (Negi et al., 2014). Mite infestation also decreases honey yield (Laigo and Morse, 1968, Camphor et al., 2005, Raffique et al., 2012), makes the colony susceptible to wax moth infestation (Laigo and Morse, 1968), and even induces colony death (Camphor et al., 2005, Burgett and Akratanakul, 1985). In some colonies with highly infestation, bald brood will be observed, a condition where worker bees remove the capping (Pettis et al., 2013)

The roles of *Tropilaelaps* mites as a vector for transferring pathogens to honey bee are not yet understood. DWV and BQCV have been identified in honey bee infested by *T. mercedesae*; nevertheless, the presence of these two viruses was not associated with the number of *T. mercedesae* infesting the pupae (Khongphinitbunjong et al., 2015). Both prevalence and titer of DWV increase with *T. mercedesae*-infestation (Khongphinitbunjong et al., 2015, Forsgren et al., 2009). DWV genome RNA can also represent almost half of the transcriptome of *T. mercedesae* (Dong et al., 2017). The negative-strand of DWV RNA was detected in *T. mercedesae* by strand-specific RT-PCR, suggesting the viral replication in the mites (Dainat et al., 2009). Therefore, these previous studies may suggest *T. mercedesae* acts as a biological vector for DWV. The puncture wound on honey bee pupae, caused by *T. mercedesae*'s feeding activity, promotes pathogens (including virus) to entry inside honey bee (Chantawannakul et al., 2018).

Compared to *V. destructor*, the capacity of *T. mercedesae* to transmit DWV to honey bee has not yet been well characterized. Furthermore, the role of every component in "Honey bee-DWV-*Tropilaelaps* mite" tripartition interaction are not yet characterized.

Section 1.4 Aims of research project

The major objective in my research project is to characterize the cross-interactions between DWV, honey bee, and the ectoparasitic mites, especially *T. mercedesae*. In order to understand the underlying the mechanisms of interactions, several questions were addressed:

1. Does *T. mercedesae* function as a vector to transmit DWV to honey bee?
2. Whether *T. mercedesae* infestation induces immune responses in honey bee? If the answer is true, what is the underlying mechanism of immune regulation in honey bee by *T. mercedesae* infestation.
3. Are there any negative impacts of DWV on *T. mercedesae*, such as reducing reproductive capacity and mite fitness?
4. Where does DWV accumulate inside ectoparasitic mites?
5. Since DWV infects honey bee and ectoparasitic mites, belonging to two distinct branches of evolutionary relationship of arthropods, DWV could potentially infect other organisms. Several

established insect cell lines, as well as honey bee primary cells were used to explore the underlying molecular and cellular mechanisms of DWV replication/infection.

For this thesis, the results of Section 2.3.1-2.3.5 were already published in *Frontiers in Microbiology* (Wu et al., 2017). The results of Section 2.2.5, 2.3.10, 4.3.2 and 4.3.5, and partial results of Section 4.3.4 were recently published in *Frontiers in Microbiology* (Wu et al., 2020).

Chapter 2 *Tropilaelaps* mite vectors DWV transmission to honey bee

Section 2.1 Brief introduction

Varroa destructor is one of the most significant drivers of colony losses, mediated through both mite's feeding activity and transmission of honey bee viruses, particularly DWV (de Miranda and Genersch, 2010, Martin et al., 2012, Rosenkranz et al., 2010). In many Asian countries, honey bee colonies are also infested by another ectoparasitic mite, *T. mercedesae*, and this mite species can co-exist with *V. destructor* in a single colony (Anderson et al., 2007, Luo et al., 2011). *Varroa destructor* and *T. mercedesae* have similar reproductive phases within capped brood cells (Fig.1.4 & Fig.1.6) and feeding activities; nevertheless, *T. mercedesae* life cycle has a relatively shorter phoretic phase, a quicker reproductive cycle and faster population build-up, suggesting a potentially greater threat for honey bee colony health. However, in contrast to *V. destructor*, the studies regarding to "Honey bee-DWV-*Tropilaelaps* mite" are limited. The proliferation of DWV was observed in honey bees colonies with *T. mercedesae* infestation, suggesting the potential vector role of DWV (Khongphinitbunjong et al., 2016, Khongphinitbunjong et al., 2015, Forsgren et al., 2009, Dainat et al., 2009). However, a recent study indicates that the vector role for the mite is not to a high degree and the major pathologies of infested honey bee are probably caused by the mite itself (Khongphinitbunjong et al., 2015), thus the vector role of *T. mercedesae* on DWV transmission needs further examination.

The innate immune system of insects consists of cellular and humoral immune responses (Laughton et al., 2011, Wilson-Rich et al., 2008), which are regulated by various immune-related genes (Christophides et al., 2002). During immune activation processes, the surface highly conserved structural motifs of pathogens (termed as Pathogen-Associated Molecular Patterns) are recognized by Pattern Recognition Receptors and their binding induces signalling cascades resulting in the hemocyte-mediated cellular immune response and phenoloxidase-regulated humoral immune responses. Hemocyte-mediated cellular immune response includes nodule formation, phagocytosis and encapsulation, and the phenoloxidase cascade regulates melanisation or coagulation of haemolymph, and antimicrobial peptides (AMP) synthesis (DeGrandi-Hoffman and Chen, 2015). As an essential component of honey bee immune system, AMP expression can be induced and delivered to the infecting microbe within a short period (Hoffmann et al., 1999, Aerts et al., 2008). As broad-spectrum antimicrobial agents, AMPs target pathogens via three mechanisms: 1) directly interacting and disrupting microbial homeostasis; 2) regulating immune responses; and 3) perturbing and rupturing the plasma membrane (Otvos Jr, 2005, Nguyen et al., 2011, Rahnamaeian and behavior, 2011, Bahar and Ren, 2013).

Four types of AMPs have been identified in honey bee, including Abaecin (Casteels et al., 1989), Apidaecin (Casteels et al., 1989), Hymenoptaecin (Casteels et al., 1993) and Defensin. The defensin family contains two peptides and encoded by *Defersin-1* and *Defersin-2* respectively (Casteels et al., 1993, Casteels-Josson et al., 1994, Qu et al., 2008). Two major NF-kB-mediated immune pathways in insects, Imd and Toll signalling pathways regulate *Hymenoptaecin* and *Defensin-1* expression respectively (Aronstein et al., 2010, Osta et al., 2004). The antimicrobial properties of defensin are against honey bee pathogens,

including *Paenibacillus larvae*, *Nosema apis*, *Melissococcus pluton* and *Ascosphaera apis* (Ilyasov et al., 2012), and reduced defensin transcription was reported in honey bee infested by *V. destructor* (Yang et al., 2004, Gregory et al., 2005). A rapidly up-regulated expression of Hymenoptaecin in response to pathogen infection was reported in adult honey bee and in brood (Danihlík et al., 2015). A large Hymenoptaecin-like antimicrobial protein was identified in *Nasonia vitripennis*, which is a parasitic wasp (Tian et al., 2010). A recent discovery indicates the transcripts of Abaecin, Hymenoptaecin and Defensin-1 were induced by coupled interaction of *V. destructor* parasitism and viral infection (Gregorc et al., 2012). These results suggest a putative immunosuppression in honey bee by *V. destructor* infestation. If the expression of any genes underlying the immune system is decreased, the immune response of honey bee may be depressed and result in a more susceptible for pathogens infection (Yang and Cox-Foster, 2005).

In this chapter, I compared the effects of *V. destructor* and *T. mercedesae* infestation on DWV prevalence and copy number in honey bee pupae by individually analysing pupae and the infesting mites from the same brood cell. Together with sequencing DWV in the paired pupae and mites, I use these data to discuss about the potential mechanisms for the stimulation of DWV replication by *V. destructor* and *T. mercedesae* in honey bees. Many previous studies analysed the pooled samples of honey bees and mites, and the results were useful to understand the general degree of DWV infection and identify the dominant variant in the colony. However, my analyses were aimed to understand micro dynamics of DWV population (as well as flow of DWV) between the pairs of honey bee pupa and infesting mite. Additionally, I examined the vector role of *T. mercedesae* on DWV transmission via artificially infesting honey bee pupa with mite, and comparing the DWV load and variants between the pupa and infesting mite. Since *V. destructor* infestation caused reduced expression of AMPs in honey bee, therefore, the infestation of *T. mercedesae* may induce similar immune suppression, and this was studied as well.

Section 2.2 Materials and Methods

Section 2.2.1 Sample collection

A single *A. mellifera* colony (*Colony #1*), sourced from a Wuxi beekeeper, was brought to Xi'an Jiaotong Liverpool University in April 2016. Honey bee pupae with purple eyes were collected by opening capped brood cells. The majority of pupae were free from mites (including *V. destructor* and *T. mercedesae*) during this first sampling period on 20-23 April, with only a small number infested by *V. destructor*. During 20-23 May 2016, purple-eyed pupae were collected from the capped brood cells and 33% of the capped brood cells were now infested by *V. destructor* and none of them contained *T. mercedesae*. The percentage of mite infestation was counted by opening approximately 100 capped brood cells and recording the number of infested cells. When purple-eyed pupae were infested by single adult *V. destructor*, both were sampled simultaneously and stored separately.

A second *A. mellifera* colony with *T. mercedesae* infestation (*Colony #2*), also sourced from a Suzhou local beekeeper, was brought to the university in October 2016. Purple-eyed pupae, with or without

infesting single *T. mercedesae*, were collected from 1-8 November 2016, as described above. *Varroa destructor* was absent in all of the opened capped brood cells in this colony.

During 2018, two *A. mellifera* colonies, sourced from the same Suzhou local beekeeper, was brought to and maintained in the university. One of the colonies was free from mite infestation (*Colony #3*) while the other one was infested by *T. mercedesae* (*Colony #4*). Honey bee pupae with pale or pink eyed-colour (stage 12-13, Fig.1.4) and adult *T. mercedesae* were collected from *Colony #3* and *Colony #4,* respectively, and used for artificial wound induction, DWV infection and *T. mercedesae* infestation experiments.

Section 2.2.2 RT-PCR analysis of DWV

Total RNA was isolated from individual pupae and mites using Total RNA Extraction Reagent (GeneSolution), according to the manufacturer's instructions. The pupal head was separately cut on pre-frozen ice tray for RNA isolation. Glycogen (1 μg) was added to facilitate isopropanol precipitation of the mite RNA samples. Reverse transcription (RT) reactions were carried out using 1 μl of total RNA, random primer (TOYOBO), ReverTra Ace (TOYOBO), and RNase Inhibitor (Beyotime). RNase H (Beyotime) was added to digest RNA in RNA/cDNA heteroduplex after cDNA synthesis. These RT products were used for subsequent RT-PCR to assess whether the honey bee or mite was infected by DWV with the primer set DWV #1 (Supplementary Table) using the conditions 2 min at 94°C, followed by 32 cycles of 10 sec at 98°C, 20 sec at 55°C, and 30 sec at 68°C. PCR products were analysed on a 2% agarose gel. PCR targeting honey bee *EF-1α*, *V. destructor β-actin*, and *T. mercedesae EF-1α* mRNAs (Supplementary Table) was utilized as controls to verify successful RT.

Section 2.2.3 qPCR analysis of DWV copy number

The qRT-PCR was preformed using a Hieff™® qRT-PCR SYBR Green Master Mix (Low Rox Plus, Yesen) and DWV primer set #2 (Supplementary Table) with a QuantStudio5 Real-Time PCR System (Thermo Fisher). To perform absolute quantification of DWV RNA, the standard curves that corresponded to DWV target RNA were firstly prepared. Target RNA was prepared by PCR, followed by purification with an AxyPrep™ PCR cleanup kit (Axygen) or QIAquick PCR Purification Kit (QIAGEN), according to the manufacturer's instructions. DNA concentration was measured using a Nanodrop 2000 spectrophotometer (Thermo Fisher) to calculate copy number using the formula as below (Dhanasekaran et al., 2010):

$$Copy\ number\ = \frac{DNA\ concentration\ (ng/\mu l)\ \times\ 6.02\ \times 10^{23}\ (copies/mol)}{Length\ (bp)\ \times\ 6.6\ \times 10^{11}\ (ng/mol)}$$

in which 6.6×10^{11} ng/mol is the average molecular mass of one base pair and 6.02×10^{23} copies/mol is Avogadro's number. Linear standard curves were then generated using target DNA of 10^{1}-10^{9} copy number per reaction, followed by plotting of Ct values against log copy number values. After RT, the copy

number of target RNA in a sample was estimated using the standard curve. The amount of cDNA added to each reaction was normalized by the Ct values of either *A. mellifera*, *V. destructor*, or *T. mercedesae* 18S rRNA (Supplementary Table).

Section 2.2.4 Sequencing of RT-PCR product

PCR products obtained by RT-PCR were purified by an AxyPrep™ PCR cleanup kit (Axygen) or QIAquick PCR Purification Kit (QIAGEN), according to manufacturer's instruction, and subsequently directly sequenced by the Sanger method. To sequence the 4 kb DWV RNA region encoding partial sequence for Lp, helicase, and all of the VP proteins, PCR was performed using DWV primer set #3 (Supplementary Table) with the conditions 2 min at 94°C, followed by 35 cycles of 10 sec at 98°C, 20 sec at 55°C, and 3.5 min at 68°C, with a final 5 min extension at 68°C. PCR products were sequenced as previously described, and categorized into DWV viral subtypes (A, B, and C).

Section 2.2.5 Artificially *T. mercedesae* infestation to honey bee pupae

Fifteen honey bee pale or pink eyed-colour pupae (stage 12-13, Fig.1.4) and 15 adult *T. mercedesae* were collected from *Colony #3* and *Colony #4*, respectively. A single mite was put inside a gelatin capsule with a pupa, incubated at 33°C with 50-60% humidity. The gelatin capsules with single pupa without mites were incubated at exactly same condition as a negative control group. Both infested and negative control groups were stored simultaneously. After 7 days incubation, mites and pupae were collected respectively and proceed for further DWV quantification (qRT-PCR) and DWV variants identification (RT-PCR products Sanger sequencing).

Section 2.2.6 Construction of phylogenetic tree

Prior to phylogenetic analysis, nucleotide sequences were aligned using Mafft (v7.307) (Katoh and Standley, 2013) and then used Gblocks (v0.91b) (Castresana, 2000) to automatically eliminate divergent regions or gaps. The best fit nucleotide substitution models were determined for the alignments by Jmodeltest (v2.1.10) with parameters set to "-g 4 –i –f – AIC –BIC –a" (Darriba et al., 2012). Mrbayes (v3.2.3) (Ronquist and Huelsenbeck, 2003) was run with the parameters set to 1,000,000 (1 sample/100 generations) until split frequencies were below 0.01. The first 25% of samples for each run were designated as the burn-in. DWV type A strain (NC_004830.2), DWV type B strain (NC_006494.1), DWV type C strain (CEND01000001.1), and Sacbrood virus (NC_002066.1) were used as references.

The maximum likelihood phylogenetic tree, which compares DWV variants between the honey bee pupa and infesting *V. destructor*, or *T. mercedesae* artificially infesting honey bee pupae and the infesting mites, was estimated using MEGA (version 7.0.26) with the best DNA substitution model (Hall and evolution,

2013). All nucleotide sequences were aligned and trimmed by MEGA prior to phylogenetic tree construction. DWV type B strain (NC_006494.1) was used as a reference.

Section 2.2.7 DWV virus isolation

Purple eye-coloured pupae with direct mite infestation were collected from *Colony #2* which was severely infested with *T. mercedesae*. They were ground into powders, followed by resuspension with Phosphate buffered saline (PBS, 1 honey bee pupa was resuspended in approximately 250 µl PBS). After 11,400 rpm 1 min 4°C centrifugation, supernatant was then cleared by filtering with 0.22 µm nylon filter membrane (Thermo Fisher). The filtrate was centrifugated through a cushion of 50% (w/v) sucrose at 36,000 rpm 4 hours 4°C (SW41 Ti, Beckman). After clearing the resulting pellet in PBS and centrifugation at 13,000 rpm 1 min 4°C, the virus pellet was finally resuspended in PBS. DWV presence in isolated virus solution was further verified by RT-PCR (with several primer sets including ABPV, BQCV, CBPV, IAPV, KBV, SBV, and DWV #1, and same PCR condition as mentioned above in Session 2.2.2) and its copy number of DWV was quantified by qRT-PCR (with primer set DWV #2 and same method as mentioned above in Section 2.2.3) (Supplementary Table).

Section 2.2.8 Artificially wound induction and DWV infection to honey bee pupae

Honey bee pupae with pink or purple eyes without direct mite infestation were gently collected from *Colony #2*. They were processed by 1) 0.2 µl DWV virus (at dilution 1:10) injection; 2) 0.2 µl PBS injection; 3) or merely needle-punching into the pupal thorax by Microliter Syringes (GAOGE). Pupae without injection and punching were utilized as a negative control group. All pupae were kept in gelatin capsule individually and incubated at 33°C with 50-60% humidity for 37 hours. In order to compare levels of DWV infection, pupal heads were further processed for RNA isolation and qRT-PCR analysis, while pupal abdomens were individually subjected for western blot analysis with anti-VP1 antibody.

Section 2.2.9 Western blot

Each honey bee abdomen was separately lysed with a homogenizer in 300 µl SDS sample buffer (2% sodium dodecyl sulfate, 10% glycerol, 10% β-mercaptoethanol, 0.25% Bromophenol blue, 50 mM Tris-HCl, pH 6.8), followed by heat denaturation at 99°C for 5 min. The lysates were centrifugated for 1 min at 10,000 xg, then the supernatants were subjected to SDS-PAGE gel. For each gel, samples were electrophoresed for approximately 80 min at 20 A and subsequently transferred to a polyvinylidene difluoride membrane (PVDF) (Millpore). Protein-loaded membranes were incubated in Blocking buffer I (5% BSA, 0.1% Tween-20, PBS) for 1 hour at room temperature, and incubated in anti-VP1 antibody diluted in Blocking buffer I at 1:1,000 overnight at 4°C. The membranes were then washed 3 times for 5 min each in PBST (0.1% Tween-20, PBS), incubated in IRDye® 680RD Donkey anti-Rabbit IgG (H+L) (LI-COR) diluted in Blocking buffer II (5% milk powder, 0.1% Tween-20, PBS) at 1:10,000 for 1 hour at room

temperature. The membranes were washed three times for 5 min each in PBST before visualization by Odysse Infrared Imager.

Section 2.2.10 qPCR analysis of *Hymenoptaecin* and *Defernsin-1 mRNAs*

The amounts of *Hymenoptaecin* and *Defernsin-1* mRNAs in the pupae with or without artificial *T. mercedesae* infestation were measured by a relative quantification qPCR method using a Hieff™ qRT-PCR SYBR Green Master Mix (Low Rox Plus, Yesen) with a QuantStudio5 Real-Time PCR System (Thermo Fisher). *Hymenoptaecin* and *Defernsin-1* mRNAs were detected by primer sets *Hymenoptaecin* and *Defensin-1*, respectively (Supplementary Table). The relative quantification was performed by the △△C_T method (Pfaffl, 2007). Honey bee *EF-1α* mRNA (Supplementary Table) was used as the reference gene. The results were expressed as a fold ratio.

Section 2.2.11 Statistical analysis

Western blot results were analysed and quantified by ImageJ (Davarinejad, 2017). Statistical analysis was carried out by *t-test* with software GraphPad Prism (v7.0) (Motulsky, 2003).

Section 2.3 1Results

Section 2.3.1 *V. destructor*'s infestation increases DWV prevalence in honey bee colony

In April 2016, purple-eyed honey bee pupae were collected from capped brood cells in *Colony #1*. During this first sample collection, there were almost no mites (*V. destructor* and *T. mercedesae*) in this colony. Approximately 61% (11 out of 18; positive signals were observed in Lane 1, 5, 7, 9-11, 13-15, 17 and 18 of Fig.2.1A) of the purple-eyed pupae were infected by DWV when analysing by RT-PCR (Fig.2.1A & C). In May 2016, there were approximately 33% of the capped brood cells in the same colony infested by *V. destructor* and none of them contained *T. mercedesae*. For this second sample collection, the same colony was more severely infested by *V. destructor* and 94% (17 out of 18; positive signals were observed in all lanes of Fig.2.1B except the Lane 10) of the pupae without direct *V. destructor* infestation were positive for DWV when analysed by RT-PCR (Fig.2.1B & D). Therefore, *V. destructor* infestation increases DWV prevalence in honey bee colony.

There are different background colours in agarose gel images of Fig.2.1A & B, for example, between Lane 1-10 and Lane 11-18, they were caused by splicing images of samples run on two agarose gels. The irregular background colour observed in all agarose gel images in this thesis was explained by the same reason.

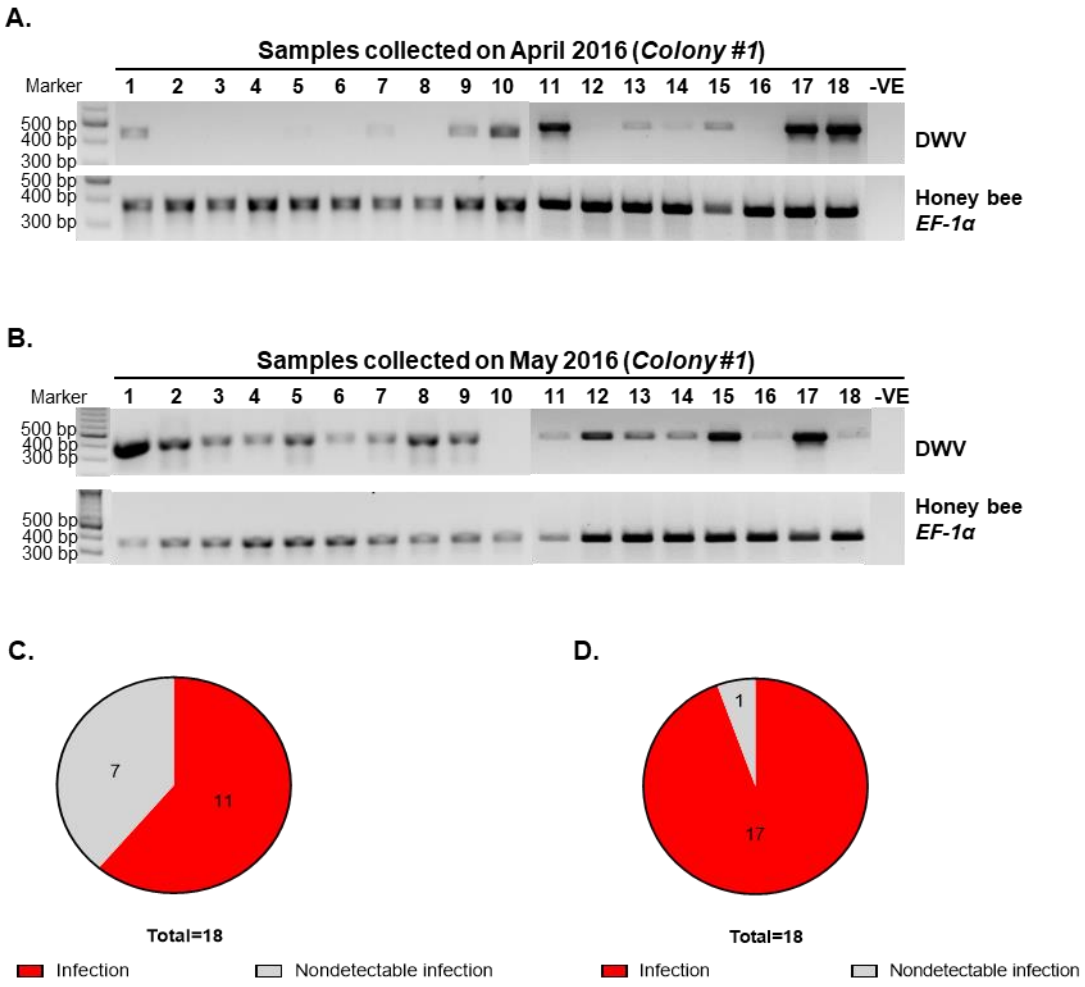

Figure 2.1 Detection of DWV in honey bee pupae without mite infestation collected in April and May 2016.

DWV was detected using RT-PCR in 18 purple eyed-pupae without mite infestation sampled in (A) April 2016 when the mite infestation in colony was low and in (B) May 2016 when the mite infestation in colony was high. Honey bee *EF-1α* mRNA was used as an endogenous positive control and water (-VE) was used as a negative control. The position of 300-500 bp of DNA molecular weight was labelled on the left of agarose gels. (C) For pupae collected in April when mite infestation was low, 11 out of 18 pupae (61%) were infected by DWV through RT-PCR. The positive bands were observed in Lane 1, 5, 7, 9, 10 11, 13, 14, 15, 17 and 18. (D) For pupae collected in May when mite infestation was high, except Lane 10, 17 out of 18 pupae (94%) were infected by DWV through RT-PCR.

Section 2.3.2 *V. destructor*'s infestation increases DWV titer and prevalence in the individual honey bee pupae and a linear correlation of DWV copy number between pupae and the infesting mites

During the second sample collection for *Colony #1* in May 2016, the purple-eyed pupae with single *V. destructor* infestation in the capped brood cells were collected, together with the infesting *V. destructor*. All *V. destructor*-infested pupae as well as the mites were positive for DWV infection (30 out of 30) (Fig.2.2A-B). The mite-infested pupae contained significantly higher DWV copy number than the control uninfested ones (*P* value = 0.004534, two-tailed *t-test*) (Fig.2.2C). Therefore, *V. destructor* infestation increases DWV titer in individual honey bee pupae.

When I measured and compared the DWV copy numbers in 23 pairs of honey bee pupa/infesting *V. destructor* isolated from the same colony, a linear correlation between DWV copy number in the pupa and infesting mite was identified (R^2 = 0.7903, *P* value = $1.439e^{-0.08}$). Specifically, the samples were grouped into two clusters, either were low (L) or high (H) DWV copy number (Fig.2.2D). There were more pairs of the pupa/mite in the cluster with low DWV copy number.

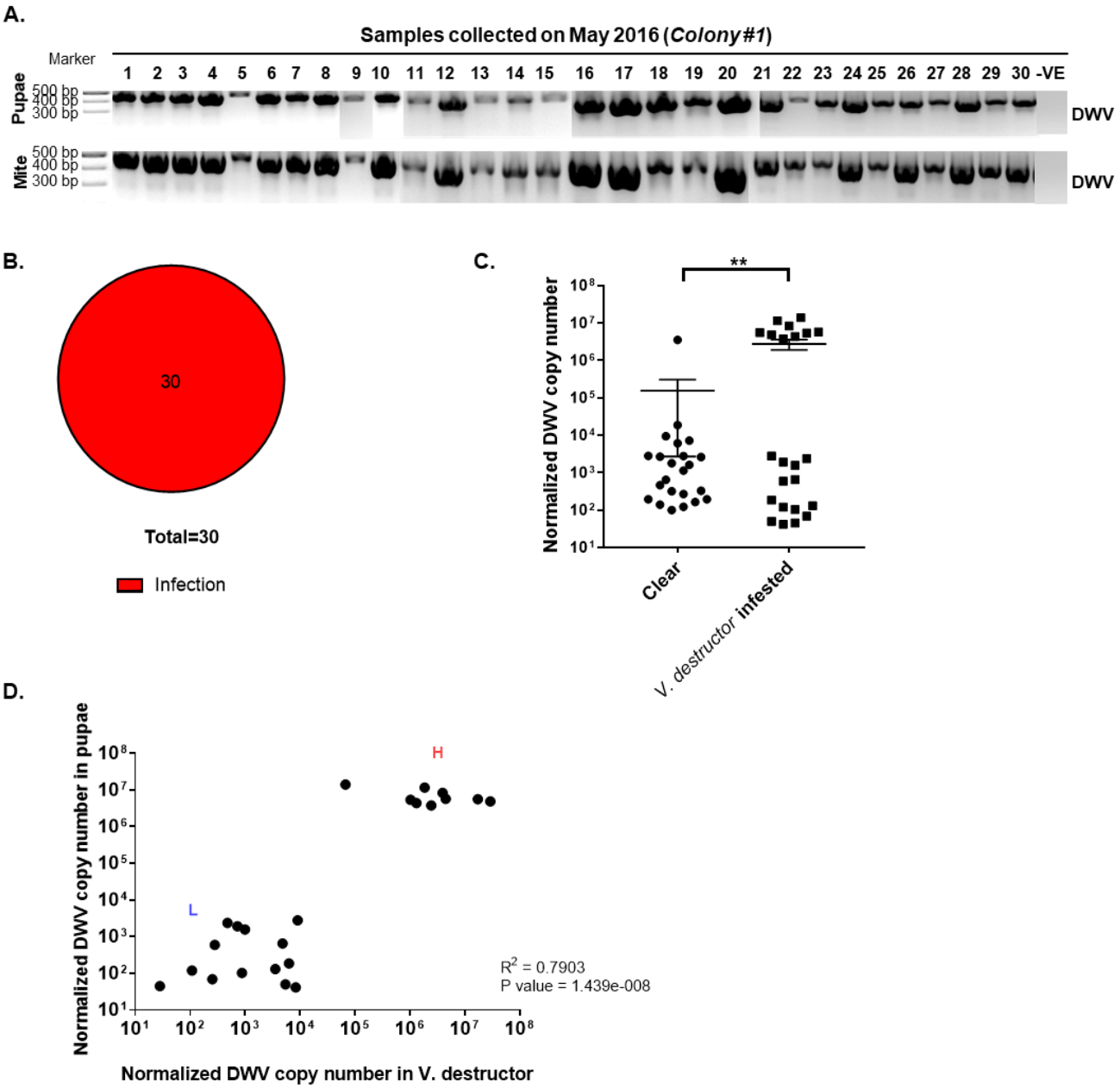

Figure 2.2. Detection and quantification of DWV in *V. destructor*-infested and clear honey bee pupae, and the correlation of DWV copy number in honey bee pupae and their infesting *V. destructor*.

(A) DWV was detected using RT-PCR in 30 purple eyed-pupae with single *V. destructor* in capped brood cells and their infesting mites sampled in *Colony #1* May 2016. Water (-VE) was used as a negative control. The position of a 300-500 bp DWV molecular weight marker is labelled on the left of the agarose gel. (B) For 30 collected purple-eyed pupae from capped brood cells with single *V. destructor* infestation, 100% (30 out of 30) were positive for DWV infection. (C) DWV copy number in purple eyed-pupae from *V. destructor* infested (n = 23) or clear (n = 23) capped cells was measured by qRT-PCR. The mean value with error bar (±SEM) is indicated for each sample. The copy number is higher in the *V. destructor* infested pupae (*P* value = 0.004534, two-tailed *t-test*). (D) DWV copy number

in individual honey bee pupae and infesting *V. destructor* are plotted in the *Y*- and *X*-axis respectively. Samples were grouped into two clusters, either were low (L) or high (H) DWV copy number. The Pearson correlation value and *P* value are shown.

Section 2.3.3 DWV strains and variants identified in the honey bee pupae and *V. destructor*

In order to examine the strain and variant of DWV detected in this experiment, RT-PCR product containing the region of VP2-VP4-VP1 was amplified, from 24 pairs of pupae and the infesting *V. destructor*, and then sequenced. The Sanger sequence electrophoretograms indicated that both pupae and mites could be infected by single or multiple DWV variants. For example, Fig.2.3A represents a single DWV variant infection since there was only single peak detected at all positions in both forward and reverse sequencing reactions. However, there were multiple peaks presented at equivalent positions in both forward and reverse reactions in Fig.2.3B, and all peaks in forward reactions were complementary to the peaks at equivalent positions in reverse reactions. These sequence traces are most parsimoniously explained by the presence of two DWV strains within the individual. Nevertheless, it is still possible that deep transcriptome sequencing may reveal the presence of variant(s) at very low copy number in the infected pupae or mites that appear to be infected by a single variant.

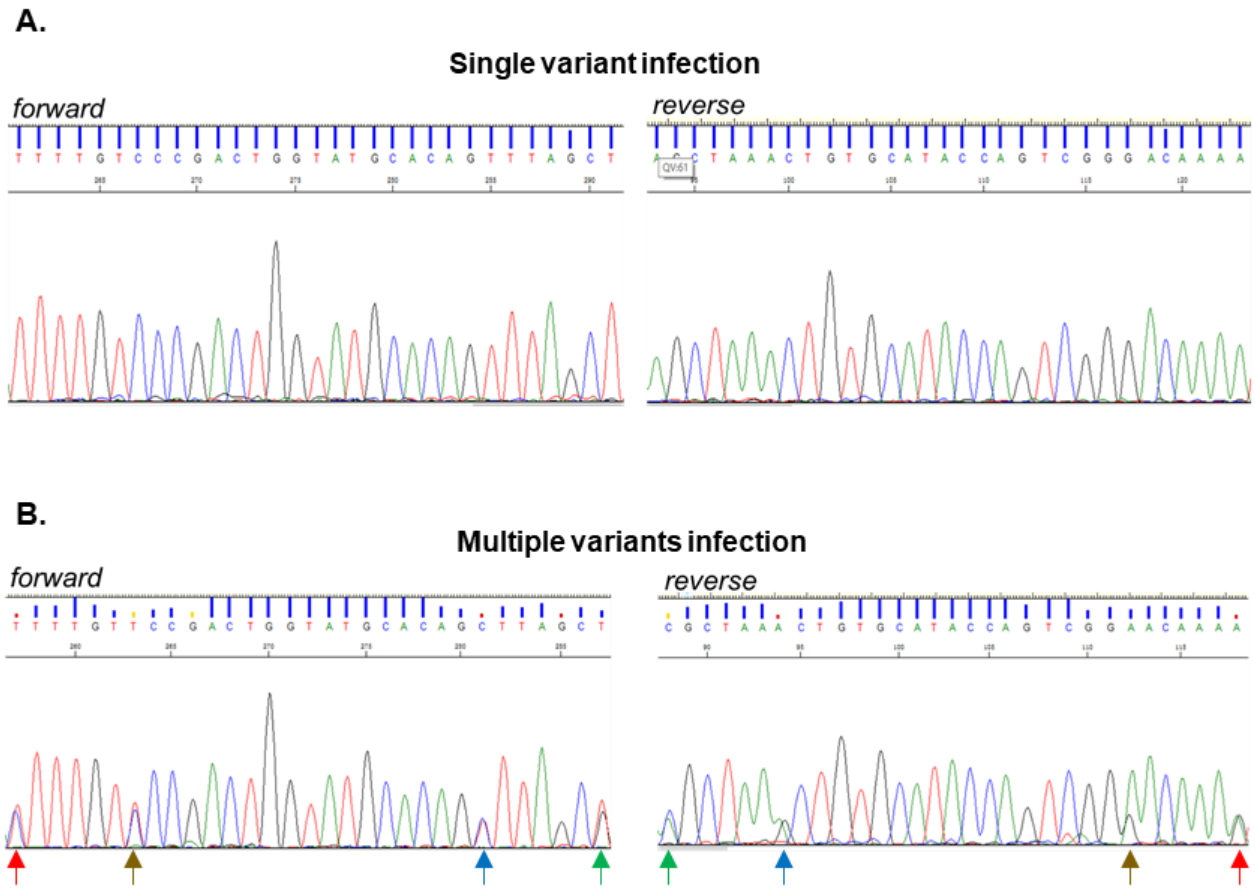

Figure 2.3. Single and multiple DWV variants infections in honey bee pupae and infesting mites.

Representative Sanger sequencing electrograms (both forward and reverse) of RT-PCR products reveal both single variant and multiple DWV variants infections in honey bee pupae and infesting *V. destructor*. (A) Only single peaks

are present at all positions of this sample but (B) two peaks are present at four positions in the second sample (marked by red, brown, blue, and green arrows in both and reverse sequences).

Based on the Sanger sequencing electrograms, 24 pairs of pupa/infesting *V. destructor* were grouped to 4 groups: single DWV variant infection in both pupa and mite (8 pairs); multiple variants infection in pupa and single variant infection in mite (3 pairs); single variant infection in pupa and multiple variants infection in mite (3 pairs); and multiple variants infection in both pupa and mite (10 pairs) (Table.2.1).

Table 2.1. The profile of DWV variants infected in honey bee pupa and the infesting *V. destructor*.

	Single DWV variant infection in honey bee pupa	**Multiple DWV variants infection in honey bee pupa**
Single DWV variant infection in *V. destructor*	7, 10, 12, 17, 20, 24, 28, 30	6, 18, 23
Multiple DWV variants infection in *V. destructor*	14, 27, 29	1, 2, 5, 8, 9, 13, 15, 16, 22, 25

The pupa/*V. destructor* pair which infected by either low or high DWV copy number in Fig.2.2D are indicated by blue and red letters, respectively. The pairs indicated by black letters were not analysed in Fig.2.2D.

These sequences were further processed for constructing Maximum Likelihood (Fig.2.4A) and Bayesian phylogenetic trees (Fig.2.4B) with published DWV type A, B, and C sequences. The Maximum Likelihood phylogenetic tree contains 38 sequences whereas there are 35 sequences for Bayesian phylogenetic tress. Both phylogenetic trees indicate similar pattern and all DWV variants in this study were related to the strain A.

A.


27B
29M
27M
25B
23B
22M
22B
18M
18B
17M
17B
16M
16B
15M
15B
14M
13M
13B
32
9M
9B
8M
8B
5B
5M
2M
2B
1M
1B
85
gi|873407447|emb|CENC01000001.1| Deformed wing virus genome assembly Devon type A scaffold Devon type A assembled genome whole genome shotgun sequence
7B
66
7M
10B
10M
65
14B
25M
23M
30B
85
30M
29B
gi|873406561|emb|CEND01000001.1| Deformed wing virus genome assembly Devon Type C scaffold Type C consensus (final) whole genome shotgun sequence
29
gi|56121875|ref|NC 006494.1| Varroa destructor virus-1 complete genome
gi|9632405|ref|NC 002066.1| Sacbrood virus complete genome
0.10

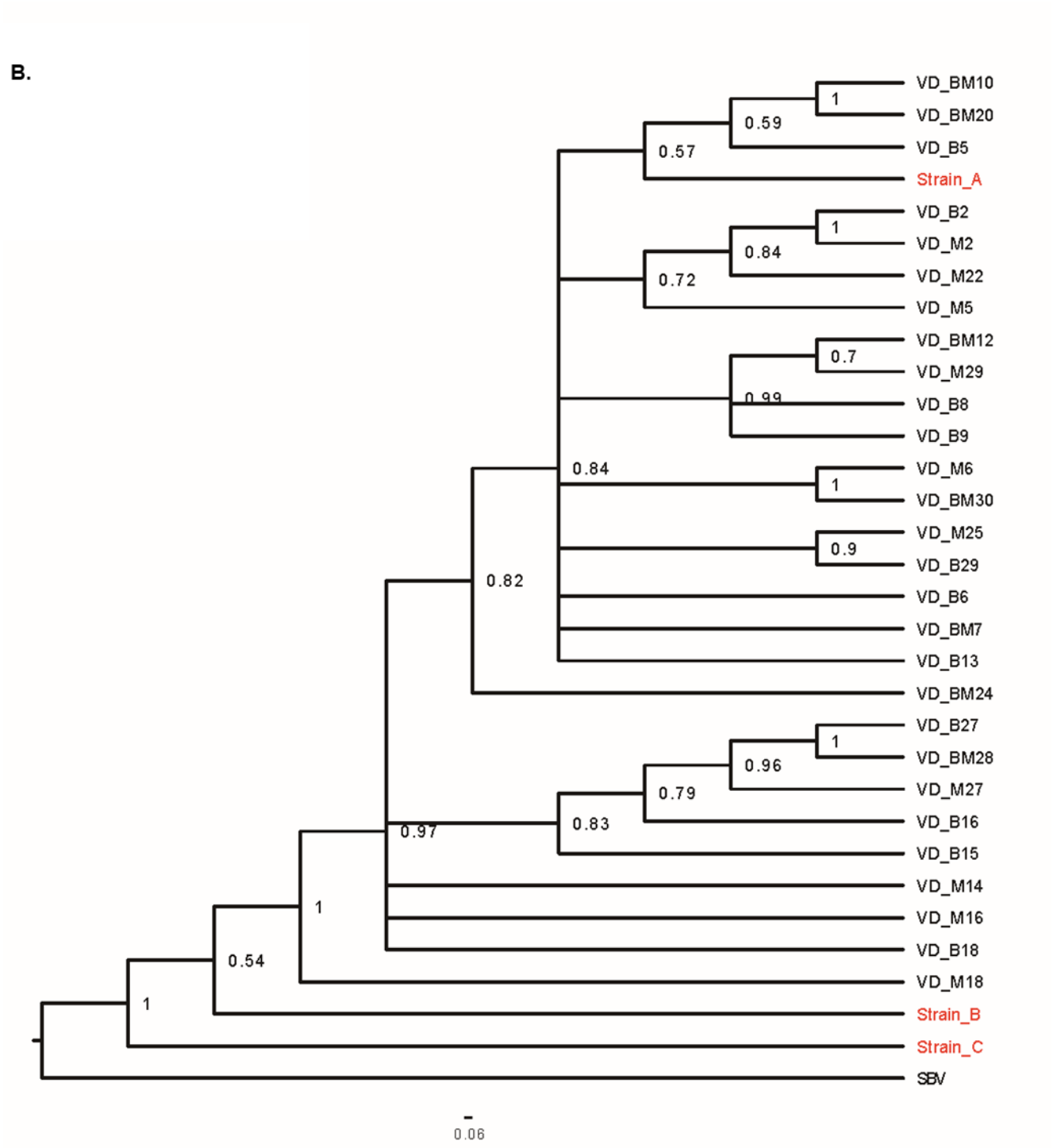

Figure 2.4. Phylogenetic trees of DWV isolates based on a 434 nt region encoding viral structural proteins for *V. destructor* and infested honey bee pupae.

(A) The maximum likelihood phylogenetic tree of DWV isolates from *V. destructor* infested honey bee pupae (indicated as "B") and matched mites (indicated as "M"). The branch lengths were measured in the number of substitutions per site base on the Tamura-3-parameter model and indicated at the corresponding node. (B) Bayesian phylogenetic tree of DWV isolates from *V. destructor* infested honey bee pupae (indicated as "VD_B") and matched mites (indicated as "VD_M"). Cases in which a pupa and infesting mites were infected by an identical single DWV variant are indicated as "VD_BM". Both trees were constructed based on same sequences including partial VP2 and VP1 and full VP4 regions, except 3 sequences were not indicated in Bayesian phylogenetic tress. Posterior probabilities are shown at the corresponding node of each branch. DWV type A, B, and C strains (with red letter) were included for analysis as references and SBV (Sac brood virus) with blue letter was used as an outgroup.

Section 2.3.4 *T. mercedesae*'s infestation increases DWV prevalence and titer within individual honey bee pupae and a linear correlation of DWV copy number between pupae and infesting mites

In November 2016, purple-eyed pupae were collected from the *Colony #2* which was infested by *T. mercedesae*. For this colony, 65% (13 out of 20; positive signals were observed in Lane 1-5, 9, 11-13, 15-17, and 20 of Fig.2.5A) of pupae without *T. mercedesae* infestation were positive for DWV (Fig.2.5A & C). Pupae with single *T. mercedesae* infestation were also collected, and 100% (30 out of 30) were positive for DWV (Fig.2.5B & D). When comparing DWV copy numbers between *T. mercedesae*-infested and uninfested pupae, the infested ones contained significantly higher DWV copy number (*P* value = 0.0001459, two-tailed *t-test*) (Fig.2.5E). *T. mercedesae*'s infestation increases DWV titer in individual honey bee pupae.

All *Tropilaelaps* mites infesting the above 30 pupae were positive for DWV (Fig.2.5B). Based on the comparison of DWV copy numbers between the paired pupa and the infesting mite, there was a linear correlation between them (R^2 = 0.6808, *P* value = $6.603e^{-0.08}$). Specifically, the samples were grouped to two clusters, either were low (L) or high (H) DWV copy number (Fig.2.5F). In contrast to *V. destructor* above, there are more pairs of pupa/mite in the cluster with high DWV copy number (*P* value < 0.0001, two-tailed *t-test*) (Fig.2.6), suggesting a greater threat for honey bee with *T. mercedesae* infestation.

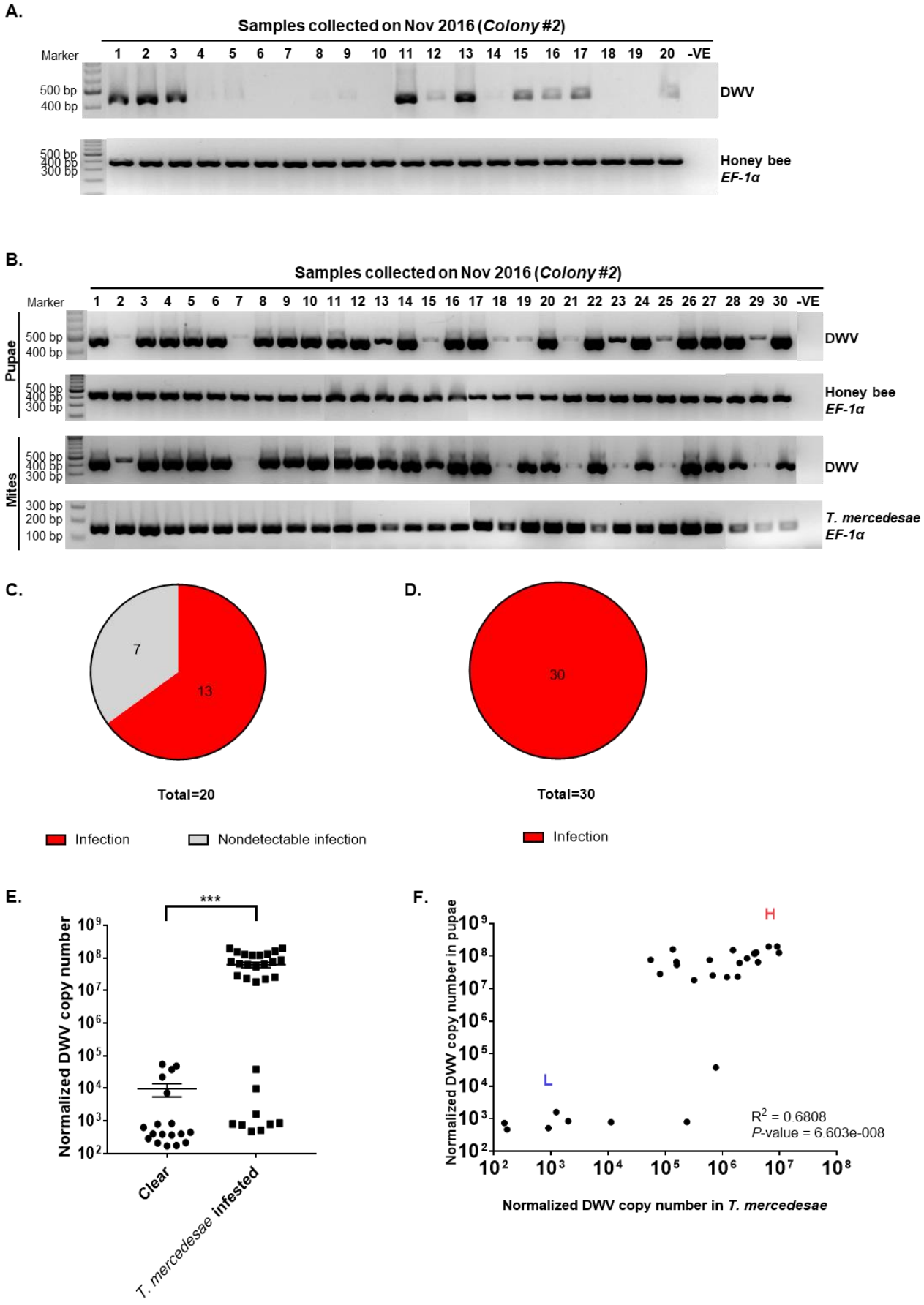

Figure 2.5. Detection and quantification of DWV in *T. mercedesae*-infested and clear honey bee pupae, and the correlation of DWV copy number in honey bee pupae and their infesting *T. mercedesae*.

DWV was detected using RT-PCR in (A) 20 purple eyed-pupae without direct mite infestation, (B) 30 purple eyed-pupae with single *T. mercedesae* in capped brood cells and their infesting mites in capped brood cells sampled in

Colony #2 on November 2016. Honey bee *EF-1α* and *T. mercedesae EF-1α* mRNAs were used as an endogenous positive control for pupae and mite samples, respectively. Water (-VE) was used as a negative control. The position of a 100-300 bp and 300-500 bp DWV molecular weight marker is labelled on the left of agarose gel. Through RT-PCR analysis, for pupae without direct mite infestation and with single *T. mercedesae* infestation, there were approximately (C) 65% (13 out of 20; positive signals were observed in Lane 1-5, 9, 11-13, 15-17, and 20) and (D) 100% (30 out of 30) positive for DWV infection respectively. The infesting mite were 100% (30 out of 30) infected by DWV. (E) DWV copy number in purple eyed-pupae from *T.* mercedesae infested (n = 29) or clear (n = 18) capped cells was measured by qRT-PCR. The mean value with error bar (±SEM) is indicated for each sample. The copy number is higher in the *T. mercedesae* infested pupae (*P* value = 0.0001459, two-tailed *t-test*). (F) DWV copy number in individual honey bee pupae and infesting *T. mercedesae* (n = 28) are plotted in the *Y*- and *X*-axis respectively. Samples were grouped into two clusters, either were low (L) or high (H) DWV copy number. The Pearson correlation value and *P* value are shown.

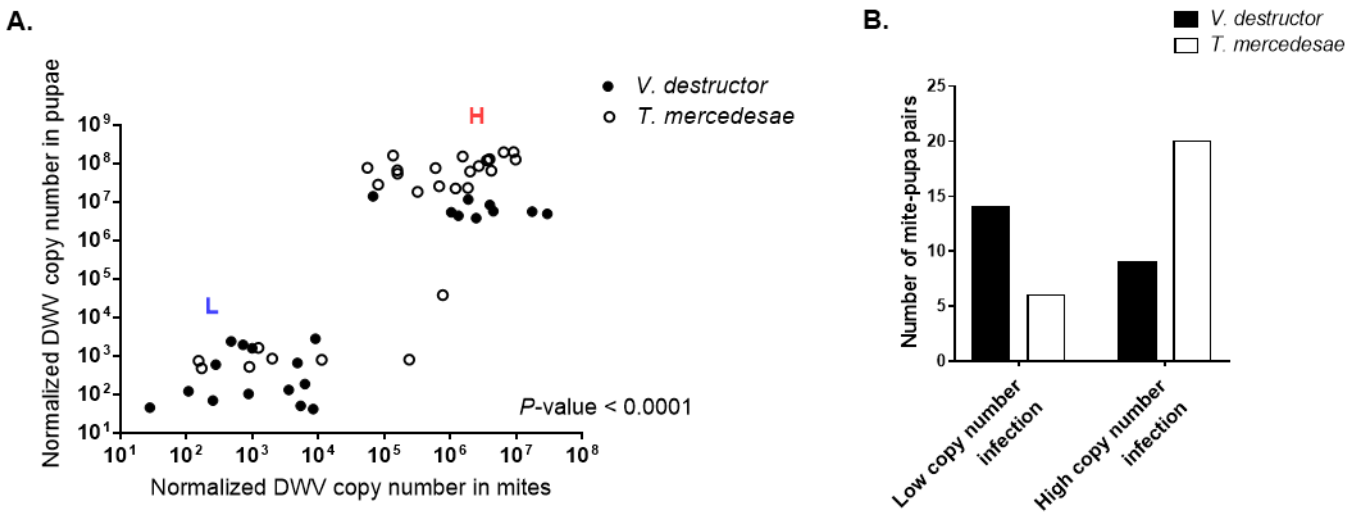

Figure 2.6 Comparison of the number of mite-pupa pairs infected by low or high DWV copy number.
(A) DWV copy number in individual honey bee pupae and infesting *V. destructor* (n = 23) or *T. mercedesae* (n = 28) were plotted in the *Y*- and *X*-axis respectively. Samples were grouped into two clusters, either were low (L) or high (H) DWV copy number. There were more mite-pupa pairs infected by high DWV copy number in *T. mercedesae*-infestation (*P* value < 0.0001, two-tailed *t-test*). (B) The amount of mite-pupa pairs infected by low or high DWV copy number indicated as bar chart.

Section 2.3.5 DWV strains and variants identified in the honey bee pupae and *T. mercedesae*

In order to determine the DWV variants in the honey bee pupae and infesting *T. mercedesae*, the same RT-PCR products were sequenced as analyzed for *V. destructor*. As shown in Table.2.2, 18 pairs of pupa/infesting *T. mercedesae* were partitioned into 4 groups: single DWV variant infection in both pupa and mite (2 pairs); multiple variants infection in pupa and single variant infection in mite (1 pairs); single variant infection in pupa and multiple variants infection in mite (1 pairs); and multiple variants infection in both pupa and mite (14 pairs). Based on the phylogenetic analysis, all DWV variants in this colony were also related to the master strain A (Fig.2.7).

Table 2.2. The profile of DWV variants infection in honey bee pupa and *T. mercedesae.*

	Single DWV variant infection in honey bee pupa	Multiple DWV variants infection in honey bee pupa
Single DWV variant infection in *T. mercedesae*	10, 13	28
Multiple DWV variants infection in *T. mercedesae*	29	1, 4, 5, 7, 14, 15, 16, 17, 18, 19, 23, 26, 27, 30

The pupa/*T. mercedesae* pair which infected by either low or high DWV copy number in Fig.2.5F are indicated by blue and red letters, respectively. The pairs indicated by black letters were not analysed in Fig.2.2F.

Since most of the posterior probabilities were less than 1 in the two phylogenetic trees for *V. destructor* and *T. mercedesae* (Fig.2.4B & Fig.2.7), I additionally sequenced an approximately 4 kb region of the viral genome encoding partial Lp protein, all of structural proteins, and partial RNA helicase from 14 representative samples including *V. destructor*, *T. mercedesae*, *V. destructor* infested pupae, *T. mercedesae* infested pupae, and pupae without the mite infestation. This phylogenetic tree further confirmed that all samples were infected by DWV type A since all isolates are distinct from DWV type B and type C and cluster together with type A (Fig.2.8). Although the isolate 2C1 branches before other isolates, including the type A (Fig.2.8), the viral genome sequence encoding the entire polyprotein, as well as the parts of 5' and 3' UTRs shows higher similarity to DWV type A (96%), rather than type B (84%) and type C (80%).

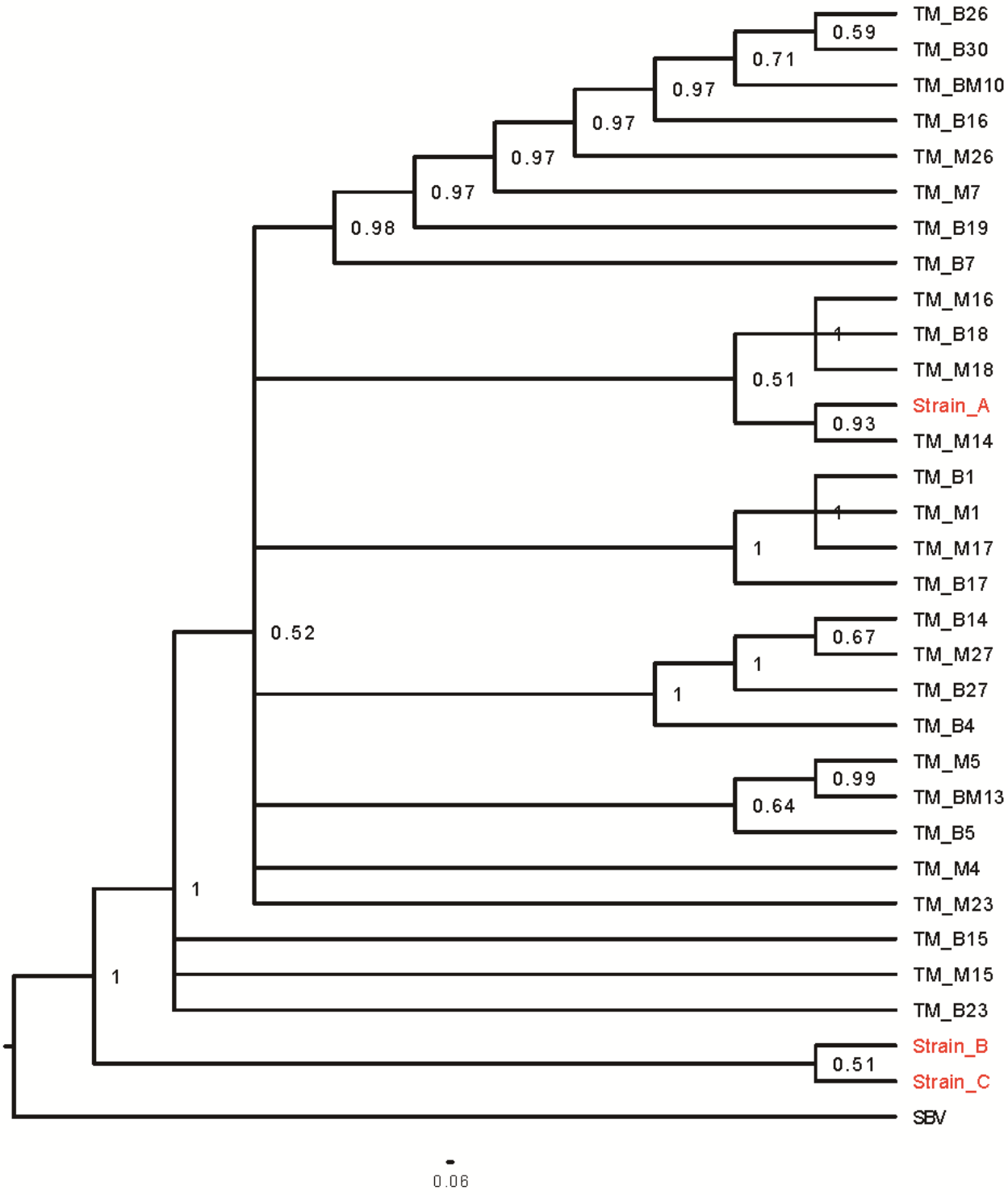

Figure 2.7 Bayesian phylogenetic trees of DWV isolates based on a 434 nt region encoding viral structural proteins for *T. mercedesae* and infested honey bee pupae.

Bayesian phylogenetic trees of DWV isolates from *T. mercedesae* infested honey bee pupae (indicated as "TM_B") and matched mites (indicated as "TM_M"), were constructed based on partial VP2 and VP1, and full VP4 sequences. Cases in which a pupa and infesting mites were infected by an identical single DWV variant are indicated as "TM_BM". Posterior probabilities are shown at the corresponding node of each branch. DWV type A, B, and C strains (with red letter) were included for analysis as references and SBV (Sac brood virus) with blue letter was used as an outgroup.

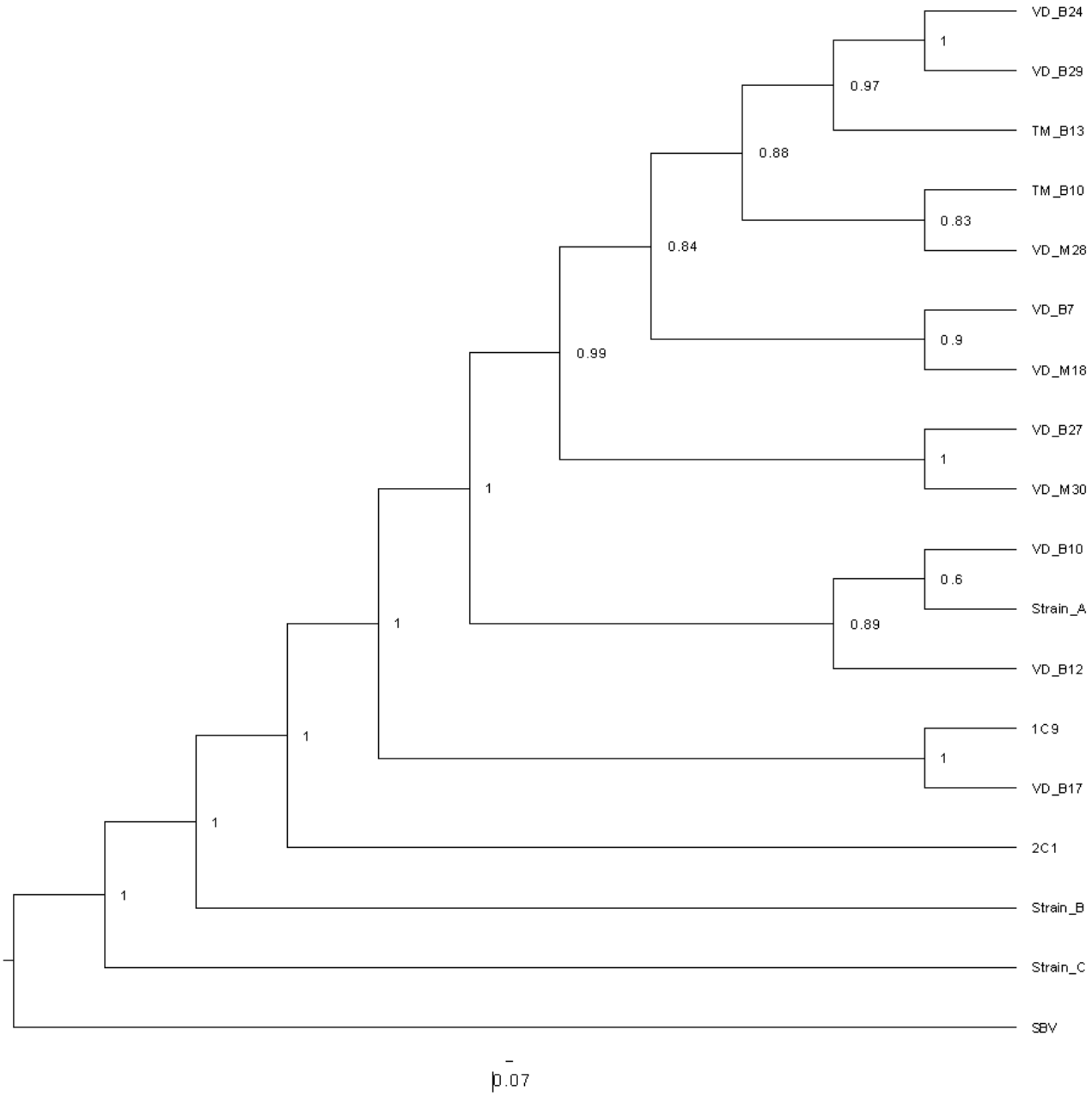

Figure 2.8 Bayesian phylogenetic tree of representative DWV isolates based on a 3633 nt region encoding partial viral structural proteins and parts of the Lp and helicase proteins.

A Bayesian phylogenetic tree of representative DWV isolates was constructed based on partial LP and helicase sequences, and full VP sequences. These 14 DWV isolates from *V. destructor* (indicated as "VD_M"), *T. mercedesae* (indicated as "TM_M"), *V. destructor* infesting pupa (indicated as "VD_B"), *T. mercedesae* infesting pupa (indicated as "TM_B"), and without infestation pupa (indicated as "C"). Posterior probabilities are shown at the corresponding node of each branch. DWV type A, B, and C strains were included for analysis as references and SBV with blue letter was used as an outgroup.

Section 2.3.6 Artificial infestation of *T. mercedesae* increases DWV copy number in honey bee pupae

In order to prove *T. mercedesae* acts as a biological vector to transmit DWV to honey bee, the pale white-eyed pupa was artificially infested by single *T. mercedesae* under laboratory condition, followed by

comparing DWV copy numbers and variants in the mite-infested and -uninfested (control) pupae as well as the infesting mites. After 7 days incubation, DWV copy numbers in the mite-infested pupae were significantly higher than those in the control pupae (*P* value= 0.0024, two-tailed *t-test*) (Fig.2.9A), indicating that artificial mite infestation increased DWV titer in honey bee pupae. When comparing DWV copy numbers between the pairs of pupa and infesting *T. mercedesae*, there was a linear correlation between them (R^2 = 0.5077, *P* value < 0.0267) and two clusters with either low (L) or high (H) DWV copy number were identified (Fig.2.9B). This is similar to the results obtained above for the honey bee pupae and the infesting *V. destructor* (Fig.2.2D) or *T. mercedesae* (Fig.2.5F) under natural condition. For this artificial infestation, the number of pairs of pupa/mite in the cluster with low copy number is slightly more than that in the cluster with high copy number.

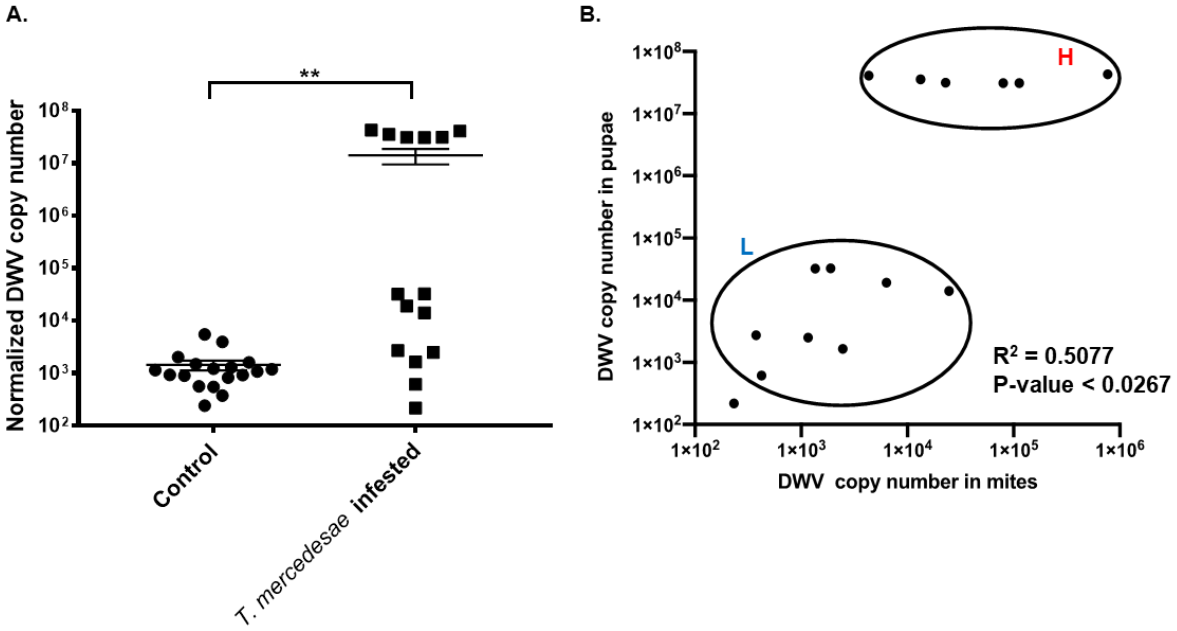

Figure 2.9 Comparison of DWV in artificially *T. mercedesae*-infested and without infestation honey bee pupae, and the correlation of DWV copy number in infested pupae and their infesting mites.

A single *T. mercedesae* was artificially infested with individual pale white-eyed pupa under laboratory condition. The pale white-eyed pupae without artificial infestation were incubated as a negative control group. (A) DWV copy number in *T. mercedesae* infested pupae (n = 15) and non-infested pupae (n = 18) were measured by qRT-PCR (*P* value = 0.0024, two-tailed *t test*). The mean value with error bar (±SEM) is indicated for each sample. (B) DWV copy number in individual artificially *T. mercedesae* infested honey bee pupa and infesting *T. mercedesae* are plotted in the *Y*- and *X*-axis respectively. Samples were grouped into two clusters, either were low (L) or high (H) DWV copy number. The Pearson correlation value and *P* value are shown.

Section 2.3.7 DWV variants identified in artificially infested-honey bee pupae and the infesting *T. mercedesae*, suggesting the vectorial role of *T. mercedesae* for DWV transmission

The same RT-PCR products derived from artificially infested-honey bee pupae and infesting *T. mercedesae* were sequenced as mentioned above to determine the DWV variants. As shown in Table.2.3, 15 pairs of pupa/infesting *T. mercedesae* are grouped to 4 categories: single DWV variant infection in both

pupa and mite (9 pairs); multiple variants infection in pupa and single variant infection in mite (2 pairs); single variant infection in pupa and multiple variants infection in mite (1 pairs); and multiple variants infection in both pupa and mite (3 pairs).

Table 2.3. The profile of DWV variants infection in artificially infested-honey bee pupa and infesting *T. mercedesae*.

	Single DWV variant infection in honey bee pupa	**Multiple DWV variants infection in honey bee pupa**
Single DWV variant infection in *T. mercedesae*	1, 3, 7, 8, 9, 10, 11, 14, 15	4, 12
Multiple DWV variants infection in *T. mercedesae*	13	2, 5, 6

The pupa/*T. mercedesae* pair which infected by either low or high DWV copy number in Fig.2.9B are highlighted by blue and red, respectively.

In order to compare DWV variants present in the artificially infested-pupae, the infesting *T. mercedesae*, and the control pupae, their RT-PCR products' sequences were further analysed for the phylogenetic relationship. In case pupae and mites were infected by multiple DWV variants, only samples in which I could identify the dominant variants were analyzed. All of 18 control pupae were infected by multiple variants and the eight samples (Bee-C #2, #6, #9, #10, #11, #14, #15, and #16) contained dominant DWV variant which is identical to the one present in seven test pupae (Bee #1, #4, #7, #8, #9, #12, and #14) and five infesting mites (Mite #1, #7, #8, #9, and #12). Three pupa-mite pairs (Bee/Mite #3, #13, and #15) contained the same variant. Mite #4 and Mite #14 shared the same variant which is different from the one present in the infested pupae (Bee #4 and Bee #14 above). Thus, these pairs represent cases where pupa and infesting mite do not share the same DWV variant. As shown in Fig.2.10, six pupa-mite pairs (Bee/Mite #3, #5, #10, #11, #13, and #15) were infected by four variants which are different from the ones present in the control pupae. These results demonstrate that these variants were transferred from the infesting mites derived from a colony different from the one all pupae were sampled.

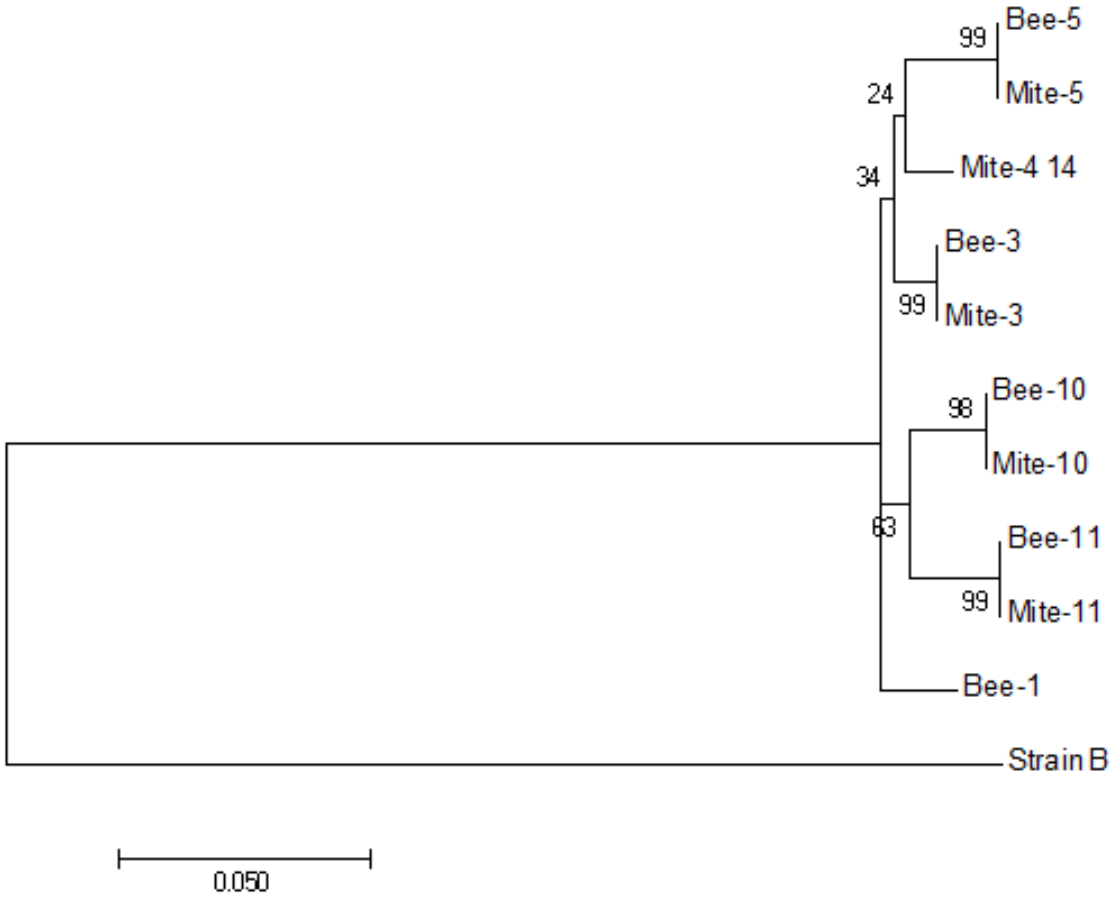

Figure 2.10. The maximum likelihood phylogenetic tree of DWV isolates from representative honey bee pupae and infesting *T. mercedesae* of artificial infestation experiment, based on a 434 nt region encoding viral structural proteins.

The maximum likelihood phylogenetic tree of DWV isolates from *T. mercedesae* artificially infested honey bee pupae (indicated as "Bee") and *T. mercedesae* (indicated as "Mite"), was constructed based on partial VP2 and VP1, and full VP4 sequences. Since the same variant is shared by three pupa/mite pairs #3, #13 and #15, only one representative is indicated. Bootstrap test was evaluated based on 1,000 repetitions and the bootstrap values are shown at the corresponding node of each branch. DWV B strain (Strain B) was included for analysis as an outgroup.

Section 2.3.8 Association between DWV variant and copy number in honey bee pupae and the infesting mites

As shown in Table 2.1, 19 pairs of honey bee pupa and the infesting *V. destructor* were previously classified to high and low DWV copy number clusters (Fig.2.2D). Among these, the same DWV variant was present in both #10 pupa/mite pair and #14 pupa (Fig.2.4A). However, #10 and #14 pairs were classified to high and low copy number clusters, respectively (Table.2.1). A similar pattern was also shown with #6 mite sample (high copy number) and #23 mite sample (low copy number) (Fig.2.4B). These results demonstrate that the same DWV type A variant can be present with either low or high copy number in both honey bee pupae and infesting *V. destructor*. Since all pairs of pupae and the infesting *T. mercedesae* with low copy number were infected by multiple DWV variants (Table.2.2), similar characterization was not possible for this mite. However, multiple DWV variants were identified in pupae and infesting *T.*

mercedesae with either low or high copy number (Table.2.2), and the single DWV variants in both #10 and #13 pupa/mite pairs with high DWV copy number were different (Fig.2.7). These results at least suggest no single DWV variant was selected for replication in honey bee pupae and infesting *T. mercedesae*.

As shown in Table 2.3 with the experiment of artificial *T. mercedesae* infestation, nine pairs were infected by single DWV variant in both honey bee pupa and the infesting *T. mercedesae* and four of them (#1, #7, #8, #9) were classified to the cluster with high DWV copy number (Fig.2.9B). These four pairs share the same DWV variant which was present in the control pupae, the mite-infested pupa #14, and *T. mercedesae* #12. All of them were classified to the cluster with low copy number (Fig.2.9B). Therefore, these results also demonstrate that the same DWV variant can be present with either low or high copy number in both honey bee pupae and infesting *T. mercedesae*.

Section 2.3.9 *T. mercedesae* acts as a mechanical vector for DWV

DWV was isolated from honey bee pupae infested by either *V. destructor* or *T. mercedesae*, and the successful isolation was further proved by RT-PCR to detect DWV and other honey bee viruses (Fig.2.11A). In order to characterize the mechanisms of DWV replication in honey bee pupae, the pupae were treated with needle-injection as a wound induction (n = 7), PBS-injection (n = 7), and isolated DWV virus-injection (n = 6), meanwhile the pupae without treatment were regarded as the negative control (n = 6). To compare the copy numbers of DWV in above honey bee pupae, the heads were individually processed for qRT-PCR to analyse DWV copy number, while the abdomens were subjected to western blot to quantify VP1 protein.

DWV copy numbers in the pupae with wound induction (P = 0.0495, two-tailed *t-test*), PBS-injection and DWV-injection (P = 0.0343, two-tailed *t-test*) are higher than those in the control pupae (Fig.2.11B); however, the difference between the control and PBS-injection is not statistically significant. VP1 protein of DWV was observed with 71% of the pupae (5 out of 7) with wound induction, 43% of the pupae (3 out of 7) with PBS-injection, and 67% of the pupae (4 out of 6) with DWV-injection. These results are consistent with the results of qRT-PCR (Fig.2.11C). By quantifying the results of western blot, VP1 expression in the pupae with wound induction was significantly higher than the control pupae (P = 0.0040, two-tailed *t-test*), and higher expression was also detected in the pupae with DWV injection (P = 0.0152, two-tailed *t-test*). Therefore, the wound to the honey bee pupae alone is sufficient to cause replication of the endogenous DWV in pupae, suggesting a mechanical vector role of *T. mercedesae* for DWV as it causes multiple wounds on the infesting honey bee pupae or larva during feeding activity.

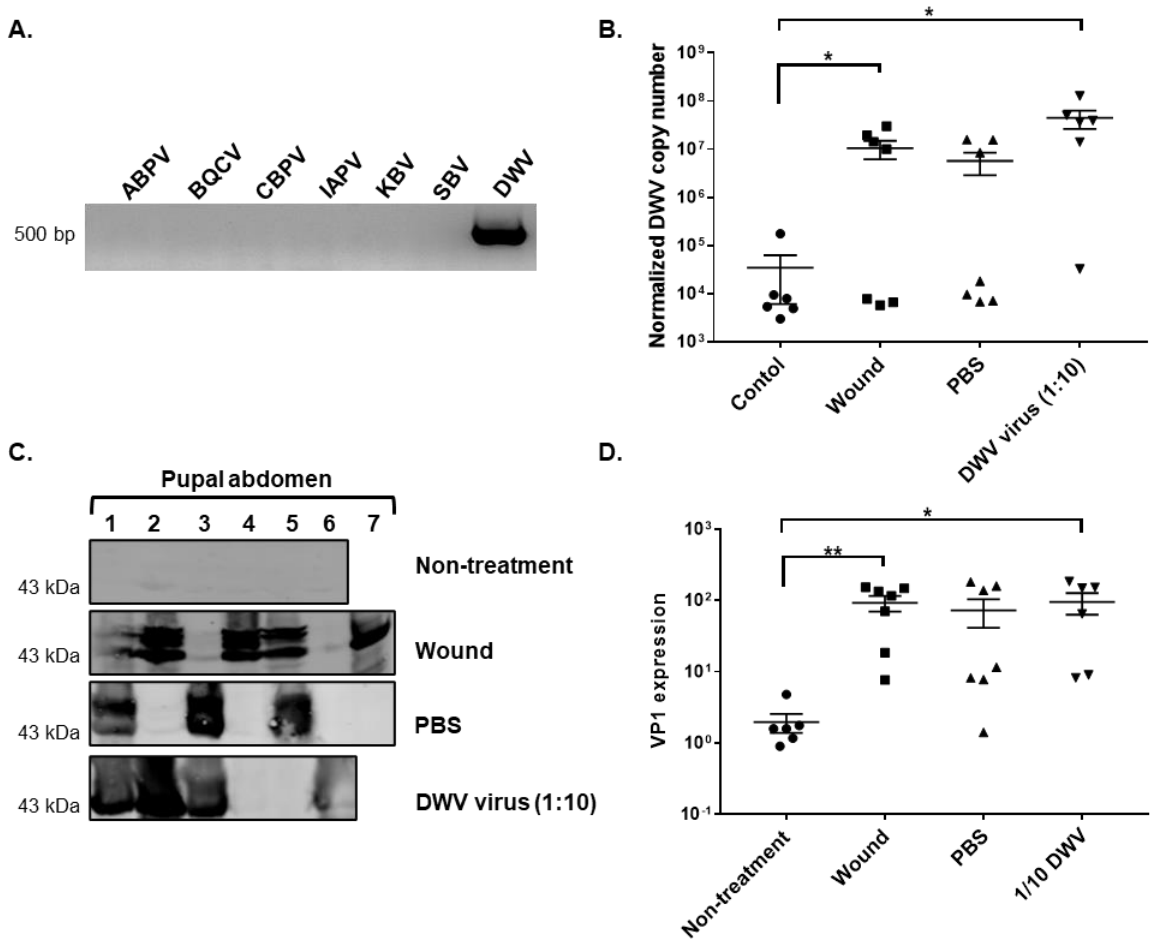

Figure 2.11 Comparison of DWV levels in honey bee pupae with different treatments.

(A) The isolated DWV virus from honey bee pupae with ectoparasitic mite infestation was examined by RT-PCR with several primer sets including DWV, ABPV, CBPV, IAPV, KBV, and SBV. (B) DWV copy numbers of individual pupae, which were treated by needle-injection as a wound induction (n = 7), PBS-injection (n = 7), and isolated DWV virus-injection at 1:10 dilution (n = 6) were analysed by qRT-PCR. Pupae without treatment (n = 6) were used as a negative control. Compare to pupae without treatment, DWV copy number in pupae with wound (*P* value = 0.0495, two tailed *t-test*) or DWV-injection (*P* value = 0.0343, two tailed *t-test*) is significantly higher. (C) Western blotting of individual pupal abdomens against anti-VP1 antibody and (D) the quantitative analysis of it. DWV VP1 expression was significantly higher in pupae with wound (*P* value = 0.0040, two tailed *t-test*) or DWV-injection (*P* value = 0.0152, two tailed *t-test*) rather than non-treatment pupae. The mean value with error bar (±SEM) is indicated for each sample (**P* value ≤ 0.05; ***P* value ≤ 0.01).

Section 2.3.10 *Hymenoptaecin* and *Defensin-1 mRNAs* were induced in honey bee pupae by *T. mercedesae* infestation

In order to assess whether *T. mercedesae* infestation induces AMPs expression in honey bee, I quantified *Hymenoptaecin* and *Defensin-1* mRNAs in pupae with and without artificially *T. mercedesae* infestation (same pupae as in Section 2.3.6-7). Both *Hymenoptaecin* (*P* value = 0.0023, two tailed *t-test*) and *Defensin-1* transcripts (*P* value = 0.0158, two tailed *t-test*) increased by the mite infestation (Fig.2.12A-B). However, there was no significant correlation between the amounts of *Hymenoptaecin* and *Defensin-1* transcripts in the individual mite-infested pupae (r = -0.08186, *P* value = 0.7718) (Fig.2.12C), suggesting

Hymenoptaecin and Defensin-1 were induced by different mechanisms through *T. mercedesae* infestation. I further compared DWV copy numbers with the amounts of either *Hymenoptaecin* or *Defensin-1* transcripts in individual infested-pupae. There is a positive correlation between DWV copy number and the amount of *Defensin-1* transcript (r = 0.2342, *P* value = 0.4009) (Fig.2.12E), but not identified for *Hymenoptaecin* (r = -0.1659, *P* value = 0.5545) (Fig.2.12D). Therefore, Defensin-1 is possibly induced by DWV infection and replication. Since *V. destructor* was reported to ingest the fat body cells of honey bee (Ramsey et al., 2019), I measured the relative amounts of honey bee 18S rRNA in the individual *T. mercedesae* to determine the degree of feeding upon the honey bee cells. There is a positive correlation between the ingestion of honey bee cells by the mite and the amount of *Hymenoptaecin* transcript (r = 0.7926, *P* value = 0.0004) (Fig.2.12F), but no association found with *Defensin-1* transcript (r = -0.06225, *P* value = 0.8256) (Fig.2.12G), suggesting that Hymenoptaecin is induced in infested honey bee probably by wound induction via mite feeding activity.

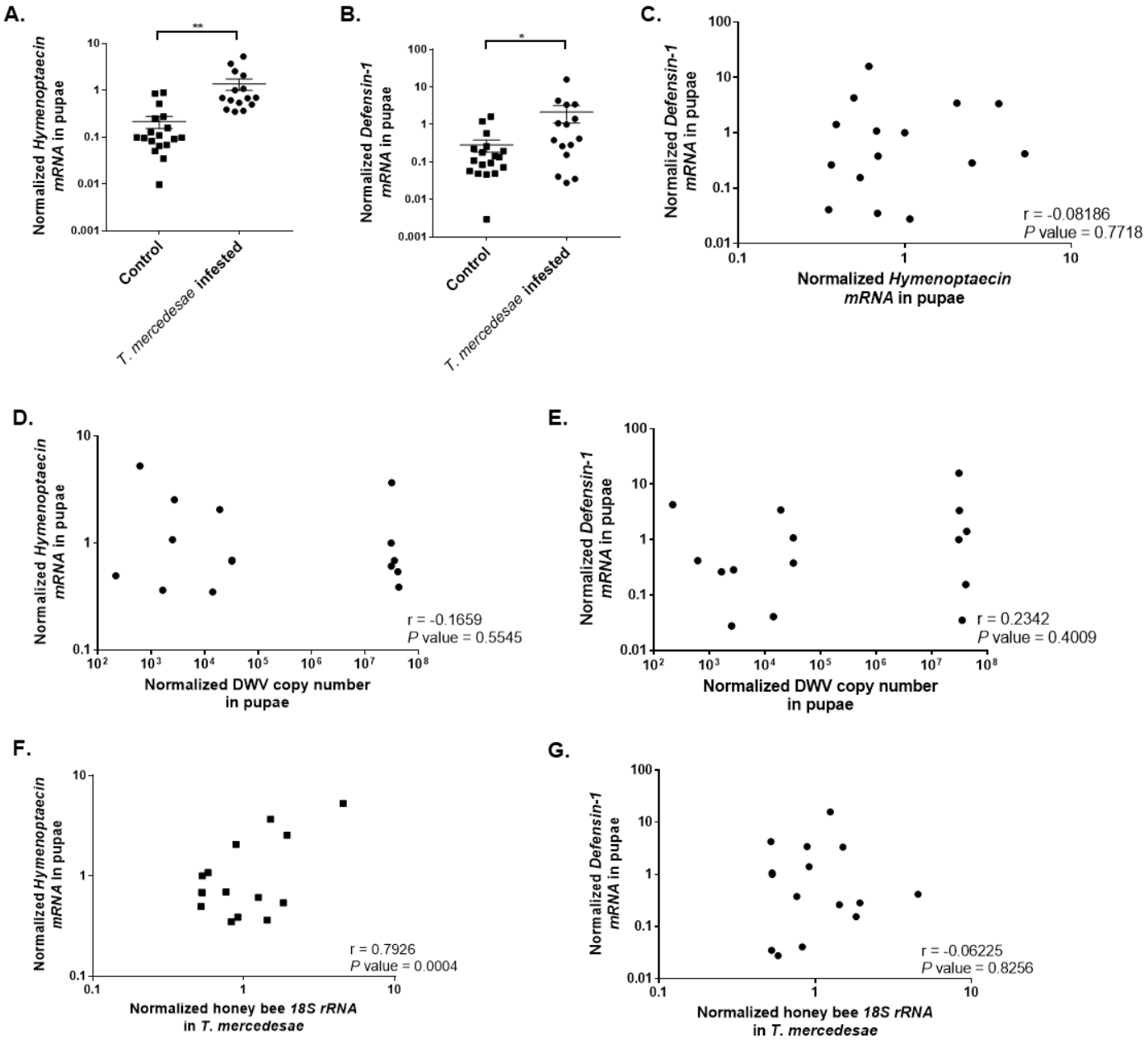

Figure 2.12 *T. mercedesae* infestation induced Hymenoptaecin and Defensin-1 mRNAs in honey bee pupae.

Relatively amounts of (A) *Hymenoptaecin* and (B) *Defensin-1* mRNAs in honey bee pupae artificially infested by *T. mercedesae* (n = 15) and the ones without mites (Control, n = 18). Both amounts of *Hymenoptaecin* (*P* value = 0.0023, two tailed *t-test*) and *Defensin-1* mRNAs (*P* value = 0.0158, two tailed *t-test*) increased in pupae with mite infestation. The mean value with error bar (±SEM) is indicated for each sample (**P* value ≤ 0.05; ***P* value ≤ 0.01). (C) Relatively amounts of *Defensin-1* and *Hymenoptaecin* mRNAs in individual infested pupae are plotted in *Y*- and *X*-axis respectively. Relatively amounts of (D) *Hymenoptaecin* and (E) *Defensin-1* mRNAs in individually infested pupae and DWV copy number in same pupae are plotted in the *Y*- and *X*-axis respectively. Relatively amounts of (F) *Hymenoptaecin* and (G) *Defensin-1* mRNAs in individually infested pupae and the amount of honey bee 18S rRNAs in the infesting *T. mercedesae* are plotted in the *Y*- and *X*-axis respectively. The Pearson correlation values and *P* values are shown.

Section 2.4 Discussion

Section 2.4.1 *V. destructor* and *T. mercedesae* infestation increase DWV copy number in honey bee pupae

Based on the results, they demonstrate increases of the *V. destructor* population in the honey bee colony enhances the prevalence of DWV infection in honey bee pupae, even without direct mite infestation. Furthermore, direct infestation of pupae with *V. destructor* or *T. mercedesae* (both naturally and artificially) dramatically increased the DWV copy number. These results demonstrate that *V. destructor* and *T. mercedesae* function as vectors for DWV and promote transmission in honey bees, similar to previous studies (Shen et al., 2005, Yue and Genersch, 2005, Forsgren et al., 2009). My study indicates that both mite species are equally effective at increasing DWV copy number in the infested honey bee pupae.

These data raise the question about the source of DWV present in honey bee pupae without direct mite infestation. DWV could be present in larval food (Yue and Genersch, 2005, Singh et al., 2010) and it may increase if honey bee workers have high DWV copy number due to the mite infestation. Furthermore, it is also possible that *V. destructor* and *T. mercedesae* carrying DWV may enter brood cells, feed on haemolymph or fat body then leave before the cell is capped. Vertical transmission of DWV from queen may also occur and the mite infestation of drone would enhance this process by producing the semen containing high titer of DWV (Chen et al., 2006a, Yue et al., 2007, De Miranda and Fries, 2008).

What is the source of DWV present in *V. destructor* and *T. mercedesae*? DWV may be vertically transmitted from the mother mites and this hypothesis is supported by a recent study demonstrating that *T. mercedesae* males and nymphs also have high copy number of DWV as females (Dong et al., 2017). In addition, the high abundance of structural DWV proteins and absence/scarce of non-structural proteins were detected in *V. destructor* (Erban et al., 2015) and *T. mercedesae* (Dong et al., 2017), and various honey bee proteins were identified in *V. destructor*, including larval and pupal haemolymph proteins (primarily hexamerins), adult honey bee proteins Vitellogenin, and Major Jelly Royal Proteins (MJRPs) (Erban et al., 2015). These results indicate that mature DWV virions are accumulated in mites via feeding activity, suggesting a horizontally viral transmission from infested pupae to *V. destructor* and *T. mercedesae*. Since the mouthparts and body shape of *T. mercedesae* do not allow to feed on adult honey bee (Anderson and Roberts, 2013), as do *V. destructor,* therefore the horizontal transmission route occurred in adult workers is only for *V. destructor*.

I have confirmed that there is a linear correlation between DWV copy number in the mite and the infested honey bee pupa, similar to previous studies (Forsgren et al., 2009, Kielmanowicz et al., 2015). For both *V. destructor* and *T. mercedesae*, the pupa/mite pairs were clustered to two groups containing either low or high DWV copy number. These results indicate that the DWV titer in infesting mite is proportional to the relative DWV titer in the honey bee pupa, which may be caused by simple viral horizontal transmission via the mite's feeding activity. If this hypothesis is correct, the dominant DWV variant present in the mite should also be the dominate variant in the pupa of pair with high DWV copy number. My study suggests that this

is the case for both *V. destructor* and *T. mercedesae*. For example, the same DWV variant was present in all pupa/*V. destructor* pairs if they were singly infected irrespective of copy number. In the pair #6, the dominated variant in the honeybee pupa was the same as the single variant present in the mite. Both pupae and *V. destructor* in the pairs of #8 and #16 were infected by multiple DWV variants, although the dominant variant was shared between them. The same pattern also occurs with pairs of pupa/*T. mercedesae* under both native and laboratory conditions. As different DWV variants were found in the honey bee pupa/mite pairs, it could be explained by the vertical transmission from the mother mite to offspring, which is supported by the observation that both mites can be infected by either a single variant or multiple DWV variants before entering the brood cell containing the 5th instar larva.

Section 2.4.2 *T. mercedesae* acts as a biological and mechanical vector for DWV transmission

Through artificial infestation of *T. mercedesae*, I found that DWV copy number was significantly increased in the mite-infested honey bee pupae and the copy number in the individual pupa was correlated to that of the infesting mite (Fig.2.9B). Based on the phylogenetic analysis, there were six mite-infested pupae with DWV variants that were distinct from ones in the control pupae. Among them, pupae #3, #10, #11, #13 and #15 were infected by single variant which is the same as variant or major variant identified in the infesting mites, even though the mite #13 was infected by multiple variants. Both pupa and mite in pair #15 were infected by the multiple variants but share the same major variant (Fig.2.10 & Table.2.3). These observations demonstrate that *T. mercedesae* transmits DWV to honey bee and increases DWV titer in the honey bee, functioning like a biological vector.

Unlike *V. destructor*, which starts feeding on larva/pupa after consuming the brood's food inside capped brood cell (Ifantidis et al., 1988), *T. mercedesae* feeds on honey bee larva and pupa in pre- and post-capped brood cells (Phokasem et al., 2019). During feeding activity, the saw-like blade chelicerae of *V. destructor* (Needham et al., 1988) usually causes 1-3 incisions into the integument of prepupae and one wound on the abdomen of pupae (Kanbar and Engels, 2004), while *T. mercedesae* inflicts multiple wounds on honey bees at the pre- and post-capped stages since its chelicerae contains a bidentate fixed digit and a spine-like terminal hook (Needham et al., 1988). Phkkasem *et al.* observed that *T. mercedesae* caused around 5 wounds on 4th instar larva, and there are approximately 32 and 5 wounds on the mite-infested and mite-free prepupae (Phokasem et al., 2019). My results indicate that wounding stimulates endogenous DWV replication in honey bee, although correlation between the degree of wound and DWV titer is not confirmed. Given the ability of *T. mercedesae* to puncture on pre- and post-capped honey bee larvae, the mite may act as a mechanical vector to stimulate DWV proliferation in honey bee colonies (Khongphinitbunjong et al., 2016, Khongphinitbunjong et al., 2015, Forsgren et al., 2009, Dainat et al., 2009). In addition, the puncture wound allow the entry of other pathogens and microbial infection as well (Brødsgaard et al., 2000).

Section 2.4.3 *V. destructor* and *T. mercedesae* mediated stimulation of DWV replication in honey bee pupa

The observation that *V. destructor* infestation increases DWV copy number in honey bees was well established before (Yue and Genersch, 2005, Shen et al., 2005) and four major mechanisms have been previously proposed: 1) *V. destructor* induces immune-suppression in honey bees, stimulating DWV replication (Yang and Cox-Foster, 2005); 2) replication-active more virulent DWV strains are selected by *V. destructor* (Martin et al., 2012); 3) DWV induces immune-suppression in honey bees at a threshold copy number (Nazzi et al., 2012, Di Prisco et al., 2016); 4) direct injection of the mixed variants of DWV to haemolymph of honey bee results in replication of the selective variant to high copy number (Ryabov et al., 2014). My results seem to be inconsistent with the first and second proposed mechanisms.

If the mite-mediated immune-suppression in honey bee occurs, DWV copy numbers found in honey bee pupae would not correlate with those in the infesting mites. However, I observed a strong correlation in copy numbers between mites and pupae. Furthermore, even though the DWV isolates in this study under natural condition were classified as the type A (Mordecai et al., 2016a, Mordecai et al., 2016c), the same variants were present in low and high copy number clusters in both honey bee pupae and mites. The patterns of DWV infection with either single or multiple variants in honey bee pupae and the infesting mites appear to be comparable (Table.2.1 & Table.2.2), suggesting that *V. destructor* and *T. mercedesae* may not select for specific type A variant. The same DWV type A variants were present in the clusters with low and high copy number in both honey bee pupae and the infesting mites as well as the control pupae. The similar pattern of DWV infection with either single or multiple variants in pupae and the infesting mites was also observed for the experiments with artificial mite infestation (Table.2.3), suggesting no specific type A variant was selected by *T. mercedesae*. These observations are similar to a previous report suggesting that a single type of virulent DWV is amplified in honey bee pupae, despite the infesting *V. destructor* contains a diverse population of DWV strains (Ryabov et al., 2014). However, this may not be the case if other types (B and C) co-exist (Mordecai et al., 2016a). Selection of specific virulent DWV types/variants may depend on the extent of replication in the mites, although the replication mechanism of DWV in honey bees and mites is not yet fully understood.

My data are most consistent with the third proposed mechanisms, that there is immune-suppression of honey bee at a threshold copy number of DWV. This support derives from my observation that two major clusters of the pupa/mite pairs were infected by low and high (but not medium) copy number of DWV (Fig.2.2D, Fig.2.5F & Fig.2.9B). When the viral load is low, DWV replication in honey bee pupae appears to be suppressed (low cluster); however, when the viral load increases and reaches to a specific threshold value, virus overcomes honey bee immune systems, resulting in proliferation and higher viral load (high cluster). Surprisingly, the same result was obtained with two different mite species, suggesting that a common mechanism is likely to operate. DWV was previously reported to adversely affect cellular and humoral immune responses in honey bee via regulating NF-kB signalling pathways (Di Prisco et al., 2016). Through transcriptome analysis of honey bee with high viral titer indicated a severe alternation of several

immune genes, inculding a member of the NF-kB gene family *dorsal-1A* (Nazzi et al., 2012). My result indicated that two AMP immune effectors, *Hymenoptaecin* and *Defensin-1* transcripts were induced in honey bee pupae by *T. mercedesae* infestation (Fig.2.12A-B), providing evidence for the immune activation as well. *Hymenoptaecin* transcripts induction was associated with mite feeding activity (Fig.2.12F), and it was proved by a previous study, in which Hymenoptaecin was significantly greater expressed in honey bee pupae with artificially wound induction alone (Kuster et al., 2014). The enhanced expression of Hymenoptaecin was observed in the pupae with wound induction for 72-120 hours, nevertheless, the induced Defensin transcripts were observed for extended period, 72-240 hours (Kuster et al., 2014). This different increased expression time for Hymenoptaecin and Defensin suggests separate induction mechanisms for them, which is proved by the results shown in Fig.2.12E-F. Since *Hymenoptaecin* and *Defensin-1* transcripts were induced by mite feeding and DWV replication, respectively, and their transcripts were reported to be under control of NF-kB-mediated Toll and Imd signalling pathways, respectively (Aronstein et al., 2010, Osta et al., 2004), therefore, these immune pathways would be independently activated by above events. Because of the association between Defensin-1 expression and DWV replication, *Defensin-1* transcripts probably have a role on regulation of the honey bee immune-suppression at a threshold copy number of DWV.

My results do not fit well to the fourth proposed hypothesis above. Many individuals of *V. destructor* and *T. mercedesae* were infected by multiple variants and most of the mite infested honey bee pupae were infected by multiple variants at either low or high copy number (Table 2.1, Table 2.2 & Table 2.3). This hypothesis may also depend on the copy number of DWV in honey bee as the third proposed mechanisms. My discussion above is based on the results obtained with 23 pupa/*V. destructor* and 44 pupa/*T. mercedesae* pairs, and thus analysing more pairs in multiple colonies will be necessary to strengthen my argument.

Chapter 3 Raising the antibodies to detect DWV

Section 3.1 Brief introduction

DWV belongs to the order *Picornavirales* and family *Iflaviridae*. It has 30 nm diameter nonenveloped icosahedral virion consisting of a 10,000-nucleotide single positive-strand RNA genome and major structural proteins including VP1 (44 kDa), VP2 (32 kDa) and VP3 (28 kDa) (Le Gall et al., 2008, Lanzi et al., 2006). The polyadenylated viral RNA genome encodes a 2,894 amino acid polyprotein, co-translationally and post-translationally cleaved into structural and non-structural proteins by the viral protease (Lanzi et al., 2006, Lamp et al., 2016). The capsid proteins locate at the N-terminal section of the polyprotein in the order of VP2, VP4, VP1, and VP3; while its C-terminal section contains the non-structural proteins including the RNA helicase, genome-liked viral protein (VPG), a-chymotrypsin-like 3C protease (3C), and RNA-dependent RNA polymerase (RdRP) (Lanzi et al., 2006) (Fig.1.2). Within families of *Picornavirales*, the most highly conserved sequences are found in polyprotein regions including the helicase, 3C protease and RdRP (Le Gall et al., 2008).

The capsid of DWV virion is pseudo-T3 icosahedral. It consists of 60 structural protomers, each of which includes major structural proteins VP1, VP2 and VP3. These protomers are arranged in 12 pentamer units of 5 protomers each (Skubnik et al., 2017). Skubnik and his colleagues determined the molecular structure of DWV virion to resolution of 3.1 Å using cryo-electron microscopy (cryo-EM) and 3.8 Å with X-ray crystallography (Skubnik et al., 2017). Based on their analyses, VP1 contains a C-terminal extension, which folds into a globular protruding (P) domain on the virion surface (Fig.3.1). The P domain positions differently in the X-ray crystallography and cryo-EM analysis and there is 39 Å shift of the centre and 145° rotation between the two alternative conformations. The alternations of pH could trigger structural changes of P domain, however, the pH level examined was not physiologically realistic. This movement and flexibility of VP1-P domain suggest that this is the putative receptor-binding site for virus infection (Skubnik et al., 2017).

Previous studies indicate that all non-structural proteins were involved in the replication of picornavirus. The helicase and VPG play essential roles for the structural and biochemical changes that are induced in the infected host cells while 3C protease and RdRP are directly related to RNA replication and synthesis processes (Paul, 2002). As a membrane of picornavirus, DWV replication requires RdRP as an essential catalytic component. During replication, DWV uses an un-cleaved precursor of 3C protease and RdRP as an intermediate, which remains inactive until this polyprotein processing is finished (Ferrer-Orta et al., 2006). As a single positive-strand RNA virus, DWV produces the negative-strand RNA during replication process and its presence indicates the active viral replication. Therefore, the negative-strand-specific RT-PCR method was often used for testing the active DWV replication (Yue and Genersch, 2005). Nevertheless, there are some problems associated with the strand-specific RT-PCR detection, including: 1) falsely primed cDNAs production during RNA reverse transcription and 2) random cDNAs synthesis due to self-priming of RNA secondary structure (Boncristiani et al., 2009, Haddad et al., 2007).

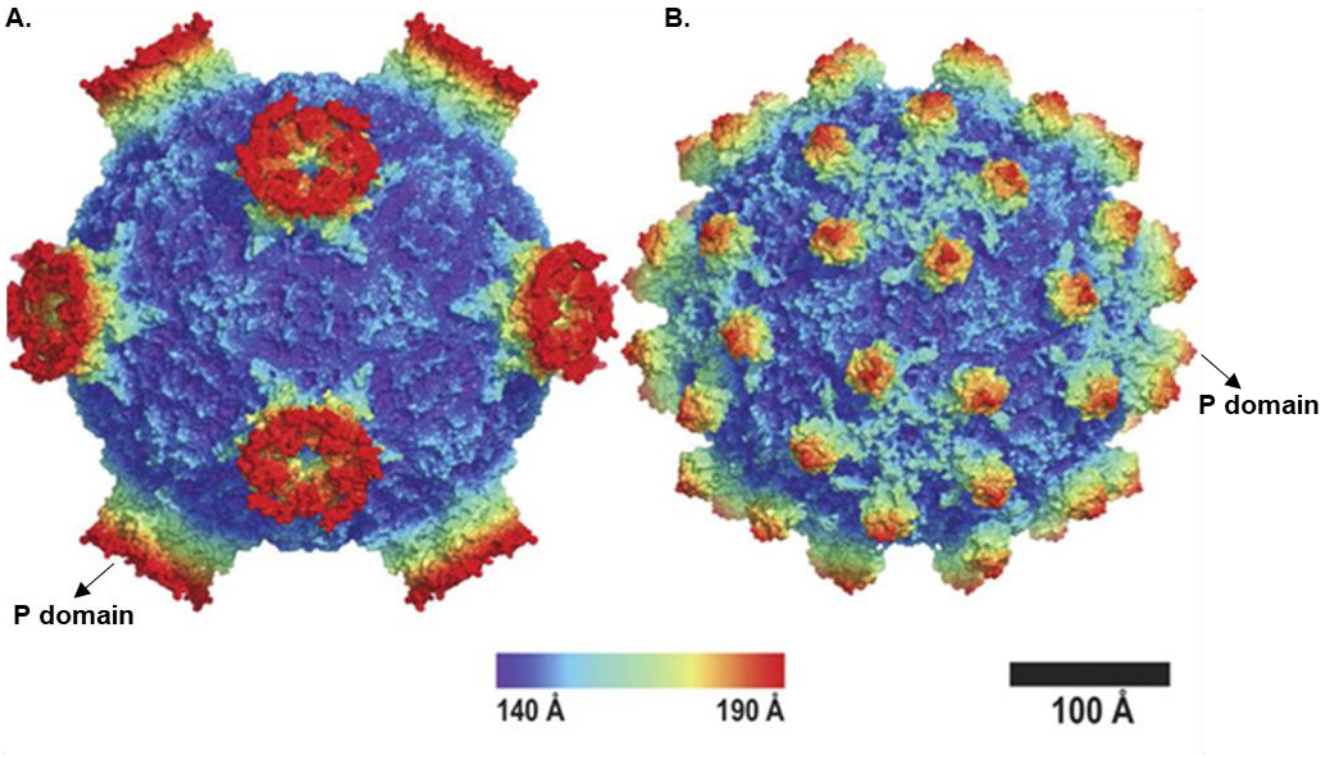

Figure. 3.1 Structures of DWV virion and its alternative conformations.

The (A) cryo-electron microscopy and (B) X-ray crystallography analysis of DWV virion surface, which is rainbow-colored according to their distances from the virion centre. The P domain of VP1 is indicated by red colour. The P domain of 5 protomers in cryo-EM image and 1 protomer in X-ray crystallography image are highlighted by arrows respectively. The P domain's positioning on the surface of DWV virion is different in cryo-EM and X-ray structures (Adapted from (Skubnik et al., 2017)).

Capsid and RdRP gene sequences (Bakonyi et al., 2002, Benjeddou et al., 2001, Philippe Blanchard et al., 2007, Chen et al., 2005b, Tentcheva et al., 2004b, Shen et al., 2005) are usually utilized to investigate RNA virus in honey bee. Therefore, VP1 and RdRP were also selected as the targets to examine DWV in my project. I raised the antibodies against VP1 and RdRP of DWV to detect DWV and DWV replication respectively. The VP1-P domain is expected at the viral surface of DWV and the peptide used to raise the 2nd RdRP antibody is expected at the surface of RdRP. Therefore, VP1-P domain and 2nd RdRP antibodies are expected to detect the targets under native condition for immunoprecipitation and immunofluorescence.

Section 3.2 Materials and Methods

Section 3.2.1 Construction of VP1 and RdRP expression vectors

The VP1 cDNA was amplified by PCR using the primer sets 5'-SacI-VP1 and 3'-HindIII-VP1 (Supplementary Table). The amplified PCR product was further purified by ethanol precipitation. The purified VP1 cDNA was treated by restriction enzymes SacI (NEB) and HindIII (NEB) separately at 37°C for 1.5 hours. The pCold vector TM I DNA vector (TaKaRa Bio Inc) was treated with the same restriction enzymes followed by further incubation with BeyoAP Alkaline Phosphatase (AP) (Beyotime) at 37°C for

30 min. The restriction-enzyme-cut products of VP1 and pCold vector were purified by Gel Extraction Kit (Qiagen), according to manufacturer's instruction, then ligated with each other using Ligation solution I (NEB) at 16°C for 1 hour. The ligation product of VP1 and pCold vector was transformed into *Escherichia coli* BL21 cells (TIANGEN) and grown on Lysogeny broth (LB) plate with Ampicillin selection.

The RdRP cDNA was amplified by PCR using the primers 5'-KpnI-RdRP and 3'-HindIII-RdRP (Supplementary Table). The amplified PCR product was further purified by ethanol precipitation. The purified RdRP cDNA was treated by restriction enzymes KpnI (NEB) and HindIII respectively at 37°C for 1.5 hours. The pCold vector was treated with the same restriction enzymes followed by further incubation with AP at 37°C for 30 min. The restriction-enzyme-cut products of RdRP and pCold vector were purified by Gel Extraction Kit, then were ligated with each other by Ligation solution I at 16°C for 1 hour. The ligation product of RdRP and pCold vector was transformed into *E. coli* BL21 cells and grown on LB plate with Ampicillin selection.

The VP1-P cDNA was amplified by PCR using the primers 5'-NdeI-P-domain and 3'-XhoI-P-domain (Supplementary Table). The amplified PCR product was further purified by ethanol precipitation. The purified VP1-P cDNA was treated by restriction enzymes NdeI (NEB) and XhoI (NEB) at 37°C for 3 hours. The pCold vector was also treated by NdeI and XhoI enzymes, however, it was then further incubated with AP at 37°C for 30 min. The restriction-enzyme-cut products of VP1-P and pCold vector were purified by Gel Extraction Kit, then were ligated using Ligation solution I at 16°C for 1 hour. The ligation product of VP1-P and pCold vector was transformed into *E. coli* BL21 cells and grown on LB plate with Ampicillin selection.

The 2nd RdRP cDNA was amplified by PCR using the primers 5'-NdeI-RdRP and 3'-XhoI-RdRP (Supplementary Table). The amplified PCR product was further purified by ethanol precipitation. The purified 2nd RdRP was treated by restriction enzymes NdeI and XhoI at 37°C for 3 hours. The pCold vector was treated with the same restriction enzymes but subsequently incubated with AP at 37°C for 30 min. The restriction-enzyme-cut products of 2nd RdRP and pCold vector were purified by Gel Extraction Kit, then were ligated using Ligation solution I at 16°C for 1 hour. The ligation product of 2nd RdRP and pCold vector was transformed into *E. coli* BL21 cells and grown on LB plate with Ampicillin selection.

Section 3.2.2 Protein expression and purification

The pCold vector containing the targeted cDNA was transfected into *E. coli* BL21 cells. Cells were grown in LB broth with Ampillicin (0.1 mg/ml) at 37°C with 200 RPM until their OD600 values reached to approximate 0.5, the cell suspension was then cooled to 15°C. Isopropyl-thio-galactoside (IPTG) was added into the culture with a concentration of 0.5 mM to initiate the expression. The expression was done by overnight shaking at 15°C with 200 RPM. The cells were collected by centrifugation at 6,500 RPM 4°C for 15 min and then resuspended in 100 ml lysis buffer (with 1 mM DTT and protease inhibitor). The sonication was performed with a Q700 Sonicator (Qsonica) at Amplitude 100 for 45 min on ice (30 sec

sonication with 3 min-interval). The sonicated suspension was centrifugated at 14,000 RPM 4°C for 30 min and the supernatant was collected. His-tag Protein Purification Resin (Beyotime) was pre-equilibrated with lysis buffer and then added into the supernatant. The suspension was gently rotated at 4°C for at least 2 hours. The resin was then sequentially washed with the washing buffer (5 x 10 ml) and elution buffer (6 x 1 ml and 2 x 5 ml). The details of lysis buffer, washing buffer and elution buffer which were specific for different proteins purification were listed in Table 3.1.

Table 3.1. Summary of specific buffers used for different proteins during purification.

Purification Buffers	**VP1**	**RdRP**	**VP1-P**	**2nd RdRP**
Lysis	Lysis buffer with 0.1% sarkosyl, 1 mM DTT and protease inhibitor	Lysis buffer with 0.1% sarkosyl, 1 mM DTT and protease inhibitor	Lysis buffer with 1 mM DTT and protease inhibitor	Lysis buffer with 0.1% sarkosyl, 1 mM DTT and protease inhibitor
Washing	Washing buffer with 0.1% sarkosyl	Washing buffer with 0.1% sarkosyl	Washing buffer	Washing buffer with 0.1% sarkosyl
Elution	Elution buffer with 0.1% sarkosyl	Elution buffer with 0.1% sarkosyl	Elution buffer	Elution buffer with 0.1% sarkosyl

Lysis buffer: 50 mM NaH_2PO_4, 300 mM NaCl, pH 8.0.

Washing buffer: 50 mM NaH_2PO_4, 300 mM NaCl, 2 mM imidazole, pH 8.0.

Elution buffer: 50 mM NaH_2PO_4, 500 mM NaCl, 250 mM imidazole, pH 8.0.

Section 3.2.3 Dialysis, condensation and protein concentration measurement

The eluted protein of VP1, RdRP and 2nd RdRP was respectively dialyzed against dialysis buffer (0.1% sarkosyl, PBS) with gently shaking at 4°C overnight. The eluted VP1-P protein was dialyzed against PBS with gentle shaking at 4°C overnight. The dialyzed protein was then concentrated with Vivaspin® 6 Polyethersulfone 10 kDa (Sartorius), followed by measuring concentration via BCA Protein Assay Kit (Beyotime), according to the manufacturer's instructions.

Section 3.2.4 Raise antibody

The purified and concentrated antigens were delivered to the company GeneScript-Nanjing to raise 4 polyclonal anti-rabbit antibodies against VP1, RdRP, VP1-P and 2nd RdRP, respectively. Table.3.2 summarizes the concentration and volume of each antibody.

Table 3.2. Summary of antibodies raised by GeneScript.

Antibody name	Immunogen	Host strain	Concentration (mg/ml)	Volume (ml)
Anti-VP1	VP1	New Zealand Rabbit	0.412	18
Anti-RdRP	RdRP	New Zealand Rabbit	0.317	16.5
Anti-VP1P	VP1-P	New Zealand Rabbit	0.754	8
Anti-2nd RdRP	2nd RdRP	New Zealand Rabbit	0.449	17

Section 3.2.5 SDS-PAGE

During protein purification, the whole cell lysate resuspended in lysis buffer, the supernatant and pellet after sonication, samples collected in washing and elution fractions were all subjected to SDS-PAGE. The samples were boiled in SDS sample buffer (2% SDS, 10% glycerol, 10% β-mercaptoethanol, 0.25% Bromophenol blue, 50 mM Tris-HCl, pH 6.8) for 5 min at 99°C before the electrophoresis. For each gel, samples were electrophoresed for approximately 80 min at 20 A. After staining with Coomassie Blue Stain buffer (0.25% Coomassie brilliant blue G-250, 40% Methanol, 10% Glacial acetic acid) and washing with Destain buffer (40% Methanol, 10% Glacial acetic acid), the bands were scanned with ChemiDoc™ MP Imaging System (BIO-RAD). All images were analysed by Image Lab™ Touch Software (BIO-RAD).

Section 3.2.6 RT-PCR analysis of DWV

Total RNA from each honey bee head were extracted using Total RNA Extraction Reagent (GeneSolution), according to the manufacturer's instructions. Reverse transcription (RT) reactions were carried out using 1 μl of total RNA, random primer (TOYOBO), ReverTra Ace (TOYOBO), and RNase Inhibitor (Beyotime). RNase H (Beyotime) was added to digest RNA in RNA/cDNA heteroduplex after cDNA synthesis. These RT products were used for subsequent RT-PCR to assess whether the honey bee was infected by DWV with the primer set DWV #1 (Supplementary Table) and the conditions 2 min at 94°C, followed by 32 cycles of 10 sec at 98°C, 20 sec at 55°C, and 30 sec at 68°C. PCR products were analysed on a 2% agarose gel. PCR targeting honey bee *EF-1α* mRNA (Supplementary Table) was utilized as controls to verify successful RT.

Section 3.2.7 Western blot

Every honey bee abdomen was individually lysed with a homogenizer in 300 μl SDS sample buffer, followed by heat denaturation at 99°C for 5 min. The lysates were centrifugated for 1 min at 10,000 xg, then the supernatants were subjected to SDS-PAGE gel. For each gel, samples were electrophoresed for approximately 80 min at 20 A and subsequently transferred to a Pure Nitrocellulose Blotting Membrane (Pall® Life Sciences) or a PVDF membrane (Millpore). Protein-loaded membranes were incubated in Blocking buffer I (5% BSA, 0.1% Tween-20, PBS) for 1 hour at room temperature, and incubated in primary

antibody diluted in Blocking buffer for 2 hours at 37°C or overnight at 4°C. The antibodies utilized including anti-VP1, anti-RdRP, anti-VP1P, and anti-2nd RdRP, all diluted at 1:1,000. The membranes were then washed 3 times for 5 min each in PBST (0.1% Tween-20, PBS), incubated in IRDye® 680RD Donkey anti-Rabbit IgG (H+L) diluted in Blocking buffer II (5% milk powder, 0.1% Tween-20, PBS) at 1:10,000 for 1-1.5 hours at room temperature. The membranes were washed three times for 5 min each in PBST before visualization by Odysse Infrared Imager.

Honey bee primary cells with DWV replication were lysed and prepared for western blot samples by the same method. The methods and conditions for western blot were also same, except the primary antibodies used were anti-RdRP and 2nd anti-RdRP antibodies, both diluted at 1:1,000.

Section 3.2.8 Transfection

BHK-21 cells were cultured at 37°C in a 5% CO_2 atmosphere in the culturing medium (DMEM, 10% heat-inactivated fetal bovine serum (FBS), 50 units/ml penicillin G, 50 µl/ml Streptomycin) and grown as monolayers. For transfection experiment, freshly confluent monolayers were washed by sterile PBS, followed by covering with 3 ml EDTA-trypsin, at room temperature for approximately 3 min. After two washes with sterile PBS, the EDTA-trypsin solution was replaced with 5 ml culturing medium and cells were re-suspended in it. One coverslip was placed inside each well of 24-well plates, and 1 x 10^5 BHK-21 cells were inoculated onto each coverslip. After culturing at 37°C overnight, cells were transfected using Lipofectamine 2000 (Invitrogen), according to the manufacturer's instructions, with the plasmid DNA which expressed VP1-P protein. Cells transfected with Lipofectamine 2000 reagent without the plasmid DNA were utilized as the negative control group. Cells were cultured in Lipofectamine® Reagent and Opti-MEM® for 24 hours, followed by culturing in the fresh medium containing DMEM, FBS and antibiotics for 24 hours.

Section 3.2.9 Immunofluorescence

Transfected and non-transfected cells were fixed in 4% paraformaldehyde (PFA) in PBS for 30 min at room temperature, followed by washing three times with PBS-Triton (0.5% Triton X-100, PBS). After blocking in Blocking buffer III (3% BSA, 1% goat serum, PBS) at 4°C overnight, coverslips were incubated with primary antibodies for 2 hours at room temperature. Primary antibodies were applied at the following dilutions in Blocking buffer III: anti-VP1P at 1:500, and pre-immune serum of anti-VP1P at 1:500. After five washes in PBS-Triton, coverslips were incubated in the secondary antibody, Alexa Fluor 555 anti-rabbit antibody (Beyotime), which was diluted at 1:1,000 in Blocking buffer III, for 1 hour at room temperature. After four washes with PBS-Triton, the coverslips were incubated with DAPI with the dilution at 1:1,000 in PBS-Triton for 5 min at toom temperature. After the last wash with PBS-Triton, the coverslips were mounted in Antifade Mounting Medium (Beyotime).

Section 3.2.10 Microscopy observation and data analysis

Images were collected using a Nikon Eclipse Ni microscopy with a Nikon Plan Fluor 10x/0.30 objective. Software ImageJ (Hartig, 2013) was utilized to analyse immunofluorescence data.

Section 3.3 Results

Section 3.3.1 Raising the antibodies to detect DWV

Expression and purification of the partial VP1 protein, and western blot results using the anti-VP1 antibody with honey bee pupal lysates

The VP1 peptide was successfully expressed in *E. coli* with the molecular weight of approximately 27 kDa. The peptide sequence was listed below (partial sequence of UniProtKB-Q8B3M2):

> VP1 [protein=partial Deformed wing virus capsid protein VP1]
GTTQHPVGCAPDEDMTVSSIASRYGLIRRVQWKKDHAKGSLLLQLDADPFVEQRIEGTNPISLYWFAPV
GVVSSMFMQWRGSLEYRFDIIASQFHTGRLIVGYVPGLTASLQLQMDYMKLKSSSYVVFDLQESNSFTF
EVPYVSYRPWWVRKYGGNYLPSSTDAPSTLFMYVQVPLIPMEAVSDTIDINVYVRGGSSFEVCVPVQPS
LGLNWNTDFILRNDEEYRAK

Based on the solubility test, most of the VP1 was insoluble (Fig.3.2A). Lysis buffer containing 0.3-2% sarkosyl can effectively increase the solubility of protein expressed in *E. coli* (e.g. glutathione S-transferase) (Hu Tao et al., 2010, Stewart Frankel et al., 1990). In my case, the lysis buffer with 0.1% sarkosyl efficiently increased the solubility of VP1, and through 6X His-tag purification method, the VP1 protein was successfully isolated with the purity higher than 85% (Fig.3.2B). Following subsequent dialysis and concentration, the VP1 peptide with the concentration of 0.4 mg/ml was delivered to GenScript to raise the polyclonal antibody in rabbit. In order to determine the capability of recognizing DWV, the raised anti-VP1 antibody was used for western blot with honey bee lysates. Western blot of the protein lysate from DWV-positive honey bee by RT-PCR (Fig.3.2C) showed two bands near 43 kDa (Fig.3.2D). These two bands of VP1 likely represent differential post-translational modifications and processing forms.

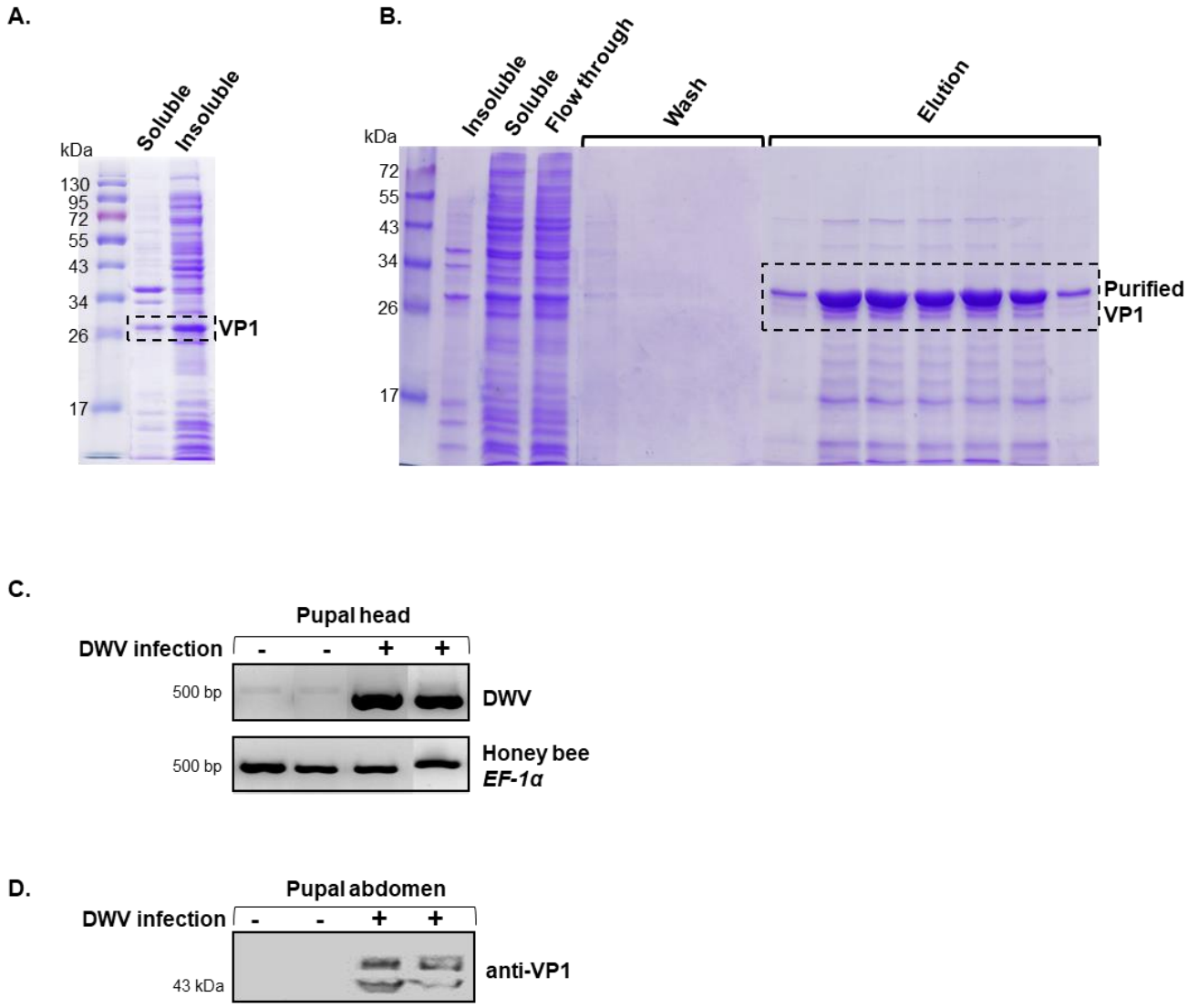

Figure 3.2 SDS-PAGE analysis of VP1 peptide expression and purification, and western blot analysis of honey bee pupae lysates using the anti-VP1 antibody.

(A) 12% SDS-PAGE analysis of the VP1 peptide's solubility in PBS, which was expressed in *E. coli*. The expressed VP1 peptide was indicated by dotted box. Lane 1. protein marker; Lane 2. the soluble proteins; Lane 3. the insoluble proteins. (B) 12% SDS-PAGE analysis of 6X His-tag purification of VP1 peptide, which was highlighted by dotted box. Lane 1. protein marker; after lysing *E. coli* with the buffer containing 0.1% sarkosyl: Lane 2. the insoluble proteins; Lane 3. the soluble proteins; during the purification: Lane 4. the unbound fraction to the resin; Lane 5-8. the washing fractions; Lane 9-15. the elution fractions. (C) DWV was detected using RT-PCR in 4 honey bee pupal heads. Two pupae were infected by DWV with the bands near 500 bp. Honey bee *EF-1α* mRNA was used as the endogenous positive control. (D) The abdominal protein lysates from the same 4 pupae were used for western blot with the anti-VP1 antibody. Two bands near 43 kDa were visualized in the pupae with DWV infection.

Expression and purification of the partial RdRP protein, and western blot results of honey bee pupal lysates using the anti-RdRP antibody

The RdRP peptide was successfully expressed in *E. coli* with the molecular weight of approximately 27 kDa. The peptide sequence was listed below (partial sequence of UniProtKB-Q8B3M2):

> RdRP [protein=partial Deformed wing virus RNA-dependent RNA polymerase]
TCLPVEKCRIPGKTRIFSISPVQFTIPFRQYYLDFMASYRAARLNAEHGIGIDVNSLEWTNLATSLSKYGTH
IVTGDYKNFGPGLDSDVAASAFEIIIDWVLHYTEEDNKDEMKRVMWTMAQEILAPSHLCRDLVYRVPCGI
PSGSPITDILNTISNCLLIRLAWLGITDLPLSEFSQNVVLVCYGDDLIMNVSDNMIDKFNAVTIGKFFSQYK
MEFTDQDKSGNTVKWRTLQTA

Based on solubility test, most of the RdRP was insoluble (Fig.3.3A). Using the lysis buffer with 0.1% sarkosyl efficiently increased the solubility of RdRP, and through 6X His-tag purification method, the RdRP protein was successfully isolated with purity exceeding 85% (Fig.3.3B). Following subsequent dialysis and concentration, the RdRP peptide with the concentration 1 mg/ml was delivered to GenScript to raise the polyclonal antibody in rabbit. In order to determine the capability of recognizing DWV, the raised anti-RdRP antibody was utilized for western blot with honey bee lysates. Western blot of the protein lysate from DWV-positive honey bee by RT-PCR (Fig.3.3C), showed two bands, one is near 95 kDa and the other one is near 55 kDa, which represented the precursor and matured RdRP respectively (Fig. 3.3D).

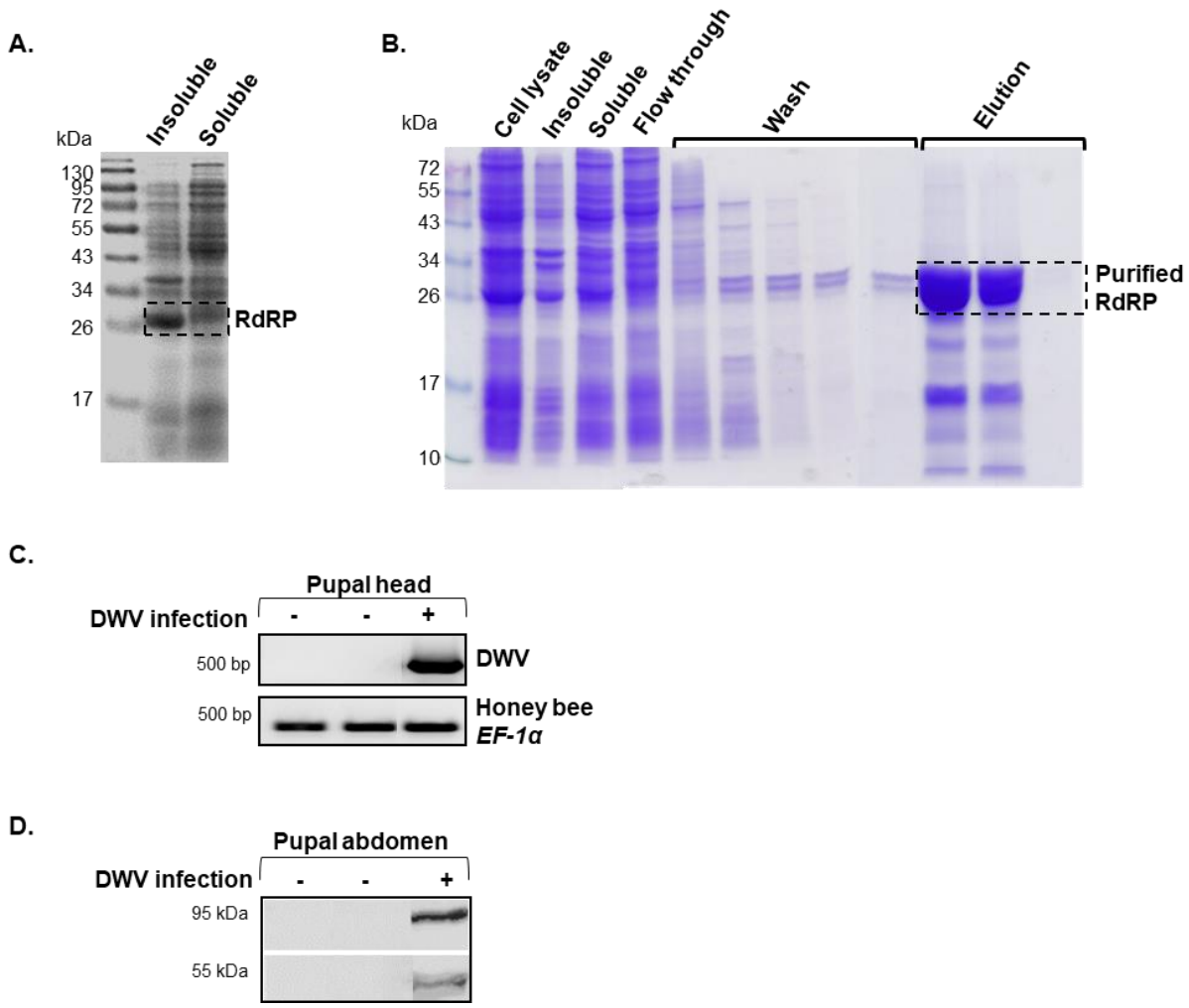

Figure 3.3 SDS-PAGE analysis of RdRP protein expression and purification, and western blot analysis of honey bee pupae lysates using the anti-RdRP antibody.

(A) 12% SDS-PAGE analysis of the RdRP peptide's solubility in PBS, which was expressed in *E. coli*. The expressed RdRP peptide was indicated by dotted box. Lane 1. protein marker; Lane 2. the insoluble proteins; Lane 3. the soluble

proteins. (B) 12% SDS-PAGE analysis of 6X His-tag purification of RdRP peptide, which was highlighted by dotted box. Lane 1. protein marker; after lysing *E. coli* with the buffer containing 0.1% sarkosyl: Lane 2. the whole expressed proteins; Lane 3. the insoluble proteins; Lane 4. the soluble proteins; during the purification: Lane 5. the unbound fraction to the resin; Lane 6-10. the washing fractions; Lane 11-13. the elution fractions. (C) DWV was detected using RT-PCR in 3 honey bee pupae heads. One pupa was infected by DWV with the bands near 500 bp. Honey bee *EF-1α* mRNA was used as an endogenous positive control. (D) The abdominal protein lysates from the same 3 pupae were used for western blot with the anti-RdRP antibody. Two bands near 95 kDa and 55 kDa were visualized in the pupa with DWV infection.

Expression and purification of VP1-P domain peptide, and western blot results of honey bee pupal lysates using the anti-VP1P antibody

The VP1-P domain peptide was successfully expressed in *E. coli* with molecular weight of approximately 21 kDa. The peptide sequence was listed below (partial sequence of UniProtKB-Q8B3M2):

> VP1-P [protein= Deformed wing virus capsid protein VP1-P domain]
MRAKTGYAPYYAGVWHSFNNSNSLVFRWGSASDQIAQWPTISVPRGELAFLRIKDGKKAAVGTQPWRT
MVVWPSGHGYNIGIPTYNAERARQLAQHLYGGGSLTDEKAKQLFVPANQQGPGTASNGNPVWEVMRA
PLATQRAHVQDFEFIEAIPE

Based on solubility test, most of the VP1-P protein was soluble (Fig.3.4A). The VP1-P protein was successfully isolated with purity higher than 85% through 6X His-tag purification method (Fig.3.4B). Following subsequent dialysis and concentration, the VP1-P peptide with concentration of 12 mg/ml was delivered to GenScript to raise the polyclonal antibody in rabbit. In order to determine the capability of recognizing DWV, the raised anti-VP1P antibody was used for western blot with honey bee lysates. Western blot of the protein lysate from DWV-positive honey bee by RT-PCR (Fig.3.4C), showed a single band near 43 kDa (Fig. 3.4D).

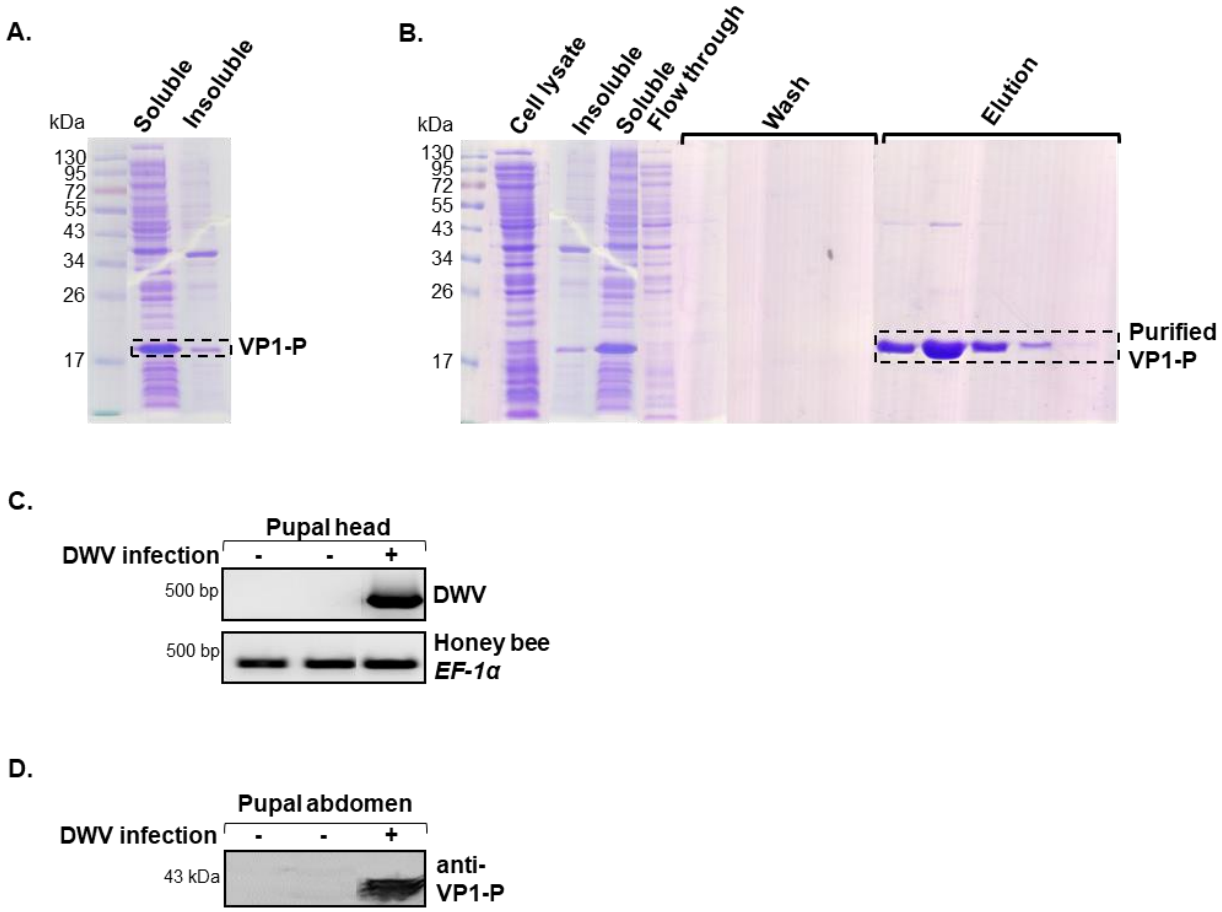

Figure 3.4 SDS-PAGE analysis of VP1-P peptide expression and purification, and western blot analysis of honey bee pupae lysates using the anti-VP1P antibody.

(A) 12% SDS-PAGE analysis of the VP1-P peptide's solubility in PBS, which was expressed in *E. coli*. The expressed VP1-P protein was indicated by dotted box. Lane 1. protein marker; Lane 2. the soluble proteins; Lane 3. the insoluble proteins. (B) 12% SDS-PAGE analysis of 6X His-tag purification of VP1-P peptide, which was highlighted by dotted box. Lane 1. protein marker; Lane 2. the whole expressed proteins in *E. coli*; Lane 3. the insoluble proteins; Lane 4. The soluble proteins; during the purification: Lane 5. the unbound fraction to the resin; Lane 6-9. the washing fractions; Lane 10-14. the elution fractions. (C) DWV was detected using RT-PCR in 3 honey bee pupae heads. One pupa was infected by DWV with the bands near 500 bp. Honey bee *EF-1α* mRNA was used as the endogenous positive control. (D) The abdominal protein lysates from the same 3 pupae were used to for western blot with the anti-VP1P antibody. A single band near 43 kDa was visualized in the pupa with DWV infection.

Expression and purification of the 2nd RdRP peptide, and western blot results of honey bee cell lysates using the 2nd anti--RdRP antibody

In order to raise an antibody which can be utilized to detect native RdRP protein, I expressed the peptide 2nd RdRP which is expected at the surface of RdRP based on X-ray crystallographic analysis of other RdRP proteins, including Foot-and Mouth disease virus RdRP, murine norovirus RdRP, and human *Entervirus* D68 RdRP. The 2nd RdRP peptide was successfully expressed in *E. coli* with molecular weight of approximately 14 kDa. The peptide sequence was listed below (partial sequence of UniProtKB-Q8B3M2):

> 2nd RdRP [protein=partial Deformed wing virus RNA-dependent RNA polymerase]
ISPVQFTIPFRQYYLDFMASYRAARLNAEHGIGIDVNSLEWTNLATRLSKGGTHIVTGDYKNFGPGLDSD
VAASAFEIIIDWVLHYTEEDNKDEMKRVMWTMAQEILAPSHLYRDLVYRV

Based on solubility test, most of the 2nd RdRP was insoluble (Fig.3.5A). Lysis buffer with 0.1% sarkosyl efficiently increased the solubility of 2nd RdRP, and through 6X His-tag purification method, the 2nd RdRP peptide was successfully isolated with purity higher than 85% (Fig.3.5B). Following subsequent dialysis and concentration, the 2nd RdRP peptide with the concentration of 0.9 mg/ml was delivered to GenScript to raise the polyclonal antibody in rabbit. In order to examine the capability of recognizing DWV, the raised 2nd anti-RdRP antibody was used for western blot with honey bee cell lysates, which were also examined by 1st anti-RdRP antibody as a reference for the presence of DWV replication. Western blot of the protein lysate from DWV replication-positive honey bee cells showed a band near 95 kDa, the same position as one of the bands recognized by the 1st anti-RdRP antibody. Nevertheless, compared to the 1st anti-RdRP antibody, there were more non-specific bands in the western blot results of the 2nd anti-RdRP antibody, and therefore, it is difficult to distinguish and verify the band near 55 kDa representing the matured RdRP (Fig. 3.5C).

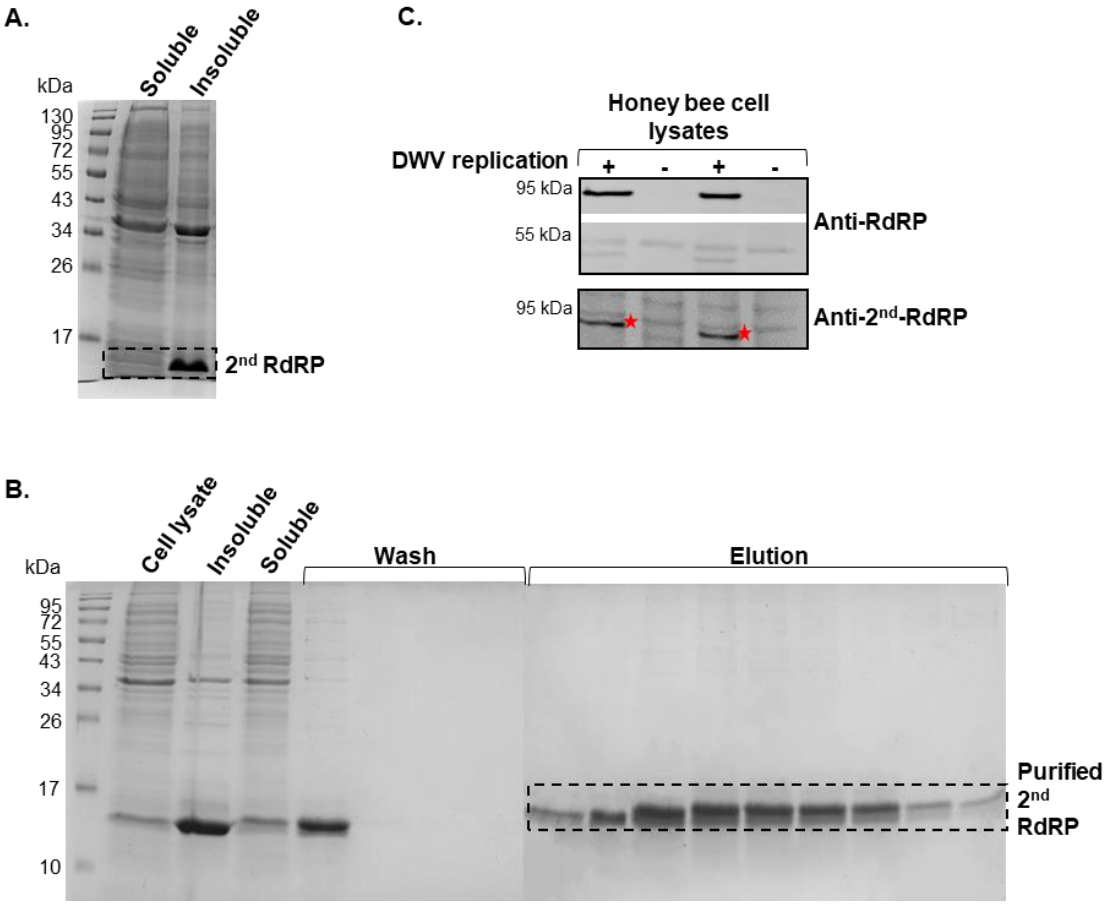

Figure. 3.5 SDS-PAGE analysis of 2nd RdRP protein expression and purification, and western blot analysis of honey bee lysates using the 2nd anti-RdRP antibody.

(A) 12% SDS-PAGE analysis of the 2nd RdRP peptide's solubility in PBS, which was expressed in *E. coli*. The expressed 2nd RdRP was indicated by dotted box. Lane 1. protein marker; Lane 2. the soluble proteins; Lane 3. the

insoluble proteins. (B) 15% SDS-PAGE analysis of 6X His-tag purification of 2nd RdRP peptide, which was highlighted by dotted box. Lane 1. protein marker; after lysing in the buffer containing 0.1% sarkosyl: Lane 2. the whole expressed proteins; Lane 3. the insoluble proteins; Lane 4. The soluble proteins; during purification: Lane 5-8. the washing fractions; Lane 9-17. the elution fractions. (C) Western blot of honey bee cell lysates with anti-RdRP and 2nd anti-RdRP antibodies. For the honey bee cell lysates with DWV replication, duple bands (near 95 kDa and 55 kDa) were visualized by anti-RdRP antibody, while a single obvious band (near 95 kDa, highlighted by red star) was visualized by 2nd anti-RdRP antibody.

Section 3.3.2 Anti-VP1P antibody can be used for immunofluorescence

Cryo-EM analysis and X-ray crystallization of DWV virion indicate the VP1-P domain is expected at the surface of DWV virion (Skubnik et al., 2017). Therefore, the anti-VP1P antibody is expected to detect DWV under native conditions, which means this antibody is available for immunoprecipitation and immunofluorescence assays. In order to examine whether anti-VP1P antibody can detect DWV under native conditions, it was used for immunofluorescence of BHK-21 cells transfected with the plasmid expressing VP1-P domain. The pre-immune serum as well as the cells without transfection were used as negative controls. The red fluorescence signals were only observed with the transfected cells using anti-VP1P antibody (Fig.3.6). These results demonstrate that anti-VP1P antibody recognizes DWV through immunofluorescence. Therefore, anti-VP1P antibody would be utilized to explore the localization of DWV inside ectoparasitic mites through immunofluorescence.

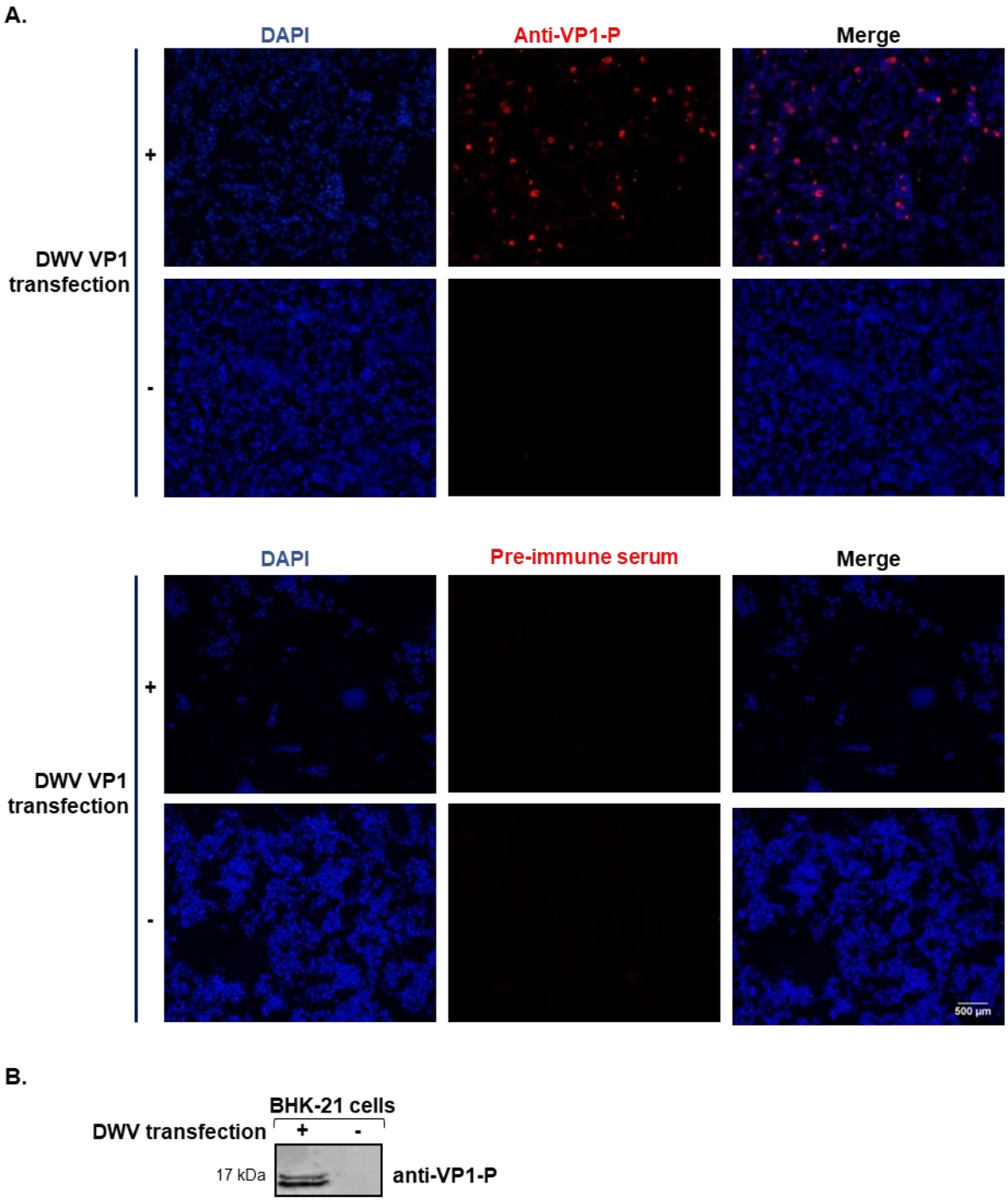

Figure 3.6 Immunofluorescence and western blot analysis with BHK-21 cells using anti-VP1P antibody. BHK-21 cells were transfected with the plasmid expressing VP1-P domain. The cells were further subjected for immunofluorescence (A) and western blot (B) with anti-VP1P antibody. The BHK-21 cells without transfection and the pre-immune serum of anti-VP1P antibody were used as the negative controls. A western blot of the transfected BHK-21 cells to show two bands near 17 kDa, indicating the successful transfection and expression of P domain. The nuclei were counterstained with DAPI (blue). Bar scale represents 500 μm, which is shared by all images in (A).

Section 3.4 Discussion

I expressed and purified both structural (VP1) and non-structural proteins (RdRP) and raised their antibodies. Both first and second anti-RdRP antibodies detected the RdRP protein of DWV, which is an essential component for the viral replication. Therefore, these two antibodies are available for testing the

degree of viral replication. The anti-VP1 and anti-VP1P antibodies, which detect DWV structural protein VP1, can be utilized to examine the virion in the samples. Anti-VP1P antibody detected VP1 under native condition and this was supported by the successful detection of VP1 in BHK-21 cells by immunofluorescence. Consequently, anti-VP1P antibody would be used for DWV localization in the ectoparasitic mite by immunofluorescence and identification of the host proteins interacting with DWV via immunoprecipitation. However, whether the 2nd anti-RdRP antibody can detect RdRP under native conditions remains to be tested.

Until now, the traditional methods to detect DWV include electron microscopy and ELISA techniques, which are not sensitive and specific (Bowen-Walker et al., 1999, Nordström, 2003, Genersch, 2005). The most common method for DWV detection is RT-PCR with various primers targeting different region in the DWV genome, including *RdRP*, *Lp*, *Helicase*, and major capsid genes (Francis et al., 2013, McMahon et al., 2016, Moore et al., 2011, Dalmon et al., 2017, Highfield et al., 2009, Genersch, 2005, Tentcheva et al., 2004a, Gauthier et al., 2007, Kukielka et al., 2008). RT-PCR with the post analysis by high resolution melt analysis (HRM) was used to distinguish different variants. DWV type A and type B were distinguished via HRM; however, DWV type C cannot be separated from type B, as they have the same dissociation curves (Mordecai et al., 2016c). More recently, qRT-PCR method was used to measure viral load (McMahon et al., 2016, Highfield et al., 2009). Next generation sequencing methods are also used to identify the viral variants, recombinants and viral load studies (Mordecai et al., 2016c, Moore et al., 2011, Dalmon et al., 2017, Mordecai et al., 2016b, Brettell et al., 2017). A monospecific antibody to DWV-VP1 was previously used to identify DWV distribution in honey bee sections via immunohistology (Fievet et al., 2006). Santillan-Galicia *et al.* also used the immunohistological method by DWV antibody to reveal the localization in *V. destructor* (Santillan-Galicia et al., 2008). To assess the viral localization, immunofluorescence with anti-VP1 antibody may not be sensitive; however, it is useful to detect DWV in specific organs or tissues (Santillan-Galicia et al., 2008). Currently, most of studies use RT-PCR to detect the negative-strand RNA of DWV genome to indicate the viral replication (Ongus et al., 2004, Yue and Genersch, 2005, Gisder et al., 2009); however, it could generate false positives via falsely-primed cDNAs synthesis in vitro during reverse transcription, which amplified by following PCR (Peyrefitte et al., 2003). The anti-RdRP antibodies I raised can overcome the problem and be used in my project to detect viral replication.

Chapter 4 Effects of DWV on *T. mercedesae*

Section 4.1 Introduction

The two major ectoparasitic mites for honey bee, *V. destructor* and *T. mercedesae*, are prevalent in most Asian countries (Anderson and Roberts, 2013, Buawangpong et al., 2015). Compared to *V. destructor*, the studies for *T. mercedesae*, including the genomic features, development, reproduction and capability of pathogen transmission are quite limited. Recently, the whole transcriptome analysis of *T. mercedesae* indicated that one-third of the transcriptome was represented by DWV sequences, and the subsequent proteomic analysis of female and male mites showed abundant peptides derived from DWV structural proteins with little non-structural proteins (Dong et al., 2017). The similar observations were made in *V. destructor* (Erban et al., 2015). These findings suggested that DWV exists as mature virion in the ectoparasitic mites and may not replicate.

As an evolutionary standpoint, honey bee and ectoparasitic mites belong to two distinct branches of arthropod radiation, which likely present some particular features of DWV infecting these different hosts. The various DWV strains, including type A, type B and recombinants of type A and type B, were reported in all body parts of honey bee (Boncristiani et al., 2011, Zioni et al., 2011, Shah et al., 2009, Mockel et al., 2011, Mazzei et al., 2014). Replication of DWV type A was observed in the head, thorax and abdomen of honey bee pupae via immunohistochemistry (Lamp et al., 2016). The structural protein of DWV type A was identified in the ocular cells, glandular system and nervous system of pupal head; in the glands of thorax; and in the connective tissue; but not in hemocytes or thorax muscles (Lamp et al., 2016). Gisder *et al.* identified both DWV type A and type B in the head and thorax of adult honey bee which was artificially infected by the virus (Gisder et al., 2018). Through fluorescence *in situ* hybridization (FISH) DWV type B was identified in the brain tissue of honey bee while type A was absent (Martin and Brettell, 2019). Compared to honey bee, studies of DWV localization in mites are very limited, especially for *T. mercedesae*. The viral particles possibly derived from DWV type B were reported in the cells of *V. destructor* (Ongus et al., 2004); however, an immunolocalization study of *V. destructor* fed with DWV-infected honey bee pupae indicated exclusive presence of DWV inside the mite midgut lumen instead of cells (Santillan-Galicia et al., 2008). The negative strand RNA of DWV type B, as an indicator for viral replication, was detected in synganglia (“brain”) of *V. destructor* (Campbell et al., 2016); however, the negative strand RNA of type A was only detected in *V. destructor* which infested pupae with high but not low DWV loads (Posada-Florez et al., 2019). The question regarding whether DWV replicates inside mites remains controversial.

Regulation of vitellogenin (Vg) synthesis is essential for insect reproduction (Carr et al., 2016), and this is also true for mites/ticks, evidence, for example, by the absence of *Vg* expression in diapausing adult female *Tetranychus urticae* (Kawakami et al., 2009). During the reproductive phase, an adult female synthesizes Vg, which is taken up by maturing oocytes and then packaged as vitellin in yolk granules to provide nutrients for embryo development (Postlethwait and Giorgi, 1985, Tufail and Takeda, 2008). For *V. destructor*, female mites do not initiate vitellogenesis until feeding on the 5th instar honey bee larva

(Steiner et al., 1994). During the vitellogenesis, the oocyte obtains nutrients and cytoplasmic components from the lyrate organ tissues, ovary, and honey bee tissues as well (Steiner et al., 1994, Dittmann and Steiner, 1997, Tewarson, 1982a, Tewarson, 1982b). *Vg* genes are members of the lipid transfer gene superfamily, and encode proteins with 1,500-1,900 amino acids (Cabrera Cordon et al., 2013). There are two *V. destructor Vgs* deposited in GenBank and both are significantly up-regulated during vitellogenesis (Cabrera Cordon et al., 2013). The *Vg* gene family was also highly expressed in females of *T. mercedesae* (Dong et al., 2017). Consequently, for these two mites, synthesis of *Vgs* is crucial for successful reproduction. Di Prisco *et al.* has recently demonstrated an enhanced fertility of *V. destructor* infesting honey bee pupae with high DWV loads, shedding light on the potentially mutualistic symbiosis between DWV and *V. destructor*. This enhanced reproduction was associated with humoral and cellular immunosuppressive responses in honey bee (Di Prisco et al., 2016).

Understanding each component within the tripartite system “Honey bee-DWV-ectoparasitic mite” and the interactions between them are essential for unravelling the mechanism of DWV transmission and infection. However, studies regarding the relationship between DWV and ectoparasitic mites are quite limited, especially for *T. mercedesae*. In this chapter, I focused on the effects of DWV on *T. mercedesae*, especially for the reproductive capability and mite fitness, and the specific localization of virus within *T. mercedesae* and *V. destructor*.

Section 4.2 Materials and Methods

Section 4.2.1 Sample collection

Two more honey bee colonies were brought from a Suzhou local beekeeper in May 2017. One colony was relatively healthy, almost without mite infestation due to miticides treatments (*Colony #5*), while the other was seriously infested by *T. mercedesae* (*Colony #6*). The pre-pupa larva collected from capped brood cell without mite infestation in *Colony #5* and female mature *T. mercedesae* collected from *Colony #6* were utilized for the reproduction test. Six female *T. mercedesae* and 40 female mites, which were collected from *Colony #2* and *Colony #6* respectively, were subsequently subjected to RNA-seq analysis. *Varroa destructor* and *T. mercedesae*, collected from *Colony #1* and *#2* respectively, were utilized for RdRP detection, while honey bee pupae aimed for this experiment were collected from the both colonies. *V. destructor* and *T. mercedesae* with distinct sexes and different development stages were collected from *Colony #4* and further processed for thin-section and immunofluorescence.

Section 4.2.2 RNA isolation, RT-PCR and qRT-PCR

Total RNA was isolated from individual *T. mercedesae* using Total RNA Extraction Reagent (GeneSolution), according to the manufacturer’s instructions. Glycogen (1 µg) was added to facilitate isopropanol precipitation of the mite RNA samples. Reverse transcription (RT) reactions were carried out using 1 µl of total RNA and all remaining total RNA were stored in -80°C. The RT products were

subsequently analysed with RT-PCR to assess DWV infection in mites with the primer set DWV #1 and PCR targeting *T. mercedesae EF-1α* mRNA or *T. mercedesae* 18S rRNA were utilized as controls to verify successful RT (Supplementary Table). The methods of RT and conditions of PCR were same as mentioned in Section 2.2.2. The absolute DWV copy number within individual *T. mercedesae* was examined via qRT-PCR as the same method mentioned in Section 2.2.3 with the primer sets DWV #*2* and normalized by *T. mercedesae* 18S rRNA (Supplementary Table).

Section 4.2.3 RNA-seq

For the 1st RNA-seq of six individual *T. mercedesae* with low, medium or high DWV copy number, their RNAs were delivered to Synbio-Suzhou on dry ice for polyA+ RNA enrichment, cDNA library preparation, and Illumina Hiseq 4000 sequencing.

For the 2nd RNA-seq, 40 *T. mercedesae* RNAs were chosen (20 RNAs with high DWV copy number infection while remaining 20 RNAs with low DWV copy number), mixed and sub-categorized into 4 groups as High_A, High_B, Low_A and Low_B. They were delivered to BGI-Wuhan with dry ice for polyA+ RNA enrichment, cDNA library preparation, and Illumina Hiseq 2500/4000 sequencing.

Section 4.2.4 Analysis of RNA-seq data

After sequencing, the raw data were filtered to remove the adaptor sequences, contamination, and low-quality reads by Synbio or BGI. The Quality control (QC) was further analyzed using FastQC. The clean reads were subsequently aligned to the assembled DWV genome and *T. mercedesae* genome using Hisat2-build indexer (Kim et al., 2015) and SAMtools (Li et al., 2009). With the default union-counting and option “-a” to specify the minimum score for alignment quality, Htseq-count in the Htseq Python package (v0.6.1) (Anders et al., 2015) was utilized to obtain raw read counts, which was further subjected to the EdgeR (v3.0) Bioconductor package (Chen et al., 2014) to compare differential expression genes. An exact test was used to conduct pairwise comparisons of differential gene expression between the RNA-seq samples. The FDR P-value < 0.01, and logFC > 0.05 and logFC < 0.05 cut-offs were utilized for significance.

Section 4.2.5 Detection of viral replication by western blot

The individual honey bee pupal head was lysed with a homogenizer in 300 µl SDS sample buffer, while 150 µl SDS sample buffer for *T. mercedesae* and *V. destructor*, followed by heat denaturation at 99°C for 5 min. After centrifugation at 10,000 xg for 1 min, supernatants were subjected for SDS-PAGE gel. For each gel, samples were electrophoresed for approximately 80 min at 20 A and subsequently transferred to a PVDF membrane. Protein-loaded membranes were incubated in Blocking buffer I at room temperature for 1 hour, followed by anti-VP1 or anti-RdRP antibody incubation at a dilution of 1:1,000 at 4°C overnight.

The membranes were then washed 3 times for 5 min each in PBST, subsequently incubated in IRDye® 680RD Donkey anti-Rabbit IgG (H+L) diluted in Blocking buffer II at 1:10,000 for 1 hour at room temperature. After three washes for 5 min each in PBST, membranes were visualized by Odysse Infrared Imager.

Section 4.2.6 Reproduction experiment

Mite-free pre-pupa honey bee larva and mature female *T. mercedesae* were collected from *Colony #5* and *#6* respectively. When collecting honey bee larva, I opened the capped brood cells and then sidled the frame in the incubator with 50-60% humidity at 33°C for 1 hour. For the pre-pupa larva (in the developing stages 9-10, Fig.1.4), slipped off capped cells were collected and placed in a gelatin capsule individually with a single mature female *T. mercedesae*. All gelatin capsule were transversely incubated at 50-60°C humidity at 33°C for 12 days. After incubation, live honey bees and *T. mercedesae* (including foundress mites and offspring) samples were simultaneously stored in pairs, which were further used to analyse DWV copy number via qRT-PCR.

Section 4.2.7 Thin-section of ectoparasitic mites

The collected ectoparasitic mites, including *T. mercedesae* and *V. destructor* with distinct sexes and developing stages, were cleaned by bleaching buffer and PBS. Fixation was conducted in 4% PFA in PBS at 4°C with gentle shaking for at least 24 hours. Samples were kept in methanol at 4°C until shipped to German for thin-sectioning by Benjamin Weiss (Johannes Gutenberg University Mainz). Samples were there embedded in Technovit 8100, according to the manufacturer's instructions, subsequently sectioned transversally from cranial to caudal with thickness 4 µm.

Section 4.2.8 Immunofluorescence

Thin-sections of ectoparasitic mites were washed with PBS 5 times for 10 min each, then they were incubated in 2 mg/mL pepsin (0.9% NaCl, pH 2.0) at 37°C for 10 min. After 3 times washes with PBS, 3 times washes with PBS-Triton (0.1% Triton-X 100, PBS), and final wash with PBS, in which 10 min for each wash, all sections were incubated in blocking buffer III at 4°C overnight. The sections which were localized on the slides adjacently were incubated in anti-VPP antibody or pre-immune serum of anti-VPP antibody respectively at 4°C overnight. The antibodies were diluted at 1:100 in blocking buffer III. After washing in PBS 8 times for 10 min each, all sections were incubated in Goat anti-Rabbit IgG (H+L) Superclonal™ Secondary Antibody, Alexa Fluor 555, diluted at 1:1,000 in Blocking buffer III for 1.5 hours at room temperature. After washing 7 times in PBS each for 10 min, sections were incubated with DAPI (Beyotime) with the dilution at 1:1,000 in PBS for 15 min at room temperature. Followed by a final wash in PBS for 10 min, sections were mounted in antifade Mounting Medium (Beyotime).

Section 4.2.9 Confocal microscopy observation

Immunohistochemistry images were obtained by LSM 880 (Zeiss) under 20x objective with the TileScan method. The signals of antigens and nuclei were taken in the Alexa 555 and DAPI channel, respectively. The software ImageJ (Hartig, 2013) was utilized for further image modifications and merge analysis.

Section 4.2.10 qPCR analysis of *Vitellogenin (Vg)*, *Hymenoptaecin* and *Defernsin-1* mRNAs

The amounts of *Vgs* mRNA in *T. mercedesae* and *Hymenoptaecin* and *Defernsin-1* mRNAs in the infested-pupa was measured by a relative quantification qPCR method using a Hieff^{TM} qRT-PCR SYBR Green Master Mix (Low Rox Plus, Yesen) with a QuantStudio5 Real-Time PCR System (Thermo Fisher). Primer sets Vg-1 and Vg-2 were used to detect different sequences of *Vgs* (Supplementary Table). *Hymenoptaecin* and *Defernsin-1* mRNAs were detected by primer sets *Hymenoptaecin* and *Defernsin-1* respectively (Supplementary Table). The relative quantification was performed by the $\triangle\triangle C_T$ method (Pfaffl, 2007). Honey bee *EF-1α* mRNA and *T. mercedesae* 18S rRNA (Supplementary Table) were used as the reference gene for honey bee immune effectors and *T. mercedesae Vg* respectively. The results were expressed as a fold ratio.

Section 4.2.11 Statistical analysis

Western blot results were analysed and quantified by ImageJ (Davarinejad, 2017). Statistical analysis was carried out by *t-test* with software GraphPad Prism (v.7).

Section 4.3 Results

Section 4.3.1 Identification of Differentially Expressed Genes (DEGs) in *T. mercedesae* with high or low DWV copy number

Transcriptomes analysis of single mites with high, medium or low DWV copy number

I previously measured and compared DWV copy numbers in 28 pairs of honey bee pupa and respective infesting *T. mercedesae*, and observed that there is a linear correlation between them. In addition, these 28 pairs were divided to two clusters that were infected by either low or high DWV copy number (Fig.2.5F). In order to determine the effects of DWV on *T. mercedesae*, I picked six mite RNA samples from 28 pairs to conduct RNA-seq analysis for the mites with low, medium or high DWV copy number. There is the duplicate for each sample and they were derived from L, M, and H in the panel A of Fig. 4.1 except one mite sample with low DWV copy number. The levels of DWV in these six samples were further confirmed by RT-PCR (Fig.4.1B).

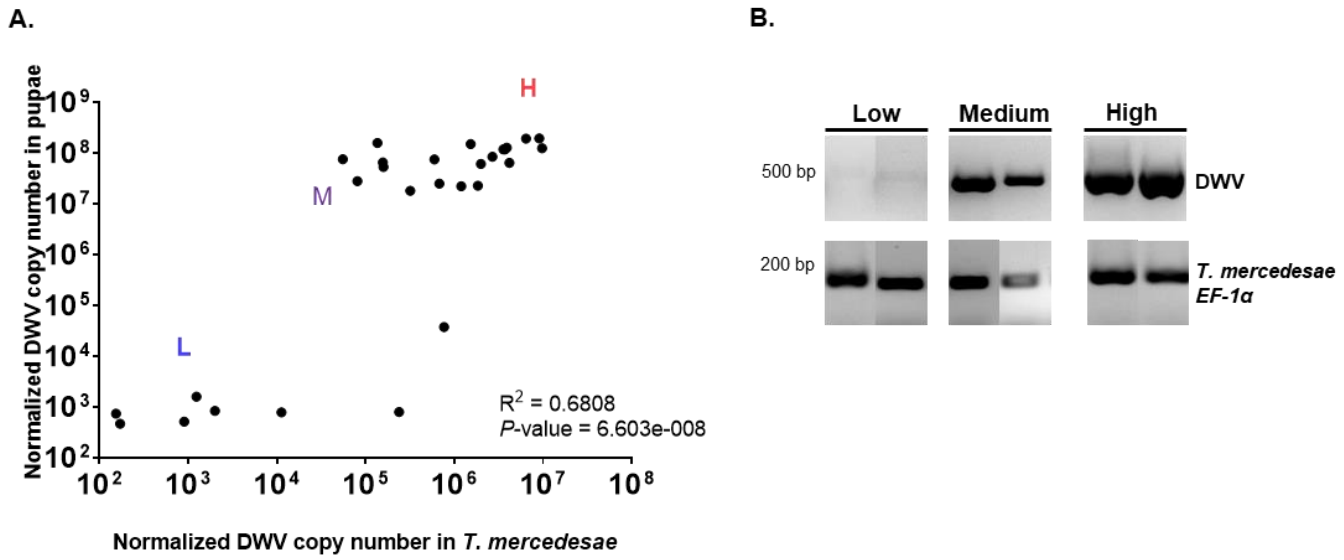

Figure 4.1. qRT-PCR and RT-PCR results of six *T. mercedesae* RNA samples for RNA-seq

(A) DWV copy number in individual honey bee pupa and infesting *T. mercedesae* were plotted on the *Y*- and *X*-axis respectively. Samples were grouped into two clusters, either were low (L) or high (H) DWV copy number. Two mites in the "H" cluster with the highest DWV copy number were selected for high DWV. Two mites in the "H" cluster with relatively lower DWV copy number (M) were selected for medium DWV. One mite in the "L" cluster was selected for low DWV and another sample contained low DWV undetected by qRT-PCR. The Pearson correlation values and *P* values are shown. (B) DWV infection was detected in six mites by RT-PCR and *T. mercedesae EF-1α* mRNA was used as an endogenous positive control. The positions of 500 bp and 200 bp representing bands for DWV and *T. mercedesae EF-1α* mRNA respectively are labelled on the left of agarose gel.

In my cases, Differentially Expressed Genes (DEGs) was determined by EdgeR based on quantifications of expressed genes derived from computational analyses of raw RNA-seq reads (including mapping and assembly) (McDermaid et al., 2019), to provide insights into the genetic influence in *T. mercedesae* caused by DWV infection. The expression differences of certain genes between pairwise comparisons was indicated as Log_2FC, in which FC means for Fold Change, and *P*-value was also calculated by *t-test* (McDermaid et al., 2019, Oshlack et al., 2010). The total RNAs of these six mites were individually subjected to transcriptome analysis and the DEGs of *T. mercedesae* were identified between the mites with low and high, low and medium, and medium and high DWV copy numbers, listed in Table 4.1. Expression of genes encoding vitellogenin, cuticle proteins, and serine protease inhibitor were down-regulated in *T. mercedesae* with higher DWV copy number, and this was common between all three comparisons. Gene predicted to encode a protease-like venom was up-regulated in *T. mercedesae* with high copy number when comparing DEGs between medium and high copy number; however, this gene is down-regulated in the comparison between low and medium copy number. This inconsistent observation was also made in several genes, including *Hypothetical protein BIW11_09464*, and *Partial hypothetical protein BIW11_04518*. There were more DEGs between the mites with low and medium DWV copy numbers. The inconsistent up- or down-regulation in the DEGs identified between above three comparisons, is probably caused by individual heterogeneity in the mites.

Table 4.1 Summary of differentially expressed gene (DEGs) in *T. mercedesae* with different DWV copy number.

1) DEGs in *T. mercedesae* with low and high DWV copy number infection.

	Annotations	**Log_2FC**	***P* value**
DEGs in *T. mercedesae* with low and high DWV copy number	vitellogenin 1-like [*Tropilaelaps mercedesae*]	-14.643	5.00E-05
	vitellogenin 2-like [*Tropilaelaps mercedesae*]	-6.77752	5.00E-05
	cuticle protein 14-like, partial [*Tropilaelaps mercedesae*]	-7.29126	5.00E-05
	PREDICTED: cuticle protein 16.8-like [*Galendromus occidentalis*]	-3.07573	5.00E-05
	serine protease inhibitor [*Argopecten irradians*] (E-12)	-4.26431	5.00E-05
	PREDICTED: serine protease inhibitor dipetalogastin-like [*Nicrophorus vespilloides*] (E-07)	-3.62226	5.00E-05
	hypothetical protein BIW11_01042 [*Tropilaelaps mercedesae*]	-2.26162	5.00E-05
	hypothetical protein BIW11_02070 [*Tropilaelaps mercedesae*]	2.70176	5.00E-05
	hypothetical protein BIW11_06807 [*Tropilaelaps mercedesae*]	-2.48233	5.00E-05
	hypothetical protein BIW11_11053 [*Tropilaelaps mercedesae*]	-3.19154	5.00E-05

2) DEGs in *T. mercedesae* with low and medium DWV copy number infection.

	Annotations	**Log_2FC**	***P* value**
DEGs in *T. mercedesae* with low and medium DWV copy number	vitellogenin 1-like [Tropilaelaps mercedesae]	-14.5174	5.00E-05
	cuticle protein 10.9-like [*Tropilaelaps mercedesae*]	-1.64754	5.00E-05
	cuticle protein 10.9, partial [*Stegodyphus mimosarum*] (E-17)	-3.05427	5.00E-05
	PREDICTED: cuticle protein 16.8-like [*Galendromus occidentalis*]	-1.48293	0.00015
	hypothetical protein BIW11_04159 [*Tropilaelaps mercedesae*], PREDICTED: serine protease inhibitor dipetalogastin-like [*Nicrophorus vespilloides*](E-10)	-3.5455	5.00E-05
	PREDICTED: serine protease inhibitor dipetalogastin-like [*Nicrophorus vespilloides*] (E-07)	-2.06658	5.00E-05
	hypothetical protein BIW11_00405 [*Tropilaelaps mercedesae*]	-2.92255	5.00E-05
	hypothetical protein BIW11_02978 [*Tropilaelaps mercedesae*]	-1.64621	0.00015
	hypothetical protein BIW11_04251 [*Tropilaelaps mercedesae*]	-2.23896	5.00E-05
	hypothetical protein BIW11_04518, partial [*Tropilaelaps mercedesae*]	-3.83626	5.00E-05
	hypothetical protein BIW11_04689 [*Tropilaelaps mercedesae*]	-1.65819	5.00E-05
	hypothetical protein BIW11_04897 *[Tropilaelaps mercedesae*]	-5.096	5.00E-05
	hypothetical protein BIW11_05105 [*Tropilaelaps mercedesae*]	-2.03273	5.00E-05
	hypothetical protein BIW11_06807 [*Tropilaelaps mercedesae*]	-1.72977	0.0001
	hypothetical protein BIW11_07325 [*Tropilaelaps mercedesae*]	-2.1103	5.00E-05
	hypothetical protein BIW11_07854 [*Tropilaelaps mercedesae*]	-1.45426	0.0003
	hypothetical protein BIW11_09464 [*Tropilaelaps mercedesae*]	3.6297	5.00E-05
	hypothetical protein BIW11_09521 [*Tropilaelaps mercedesae*]	-3.55962	5.00E-05

	hypothetical protein BIW11_10521, partial [*Tropilaelaps mercedesae*]	-1.76608	0.0003
	hypothetical protein BIW11_10715 [*Tropilaelaps mercedesae*]	-2.61456	0.00015
	hypothetical protein BIW11_12564 [*Tropilaelaps mercedesae*]	-3.5474	5.00E-05
	hypothetical protein BIW11_14202 [*Tropilaelaps mercedesae*]	-3.70207	5.00E-05
	cytochrome P450 4c3-like [*Tropilaelaps mercedesae*], Tm_01415	2.25036	5.00E-05
	cytochrome P450 4V2-like, partial [*Tropilaelaps mercedesae*], Tm_06642	2.08724	5.00E-05
	thromboxane-A synthase-like, partial [*Tropilaelaps mercedesae*], PREDICTED: cytochrome P450 3A6-like [*Galendromus occidentalis*] (E-65), Tm_07853	1.93953	0.0001
	thromboxane-A synthase-like [*Tropilaelaps mercedesae*], PREDICTED: cytochrome P450 3A6-like [*Galendromus occidentalis*] (E-167)	1.64505	5.00E-05
	PREDICTED: venom protease-like [*Cyphomyrmex costatus*] (E-08)	-3.97239	5.00E-05
	alpha-tocopherol transfer protein-like [*Tropilaelaps mercedesae*]	3.06173	5.00E-05
	alpha-tocopherol transfer protein-like [*Tropilaelaps mercedesae*]	1.52579	5.00E-05
	actin, partial [*Tropilaelaps mercedesae*]	-1.64565	0.0001
	actin [*Tropilaelaps mercedesae*]	-1.81519	5.00E-05
	transmembrane protein-like [*Tropilaelaps mercedesae*], PREDICTED: heat shock protein 67B2 [*Drosophila bipectinata*] (E-15)	-1.6168	5.00E-05
	chymotrypsin elastase family member 3B-like [*Tropilaelaps mercedesae*]	2.43893	5.00E-05
	TBC1 domain family member 20-like [*Tropilaelaps mercedesae*] GAP	1.7134	0.0002
	facilitated trehalose transporter Tret1-like [*Tropilaelaps mercedesae*]	1.43694	0.0001
	PREDICTED: pappalysin-1-like [*Saccoglossus kowalevskii*] (E-92)	-2.5803	5.00E-05
	ribonuclease UK114-like [*Tropilaelaps mercedesae*], RidA family protein [*Clostridium baratii*] (E-41)	-1.21275	0.00025
	acetylcholine receptor subunit alpha-type acr-16-like [*Tropilaelaps mercedesae*]	-2.66034	5.00E-05
	hypothetical protein BIW11_10956 [*Tropilaelaps mercedesae*], PREDICTED: skin secretory protein xP2-like [*Galendromus occidentalis*] (E-15)	-3.39952	5.00E-05
	phospholipase A2-like [*Tropilaelaps mercedesae*]	1.98007	5.00E-05

	gamma-butyrobetaine dioxygenase-like [*Tropilaelaps mercedesae*]	1.3396	0.0002
	palmitoyl-protein thioesterase 1-like [*Tropilaelaps mercedesae*]	-1.30455	0.0002
	ganglioside GM2 activator-like [*Tropilaelaps mercedesae*]	-3.77396	5.00E-05
	dimethylaniline monooxygenase-like [*Tropilaelaps mercedesae*]	1.64085	0.00015
	aminoglycoside phosphotransferase domain-containing protein 1-like [*Tropilaelaps mercedesae*], PREDICTED: hydroxylysine kinase [*Galendromus occidentalis*](E-95)	1.9255	5.00E-05
	receptor-transporting protein 2-like [*Tropilaelaps mercedesae*]	1.66205	5.00E-05
	lipase member H-A-like [*Tropilaelaps mercedesae*]	-3.33681	0.0002
	elongation of very long chain fatty acids protein-like [*Tropilaelaps mercedesae*] Up	1.40236	0.0003
	proton-coupled folate transporter-like [*Tropilaelaps mercedesae*], putative adenylate cyclase, partial [*Amblyomma sculptum*] (E-98)	-3.36304	0.00025
	hypothetical protein BIW11_05523 [*Tropilaelaps mercedesae*], Fuseless [*Daphnia magna*] (E-24)	1.43686	5.00E-05
	microsomal triglyceride transfer protein large subunit-like [*Tropilaelaps mercedesae*]	-2.58786	5.00E-05
	4-hydroxyphenylpyruvate dioxygenase-like [*Tropilaelaps mercedesae*]	-1.39131	0.00015

3) DEGs in *T. mercedesae* with medium and high DWV copy number infection.

	Annotations	**Log_2FC**	***P* value**
DEGs in *T. mercedesae* with medium and high DWV copy number	vitellogenin 2-like [*Tropilaelaps mercedesae*]	-2.88321	5.00E-05
	PREDICTED: cuticle protein 16.8-like [*Galendromus occidentalis*]	-2.11668	5.00E-05
	PREDICTED: serine protease inhibitor dipetalogastin-like [*Nicrophorus vespilloides*] (E-08)	-2.80799	5.00E-05
	hypothetical protein BIW11_02070 [*Tropilaelaps mercedesae*]	2.21348	5.00E-05
	hypothetical protein BIW11_04518, partial [*Tropilaelaps mercedesae*]	3.07375	5.00E-05
	hypothetical protein BIW11_09464 [*Tropilaelaps mercedesae*]	-2.3642	5.00E-05
	hypothetical protein BIW11_11053 [*Tropilaelaps mercedesae*]	-1.99163	5.00E-05
	hypothetical protein BIW11_14202 [*Tropilaelaps mercedesae*]	-2.06143	5.00E-05
	PREDICTED: venom protease-like [*Cyphomyrmex costatus*]	3.66102	5.00E-05
	secreted salivary gland, partial [*Ornithodoros brasiliensis*] (E-21)	-1.8147	5.00E-05
	cathepsin L-like [*Tropilaelaps mercedesae*]	-1.73661	5.00E-05

The value of Log_2FC indicates expression differences of the specific gene between pairwise comparisons, and the greater absolute value of Log_2FC means larger differences between two comparisons. The positive and negative

Log_2FC respectively designate up-regulated and down-regulated genes in *T. mercedesae* by higher DWV copy number infection. *P*-value was calculated by *t-test*.

Comparison of the transcriptomes for 20 T. mercedesae with high or low DWV copy number

In order to decrease the influence of individual mite heterogeneity on transcriptome analysis, I selected 40 *T. mercedesae* with either high or low DWV copy number for the RNA-seq. Based on their RT-PCR and qRT-PCR results for DWV and 18S rRNA, these 40 mites were divided to 4 groups as High_A, High_B, Low_A and Low B and each group consisted of 10 mites' total RNAs. For High_A and High_B, all mites contained high DWV copy numbers, while Low_A and Low_B had low DWV copy numbers. Their RT-PCR results were consistent with either low or high DWV copy number in the individual mite (Fig.4.2A).

The assembled RNA-seq reads of each sample were first mapped to the genome of *T. mercedesae* and DWV genome. Very few reads of both Low_A and Low_B samples mapped to DWV genome, whereas 22-23% of total reads in High_A and High_B samples mapped to DWV genome (Fig.4.2B-C). Using the threshold value of adjustment *P* value as 0.01 and FDR value as 0.05, there were totally 15 DEGs identified between Low and High groups.

A.

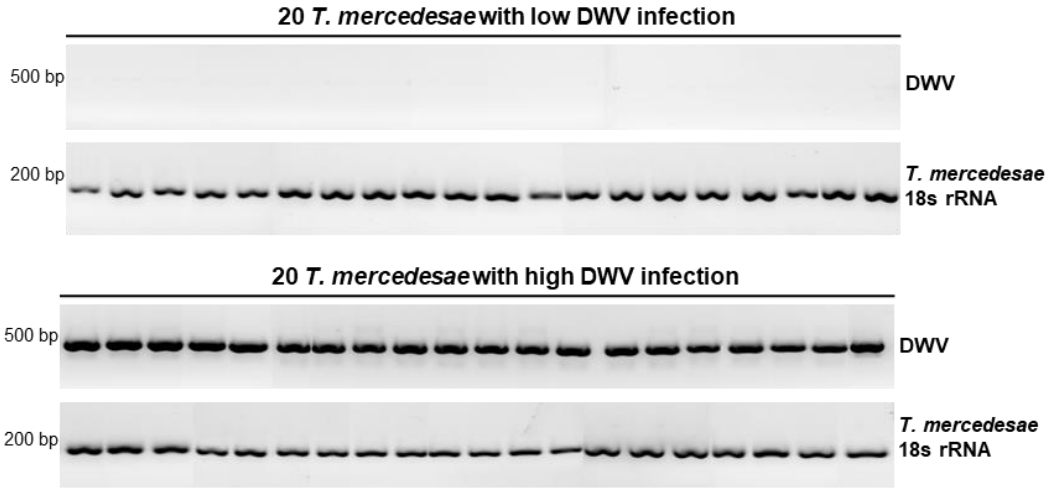

B.

Overall alignment rates of RNA-seq reads

Sample	Against *T. mercedesae* genome	Against DWV genome
High_A	37.73%	22.45%
High_B	39.64%	23.12%
Low_A	80.44%	0.08%
Low_B	85.53%	0.01%

C.

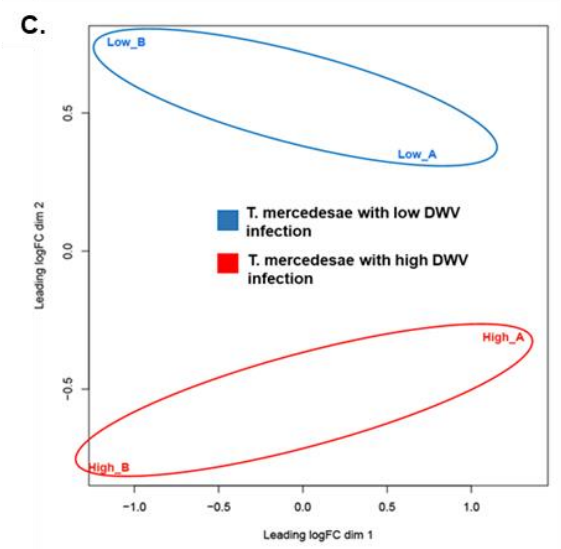

Figure 4.2 *T. mercedesae* RNA samples with high or low DWV copy number for RNA-seq.

Forty *T. mercedesae* were selected for RNA-seq and divided to 4 groups, High_A, High_B, Low_A and Low_B. Each group consisted of 10 mites' RNAs. (A) DWV was detected in 40 *T. mercedesae* by RT-PCR and *T. mercedesae* 18S rRNA was used as the endogenous positive control. The positions of 500 bp and 200 bp representing bands for DWV and *T. mercedesae* 18S rRNA respectively are labelled on the left of agarose gel. (B) The assembled RNA-seq reads of 4 groups were aligned against *T. mercedesae* genome and DWV genome. (C) Multidimensional scaling plots of 4 RNA samples. The distance between 2 samples reflects the leading fold-change of the corresponding RNA samples. The leading logFC is the root mean square value for 500 genes most divergent between these two RNA samples. High_A and High_B are coloured by red, while Low_A and Low_B are coloured by blue.

As shown in Table.4.2, there were only 10 down-regulated and 5 up-regulated genes in *T. mercedesae* by high DWV copy number. Among these 15 DEGs, six were also identified in the transcriptome analysis of six individual *T. mercedesae* with different DWV copy numbers. These are *Vitellogenein-1-like* and *Larval cuticle protein A3A-like* (down-regulated), and *Lipase member H-A-like*, *Chymotrypsin elastase family member 3B-like*, *Hypothetical protein BIW11_04159* (predicted: serine protease inhibitor dipetalogastin-like [*Nicrophorus vespilloides*]) and *Hypothetical protein BIW11_12564* (up-regulated) (Table.4.1). Since the number of DEGs in *T. mercedesae* with high DWV copy numbers is few, suggesting high level of DWV presenting in the mites without active replication. Additionally, the down-regulated expression of *Vg* in the mites with high DWV copy number suggests the potential negative influence of virus on the mite's reproductive capability.

Table. 4.2 Summary of down- and up-regulated genes in *T. mercedesae* with DWV infection.

1) Down-regulated *T. mercedesae* genes by DWV infection.

Annotations	**Gene**	**Log_2FC**	***P* value**
Vitellogenin 1-like	OQR79705.1	1.309646324	1.71E-05
Hypothetical protein BIW11_07447	OQR76942.1	2.156576728	2.57E-06
Hypothetical protein BIW11_11788	OQR70191.1	2.172344236	1.85E-08
Cement protein RIM36-like	OQR75105.1	4.027534008	6.01E-06
Larval cuticle protein A3A-like	OQR67513.1	5.187458547	1.70E-05
Hypothetical protein BIW11_00866	OQR74958.1	5.205619337	1.68E-06
Nose resistant to fluoxetine protein 6-like	OQR67746.1	7.436117627	7.87E-07
Hypothetical protein BIW11_11234	OQR71056.1	7.732854356	1.03E-06
Hypothetical protein BIW11_12957	OQR68367.1	8.176909031	1.22E-06
Zinc finger protein-like	OQR70206.1	9.327941587	1.80E-14

2) Up-regulated *T. mercedesae* genes by DWV infection.

Annotations	**Gene**	**Log_2FC**	***P* value**
Hypothetical protein BIW11_12564	OQR68960.1	-0.91429	4.31E-05
Chymotrypsin elastase family member 3B-like	OQR72005.1	-1.01624	8.45E-06
Hypothetical protein BIW11_06990, partial	OQR77579.1	-1.0391	5.30E-05
Hypothetical protein BIW11_04159	OQR70413.1	-1.08955	3.44E-06
Lipase member H-A-like	OQR67497.1	-1.13119	1.50E-06

The value of Log_2FC indicates expression differences of the specific gene between pairwise comparisons, and the greater absolute value of Log_2FC means larger differences between two comparisons. The positive and negative Log_2FC respectively designate down-regulated and up-regulated genes in *T. mercedesae* by high DWV copy number infection. *P*-value was calculated by *t-test*.

Section 4.3.2 RdRP was not detected in *V. destructor* and *T. mercedesae* with high DWV, suggesting DWV does not replicate

In order to test whether DWV replicates in the ectoparasitic mites, their protein lysates were subjected to western blot using the anti-RdRP antibody. The anti-VP1 antibody was also utilized to detect endogenous DWV by structural protein, VP1. As the essential component for DWV replication, RdRP was not detected in either *T. mercedesae* nor *V. destructor* with high DWV load; however, it was detected in the infected honey bee (Fig.4.3A). The quantitative western blot analysis also indicates that the ratio of RdRP to VP1 was significantly lower in both *T. mercedesae* (*P* value = 0.0004, two-tailed *t test*) and *V. destructor* (*P* value = 0.0011, two-tailed *t test*) compared to that of honey bee (Fig.4.3B). These results provide evidence that DWV does not replicate in the mites.

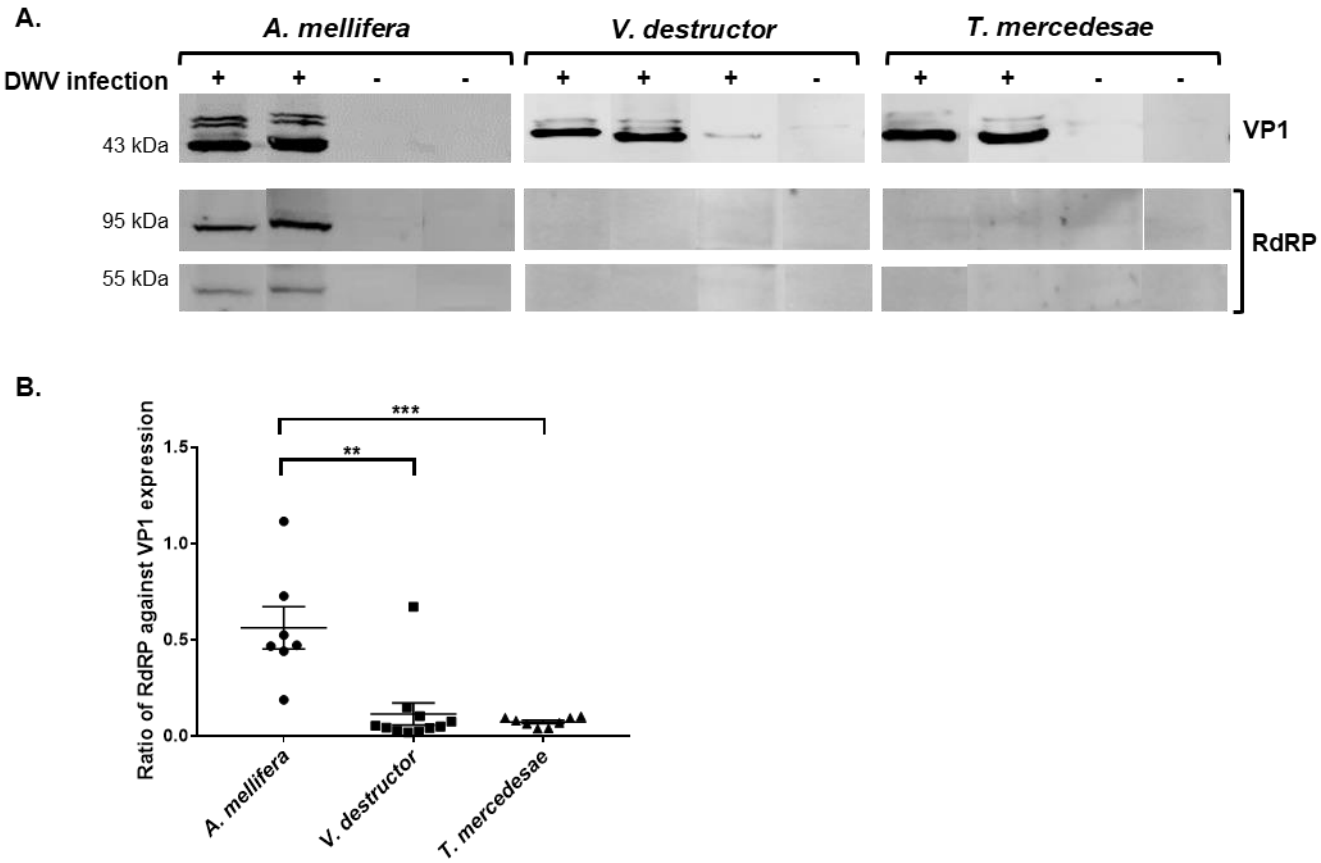

Figure 4.3. Detection of DWV replication in honey bee, *V. destructor* and *T. mercedesae*.

(A) The protein lysates of honey bee pupal head, *V. destructor* and *T. mercedesae* were subjected to western blot with anti-RdRP antibody and anti-VP1 antibody. The clear band near 43 kDa corresponds to VP1 while duplex bands near 95 kDa and 55 kDa for RdRP. (B) The quantitative analysis of western blot results by calculating the ratios of RdRP against VP1 expression. The RdRP/VP1 expression ratio was significantly lower in *V. destructor* (*P* value = 0.0011, two tailed *t-test*) and *T. mercedesae* (*P* value = 0.0004, two tailed *t-test*) compared to in honey bee. The mean value with error bar (±SEM) is indicated for each sample (**P* value ≤ 0.05; ***P* value ≤ 0.01).

Section 4.3.3 Negative correlation between reproductive capability of *T. mercedesae* and the DWV copy number

Vitellogenin is the precursor of a major yolk protein, vitellin, which is the critical nutrient for embryo development in many oviparous animals (Postlethwait and Giorgi, 1985, Tufail and Takeda, 2008). *Vg* mRNA appeared to decrease with high DWV copy number in *T. mercedesae* (Table.4.1 & Table.4.2), suggesting that DWV probably affects mite's reproductive capability via regulating *Vg* expression. In order to test whether DWV has the negative effects on reproductive capability, I conducted a reproduction test, in which single matured female mite was inoculated with single honey bee larva inside a gelatin capsule under laboratory condition. After 12 days incubation, the number of progeny was counted and investigated the association with DWV copy number in the foundress mite.

There were 4, 5, and 8 foundress mites producing 2, 1, and no progenies, respectively. DWV copy numbers in the foundress mites without progeny were higher than those in the foundress mites with single or two progenies, but this correlation was not significant (*P* value > 0.05, two-tailed *t-test*) (Fig.4.4A). Compared to the reproductive female mites, DWV copy numbers in the non-reproductive mites was significantly higher (*P* value = 0.0357, two tailed *t-test*) and more non-reproductive mites contained DWV higher than 10^6 copy number than reproductive mites (Fig.4.4B). These results suggest the adverse effect of high DWV load on *T. mercedesae*'s reproductive capability.

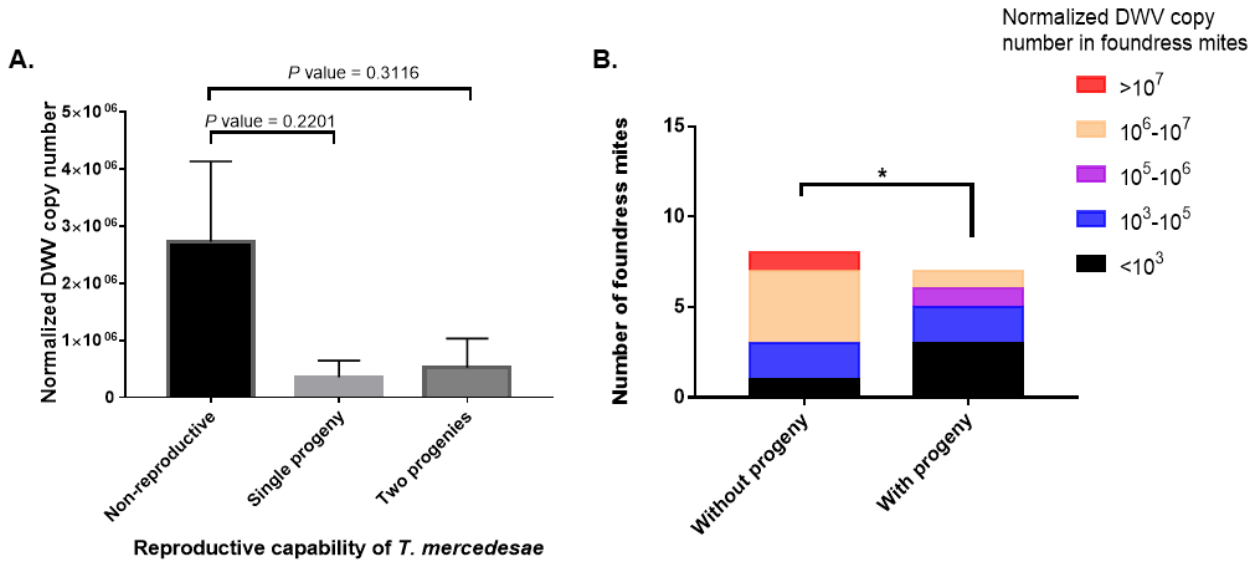

Figure 4.4. Reproductive capability of foundress *T. mercedesae* with different copy numbers of DWV.
(A) The DWV copy number in foundress *T. mercedesae* with one progeny (n = 5), two progenies (n = 4), and without progeny production (n = 8). (B) The profile of DWV copy numbers in foundress mites with (n = 9) or without (n = 8) progeny production. The mean value with error bar (±SEM) is indicated for each sample (**P* value ≤ 0.05).

Section 4.3.4 The localization of DWV in *V. destructor* and *T. mercedesae*

The localization of DWV inside the ectoparasitic mites provides insight into the relationship between DWV and mites. As mentioned in Section 3.3.2, DWV structural protein, VP1, was successfully detected by anti-

VP1P antibody via immunofluorescence. Therefore, this antibody was used to localize the virus inside *V. destructor* and *T. mercedesae*. Both ectoparasitic mites, *V. destructor* and *T. mercedesae* were sectioned transversally from cranial to caudal. The sections were alternatively subjected for immunofluorescence using anti-VP1P antibody or the pre-immune serum to compare the staining patterns of two adjacent sections.

In all sections of female, male and nymph *T. mercedesae*, DWV was primarily detected in the middle and posterior regions of bodies but absent in the anterior cranial and mouthpart regions. The signals were aggregated in the gastric and intestinal tissues. For female sections of *T. mercedesae*, DWV signals were also detected in muscle tissues located in the middle region of mite body, and DWV signals located in intestinal regions were primarily in the post-colon, which is the distal part of the midgut (Fig.4.5). The gastric caecum, rectum and colon showed the specific staining in all sections of male *T. mercedesae* (Fig.4.6). Due to the incomplete development and maturation of nymph mites, their specific body structures are difficult to determine. Nevertheless, DWV appears to be located in the gastric caecum and rectum (Fig.4.7). Compared to female and nymph mites, strong signals were observed in males perhaps because of higher DWV load.

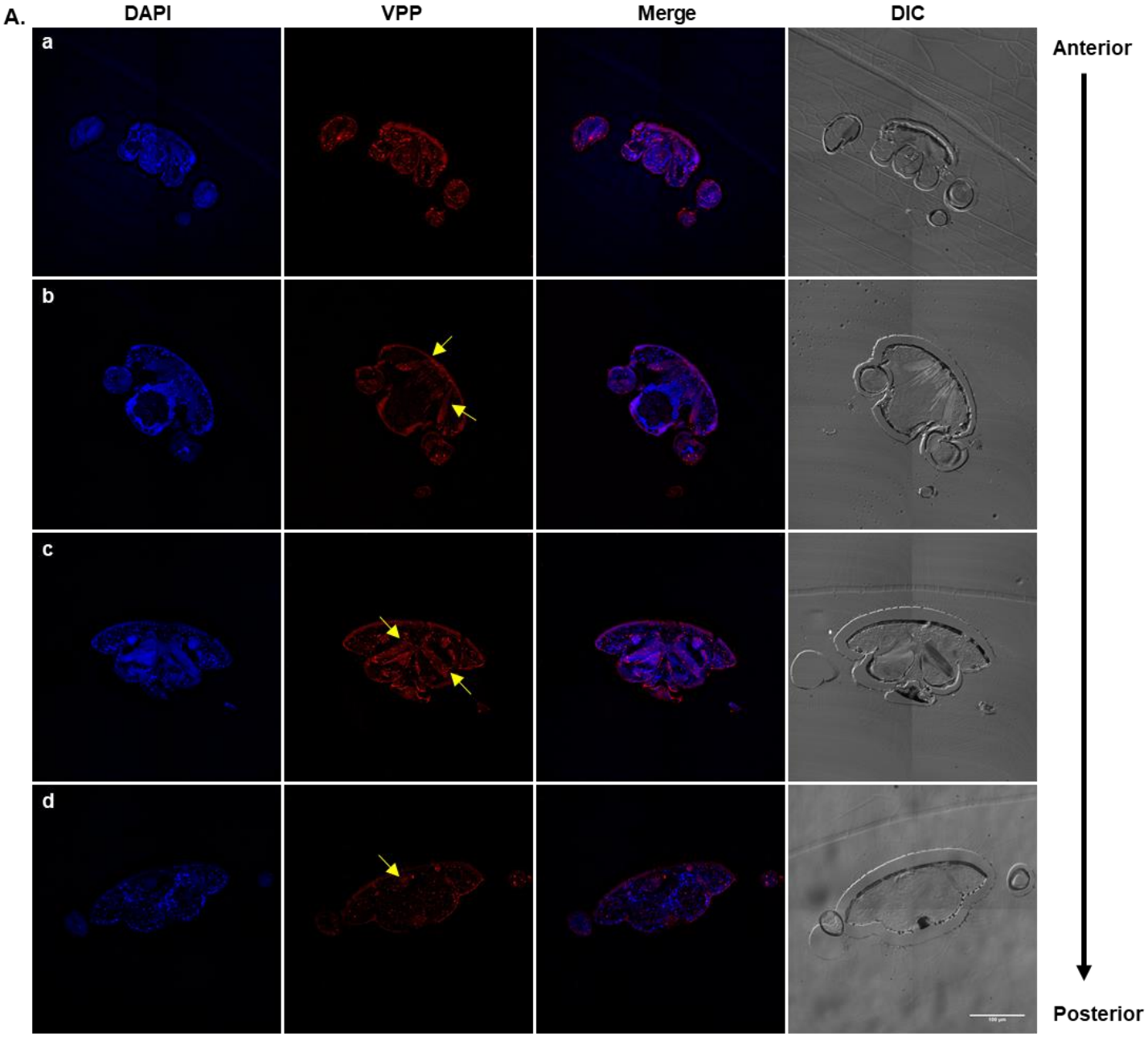
A.
DAPI
VPP
Merge
DIC
a
b
c
d
Anterior
Posterior

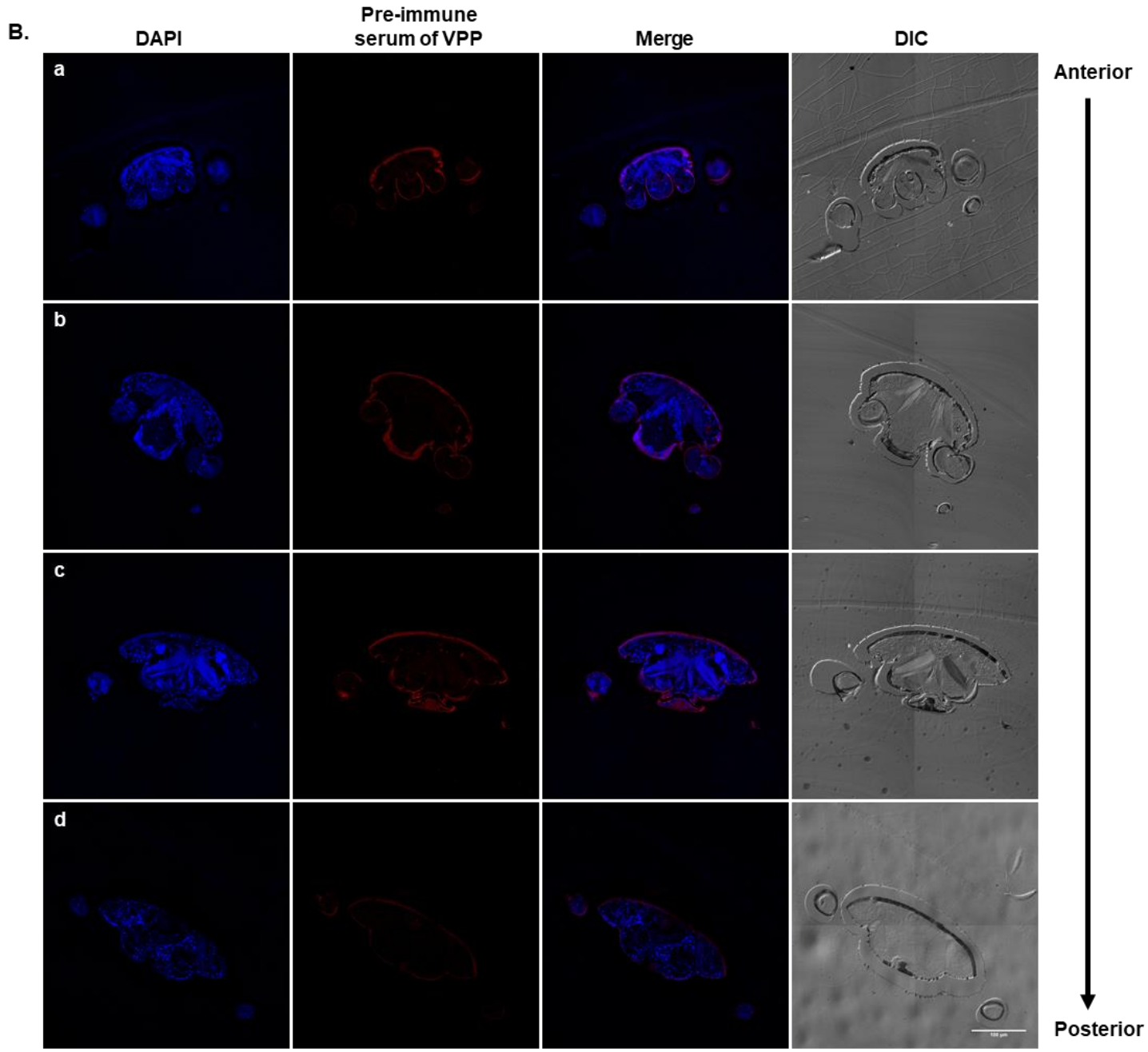

Figure. 4.5. Localization of DWV in transversal sections of female *T. mercedesae*.

The transversal sections of female *T. mercedesae* were subjected to (A) anti-VP1P antibody or (B) pre-immune serum of anti-VP1P antibody. The a-d indicates sections from cranial to caudal. Detection of antigens were taken in the Alexa 555 channel and indicated as red colour. The nuclei were counterstained with DAPI (blue). The signals of binding to DWV were highlighted by yellow arrows. Bar scale representing 100 µm was shared by all images.

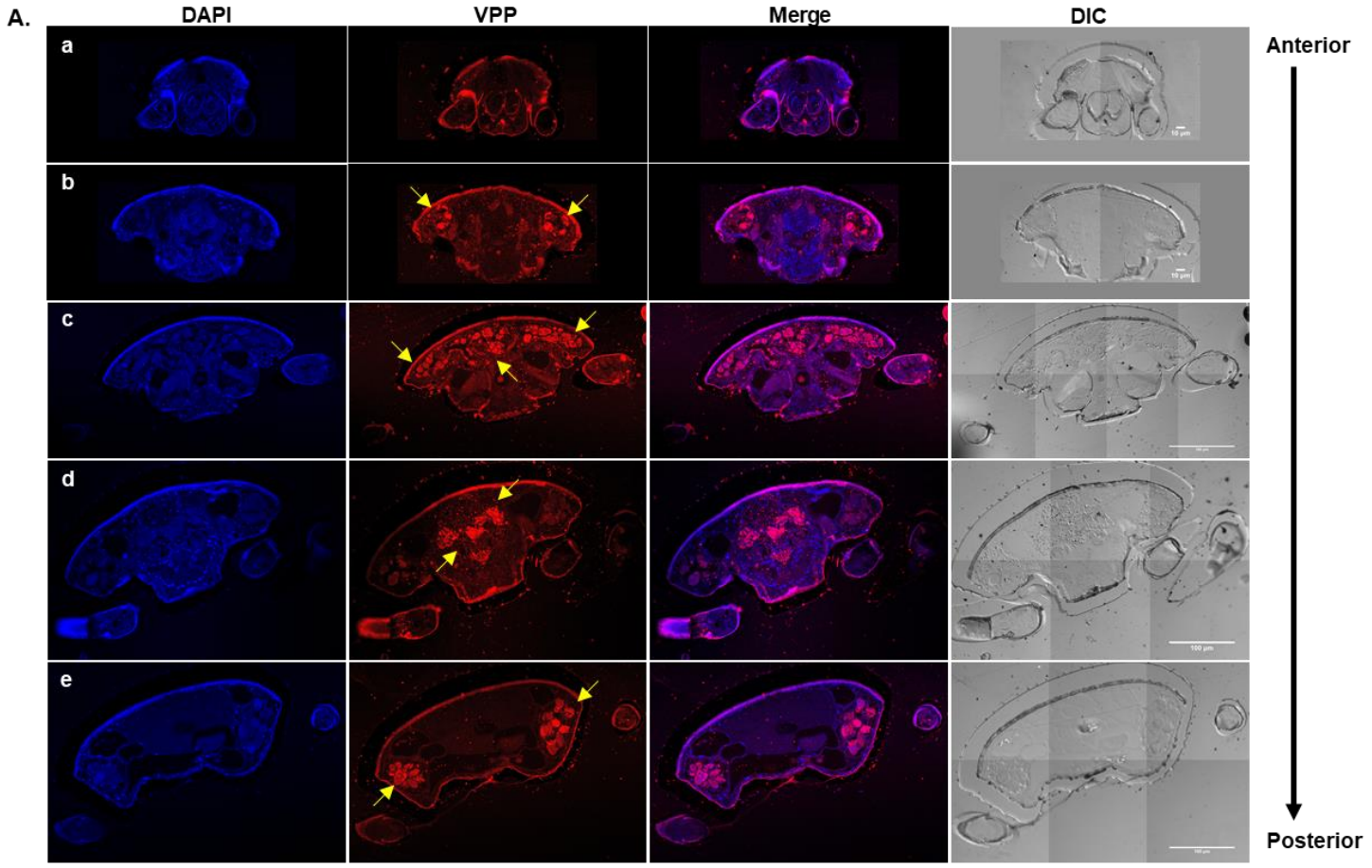
A.
DAPI
VPP
Merge
DIC
a
b
c
d
e
Anterior
Posterior

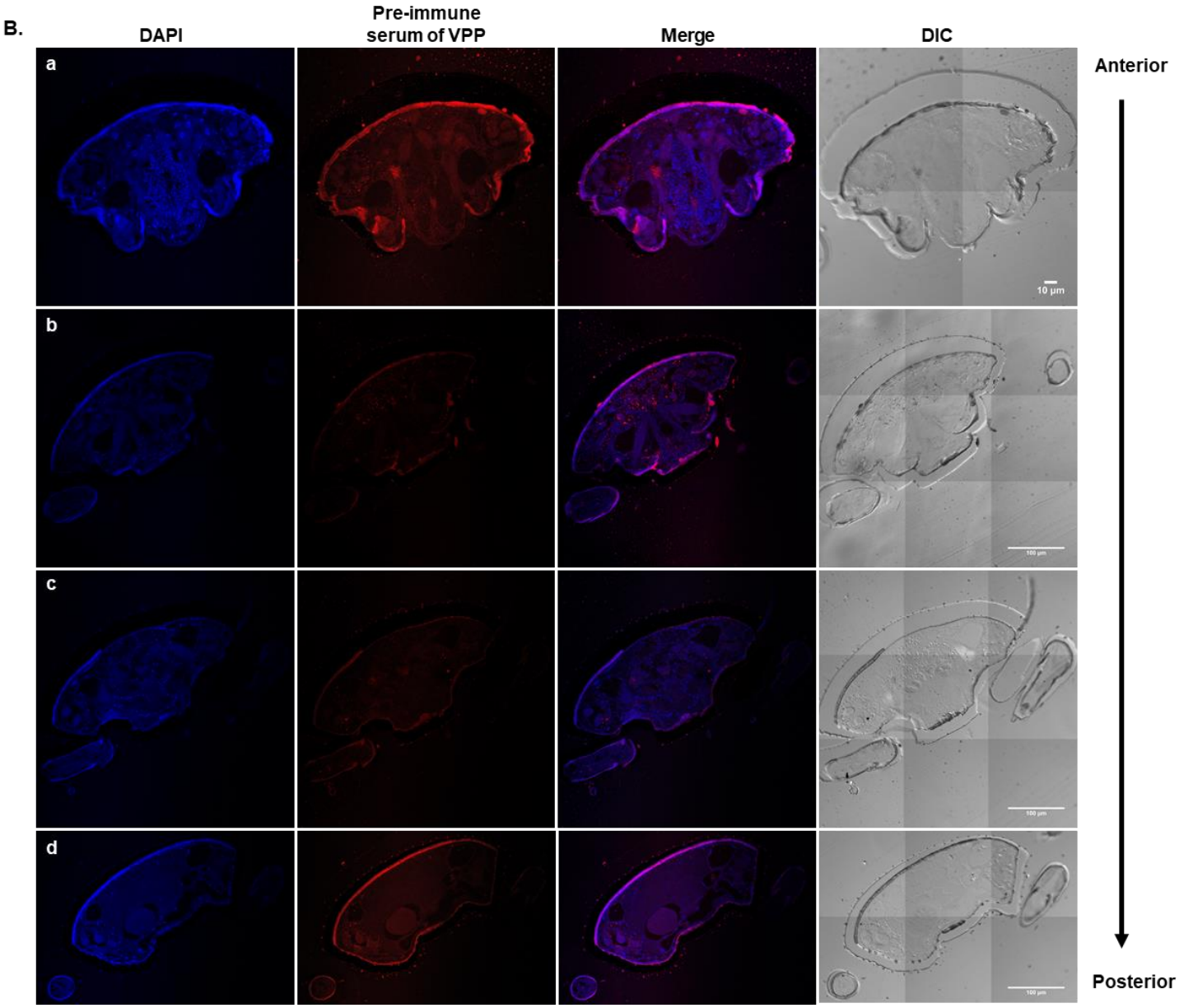

Figure. 4.6. Localization of DWV in transversal sections of male *T. mercedesae*.

The transversal sections of male *T. mercedesae* were subjected to (A) anti-VP1P antibody or (B) pre-immune serum of anti-VP1P antibody. The a-e(d) indicates sections from cranial to caudal. Detection of antigens were taken in the Alexa 555 channel and indicated as red colour. The nuclei were counterstained with DAPI (blue). The signals of binding to DWV were highlighted by yellow arrows. Bar scale, which represents 10 or 100 µm and is shown at the bottom of DIC image, was shared by the same section taken under different channels.

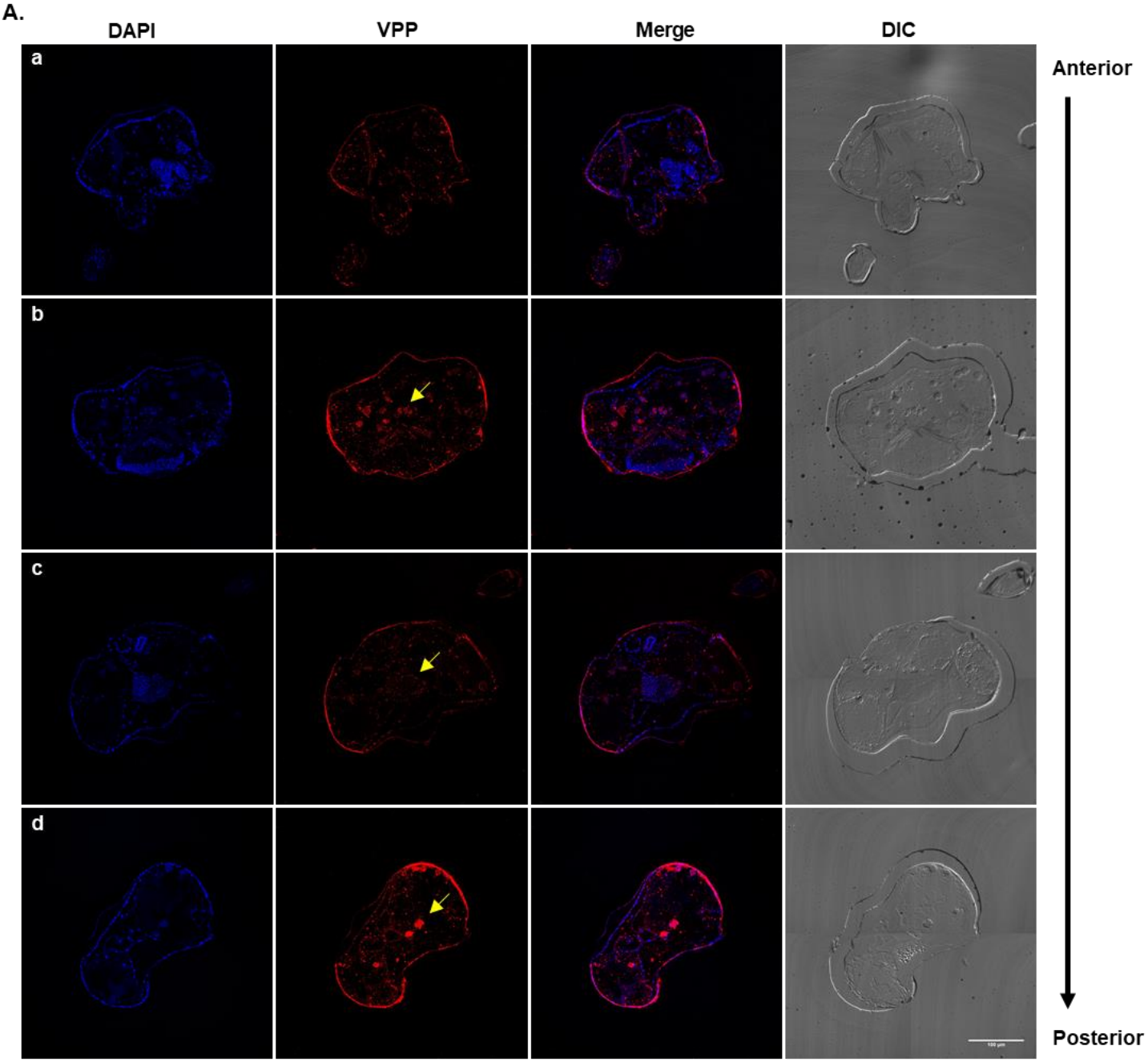
A.
DAPI
VPP
Merge
DIC
a
b
c
d
Anterior
Posterior

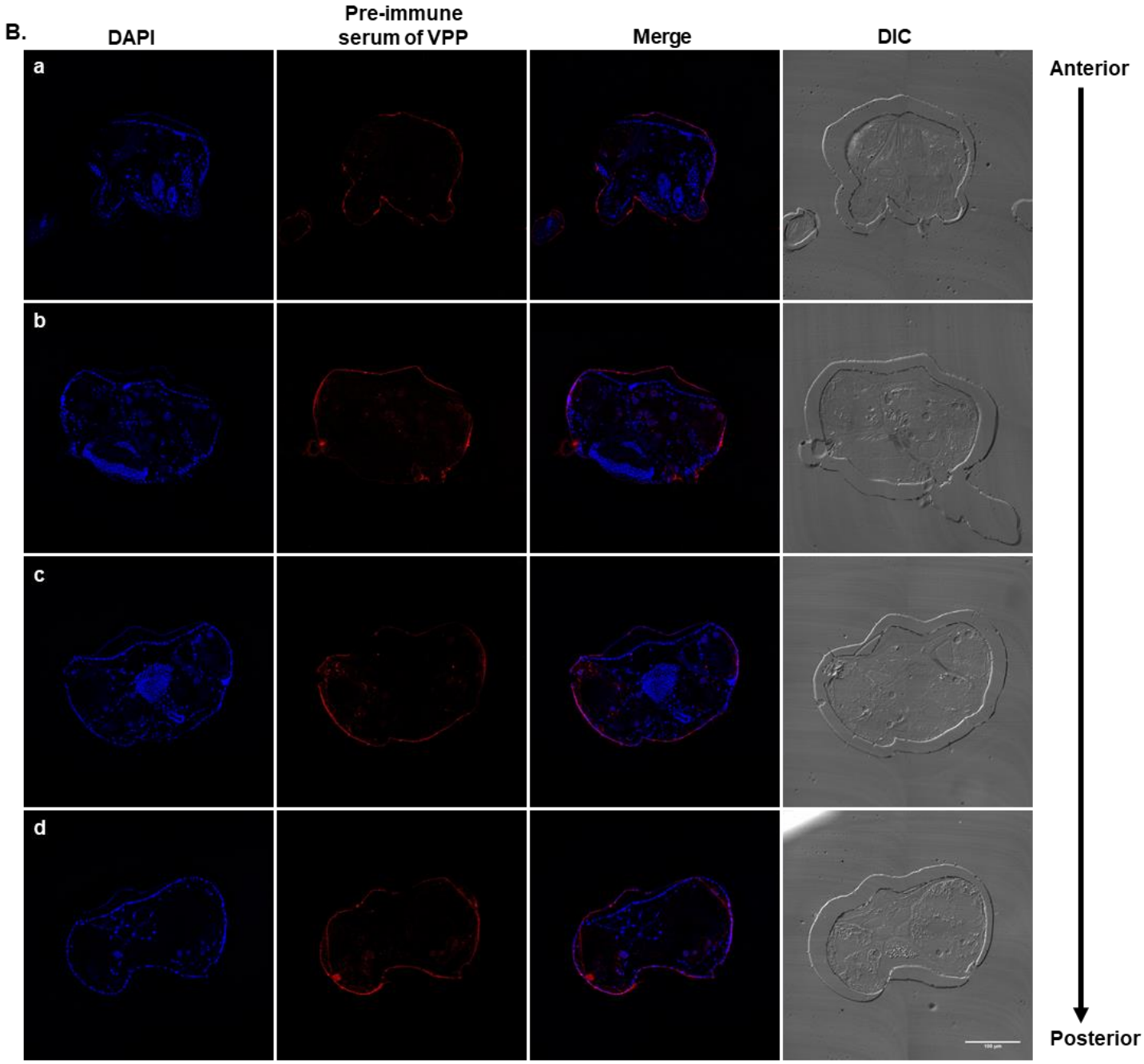

Figure. 4.7. Localization of DWV in transversal sections of nymphal *T. mercedesae*.

The transversal sections of nymphal *T. mercedesae* were subjected to (A) anti-VP1P antibody or (B) pre-immune serum of anti-VP1P antibody. The a-d indicates sections from cranial to caudal. Detection of antigens were taken in the Alexa 555 channel and indicated as red colour. The nuclei were counterstained with DAPI (blue). The signals of binding to DWV were highlighted by yellow arrows. Bar scale representing 100 μm was shared by all images.

Varroa destructor was also sectioned transversally from cranial to caudal, and all sections were immunostained as above. Unfortunately, there were no significant specific signals in all nymphal sections tested, perhaps because of the low DWV load. For all sections of female and male *V. destructor*, the specific signals were primarily visualized in the middle and posterior parts of body, which was similar to *T. mercedesae*. In female mites, DWV signals were observed in the gastric caecum, rectum, colon, and lyrate organ and primarily detected as the dense spheres (Fig.4.8). Compared to female *V. destructor*, male mites have distinct body shape and structure with weaker sclerotization. Therefore, the specific organs

and tissues inside male mites are difficult to determine. Based on its immunofluorescent images, the signals were localized in the gut tissues, probably gastric caecum and rectum (Fig.4.9).

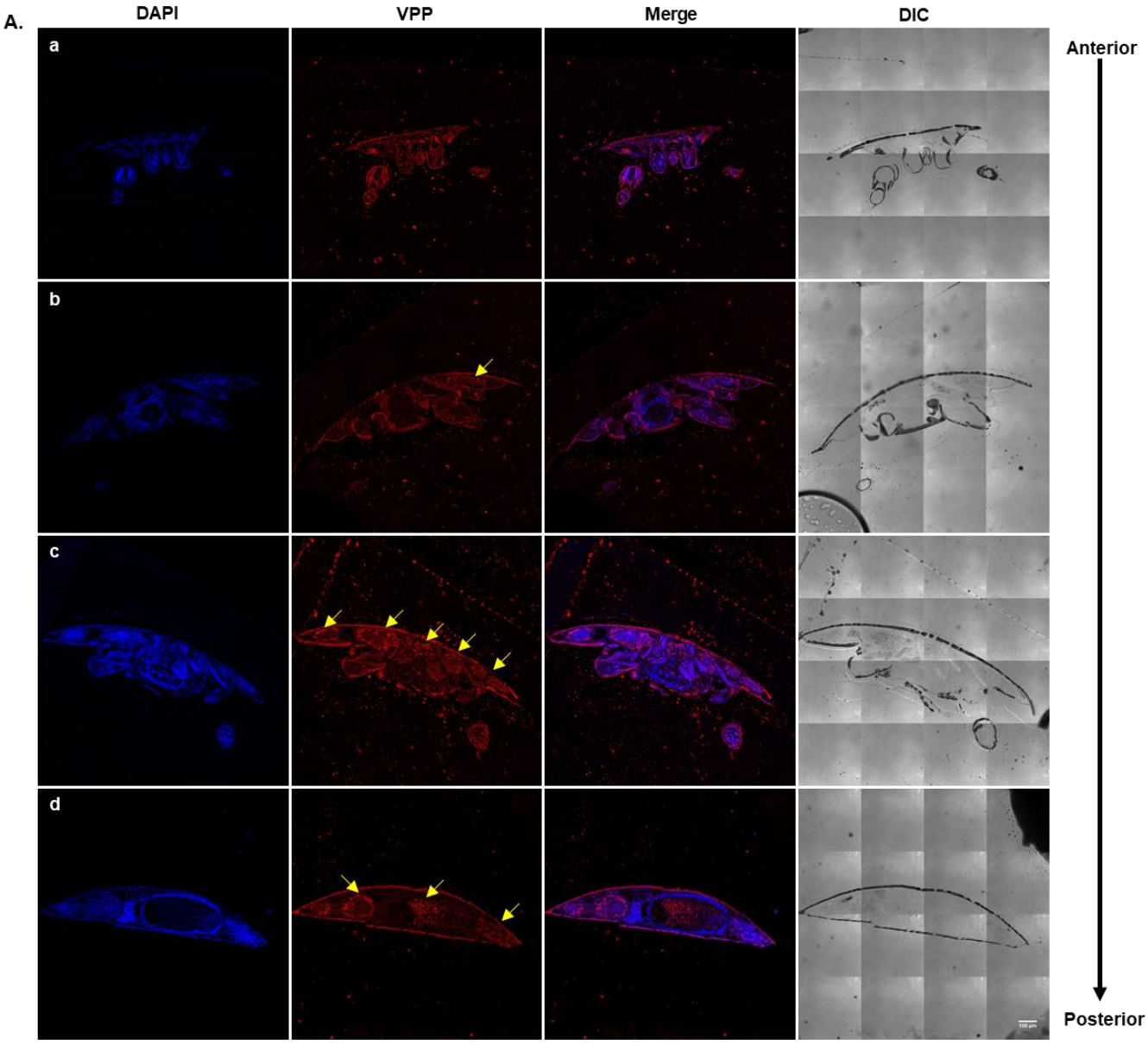

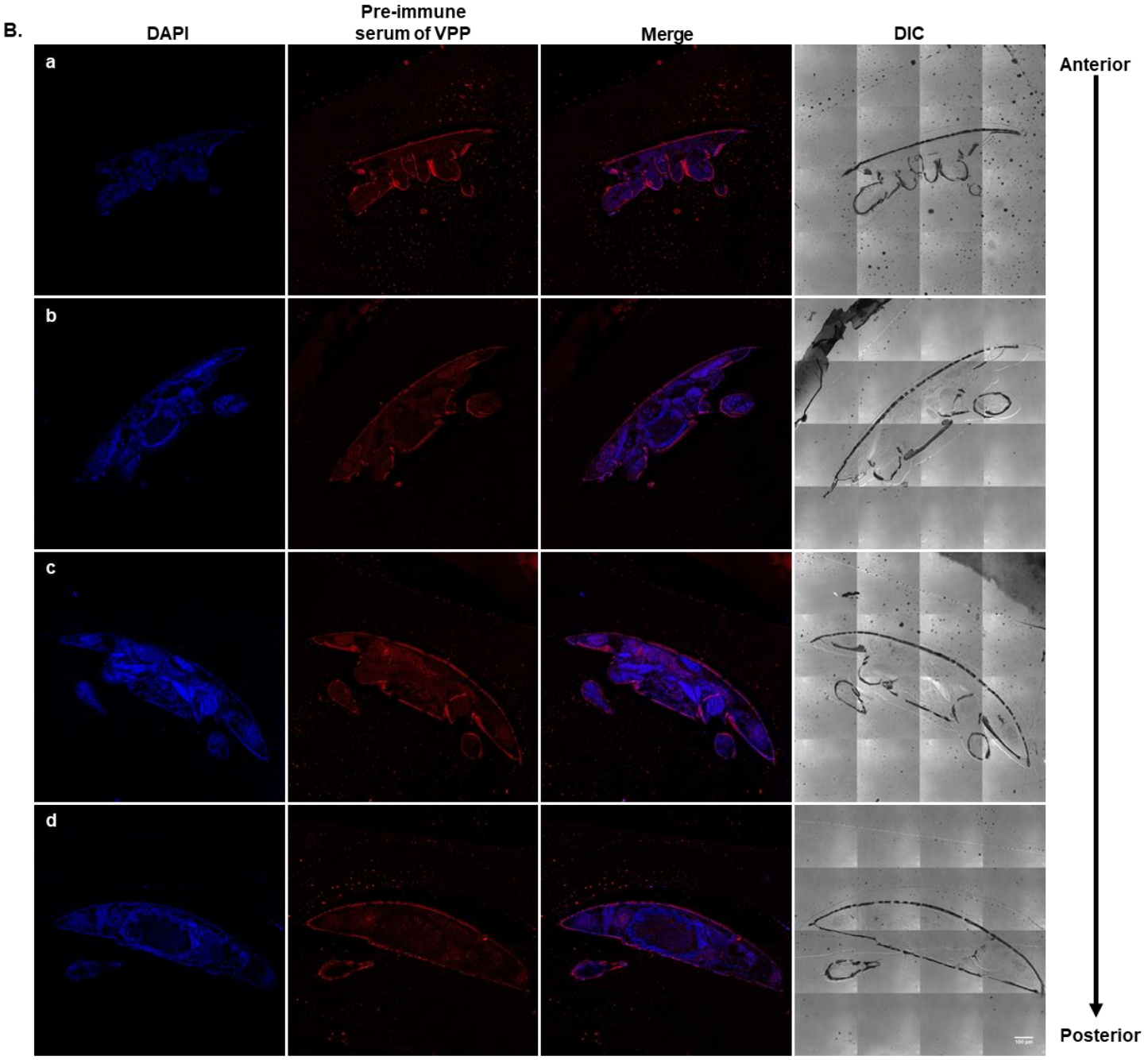
B.
DAPI
Pre-immune serum of VPP
Merge
DIC
a
b
c
d
Anterior
Posterior

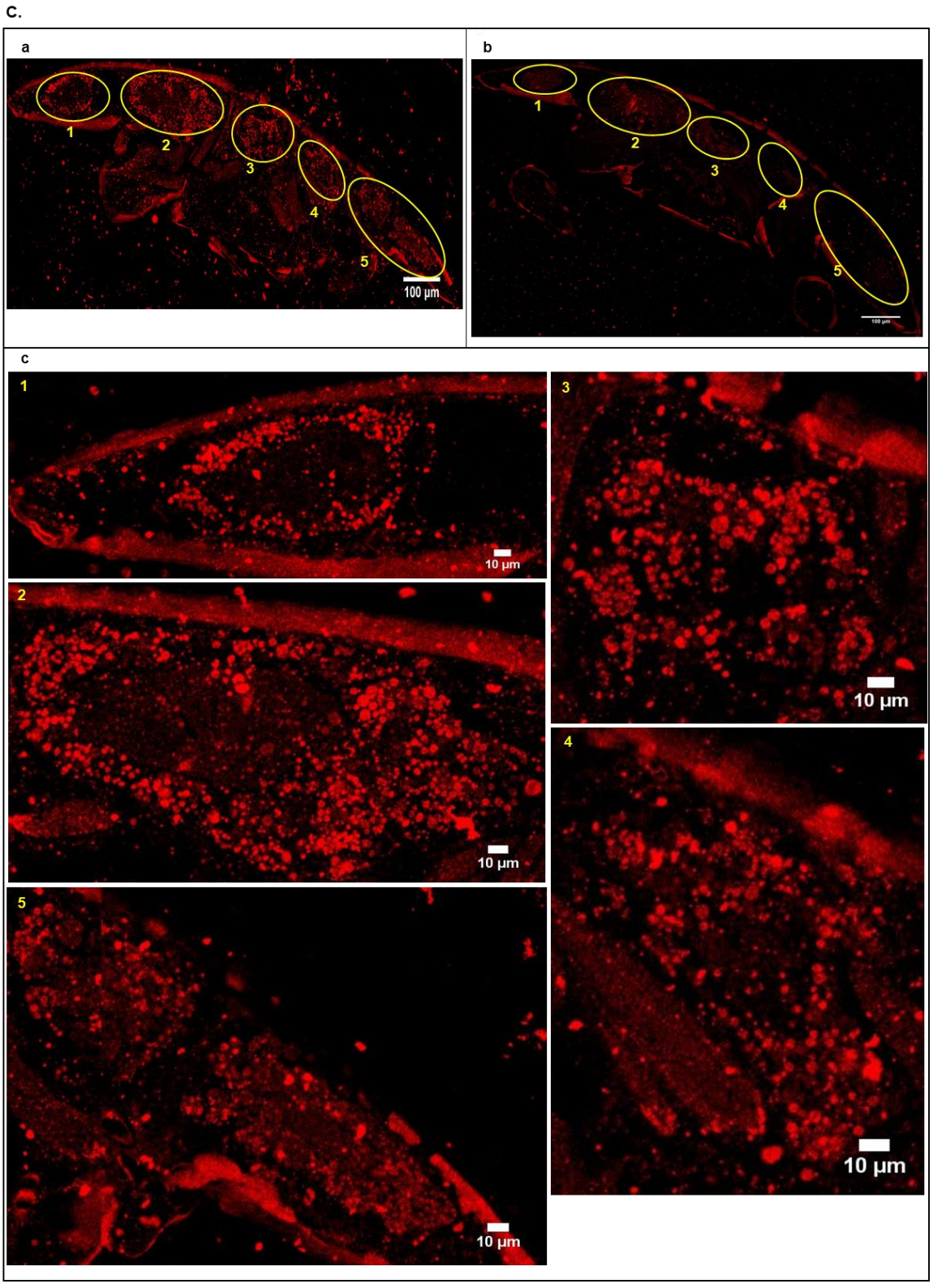

Figure. 4.8. Localization of DWV in transversal sections of female *V. destructor*.

The transversal sections of female *V. destructor* were subjected to (A) anti-VP1P antibody or (B) pre-immune serum of anti-VP1P antibody. The a-d indicates sections from cranial to caudal. Detection of antigens were taken in the Alexa 555 channel and indicated as red colour. The nuclei were counterstained with DAPI (blue). The signals of binding to DWV were highlighted by yellow arrows. Bar scale representing 100 µm was shared by all images. (C) The comparison of anti-VP1P and pre-immune serum of anti-VP1P signals of binding to DWV in the sections cut serially. Through comparing the magnifying cropped images of A-c (a) and B-c (b), the DWV signals were highlighted by yellow circles and detailed images for each circle were indicated from 1 to 5. Bar scales were indicated at the bottom right of each image.

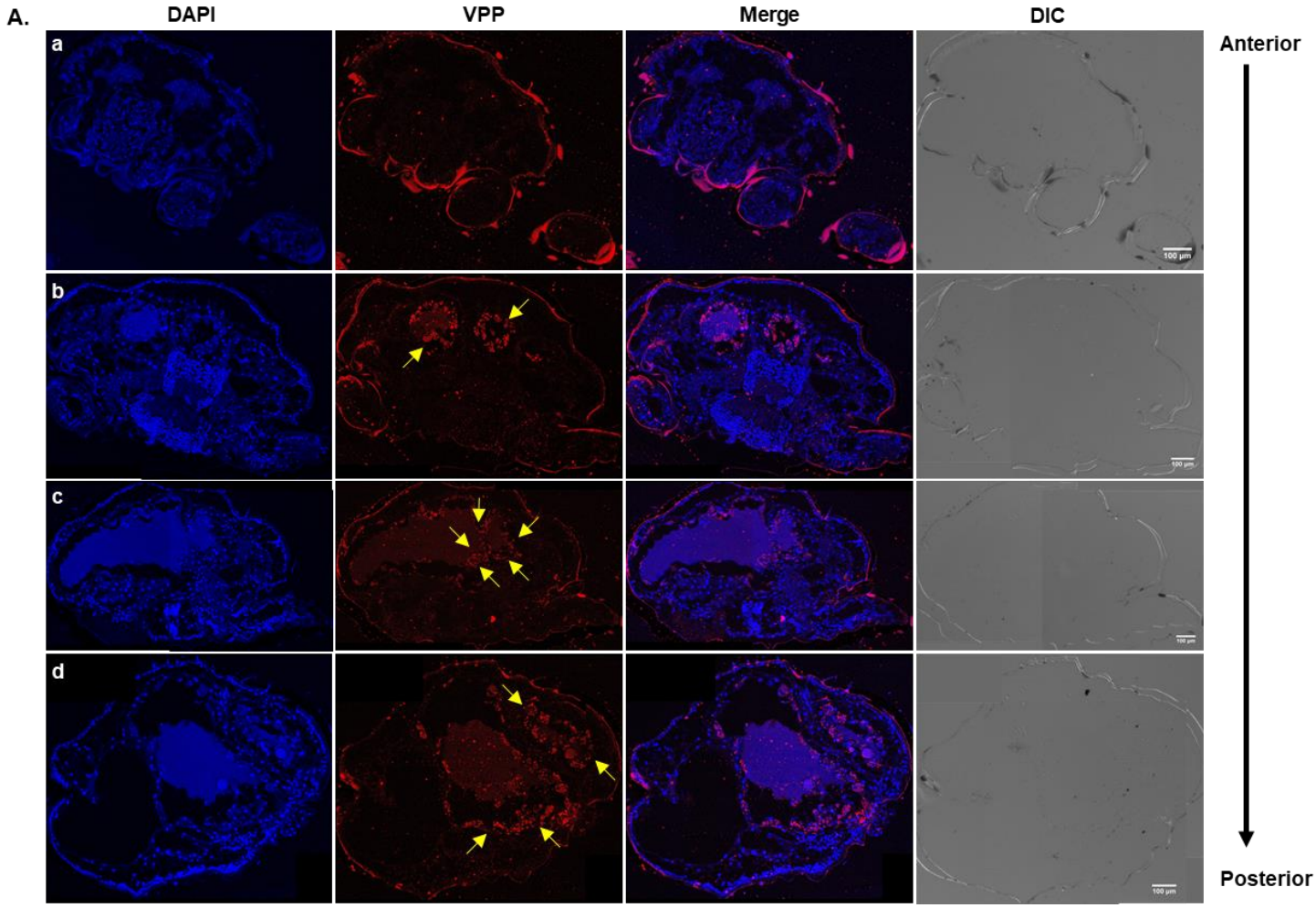
A.
DAPI
VPP
Merge
DIC
a
b
c
d
Anterior
Posterior

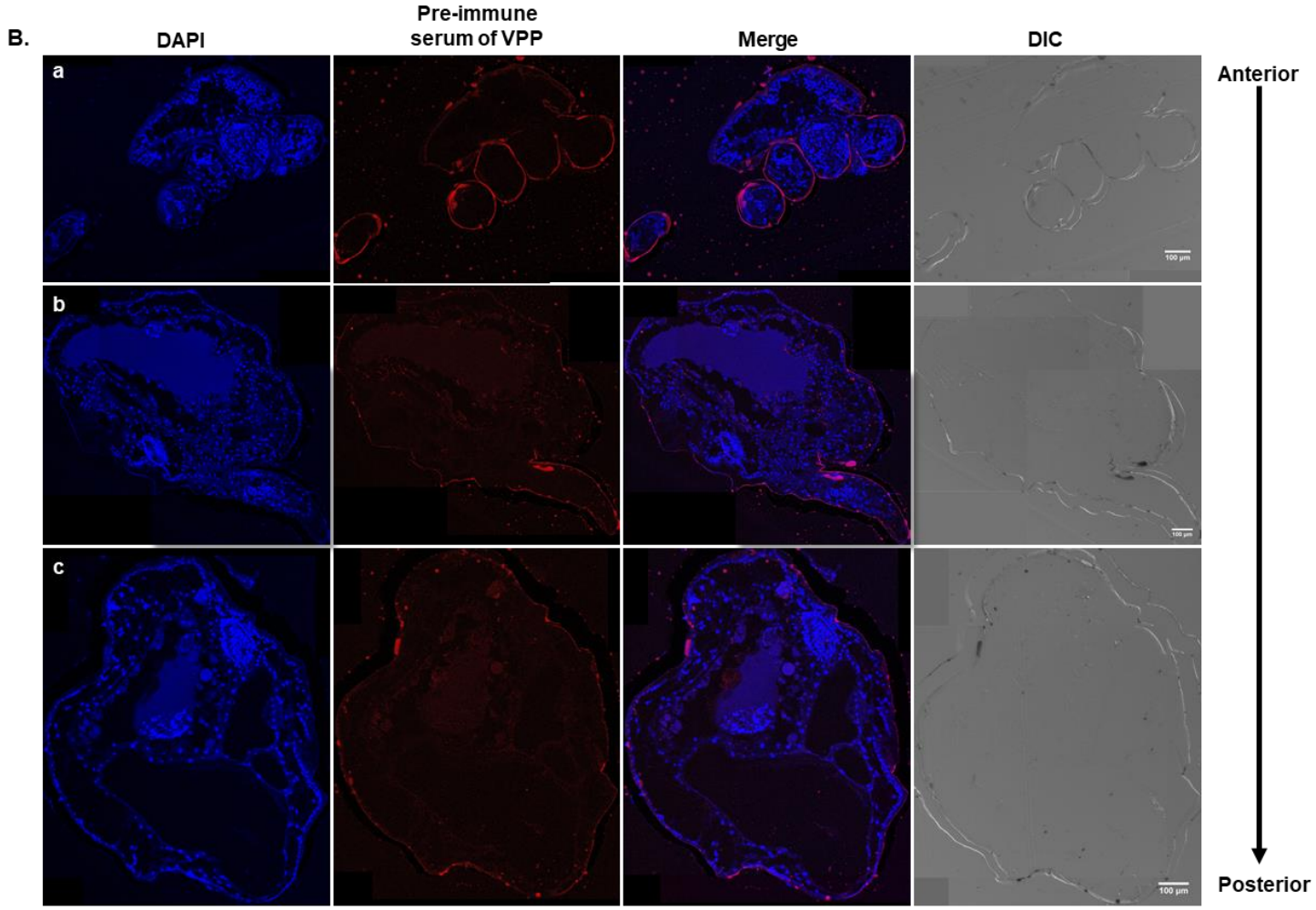

Figure. 4.9. Localization of DWV in transversal sections of male *V. destructor*.

The transversal sections of male *V. destructor* were subjected to (A) anti-VP1P antibody or (B) pre-immune serum of anti-VP1P antibody. The a-d(c) indicates sections from cranial to caudal. Detection of antigens were taken in the Alexa 555 channel and indicated as red colour. The nuclei were counterstained with DAPI (blue). The signals of binding to DWV were highlighted by yellow arrows. Bar scale, which represents 100 µm and is shown at the bottom of DIC image, was shared by the same section taken under different channels.

Based on these immunofluorescent images of both ectoparasitic mite species, even though there is variation in the signals with specific tissues and organs, DWV signals are primarily localized in the intestinal organs (gastric caecum, rectum and colon) in all female, male and nymphal *T. mercedesae*, and female and male *V. destructor* tested (Table.4.3). The signals were visualized as dense spheres in the intestinal organs (Fig.4.10). Especially, in the case of male *T. mercedesae*, DWV binding signals form several large and aggregated dense clumps at the end of rectum (Fig.4.10a-b).

Table. 4.3 Summary of immunofluorescence results of DWV localization in *T. mercedesae and V. destructor*.

Figure	Mite	Localization of DWV signals
4.5	Female *T. mercedesae*	Gastric and intestinal tissues, muscle tissues localized in the middle region of body
4.6	Male *T. mercedesae*	Gastric and intestinal tissues
4.7	Nymphal *T. mercedesae*	Tissues probably are gastric caecum and rectum
4.8	Female *V. destructor*	Gastric and intestinal tissues, lyrate organ
4.9	Male *V. destructor*	Tissues probably are gastric caecum and rectum

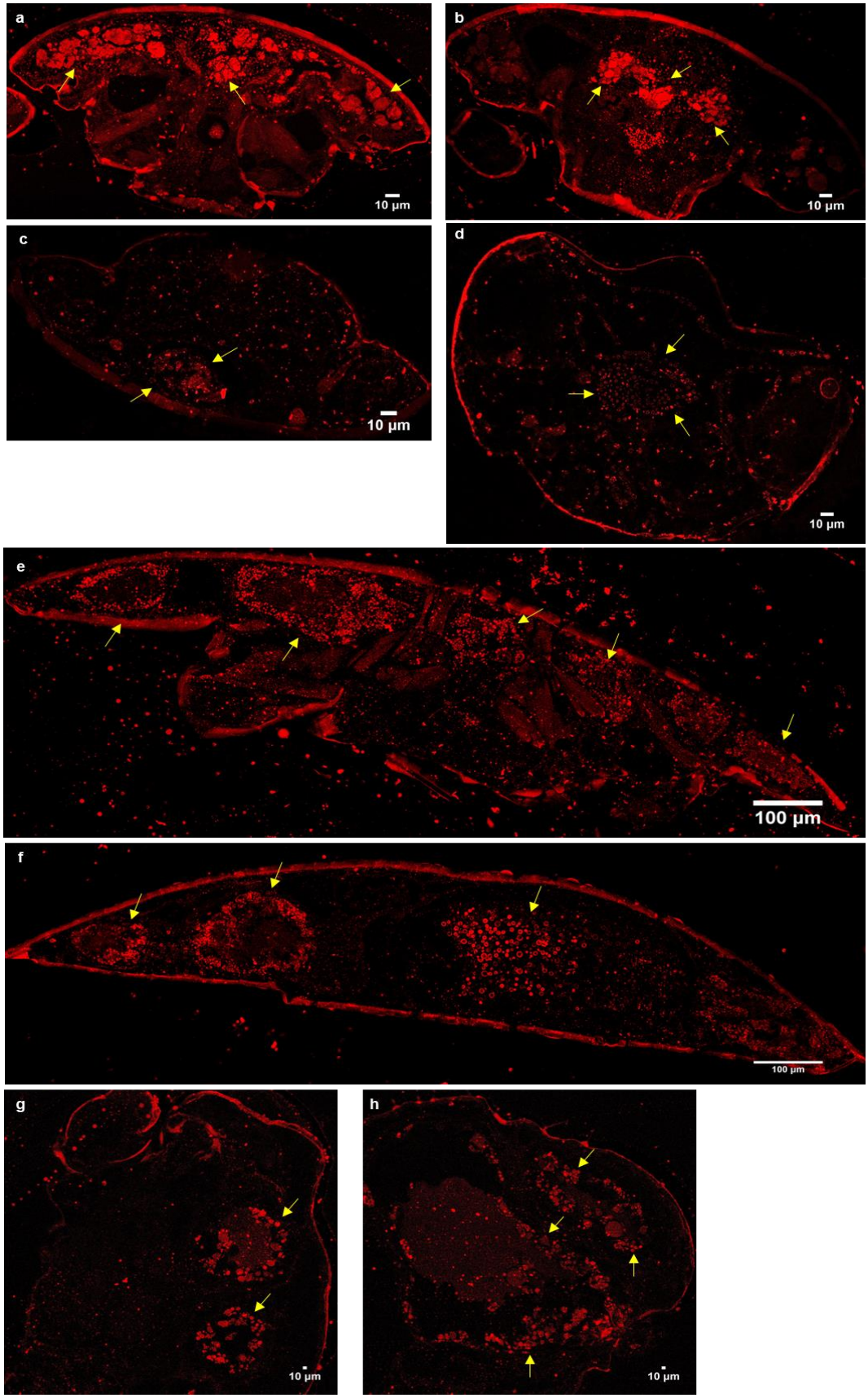

Figure. 4.10. Detection of anti-VP1P antibody binding to DWV in intestinal organs of ectoparasitic mites. The signals of anti-VP1P antibody binding to DWV were identified in intestinal organs of (a-b) male, (c) female, and (d) nymphal *T. mercedesae*, and (e-f) female and (g-h) male *V. destructor*. The specific organs of tissues showing signals are (a-b) gastric caecum, rectum and colon, (c) rectum and colon, (d) gastric caecum, (e) gastric caecum and lyrate organ, (f) colon and lyrate organ, (g-h) gastric caecum, rectum and colon. The signals were highlighted by yellow arrows. Bar scales were labelled at the right bottom of each image.

Section 4.3.5 Correlation between honey bee immune effectors and *T. mercedesae Vitellogenin (Vg)* gene

As mentioned previously, expression of the immune effector molecules, such as *Hymenoptaecin* and *Defensin-1* were induced in the honey bee pupae infested by *T. mercedesae* (Fig.2.12A-B). They could affect physiology of the mite via the intake through feeding on the fat body or other tissues of honey bee. *Vg* mRNA was down-regulated in *T. mercedesae* with high DWV copy number (Table.4.1 & Table.4.2), which could be associated with honey bee immune effectors. To assess this hypothesis, I tested the correlation between the amount of *Vg* mRNA in *T. mercedesae* and either *Hymenoptaecin* or *Defensin-1* mRNA in the mite-infested honey bee pupae. There was a negative correlation between *Hymenoptaecin* mRNA and *Vg-1* (r = -0.508, *P* value = 0.0266) or *Vg-2* (r = -0.4212, *P* value = 0.05); however, no significant correlation was observed between *Defensin-1* mRNA and *Vg-1* (r = -0.112, *P* value = 0.3458) or *Vg-2* (r = -0.3125, *P* value = 0.1284). These results suggest that the expression of *T. mercedesae Vg* gene is potentially down-regulated by honey bee Hymenoptaecin.

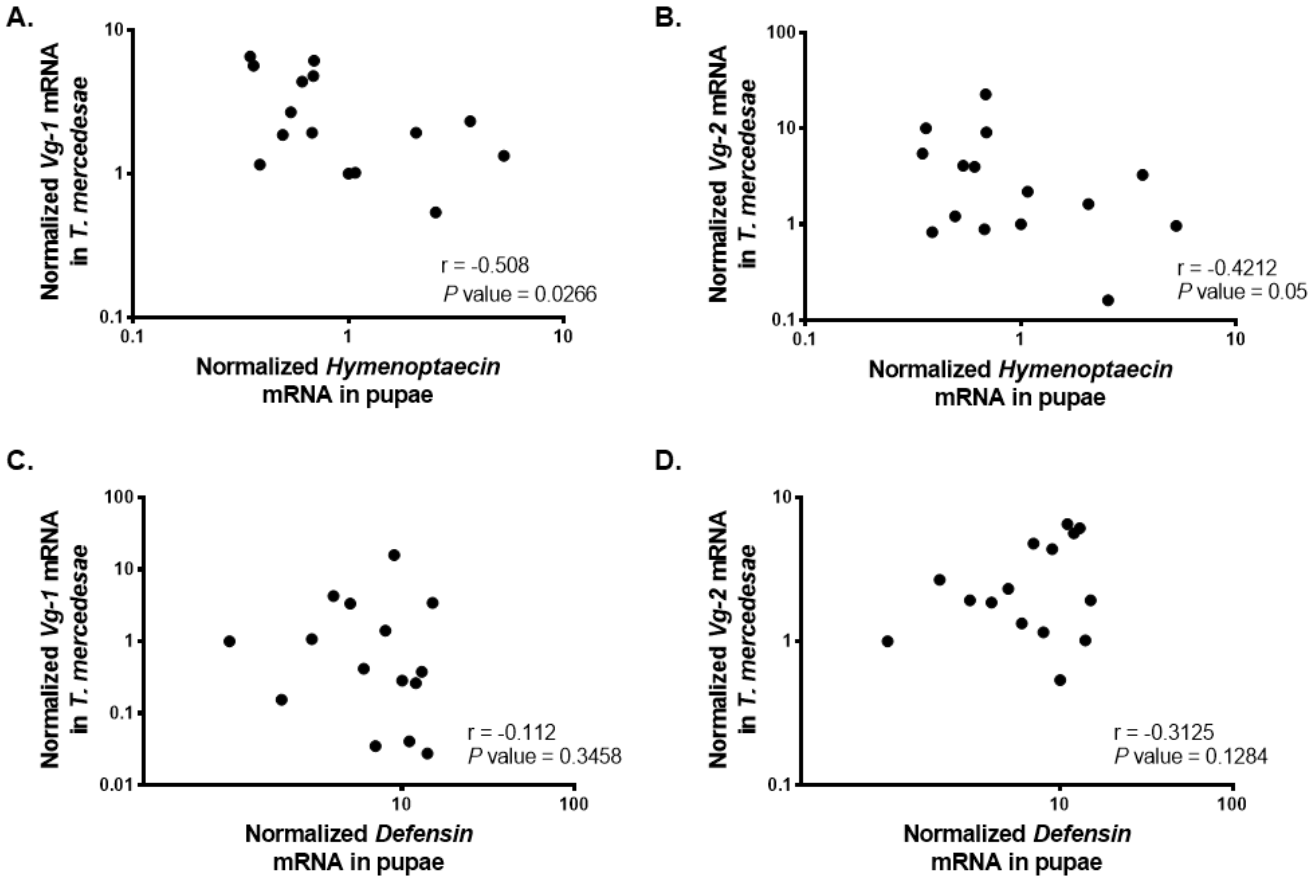

Figure 4.11 Relationship between *Vitellogenin (Vg)* mRNAs in *T. mercedesae* and either honey bee *Hymenoptaecin* or *Defernsin* mRNA.

There was a negative correlation between the amount of *Hymenoptaecin* mRNA and either (A) *Vg-1* or (B) *Vg-2* mRNA in *T. mercedesae*. However, there was no significant correlation detected in the amount of *Defensin* mRNA and either (C) *Vg-1* or (D) *Vg-2* mRNA. The Pearson correlation values and *P* values are shown on each graph.

Section 4.4 Discussion

Section 4.4.1 Ectoparasitic mites contain high DWV load without the active replication

Even though there is strong correlation of DWV copy numbers between honey bee pupae and the infesting *V. destructor* or *T. mercedesae* individual (Fig.2.2D, Fig.2.5F & Fig.2.9B), there is still controversy regarding whether DWV replicates in the mites. My results indicated that RdRP cannot be detected in *V. destructor* and *T. mercedesae* carrying a high load of DWV (Fig.4.3), suggesting that the active replication of DWV may not occur in the mite host. However, some previous studies indicated DWV replication inside *V. destructor* via detecting the negative-strand of DWV genome RNA (Ongus et al., 2004, Yue and Genersch, 2005). Gisder *et al.* also observed the negative RNA strand in *V. destructor* collected from honey bee with deformed wings but it was absent in mites collected from asymptomatic bees (Gisder et al., 2009). Campbell *et al.* failed to detect the negative-strand of DWV genome RNA in any tissues of *V. destructor* as well (Campbell et al., 2016). There was no evidence of DWV replication in the mites based on previous histological studies. There are three reasons to explain these controversial observations: 1) different DWV master variants with the distinct replication capability; 2) DWV is accumulated by the intake through mite's feeding activity instead of active replication; 3) the sensitivity of the detecting techniques.

Since the specific DWV master variant was not characterized in this study, the question regarding whether viral replication in mite associates with the different master variants cannot be answered. Through immunofluorescent experiment, I found the localization of DWV was primarily inside the intestinal tissues of *V. destructor* and *T. mercedesae*, which is consistent with the previous observation of DWV in the *V. destructor* gut (Santillan-Galicia et al., 2008, Zhang et al., 2007). The intestinal region is the major site for mite digestion and absorption activities (Evans, 1992), suggesting that DWV was ingested through fat body or other tissues of honey bee. The ingested virus then accumulates and remains with the ingested material in this region. There was high abundance of structural DWV proteins while non-structural proteins are reported to be rare in *V. destructor* and *T. mercedesae* (Erban et al., 2015, Dong et al., 2017). DWV load in *V. destructor* which started to feed on pupae was lower than that in the mites which have infested for 12 days (Martin et al., 2013), supporting that the hypothesis that accumulated DWV inside mites is derived from the feeding activity instead of the viral replication. The current method to detect DWV replication in the mites was based on testing the negative-strand of DWV genome RNA via RT-PCR. Compared to serological techniques, PCR techniques are more sensitive; however it could generate false positives via falsely-primed cDNAs synthesis *in vitro* during the reverse transcription (Peyrefitte et al., 2003). A new method using biotinylated primers combined with streptavidin-coated beads was recently proposed to eliminate the false positives during negative strand RNA detection (Boncristiani et al., 2009). Nevertheless, in order to verify whether DWV replicates within mites, the new method to separate replicated DWV virus from viral replication complex ingested from host tissues is still necessary.

Section 4.4.2 DWV negatively affects reproduction of *T. mercedesae*

Through the transcriptome analysis, *Vg* mRNA was down-regulated in *T. mercedesae* with high DWV copy number (Table.4.1 & Table.4.2). For female insects, the synthesis of Vg and its uptake by maturing oocytes play a critical role on successful reproduction (Roy et al., 2017). The observation of decreased reproductive capability in female *T. mercedesae* with high copy number DWV (Fig.4.4) suggests a negative effect of DWV on the mite's fertility via regulating Vg synthesis. The tissues for Vg synthesis in mites are still unknown, since they lack a tissue equivalent to fat body, which is the essential site for Vg synthesis in insects and ticks (Cabrera et al., 2009, Tufail et al., 2000, Thompson et al., 2005, Thompson et al., 2007). Alternatively, the synthesis of Vg occurs in the midgut of ticks (Thompson et al., 2005, Khalil et al., 2011) or the ovaries of insects (Swevers et al., 2005). Therefore, the lyrate organ and midgut are probably the site for Vg synthesis in *V. destructor* and *T. mercedesae*. Lyrate organ consists of paired, distinct flattened arms separated vaguely into various segments. It is a specialized trophic tissue related to the ovary and connects with the maturing follicles via a nutritive cord, thus it is a channel to provide nutrimental and cytoplasmic components to the oocytes during vitellogenic period (Alberti and Zeck‐Kapp, 1986, Steiner et al., 1995, Sato, 2012). Through immunofluorescent experiments, I observed the signals of DWV in the intestinal tissues of all female, male and nymphal *T. mercedesae*, and female and male *V. destructor*. Additionally, the signal was also observed in the lyrate organ of female *V. destructor*. These results support the negative-regulation of Vg synthesis in mites by high DWV load.

Transcriptome analysis of *T. mercedesae* with different DWV loads also indicated down-regulated gene expression for cuticle proteins (Table.4.1 & Table.4.2). They belong to the exoskeleton proteins and function as strong barrier against most pathogens (Fraczek et al., 2013). Down-regulation of a gene encoding a serine protease inhibitor was detected in the transcriptome analysis of six individual *T. mercedesae* (Table.4.1). Serine protease inhibitors regulate several innate defensive responses connected to blood coagulation, surface melanisation, and antimicrobial peptides synthesis (Muta and Iwanaga, 1996, Zou et al., 2006, Vilcinskas, 2010). The protease inhibitor of thrombin, which is one of the major serine proteases and necessary for mammal haemostasis, has been identified in numerous blood-sucking arthropods (Liao et al., 2009). Previous researches with *V. destructor* suggested that the serine protease inhibitor limits honey bee haemolymph coagulation and facilitate the uptake of haemolymph (Fraczek et al., 2013). Therefore, down-regulation of genes encoding Vg, cuticle proteins and serine protease inhibitors in *T. mercedesae* with high copy number of DWV suggests the negative effects of DWV on mite fitness.

Section 4.4.3 Suppressed reproduction of *T. mercedesae* is associated with honey bee immune effector, Hymenoptaecin

As mentioned previously, expression of the immune effector molecules, *Hymenoptaecin* and *Defensin-1* was induced in honey bee pupae with *T. mercedesae* infestation (Fig.2.12A-B). These honey bee AMPs could affect physiology of mites via intake by feeding activity of host's fat body or other tissues. *Vg* mRNA

was down-regulated in *T. mercedesae* with high DWV copy number (Table.4.1 & Table.4.2) and negative correlation was found between the amount of *T. mercedesae Vg* mRNA and *Hymenoptaecin* mRNA in the infested-pupa (Fig.4.11A-B), suggesting down-regulation of mite *Vg* expression by Hymenoptaecin derived from the honey bee tissues. Therefore, the decreased reproductive capability in *T. mercedesae* with high DWV load may be caused by Hymenoptaecin down-regulating *Vg* expression. My previous result, shown in Fig.2.12, indicates that *Hymenoptaecin* and *Defensin-1* are expressed following wound induction subsequent to mite feeding activity and DWV infection/replication, respectively, and previous reports indicated that *Hymenoptaecin* and *Defensin-1* are under the control of Imd and Toll signalling pathways, respectively (Aronstein et al., 2010, Osta et al., 2004). These observations may explain the negative correlation between *Hymenoptaecin* and *Vg* while no relationship identified between *Defensin-1* and *Vg*, and suggest that Imd and Toll immune signalling pathways would be independently activated in honey bee by different events. However, the underlying mechanism of down-regulation between Hymenoptaecin and Vg still needs further studies to uncover.

The negative effects of host AMPs on parasites were reported before. For example, Abaecin, Defensin and Hymenoptaecin suppressed the growth of eight different strains of *Crithidia bombi*, which is the trypanosome infecting bumble bees, *Bombus terrestris* (Marxer et al., 2016). Compared to Hymenoptaecin, the production of Defensin in honey bee is relatively low and considerably delayed (Casteels-Josson et al., 1994, Suguru et al., 1990). Only *Apidaecin* and *Hymenoptaecin* mRNAs, not *Abaecin* or *Defensin* mRNAs, were detected in honey bee with minor infection of pathogens in the wild (Casteels-Josson et al., 1994). Therefore, Apidaecin and Hymenoptaecin probably play the major role on killing or restricting pathogens while Defensin maintains the immunological abilities during the later infection period (Xu et al., 2009). The negative effect of induced Hymenoptaecin on *T. mercedesae* reproduction may help limiting the mite infestation and establishing the equilibrium between host (honey bee) and parasite (mite).

Chapter 5 Essential factors for DWV infection and replication

Section 5.1 Brief introduction

Cell line establishment and primary culture methods are widely used for understanding the mechanisms of pathogen transmission and pathogenesis in insects. However, established honey bee cell lines are not widely available (Goblirsch et al., 2013), and there are very limited studies on culturing honey bee embryonic cells (Giauffret et al., 1967, Bergem et al., 2006, Chan et al., 2010), and larval and pupal cells (Stanley, 1968, Giauffret, 1971, Gascuel et al., 1994, Kreißl and Bicker, 1992, Gisselmann et al., 2003, Hunter and Biology-Animal, 2010). Honey bee cells from these studies had limited survival period, and gene transfection was used to overcome this difficulty. By introducing human *c-myc* to honey bee embryonic cells via lipofection, a cell line was established and remained viable for 8 months (Kitagishi et al., 2011)., However, there is no evidence that they are immortalized, and can grow indefinitely (Goblirsch et al., 2013). Recently, a cell line named *AmE-711*, derived from embryonic tissues, was established (Goblirsch et al., 2013). Unfortunately, *AmE-711* cell line is persistently infected with DWV (Carrillo-Tripp et al., 2016), thus it is not appropriate for my study. Further, they have been already lost. DWV was detected in honey bee and ectoparasitic mites (*V. destructor* and *T. mercedesae*), belonging to distinct orders within the arthropod radiation, may have a potential capability to infect other organisms. Therefore, I tested DWV infection in several distinct established insect cell lines to identify an alternative model substituting honey bee cell line.

The *Sf9* cell line is a clonal isolate derived from the parental *Spodoptera frugiperda* cell line *IPLB-Sf-21-AE* (Vaughn et al., 1977) and it is widely used to produce protein by the Baculoviral system. The availability of *Sf9* genome sequence and various Baculovirus-related studies (Nandakumar et al., 2017) aid testing DWV infection and replication. *S2* cell line was derived from the primary culture of *Drosophila melanogaster* at late embryonic stages (20-24 hours AEL) (Schneider, 1972). This cell line has several advantages, including the ease of culturing and availability of genetic techniques like RNAi (Cottrell and Doering, 2003), and a complete genome sequence (Adams et al., 2000). Furthermore, *S2* cell line was used as the model to study the entry mechanisms and specific replication sites of cricket paralysis virus (CrPV) and Drosophila C virus (DCV) (Cherry and Perrimon, 2004, Cherry et al., 2006). These make S2 cell line an attractive model for investigating DWV infection and replication.

There are 20 amino acid encoded by 64 different nucleotide triplet codons. Different triplets coding the same amino acid are known as “synonymous codons”. The phenomena of preferential use of certain codons for translation is “codon usage bias” (Behura and Severson, 2013). Since codon usage is heavily biased in DWV, especially for the Position 3 of codon, DWV is more likely replicate in a host with an A/T-rich genome. Regarding arthropods with high AT genome, the sandfly and *Culicoides* midge genomes have relatively low GC%, which are approximately 33% and only 28%, respectively (Morales-Hojas et al., 2018, Bell-Sakyi et al., 2018). A novel sandfly cell line *LLE/LULS 40* was derived from embryonic *Lutzoyis longipalpis* (Bell-Sakyi et al., 2018), and a widely-used biting midge cell line *KC* was derived from *Culicoides sonorensis* (Wechsler et al., 1991), which was used for investigating infection and

dissemination of Bluetongue virus (Veronesi et al., 2013), were here used to establish DWV replication and infection due to their high A/T-rich genomes.

Figure.5.1 provides a general infection cycle of positive-strand RNA virus. After a positive-strand RNA virus enters an animal cell via endocytosis, or wound for plant cell, the positive-strand RNA is released to the cytosol and then translated to produce the viral proteins by the host ribosomes. Viral replication proteins recruit other factors, forming viral replication complexes (VRCs) on subcellular membrane surfaces, to synthesize the negative-strand RNA, which further used for positive-strand RNA synthesis. The positive-strand RNAs released from VRCs, undergo additional translation and replication cycle or encapsidated to exit out host cell (Nagy and Pogany, 2012). As a result, host factors are necessary for the major steps of positive-strand RNA viral infection, including the entry, replication protein translation, VRCs assembly and release from the host cells. Moreover, host gene expression and defences are modulated by virus via targeting host factors (Ahlquist et al., 2003). DWV, as a member of positive-strand RNA virus, is supposed to interact and recruit the honey bee proteins during its infection. RdRP is a critical component for DWV replication. For DWV replication, the genomic RNA is translated to RdRP, and requires several additional replication factors for targeting membrane, RNA capping and template recruitment *et al.* (Ahlquist et al., 2003).

In this chapter, I attempted to identify an alternative insect cell line to investigate the underlying molecular and cellular mechanisms of DWV infection and replication by testing DWV infection in four insect cell lines and honey bee primary cells. The honey bee primary cells were mainly used for identifying essential factors for DWV replication and viral binding receptors.

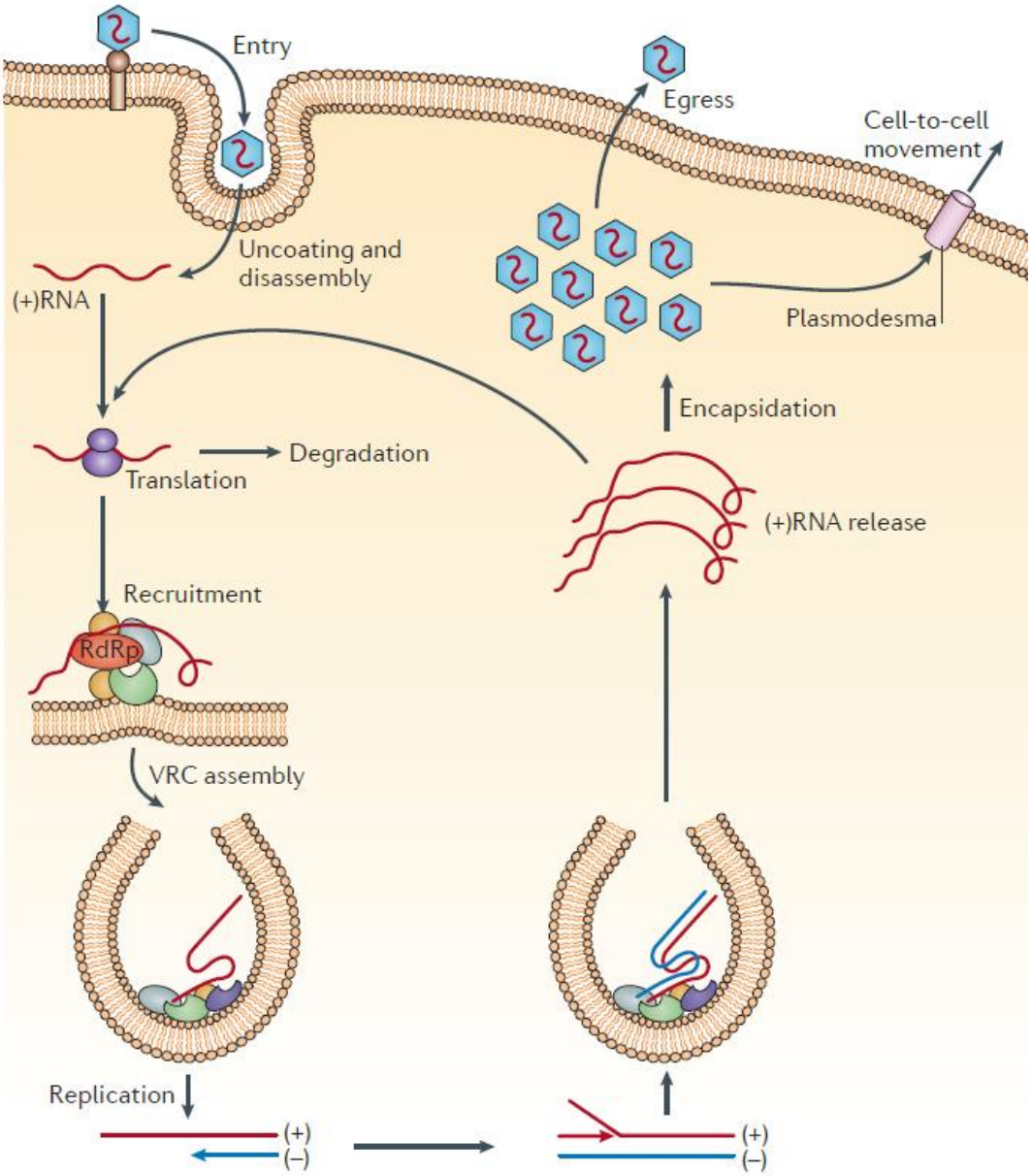

Figure 5.1. Schematic infection cycle of positive-strand RNA viruses.

After entering host cell, the positive-strand RNA is released to cytosol, followed by translation to produce the viral proteins. Viral replication proteins recruit other factors, forming viral replication complexes (VRCs) on subcellular membrane surfaces, to synthesize negative-strand RNAs using the positive-strand RNA as a template. The positive-strand RNAs are synthesized using the newly synthesized negative-strand as a template. The positive-strand RNAs are released from VRCs, undergo additional translation and replication cycle or encapsidated to exit out host cells. Encapsidated animal viruses egress host cells while plant viruses move to neighbouring cells via plasmodesmata (Adapted from (Nagy and Pogany, 2012)).

Section 5.2 Materials and Methods

Section 5.2.1 Cell culture medium and supplements

The complete medium for *S2* cells was Schneider's Drosophila Medium containing 10% heat-inactivated foetal bovine serum (FBS), and Penicillin-Streptomycin. The incubation temperature was 25°C.

LLE/LULS40 cell line medium contained L-15 medium, L-15B medium and H-Lac medium in a ration 1:1:1. L-15 medium contains L-15 (Leibovitz) medium, 10% Tryptose phosphate broth, 20% heat-inactivated FBS, 200 mM L-glutamine and Penicillin-Streptomycin. L-15B medium contained L-15B medium (Munderloh et al., 1989), 10% Tryptose phosphate broth, 5% heat-inactivated FBS, 0.1% Bovine lipoprotein, 200 mM L-glutamine, and Penicillin-Streptomycin. The final pH of L-15B medium was adjusted to a nice orange colour by sterile 1 N sodium hydroxide. H-Lac medium contained 0.5% Lactalbumin hydrolysate, 20% heat-inactivated FBS, 200 mM L-glutamine, and Penicillin-Streptomycin in Hanks balanced salt solution. The incubation temperature was 26°C.

The same Grace medium with 10% FBS and Penicillin-Streptomycin was shared for *Sf9* and *KC* cell lines and honey bee primary cells. The incubation temperature for *Sf9* cell line, *KC* cell line, and honey bee primary cell were 25°C, 26-33°C, and 33°C, respectively.

The final concentration of Penicillin-Streptomycin in all cell medium mentioned above was 50 units penicillin G and 50 µg streptomycin sulfate per milliliter of medium.

Section 5.2.2 Honey bee primary culture

Honey bee pupae were collected from capped brood cells without ectoparasitic mites' infestation. They were surface sterilized with three times washes of bleach, followed by three times washes with sterile PBS, and every wash was 5 min. A single pupa was dissected in 5 ml sterile PBS. The head part was dissected into approximately equal two parts and placed in the tube with 100 µl culture medium separately. The following procedures for pupal head cells varied depending on different experiments. The abdomen part was frozen at -20°C directly for detection of original endogenous DWV infection in the pupa.

Section 5.2.3 Artificial DWV infection in *Sf9*, *S2*, *LLE/LULS40* and *KC* cell lines

For the *Sf9* cells, 1 x 10^6 cells were infected by 1 x 10^7 copy number or 5 x 10^7 copy number DWV virus, regarded as with low or high copy number infection, respectively. Cells without infection were used for a negative control. After the initial 8 hours incubation with 200 µl culture medium, fresher medium was added and cells allowed to incubate in nearly 2 ml medium. The *Sf9* cells were collected on Day 2, 5, 8, 14, and 18. For each collection, cells were resuspended with medium and dissociated by centrifugation at 500 xg for 10 min. After three times washes with sterile PBS with 5 min for each, the *Sf9* cells were then subjected for DWV detection and quantification via RT-PCR, qRT-PCR and western blot.

For *S2* cells, 1 x 10^5 cells were infected by 1 x 10^5 copy number or 1 x 10^6 copy number DWV virus, regarded as with low or high copy number infection, respectively. Cells without infection were used for a negative control. After the initial 4 hours incubation with 200 µl culture medium, fresher medium was added

and allowing cells incubated in nearly 400 µl medium. The *S2* cells were collected on Day 2, 3, 5 and 8. The methods of collection, DWV detection and quantification were same as the one used for the *Sf9* cells.

For *LLE/LULS40* cells and the *KC* cells, 6 x 10^6 and 7 x 10^6 cells were respectively seeded and attached to well-plate at 26°C overnight. They were infected by 1 x 10^7 copy number DWV virus on the next day while cells without infection were used as a negative control. Each infected sample consisted of three biological replicates. After the initial 2 hours incubation with 200 µl culture medium, around 1 ml fresh medium were added to allow longer incubation. Cells with initial 2 hours infection were collected as 'Day 0', then the *LLE/LULS40* cells were collected every 4 days until to Day 12, whereas the *KC* cells were collected every 2 days until to Day 16. The methods of collection, DWV detection and quantification were same as the one used for the *Sf9* cells.

Section 5.2.4 RdRP detection in honey bee primary cells and the *KC* cells with DWV infection

Honey bee primary cells were cultured from pupal head and abdomen separately. The primary cells cultured from the same pupa was infected by DWV virus or without infection, and the latter one was used as a negative control. Cells were collected after 6, 12, and 24 hours infection by removing the medium, serial washes with sterile PBS and homogenization with SDS sample buffer. Cell lysates were then subjected to western blot for RdRP detection by anti-RdRP antibody.

The method for RdRP detection in the *KC* cells was same as honey bee primary cells, except the *KC* cells were collected after 2 hours, and 2 days infection, corresponding to "Day 0" and "Day 2" respectively.

Section 5.2.5 Detection of DWV replication in pupal cells infected by antibody-DWV

DWV virus was incubated with anti-VP1P (DWV-VP1P) or anti-VP1 antibody (DWV-VP1), the latter used as a negative control, at room temperature for at least 30 min. Both antibodies were diluted at the concentration 0.377 mg/ml, 0.0377 mg/ml, and 0.00377 mg/ml. The head and abdomen from the same single pupa were used for cell culture and original endogenous DWV detection, respectively. Honey bee primary cells derived from a pupal head were roughly divided into two equal parts, one infected by DWV-VP1P while the other infected by DWV-VP1. After 1 hour incubation in nearly 100 µl medium at 33°C, 400 µl fresh medium was added and incubated at 33°C overnight. Cells were collected by resuspending with medium and then dissociated by centrifugation at 300 xg for 5 min. After three times washes with sterile PBS, cells were homogenized in 150 µl RAPI buffer (20 mM Tris-HCl pH 7.5, 150 mM NaCl, 1 mM Na_2EDTA, 1 mM EGTA, 1% NP-40, 1% sodium deoxycholate, 2.5 mM sodium pyrophosphate, 1 mM β-glycerophosphate, 1 mM Na_3VO_4, 1 µg/ml leupeptin). The abdomen from the paired pupa was homogenised in 400 µl RIPA buffer. After centrifugation at 1,000 xg for 3 min, the supernatant was analysed by Enhanced BCA Protein Assay Kit (Beyotime) to measure the protein concentration, according

to the manufacturer's instructions. Subsequently, cell lysates were normalized by SDS sample buffer and subjected to western blot and SDS-PAGE.

Section 5.2.6 Detection of DWV replication in pupal cells with pre-incubation of VP1-P protein

Honey bee primary cells derived from a pupal head were roughly divided into two equal parts; one was pre-incubated with purified VP1-P protein while the other was used as a negative control. The abdomen from the same pupa was used to detect the endogenous DWV infection in this pupa. Different volumes of P protein were examined including 1, 2.5, 5 and 10 µl. Pupal cells were incubated with P protein in nearly 100 µl medium for 1 hour at room temperature, then infected by DWV virus at 33°C overnight. Cells were collected, homogenized and normalized as per the method in Section 5.2.5, followed by DWV replication detection via western blot.

Section 5.2.7 DWV Binding assay

Binding assay of DWV to honey bee cells was examined in the presence of anti-VP1P antibody or VP1-P protein. In the case of anti-VP1P antibody, DWV virus was incubated with the antibody at room temperature for 30 min followed by cooling for at least 30 min. Anti-VP1 antibody was used at same condition as a negative control. Both antibodies were diluted at the concentration 0.377 mg/ml, 0.0377 mg/ml, and 0.00377 mg/ml. The pre-cooled antibody-DWV was used to infect honey bee primary cells which were derived from half pupal head and pre-cooled for 30 min. The condition of infection was at cold temperature for 2 hours in nearly 100 µl medium. Cells were then collected by centrifugation at 300 xg for 5 min and subsequent three times washes in sterile PBS. Cells were homogenized in RIPA buffer and the normalized cell lysates were subjected to western blot to assess bound DWV by anti-VP1 and/or anti-VP1P antibody, or followed by RNA isolation, RT-PCR and qRT-PCR to measure the bound DWV as absolute copy numbers.

In the case for detecting the effects of VP1-P protein on DWV binding, pupal cells were pre-incubated with P protein in 25 µl medium at room temperature for 30 min, followed by cooling down for at least 30 min. These pre-cooled cells were then infected by pre-cooled DWV virus at cold temperature for 2 hours in nearly 100 µl medium. The following methods for assessing DWV bound to cells were same as mentioned above.

Section 5.2.8 Detection of DWV replication in pupae with different developmental stages

Honey bee pupae with different developmental stages were collected from capped brood cells without *V. destructor* or *T. mercedesae* infestation. Each developmental stage consisted of three representative replicates. The pupal cells derived from half head was initially infected with DWV in nearly 100 µl at 33°C for 1 hour, followed by overnight incubation with additional 400 µl fresh medium. The cells derived from

the remaining half head were used as a negative control without infection. Cells were collected by resuspending with medium and subsequently dissociated by centrifugation at 300 xg for 5 min. After three times washes with sterile PBS, cells were homogenized in 150 µl RAPI buffer and then normalized by Enhanced BCA Protein Assay Kit (Beyotime). The normalized cell lysates were subsequently subjected to western blot to assess DWV replication by anti-RdRP antibody.

Section 5.2.9 RT-PCR and qRT-PCR

Total RNA was isolated from cells using Total RNA Extraction Reagent (GeneSolution), according to the manufacturer's instructions. RT reactions were carried out by using 1 µl of total RNA and all remaining RNA were stored in -80°C. The RT products were subsequently analysed with RT-PCR to assess DWV infection in cells with the primer set DWV #1 and PCR targeting *LLL* 18S rRNA, *KC EF-1α* mRNA or honey bee *EF-1α* mRNA (Supplementary Table) was utilized as controls to verify successful RT. The absolute DWV copy number was examined via qRT-PCR with the primer sets DWV #2 (Supplementary Table) while using the primer sets *Sf9* 16S rRNA, *Drosophila RP* mRNA, *LLL* 18S rRNA, *KC EF-1α* mRNA and Honey bee *EF-1α* mRNA (Supplementary Table) for normalization in *Sf9*, *S2*, *LLE/LULS40*, *KC* and honey bee primary cells, respectively. The methods and conditions for RT, RT-PCR and qRT-PCR were as noted in Section 2.2.2. and Section 2.2.3.

Section 5.2.10 Detection of negative-strand DWV RNA

Reverse transcription (RT) reactions were carried out using 1 µl of total RNA, ReverTra Ace (TOYOBO), RNase Inhibitor (Beyotime) and tag-F15 primer (Supplementary Table). RNase H (Beyotime) was added to digest RNA in RNA/cDNA heteroduplex after cDNA synthesis. RT products were subsequently analysed by RT-PCR to assess negative-strand DWV with the primer sets tag and B23 (Supplementary Table). The condition for PCR was same as mentioned in Section 2.2.2.

Section 5.2.11 RNA-seq

Twenty honey bee pupae were picked from capped brood cells without ectoparasitic mite infestation, 10 in the early developmental stage with white-pale eyes (W), and an additional 10 pupae with black eyes and yellow body representing in the late developmental stage (Y). The total RNAs of 5 pupae at the same developmental stage were mixed and then these 4 mixed samples (W1, W2, Y1 and Y2) were delivered to BGI-Wuhan with dry ice for polyA+ RNA enrichment, cDNA library preparation, and Illumina Hiseq 2500/4000 sequencing.

Section 5.2.12 Transcriptome analysis and GO enrichment analysis

After sequencing, the raw data were filtered to remove the adaptor sequences, contamination, and low-quality reads by BGI. The Quality control (QC) was further analyzed using FastQC. The clean reads were then aligned to the honey bee genome Amel_HAv3.1 (NCBI) using STAR software (Dobin et al., 2013) with default settings. Subsequently, with the default union-counting and option "-a" to specify the minimum score for alignment quality, Htseq-count in the Htseq Python package (v0.6.1) (Anders et al., 2015) was utilized to obtain raw read counts, which was further subjected to the EdgeR (v3.0) Bioconductor package (Chen et al., 2014) to compare differential expression genes. Exact test was used to conduct pairwise comparisons of differential gene expression between the RNA-seq samples. The FDR P-value < 0.01, and logFC > 0.05 and logFC < 0.05 cut-offs were utilized for significance. GO terms (Biological process, Molecular function, and Cellular component) were assigned for each gene based on EnsemblMetazoa. Genes were then classified based on the GO term and GO enrichment.

Section 5.2.13 Western blot

After heat denaturation at 99°C for 5 min and centrifugation at 10,000 xg for 1 min, the supernatants of cell lysates were subjected to SDS-PAGE gel. For each gel, samples were electrophoresed for approximately 80 min at 20 A and subsequently transferred to a nitrocellulose filter membrane. Protein-loaded membranes were incubated in Blocking buffer I at room temperature for 1 hour, followed by anti-VP1, anti-VP1P or anti-RdRP antibody incubation with dilution of 1:1,000 at 4°C overnight. The membranes were then washed 3 times for 5 min each in PBST, subsequently incubated in IRDye® 680RD Donkey anto-Rabbit IgG (H+L) diluted in Blocking buffer II at 1:10,000 for 1 hour at room temperature. After three times washes for 5 min each in PBST, membranes were visualized by Odysse Infrared Imager.

Section 5.2.14 Immunoprecipitation

The 75.4 µg anti-VP1P antibody was coupled with Protein A Agarose (Fast Flow) (Beyotime) at 4°C for 4 hours. After washing three times with 0.2 M sodium borate (pH 9.0), anti-VP1P antibody + Protein A agarose was crosslinked by Dimethyl pimelimidate·2 HCl (Thermo Fisher) in 0.2 M sodium borate buffer with rocking at room temperature for 40 min, followed by quenching in 0.2 M ethanolamine (pH 8.0) with rocking for 1 hour. After three washes with 0.58% (v/v) acetic acid + 150 mM NaCl, followed by three washes with cold PBS, they were mixed with honey bee protein lysates and rocked at 4°C overnight. Following incubation, the agarose was washed three times with washing buffer (150 mM NaCl, 50 mM Tris, 10 mM EGTA, 0.2% NP-40), and additional three washes with 50 mM ammonium bicarbonate. The agarose was re-suspended in 50 µl 50 mM ammonium bicarbonate and boiled at 95°C for 5 min. The supernatant was subsequently analysed by Mass Spectrometry (MS). The pre-immune serum of anti-VP1P antibody was examined under same condition to verify the specific binding in the immunoprecipitation product.

Section 5.2.15 Sliver staining

The immunoprecipitation product was mixed with SDS sample buffer, followed by electrophoresis. The gel was stained by ProteoSilver™ Silver Stain Kit (Sigma), according to manufacturer's instruction. Compared to the staining gel of pre-immune serum of anti-VP1P antibody + Protein A agarose, the specific bands in the gel of anti-VP1P antibody + Protein A agarose were cut and digested with 5-10 ng/μl separately, followed by MS analysis. Alternatively, the supernatant of immunoprecipitation product was digested directly and subjected to MS as well.

Section 5.2.16 Mass Spectrometry

Mass spectrometric detection was accomplished by using an Easy-nLC 1,000 coupled to an LTQ Orbitrap Elite mass spectrometer (Thermo Fisher). It was equipped with a nanoelectrospray source and operated in a data-dependent acquisition (DDA) mode with following settings: spray voltage 2100 V, s-lens RF level 50%, capillary temperature 300°C, scans 150-2000 m/z. Peptide separation was used by a 15 cm analytical RSLC column (Acclaim™ PepMap™ 100 C18 2 μm pore size, 150 mm length, 50 μm i.d.) with the gradient of buffer B (99.9% acetonitrile, 0.1% formic acid): 0%-5% for 3 min, 5%-25% for 135 min, 40% for 15 min, 40%-95% for 10 min, and stayed at 95% for 17 min.

Tandem mass spectra were extracted by Mascot Distiller 2.7 (v2.4.1) (Matrix Science, UK) and searched against the database of *Apis. mellifera* or Deformed Wing Virus. The software Scaffold (v4.8.9) (Searle, 2010) was used to validate peptide and protein identification

Section 5.2.17 Codon usage analysis

The sequence of DWV (#198112), *A. mellifera* (#7460), and *V. destructor* (#109461), which from the database RefSeq, and the genomic sequence of *T. mercedesae* (#418985), from GenBank, were used for codon usage analysis. The GC content (%) of codon usage and codon usage frequency were analysed by Codon/Codon Pair Usage Tables (TissueCoCoPUTs, HIVE-CUTs) (Athey et al., 2017).

Section 5.2.18 Statistical analysis

Western blot results were analysed and quantified by ImageJ (Davarinejad, 2017). Statistical analysis was carried out by two tailed *t-test* with software GraphPad Prism (v7).

Section 5.3 Results

Section 5.3.1 Testing DWV replication/ infection in the established insect cell lines

Sf9 cell line

In order to investigate whether DWV infects and replicates in this cell line, previously isolated DWV (Fig.2.11A) was used to infect *Sf9* cells and then the dynamics of DWV load during the infection period was examined. *Sf9* cells were infected by either low or high DWV copy number, and cells without infection were used as the control. The cells harvested on Day 2, 5, 8, 14 and 18 after infection, were positive for DWV via RT-PCR; however, the band corresponding to DWV became weaker on Day 14 and weakest on Day 18 (Fig.5.2A). Absolute DWV copy number was also quantified via qRT-PCR and further analysed without and with normalization by *Sf* 18S rRNA. DWV copy number basically decreased during the infection periods. DWV copy numbers in *Sf9* cells infected by low and high DWV copy number on Day 18 were approximately 4% and 2% of those on Day 2, respectively. With normalization, these values are 4% and 4.5%, respectively (Fig.5.2B-C). Based on these results, DWV replication and infection do not occur with *Sf9* cells and thus they are not appropriate as a model for DWV infection study.

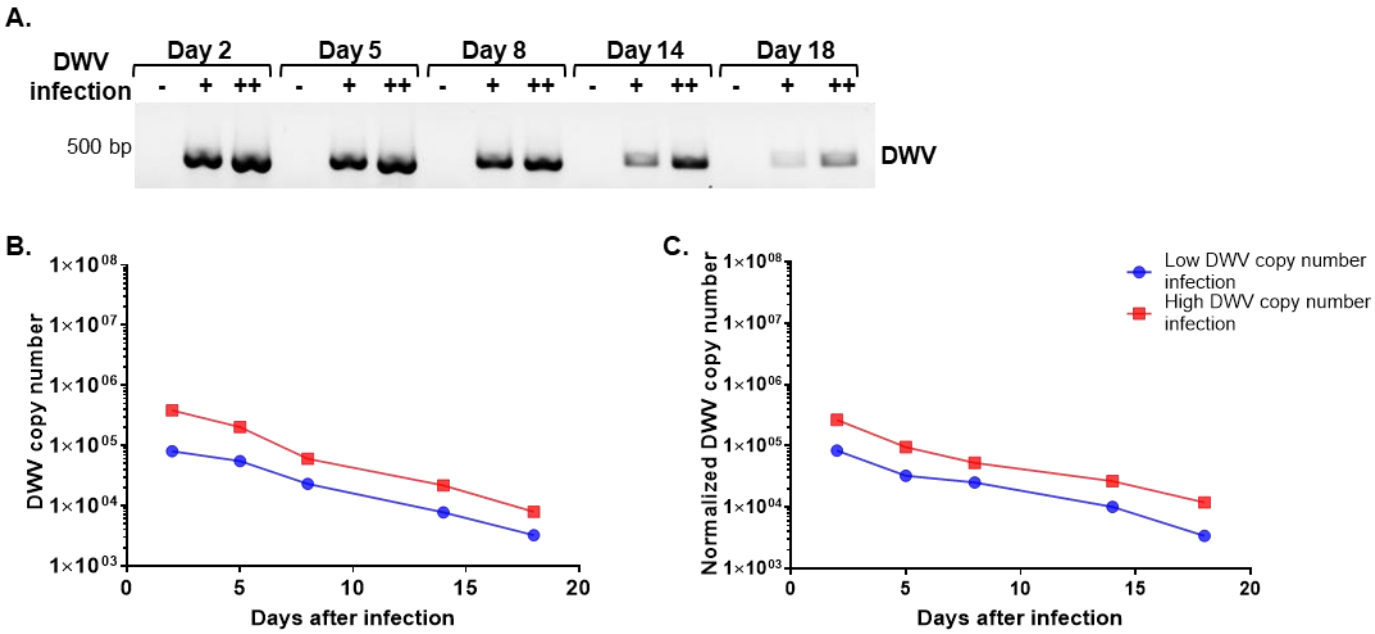

Figure 5.2 Detection and quantification of DWV in *Sf9* cells after infection.

Sf9 cells were infected by either low (blue) or high (red) DWV copy number and collected after 2, 5, 8, 14, and 18 days infection. (A) DWV detection was conducted via RT-PCR. The low and high copy number infection were indicated by "+" and "++" respectively. Cells without infection were used as a negative control and indicated as " – ". The position of 500 bp was indicated on the left of agarose gel. The absolute DWV copy number (B) without normalization or (C) with normalization was quantified by qRT-PCR. Normalization was carried out by *Sf9* 18S rRNA.

S2 cell line

Fruit fly *S2* cells were infected as above for *Sf9* cells, and harvested at 2, 3, 4, and 8 days after infection. The absolute DWV copy number quantified via qRT-PCR increased during the infection period (Fig.5.3A).

If the DWV copy number was normalized by fruit fly ribosomal protein mRNA, it remained approximately constant (Fig.5.3B). These results should be due to the increase of *S2* cell number during the infection period and the non-specific association with DWV, suggesting that DWV replication and infection do not occur and thus *S2* cells are not appropriate as a model for DWV infection study.

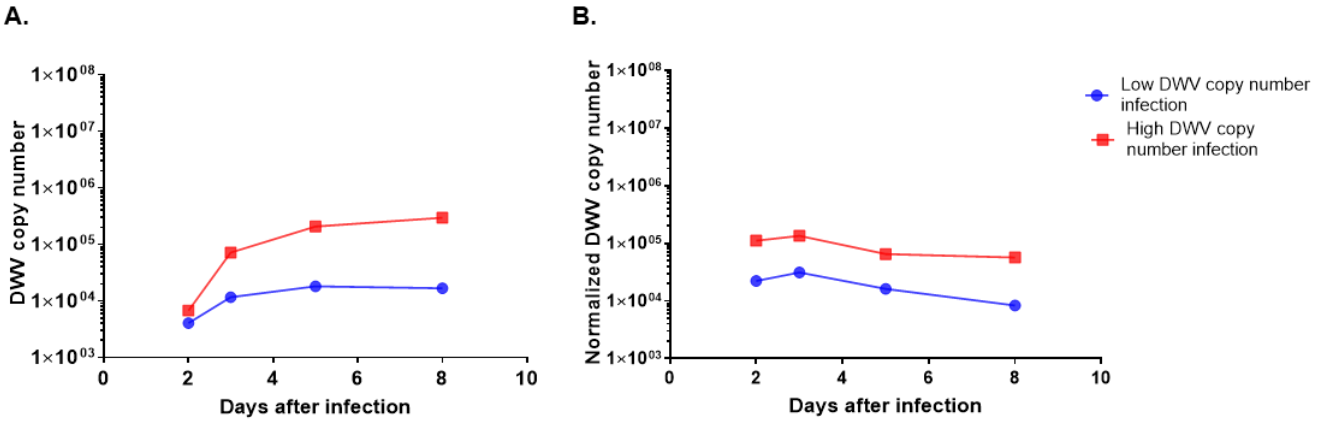

Figure 5.3 Quantification of DWV in *S2* cells after infection.

S2 cells were infected by either low (blue) or high (red) DWV copy number and collected after 2, 3, 5, 8 days incubation. The absolute DWV copy number (A) without normalization or (B) with normalization was quantified via qRT-PCR. Fruit fly ribosomal protein mRNA was used for the normalization.

LLE/LULS 40 cell line

LLE/LULS 40 cell was provided by Prof. Bell-Sakyi (University of Liverpool). *LLE/LULS 40* cells were infected by DWV for 4, 8 and 12 days. Cells harvested at 2 hours after infection represented as Day 0. All infected *LLE/LULS 40* cells were positive for DWV detection via RT-PCR (Fig.5.4A). DWV copy number slightly increased during the experiment (Fig.5.4B-C). The negative-strand RNA of the DWV genome was also detected in *LLE/LULS 40* cells except for one replicate on Day 0 (Fig.5.4A). These results suggest that DWV replication may occur in *LLE/LULS 40* cells.

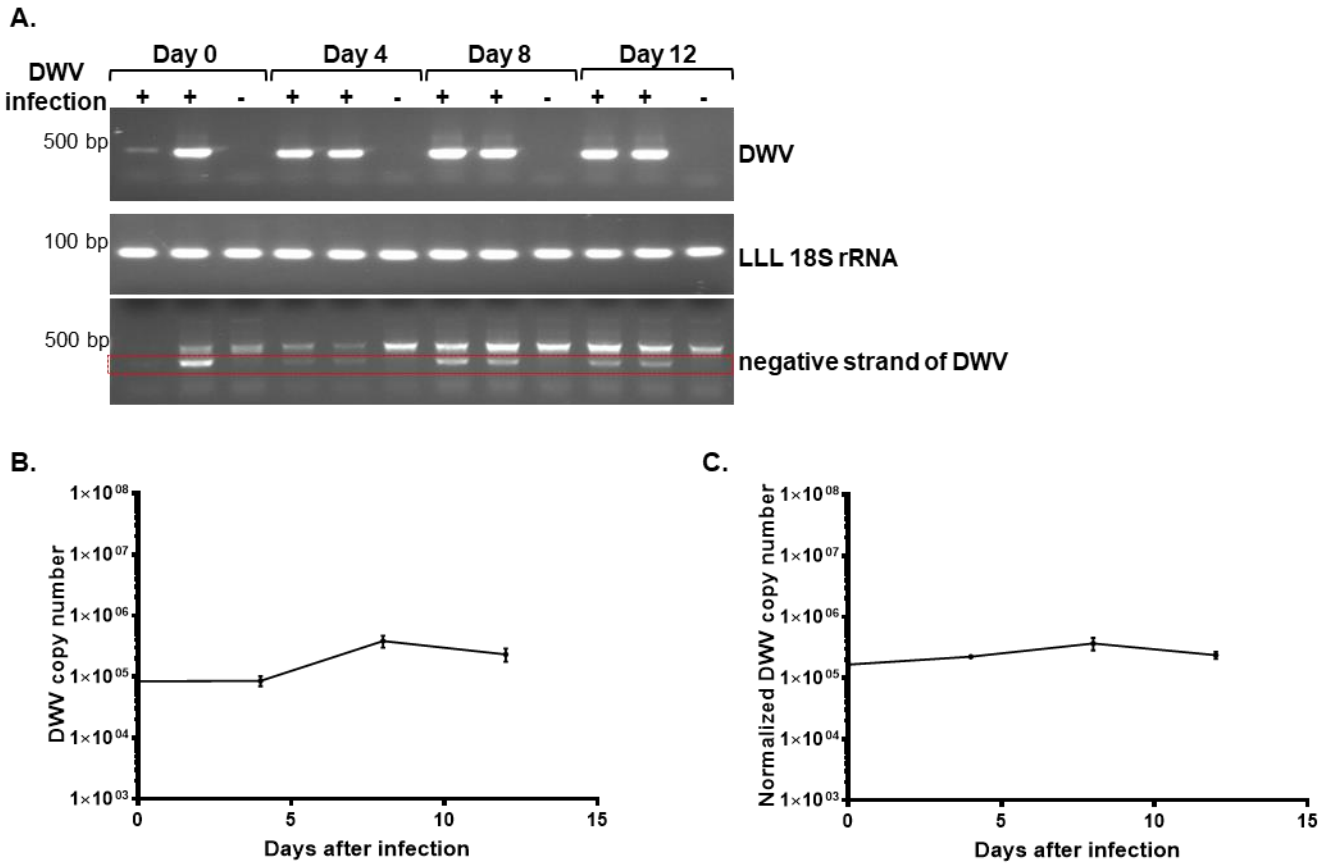

Figure 5.4 Detection and quantification of DWV in *LLE/LULS 40* cells after infection.

LLE/LULS 40 cells were infected by DWV and collected after 2 hours (represented as Day 0), and 4, 8, 12 days incubation. (A) DWV and the negative-strand were analysed via RT-PCR and the position corresponding to negative-strand was indicated by red box. *LLE/LULS 40* 18S rRNA was used as an endogenous positive control. Cells with and without infection were indicated by "+" and "-" respectively and the position of 500 bp or 100 bp was indicated on the left of agarose gel. The absolute DWV copy number without (B) or with (C) normalization was quantified via qRT-PCR. The mean value with error bar (±SEM) is indicated for each sample and the error bar is too short to be seen for some points.

KC cell line

KC cell was provided by Prof. Bell-Sakyi and were infected with DWV as above. Cells harvested at 2 hours after infection were represented as Day 0 and cells were collected every 2 days infection until to Day 16. DWV was detected except one sample for Day 12 and two samples for Day 16 (Fig.5.5A). DWV copy number tended to increase up to day 10 and then decrease (Fig.5.5B-C). The negative-strand RNA of DWV genome was also detected in the infected *KC* cells (Fig.5.5D). Therefore, based on these results, DWV replication may occur in KC cells.

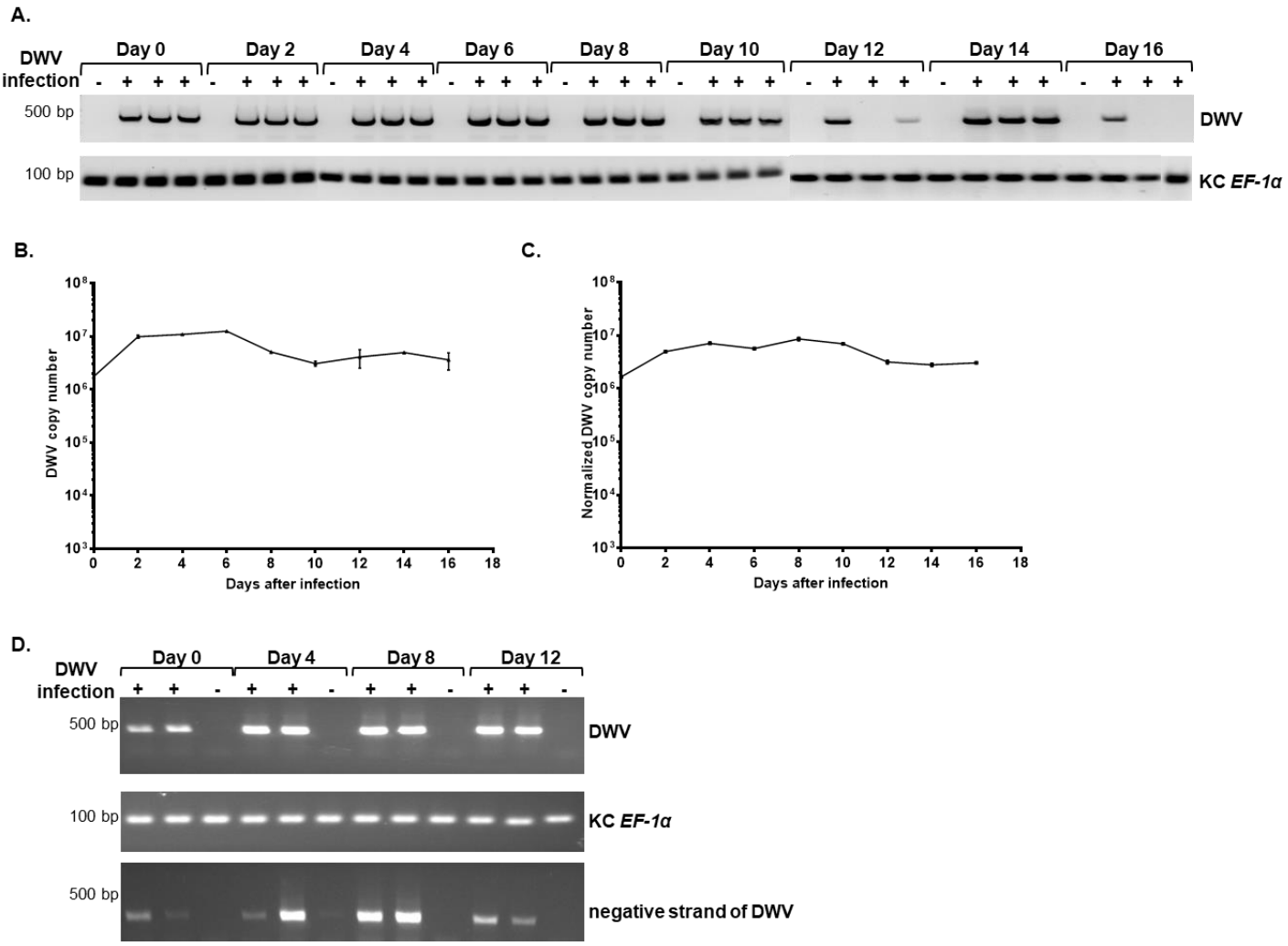

Figure 5.5 Detection and quantification of DWV in *KC* cells after infection.

(A) *KC* cells were infected by DWV and collected after every two days after infection. Day 0 represented the cells collected after 2 hours infection. DWV was detected via RT-PCR and *KC EF-1α* mRNA was used as an endogenous positive control. The absolute DWV copy number (B) without normalization or (C) with normalization was quantified via qRT-PCR. Normalization was carried out by *KC EF-1α* mRNA. The mean value with error bar (±SEM) is indicated for each sample and the error bar is too short to be seen for some points. (D) The negative-strand of DWV was detected by RT-PCR for cells collected after every four days. Cells with and without infection were indicated by "+" and "-" respectively. The position of 500 bp or 100 bp was indicated on the left of agarose gel.

Section 5.3.2 Comparison of DWV infection/replication between honey bee primary cells and *KC* cell line

Compared to *LLE/LULS 40* cells, normalized DWV copy number increased more in *KC* cells during the first 8 days infection, thus the *KC* cell line would be better for DWV replication study. In order to confirm whether the KC cell line would be sensitive to DWV infection/replication, I compared DWV replication between honey bee primary cells and KC cells. The honey bee primary cells derived from pupal head and abdomen were infected by DWV for 6, 12, and 24 hours. RdRP was successfully detected after 12 hours infection and then decreased after 24 hours infection (Fig.5.6A). Therefore, DWV infection and replication happened in the period of 6-12 hours infection and then reduced in the following 12 hours. RdRP was not

detected in *KC* cells infected by DWV for 6 or 11 hours. The infection period was elongated to two days; nevertheless, RdRP was still not detected. The detection of DWV positive- and negative-strands in the infected *KC* cells, and non-detectable RdRP in the cells with expressed VP1-P (Fig.5.6B), demonstrated that DWV genome RNA was not translated in *KC* cells. Therefore, *KC* cells consists of a distinct DWV infection/replication mechanism rather than the mechanism inside honey bee and certain specific honey bee proteins are probably required for DWV genome RNA translation.

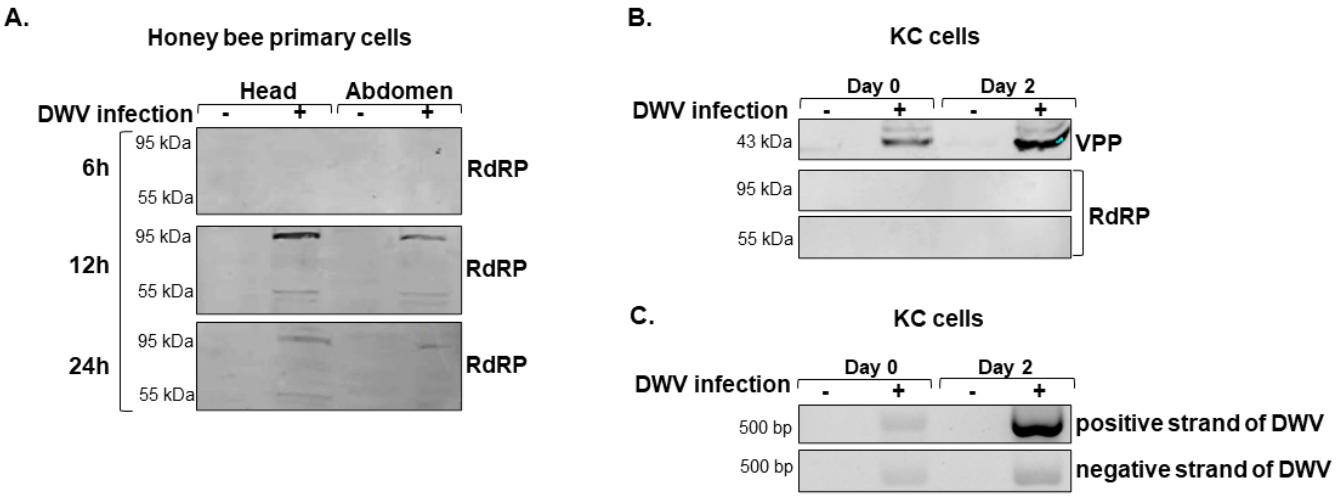

Figure 5.6 Expression of RdRP in honey bee primary cells but not *KC* cells after DWV infection.

(A) Honey bee primary cells were derived from pupal head or abdomen, and infected by DWV for 6, 12 and 24 hours. Expression of RdRP was detected by western blot and indicated as two bands near around 95 kDa and 55 kDa separately. The *KC* cells were infected by DWV virus for 2 hours (Day 0) or 2 days (Day 2). (B) Expression of VP1-P and RdRP were detected by western blot. The bands corresponding to VP1-P are near 43 kDa and the two bands for RdRP should position around 95 kDa and 55 kDa. (C) The positive- or negative-strand RNA of DWV genome was detected via RT-PCR and indicated as a band near 500 bp. Cells with and without infection were indicated by "+" and "-" respectively.

Section 5.3.3 Explore DWV replication/infection in honey bee primary cells

Shielding P-domain suppresses DWV replication

Since *S2*, *Sf9*, *LLE/LULS 40*, and *KC* cell lines cannot be used to study the mechanism of DWV replication, I decided to use honey bee primary cells for subsequent experiments. Asp294, His277, and Ser278 of P domain in VP1 locate closely and constitute a catalytic triad (Guy Dodson and Wlodawer, 1998). Ser278, Ala192, Ser293, and Asp294 of P domain adopt alternative conformations, suggesting the structure flexibility of P domain which is present at the bulge region of viral surface. Therefore, P domain may bind to DWV receptor(s) in honey bee cells to enter for the infection and replication (Skubnik et al., 2017).

As mentioned previously, the anti-VP1P antibody was raised against the P domain of DWV (Fig.3.4). In order to test whether P protein is critical for DWV entry to the cell, honey bee pupal cells were infected by DWV, which was pre-incubated with anti-VP1P antibody to mask the P domain. The pre-incubation with anti-VP1 antibody was used as the negative control. RdRP was not detected in the pupal cells when more

than 0.1 μl of anti-VP1P antibody was added (Fig.5.7A). Through the quantitative analysis, RdRP was significantly lower in the pupal cells with DWV-VP1P rather than by DWV-VP1 (0.01 μl, *P* value = 0.0426; 0.1 μl, *P* value = 0.0112; 1 μl, *P* value = 0.0316, two-tailed *t-test*) (Fig.5.7B). In order to guarantee this reduced RdRP expression was not caused by distinct protein concentrations in different samples, the same protein lysates for western blot, which were already normalized by BCA kit, were subjected to SDS-PAGE and CBB staining and similar band patterns and intensities were observed in different protein lysates derived from pupal cells infected by DWV pre-incubated with anti-VP1P or anti-VP1 antibody (Fig.5.7C). Therefore, DWV infection/replication was suppressed when the surface P-protein was blocked by the antibody, suggesting the critical role for DWV infection/replication.

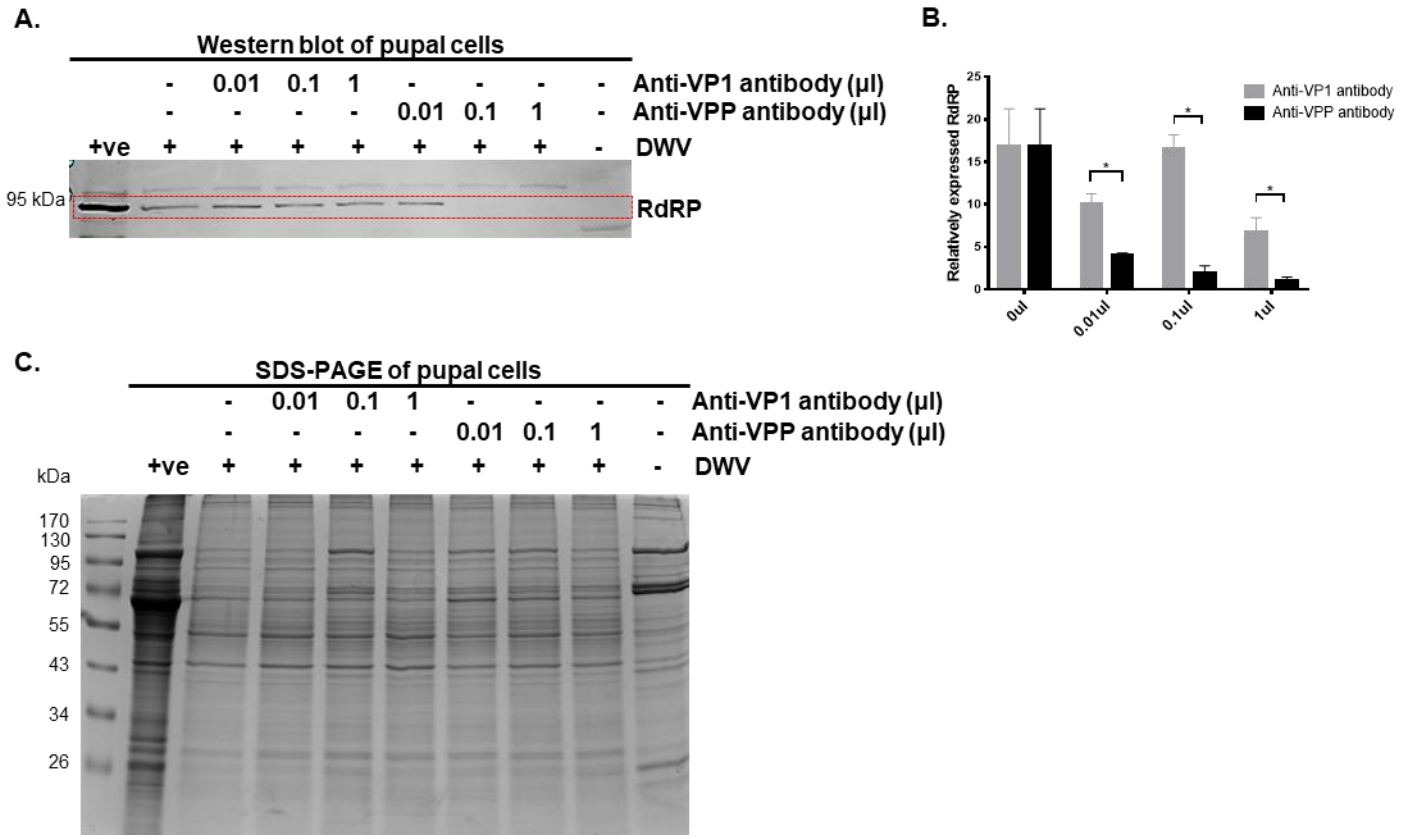

Figure 5.7 Blocking the P-protein suppresses DWV infection/replication in honey bee pupal cells.
Honey bee pupal cells were infected by DWV which was pre-incubated with different volumes of anti-VP1P or anti-VP1 antibody. (A) RdRP in the pupal cell lysates was detected by western blot. A band near 95 kDa corresponds to RdRP. (B) The quantitative analysis of RdRP detected by the western blot. The mean value with error bar (±SEM) is indicated for each sample and asterisks show statistically significant differences (*P value ≤ 0.05). (C) The same pupal cell lysates were subjected to SDS-PAGE and CBB staining. A protein marker was shown on the left of the gel. Cells with and without infection were indicated by "+" and "-" respective

P domain was not the binding site for DWV entry

Since the blocking of P protein domain by anti-VP1P antibody suppressed DWV infection/replication, P domain could be supposed the potential binding site for DWV infection. In order to test this hypothesis, I incubated honey bee pupal cells with the P domain, which was expressed and purified previously

(Fig.3.4A-B), followed by DWV infection. If the P domain is the binding site for DWV, the purified P domain binds to the DWV receptor(s) on honey bee cell, and hence blocking the subsequent viral entry and replication. RdRP was present in the pupal cells with or without pre-incubation with P domain (Fig.5.8A). Through the quantitative analysis, comparable level of RdRP was detected in the cells with and without incubation with P domain protein except when10 µl was used (*P* value = 0.0199, two-tailed *t-test*) (Fig.5.8B).

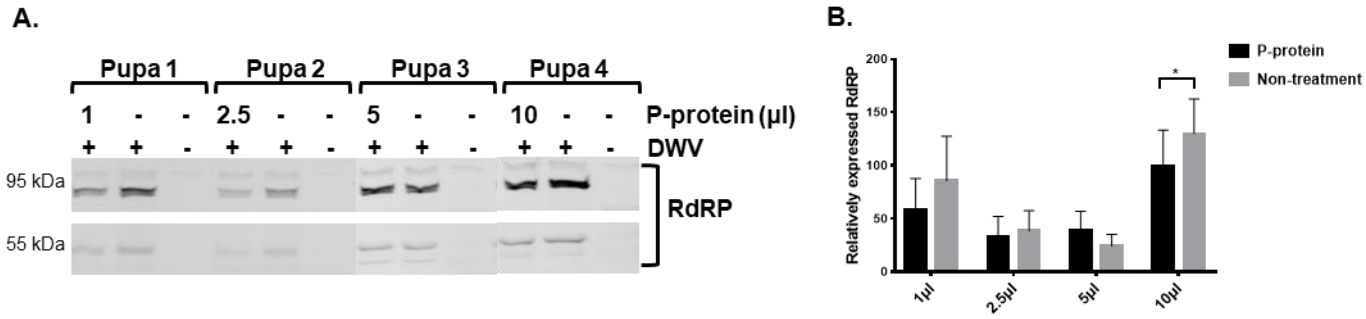

Figure 5.8 RdRP in honey bee pupal cells pre-incubated with P domain protein.

The honey bee pupal cells were pre-incubated with different amounts of purified P domain protein, followed by DWV infection. (A) RdRP in the pupal cell lysates was detected by western blot. The bands near 95 kDa and 55 kDa corresponded to RdRP. Cells with and without DWV infection were indicated by "+" and "-" respectively. (C) The quantitative analysis of western blot results. The mean value with error bar (±SEM) is indicated for each sample and asterisks show statistically significant differences (**P* value ≤ 0.05).

The binding/entry assay was further used to test whether P domain is the binding site for the DWV receptor in honey bee cells. DWV was pre-incubated with anti-VP1P antibody (DWV-VP1P) to block the P domain on the viral surface, while pre-incubation with anti-RdRP antibody (DWV-RdRP) was used as the negative control. If P domain is the binding site for DWV receptors, the blocking would suppress DWV binding to honey bee cells. After 2 hours incubation with treated DWV at low temperature (preventing viral entry), the honey bee pupal cells were subsequently subjected to western blot to detect the bound DWV. However, DWV could not be detected by western blot due to the low amount (Fig.5.9A). Thus, I decided to detect DWV bound to the pupal cells via RT-PCR and qRT-PCR. Anti-VP1 antibody (DWV-VP1) was used as the negative control in this case. Through the RT-PCR and qRT-PCR results, an equal level of DWV was detected in the pupal cells incubated with DWV treated by either DWV-VP1P or DWV-VP1 (Fig.5.9B-C).

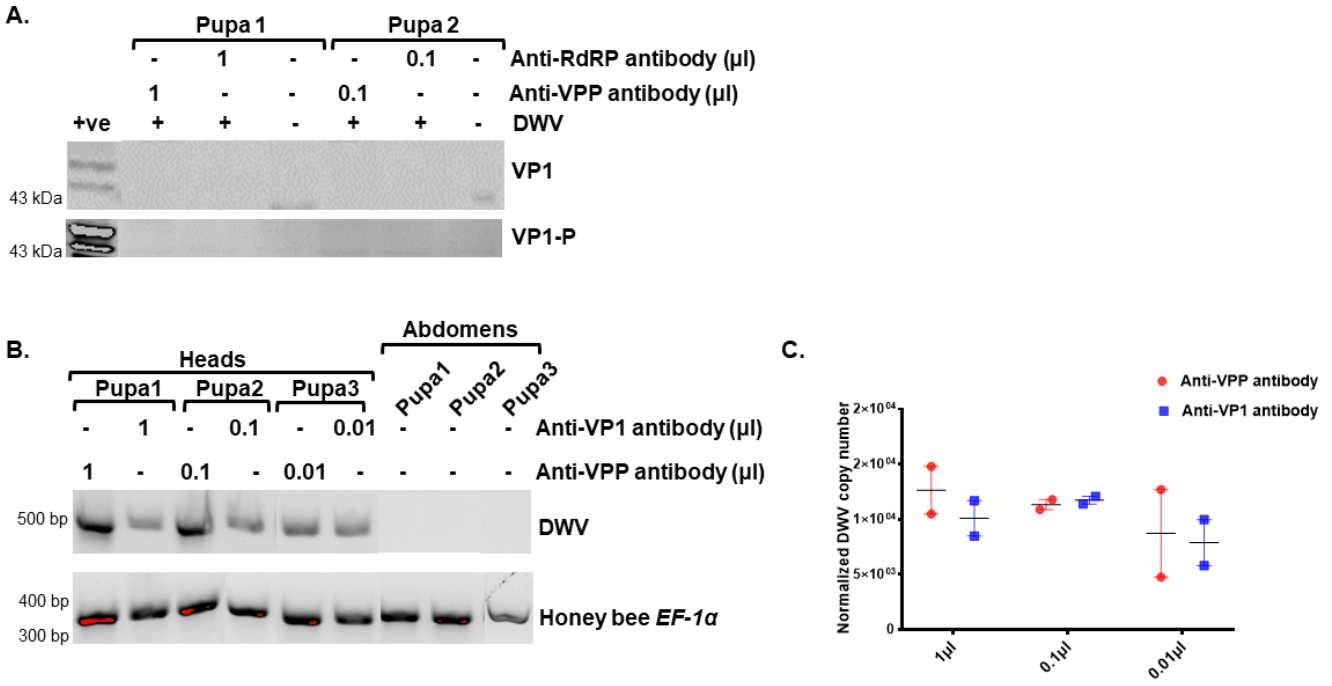

Figure 5.9 The binding assay of DWV treated with anti-VP1P antibody

(A) DWV was pre-incubated with 1 μl or 0.1 μl of anti-RdRP or anti-VP1P antibody, followed by incubation with pre-cooled honey bee pupal cells under 4°C for 2 hours. The cell lysates were subjected to western blot and the band near 43 kDa should correspond to VP1. Cells with and without DWV were indicated by "+" and "-" respectively. (B) DWV was pre-incubated with 1 μl, 0.1 μl or 0.01μl of anti-VP1P antibody or anti-VP1 antibody, followed by incubation with pre-cooled pupal cells under 4°C for 2 hours. DWV was detected via RT-PCR and honey bee *EF-1α* mRNA was used as the endogenous positive control. The position of 500 bp and 300-400 bp of DNA molecular weight was labelled on the left of agarose gels. (C) The normalized DWV copy number was quantified via qRT-PCR and the mean value with error bar (±SEM) is indicated for each sample.

The binding assay was also carried out with honey bee pupal cells pre-incubated with P domain protein. If P domain is the binding site for DWV, this pre-incubation would block the binding of DWV to honey bee cells. The pre-incubation with PBS was used as the negative control. P domain or PBS-treated pupal cells were then incubated by DWV under 4°C for 2 hours. The amount of bound DWV was too low to be detected by western blot (Fig.5.10A). The bound DWV was detected in both P domain- and PBS-treated pupal cells via RT-PCR (Fig.5.10B); however, the normalized DWV copy number in the P domain treated cells was lower than that in PBS-treated cells but no significance (Fig.5.10C).

Based on these results, the blocking of P-domain suppresses DWV infection/replication; however, the binding of DWV to honey bee cells appears intact.

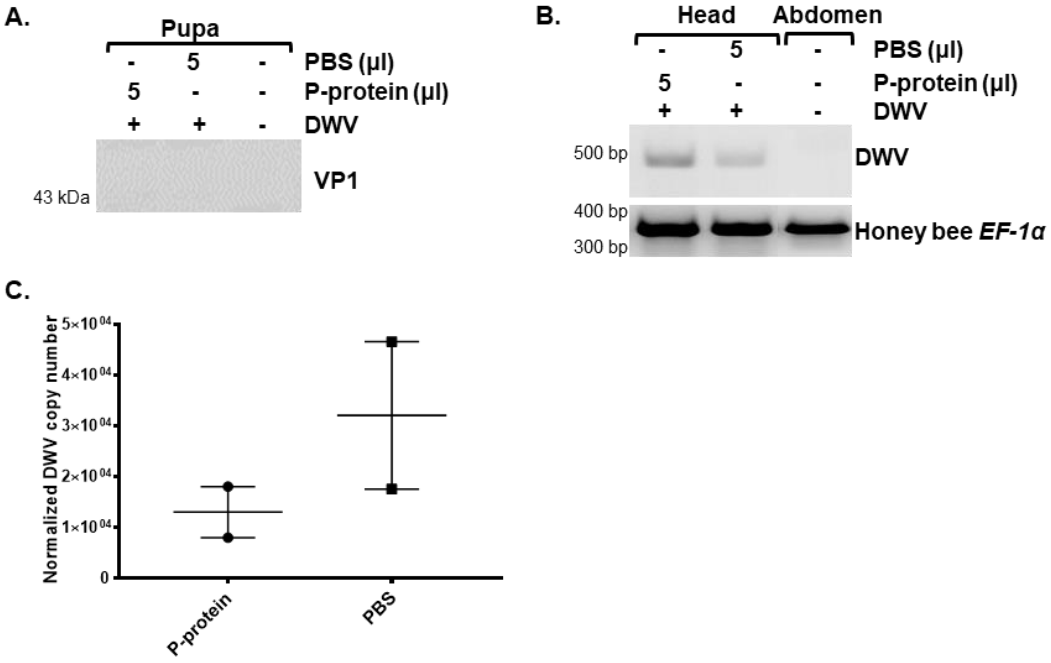

Figure 5.10 Binding assay of DWV with honey bee pupal cells pre-incubated by P-domain.

Honey bee pupal cells were pre-incubated with 5 µl of P domain protein, followed by incubation with DWV under 4°C for 2 hours. (A) DWV bound to the pupal cells was detected by western blot and the band near 43 kDa should correspond to VP1. (B) The bound DWV was detected via RT-PCR and honey bee *EF-1α* mRNA was used as the endogenous positive control. The position of 500 bp and 300-400 bp of DNA molecular weight was labelled on the left of agarose gels. Cells with and without incubation were indicated by "+" and "-" respectively. (C) The normalized DWV copy number was quantified via qRT-PCR and the mean value with error bar (±SEM) is indicated for each sample.

DWV infection/replication is inefficient in pupal cells at the late developmental stages

Honey bee pupae without ectoparasitic mite infestation were collected and divided into groups at different developmental stages, based on colours of eyes and body. Group A to D indicated the earlier to older stages of pupae, each with 3 representatives (Fig.5.11A-B). For each pupa, the head was dissected to half, and one part was infected by DWV, while the other was uninfected as the negative control. Since the previous experiment indicated that pupal head cells expressed RdRP after 12 hours infection (Fig.5.6A), these pupal cells at the different developmental stages were infected by DWV overnight then test for RdRP. RdRP was clearly detected in Group A but not Group D. RdRP decreased in the order of Group A, B, and C (Fig.5.11C). The quantitative analysis was consistent with this observation. Compared to cells without DWV infection, RdRP was significantly higher in the infected cells of Group A (*P* value = 0.0329, two-tailed *t-test*), B (*P* value = 0.0257, two-tailed *t-test*), and C (*P* value = 0.0163, two-tailed *t-test*). However, there was no significant difference between the cells with and without DWV infection in Group D. DWV infection/replication becomes inefficient in pupae at late stages (Fig.5.11D).

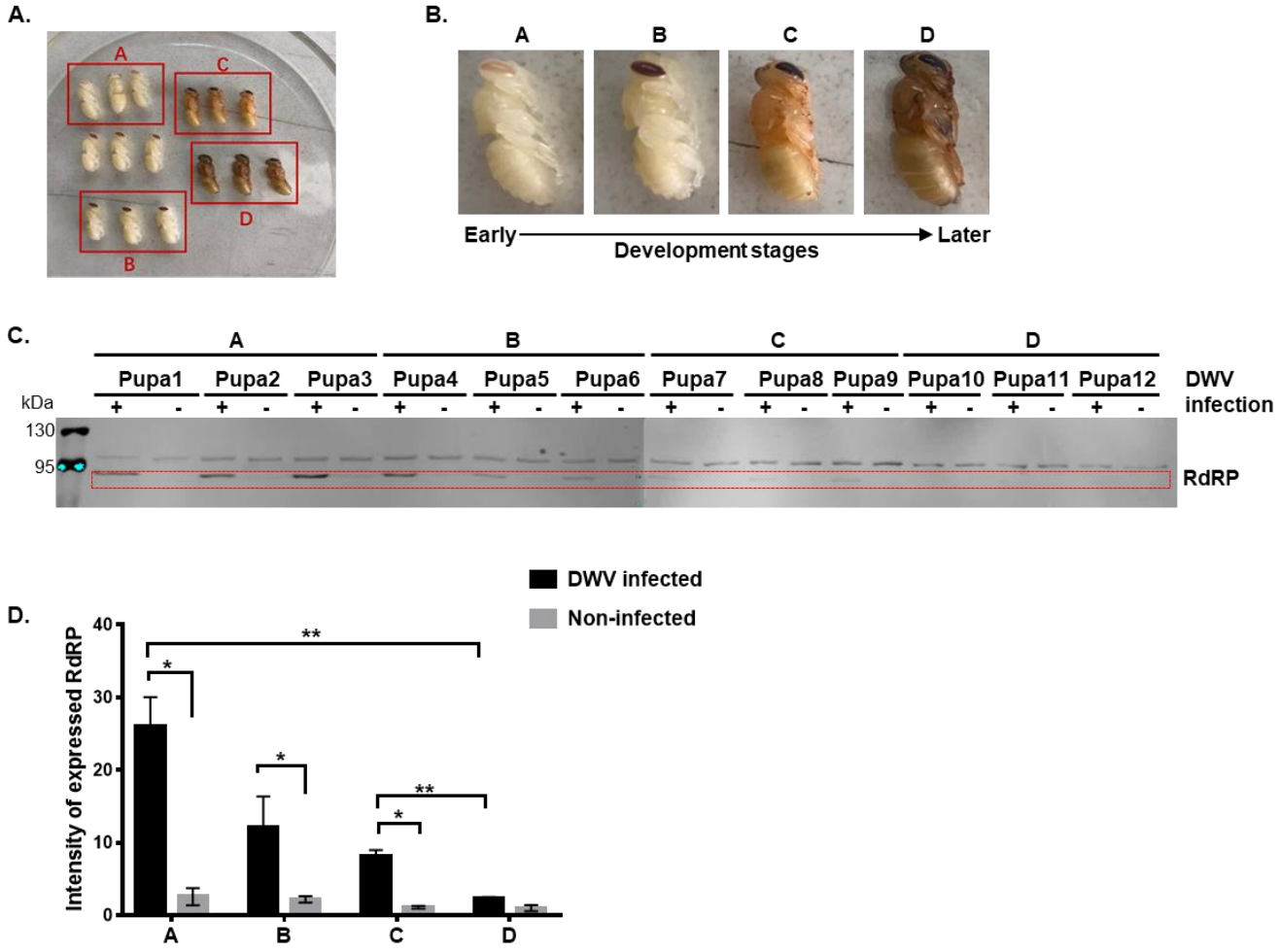

Figure 5.11 RdRP in honey bee pupal cells at different developmental stages.

(A) Honey bee pupae at the different developmental stages were collected from capped cells without mite infestation. Based on colours of pupal eyes and body, 12 pupae were divided to 4 groups, A-D, indicating the earlier to older stage and each group containing 3 representatives. (B) Comparison of the pupae representing different developmental stages. (C) Western blot of pupal head cells with or without DWV infection using anti-RdRP antibody. The band near 95 kDa represents RdRP. (D) The quantitative analysis of RdRP based on western blot results. The mean value with error bar (±SEM) is indicated for each sample and asterisks show statistically significant differences (*P value ≤ 0.05; **P value ≤ 0.01).

Section 5.3.4 Identification of potential honey bee genes critical for DWV replication via RNA-seq

Since DWV infection/replication is inefficient in honey bee pupal cells at late developmental stage, the critical components for DWV infection/replication were decreased in the older pupae or adult bees. In order to identify these components, 10 pupae with pale-white eyes (W) and 10 pupae with black eyes and yellow body (Y) were picked, representing the early and late pupae, respectively (Fig.5.12A). Their total RNAs were individually isolated and all samples were found to be negative for DWV via RT-PCR (Fig.5.2B). Total RNAs of five pupae in either Y or W were pooled for the subsequent Illumina RNA sequencing analysis.

A.

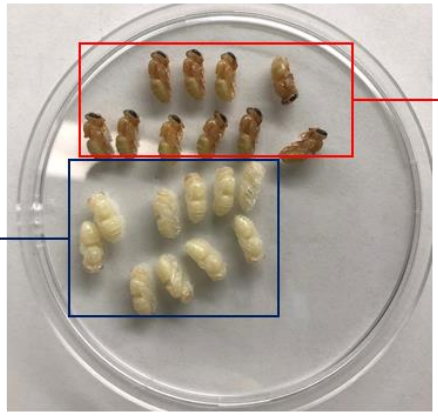

B.

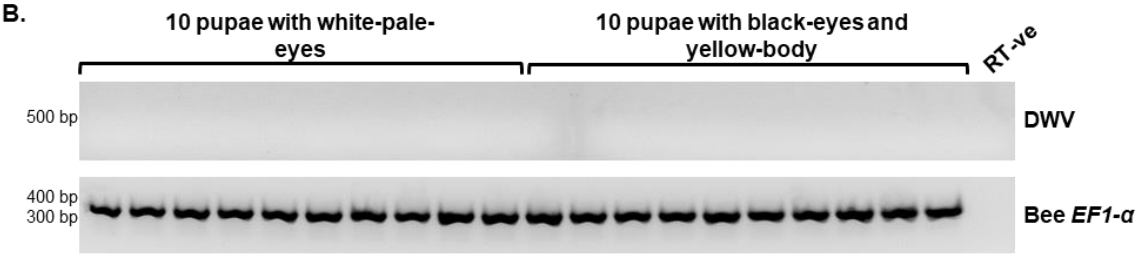

C.

Overall alignment rates of RNA-seq reads

Sample	Against honey bee genome
W1	94.67%
W2	94.41%
Y1	94.12%
Y2	94.41%

Figure 5.12 Honey bee pupal RNA samples selected for RNA-seq to identify the differentially expressed genes between pupae at early and late developmental stages.

(A) 10 honey bee pupae at early (W) or late (Y) developmental stages were picked and (B) their DWV infections were tested via RT-PCR. Honey bee *EF-1α* mRNA was used as the endogenous positive control while water (RT-ve) as the negative control. The position of a 500 bp and 300-400 bp DWV molecular weight marker is labelled on the left of agarose gel. (C) The overall mapping rates of the assembled reads from RNA-seq to honey bee genome.

The assembled reads from RNA-seq were mapped to honey bee genome first and approximately 94% of the total reads were mapped to the genome for each sample (Fig.5.12C). Then I assessed DEGs between early (W) and late pupa (Y) by using the threshold value of $\log_2$Fold Change as 1 and the adjustment *P* value as 0.01. There were in total 1861 DEGs, including 1332 up-regulated and 529 down-regulated genes in late pupae. After Geno Ontology (GO) enrichment analysis, the most enriched GO category for the up-regulated genes in late pupae was integral component of membrane. Additionally, genes involved plasma membrane and membrane belonging to cellular component, were up-regulated as well. The enriched membrane proteins in late pupae is due to brain formation with millions of developing neurons. The down-regulated genes in late pupae are involved in nucleus, sequence-specific binding, regulation of DNA-templated transcription, multicellular organism development *et al*.

Since host membrane proteins contain several critical roles on viral replication, especially for positive-strand RNA virus (Ahlquist et al., 2003), I therefore decided to focus on the down-regulated genes

categorized within the GO enriched term membrane component, which are listed in Table.5.1. They should potentially function critical roles on DWV infection/replication, such as providing localization for VRC assembly, protecting VRC, and DWV binding receptor(s).

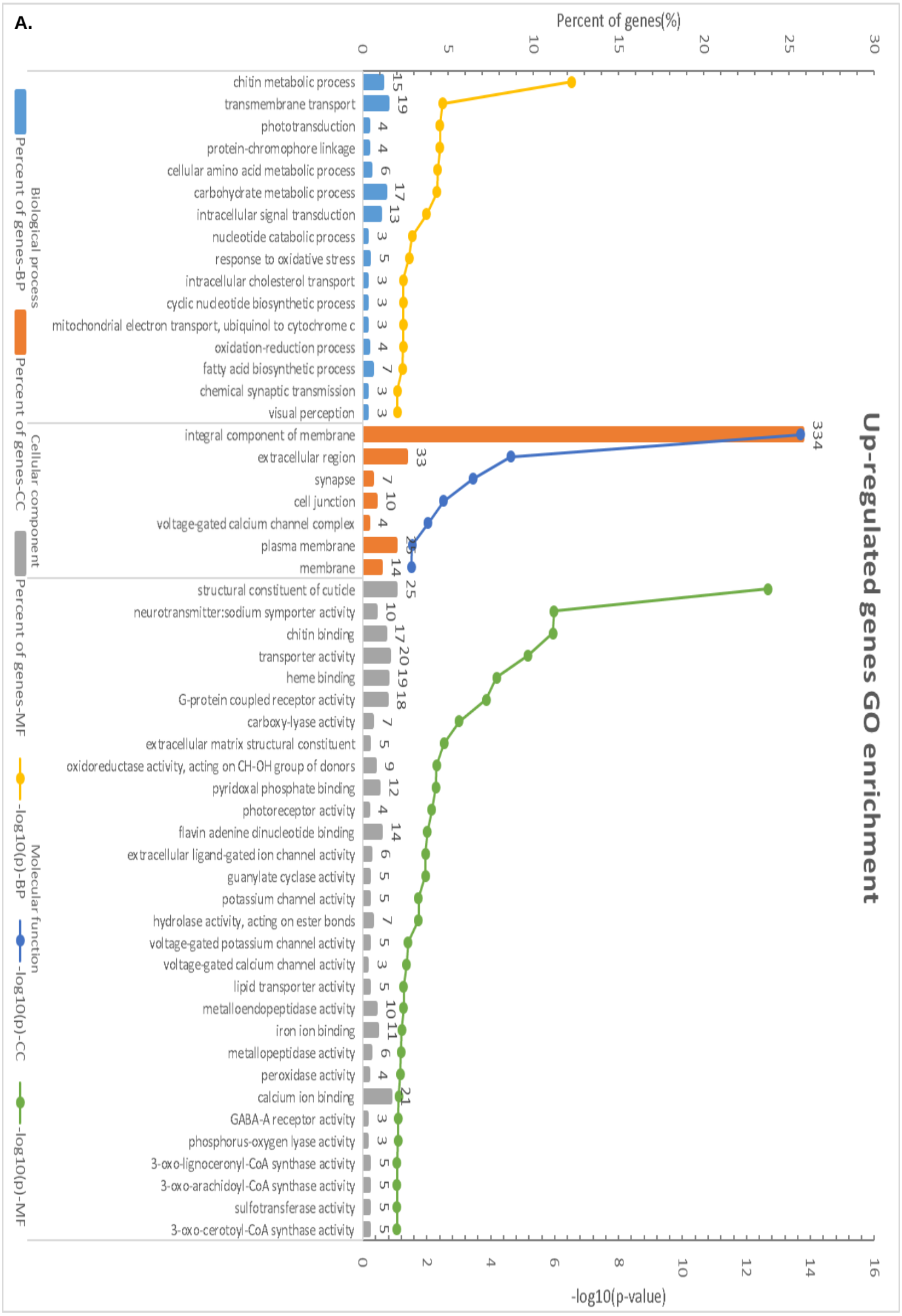
A.
Up-regulated genes GO enrichment
Percent of genes(%)
-log10(p-value)
Biological process
Cellular component
Molecular function
Percent of genes-BP
Percent of genes-CC
Percent of genes-MF
-log10(p)-BP
-log10(p)-CC
-log10(p)-MF
chitin metabolic process
transmembrane transport
phototransduction
protein-chromophore linkage
cellular amino acid metabolic process
carbohydrate metabolic process
intracellular signal transduction
nucleotide catabolic process
response to oxidative stress
intracellular cholesterol transport
cyclic nucleotide biosynthetic process
mitochondrial electron transport, ubiquinol to cytochrome c
oxidation-reduction process
fatty acid biosynthetic process
chemical synaptic transmission
visual perception
integral component of membrane
extracellular region
synapse
cell junction
voltage-gated calcium channel complex
plasma membrane
membrane
structural constituent of cuticle
neurotransmitter:sodium symporter activity
chitin binding
transporter activity
heme binding
G-protein coupled receptor activity
carboxy-lyase activity
extracellular matrix structural constituent
oxidoreductase activity, acting on CH-OH group of donors
pyridoxal phosphate binding
photoreceptor activity
flavin adenine dinucleotide binding
extracellular ligand-gated ion channel activity
guanylate cyclase activity
potassium channel activity
hydrolase activity, acting on ester bonds
voltage-gated potassium channel activity
voltage-gated calcium channel activity
lipid transporter activity
metalloendopeptidase activity
iron ion binding
metallopeptidase activity
peroxidase activity
calcium ion binding
GABA-A receptor activity
phosphorus-oxygen lyase activity
3-oxo-lignoceronyl-CoA synthase activity
3-oxo-arachidoyl-CoA synthase activity
sulfotransferase activity
3-oxo-cerotoyl-CoA synthase activity

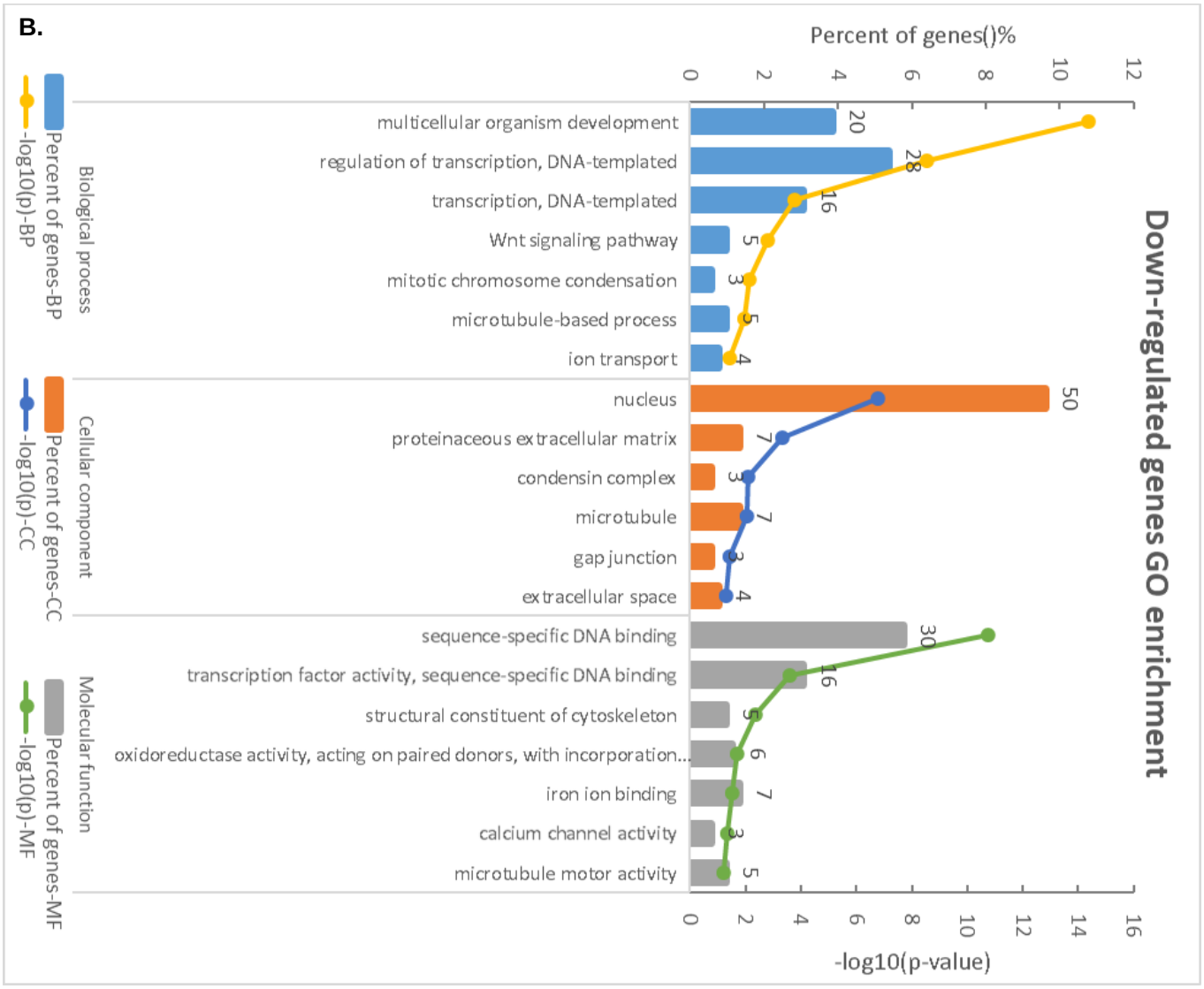

Figure 5.13 GO enrichment analysis of up- and down-regulated DEGs between honey bee pupae at early and late stages.

Compared to the early developmental pupae (W), the (A) up- and (B) down-regulated genes in late developmental pupae (Y) were assigned for GO terms separately via EnsemblMetazoa. The enriched genes were classified into biological process, cellular components or molecular function.

Table 5.1 Profile of down-regulated genes in GO term of membrane components.

Gene ID	Description	Log_2FC	*P* value
LOC102655009	elongation of very long chain fatty acids protein AAEL008004 [*Apis mellifera*]	-9.7369	6.77E-21
LOC100578715	protein wntless [*Apis mellifera*]	-2.10347	9.59E-106
LOC100578467	protein Star [*Apis mellifera*]	-1.52782	3.32E-110
LOC100576449	protein patched [*Apis mellifera*]	-1.78986	2.36E-96
LOC100576414	putative fatty acyl-CoA reductase CG5065 [*Apis mellifera*]	-2.04047	6.65E-12
18-w	18-wheeler [*Apis mellifera*]	-1.2342	2.69E-30
Or2	Odorant receptor 2 [*Apis. mellifera*]	-1.39083	2.09E-10
LOC107964338	transient receptor potential-gamma protein [*Apis mellifera*]	-2.15162	2.08E-31
LOC107964339	short transient receptor potential channel 6-like [*Apis mellifera*]	-2.26981	3.28E-26

LOC408398	cytochrome P450 306a1 [*Apis mellifera*]	-1.23117	1.14E-16
LOC408447	neurotactin [*Apis mellifera*]	-1.93556	1.42E-160
LOC408451	NADPH oxidase 5 [*Apis mellifera*]	-1.32126	5.51E-10
LOC408777	no mechanoreceptor potential C [*Apis mellifera*]	-4.10757	2.70E-216
LOC409265	dolichyl-diphosphooligosaccharide--protein glycosyltransferase subunit STT3A [*Apis mellifera*]	-1.05544	7.88E-41
LOC409905	2-acylglycerol O-acyltransferase 1 [*Apis mellifera*]	-1.21337	2.26E-24
LOC410190	tyrosine-protein kinase Dnt [*Apis mellifera*]	-2.27577	8.42E-72
LOC410229	toll-like receptor 6 [*Apis mellifera*]	-1.00777	1.90E-40
LOC410231	toll-like receptor Tollo [*Apis mellifera*]	-3.63637	3.65E-152
LOC410246	netrin receptor UNC5B [*Apis mellifera*]	-1.29648	6.31E-62
LOC410683	sodium-coupled monocarboxylate transporter 2 [*Apis mellifera*]	-2.42562	1.16E-05
LOC410825	leucine-rich repeat and immunoglobulin-like domain-containing nogo receptor-interacting protein 3 [*Apis mellifera*]	-1.3906	3.38E-65
LOC410853	irregular chiasm C-roughest protein [*Apis mellifera*]	-1.06179	7.10E-52
LOC410913	sodium/potassium-transporting ATPase subunit alpha [*Apis mellifera*]	-1.74896	9.86E-08
LOC410920	putative inorganic phosphate cotransporter [*Apis mellifera*]	-1.2082	2.13E-15
LOC410967	ABC transporter G family member 22 [*Apis mellifera*]	-1.27686	1.38E-27
LOC411023	cadherin-23 [*Apis mellifera*]	-1.71536	0.0003635
LOC411086	protein jagged-1 [*Apis mellifera*]	-1.38261	1.59E-69
LOC411685	ATP-binding cassette sub-family D member 1 [*Apis mellifera*]	-1.05801	9.13E-23
LOC412399	organic cation transporter protein [*Apis mellifera*]	-1.4182	1.15E-36
LOC412788	scavenger receptor class B member 1 [*Apis mellifera*]	-2.02322	2.51E-53
LOC413020	two pore potassium channel protein sup-9 [*Apis mellifera*]	-1.15731	6.08E-15
LOC413168	retinol dehydrogenase 14 [*Apis mellifera*]	-1.54186	5.86E-10
LOC413263	putative inorganic phosphate cotransporter [*Apis mellifera*]	-1.03717	6.52E-12
LOC413333	hemicentin-2 [*Apis mellifera*]	-1.52942	1.86E-12
LOC413844	ATP-binding cassette sub-family G member 5 [*Apis mellifera*]	-1.59226	3.86E-101
LOC550828	elongation of very long chain fatty acids protein AAEL008004 [*Apis mellifera*]	-2.52439	1.33E-31
LOC550965	probable cytochrome P450 6a14 [*Apis mellifera*]	-3.0207	5.67E-71
LOC551124	frizzled-2 [*Apis mellifera*]	-1.23309	6.49E-29
LOC551165	innexin inx3 [*Apis mellifera*]	-2.26693	4.62E-177
LOC551168	protein sidekick [*Apis mellifera*]	-1.52399	3.29E-80
LOC551263	monocarboxylate transporter 13 [*Apis mellifera*]	-1.53569	6.20E-13
LOC551508	vang-like protein 1 [*Apis mellifera*]	-1.0056	2.91E-23
LOC551848	protocadherin-like wing polarity protein stan [*Apis mellifera*]	-2.32656	9.00E-261
LOC552313	sterol O-acyltransferase 1 [*Apis mellifera*]	-1.04381	2.22E-24
LOC552546	protocadherin Fat 4 [*Apis mellifera*]	-2.71427	2.71E-125
LOC724378	BMP and activin membrane-bound inhibitor homolog [*Apis mellifera*]	-1.67898	1.09E-122

LOC724760	G-protein coupled receptor Mth2 [*Apis mellifera*]	-1.24673	5.06E-13
LOC724832	innexin inx2 [*Apis mellifera*]	-1.49109	1.48E-102
LOC725008	protein trapped in endoderm-1 [*Apis mellifera*]	-1.06065	1.33E-24
LOC725026	retinol dehydrogenase 10-A [*Apis mellifera*]	-7.35703	1.48E-191
LOC725284	chitin synthase chs-2 [*Apis mellifera*]	-1.02603	4.12E-22
LOC725922	mitochondrial basic amino acids transporter [*Apis mellifera*]	-3.62102	7.36E-120
LOC726158	glutathione hydrolase 1 proenzyme [*Apis mellifera*]	-1.28424	2.32E-19
LOC726513	ATP-binding cassette sub-family G member 5 [*Apis mellifera*]	-1.50201	1.66E-99
LOC726677	protein singles bar [*Apis mellifera*]	-1.32928	1.79E-08

The value of Log_2FC indicates expression differences of the specific gene between pairwise comparisons, and the greater absolute value of Log_2FC means larger differences between two comparisons. The negative Log_2FC designate down-regulated genes in honey bee pupae at late developmental stages. *P*-value was calculated by *t-test*.

Section 5.3.5 Interactions between DWV structural protein and honey bee proteins

To access the protein interactions between honey bee and DWV, the protein lysates derived from DWV infected honey bee pupae were immunoprecipitated with anti-VP1P antibody, and the pre-immune serum was used as the negative control. As shown in Fig.5.14, there were 7 specific bands in the immunoprecipitated fraction via sliver staining. Through protease digestion of the proteins extracted from above 7 bands followed by the mass spectrometric analysis, the proteins in the bands 1-4 corresponded to DWV structural protein VP1 while the band 5, 6, 7 was a mixture of structural proteins of VP1 and VP2, VP2 and VP3, and VP2 and VP3, respectively (Fig.5.14). However, searching the *A. mellifera* database provided no significant hit. Therefore, I used the whole anti-VP1P immunoprecipitated fraction for the direct MS analysis to identify the interaction between VP1 and honey bee proteins. The whole immunoprecipitated fraction from the pre-immune serum was analysed by MS as well and the identified proteins were regarded as the non-specific. The honey bee proteins potentially interacting with VP1 were listed in Table.5.2. Most of proteins were cuticle and cuticle related proteins, and 5 peptides were actin and actin-related proteins. Heat shock protein 60A was also identified as well (Table.5.2).

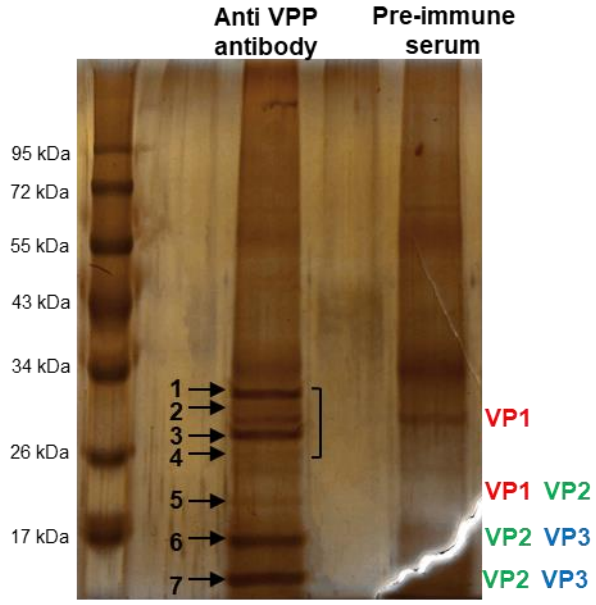

Figure 5.14 Sliver staining of immunoprecipitated proteins by anit-VP1P antibody.

Sliver staining of immunoprecipitated proteins by anti-VP1P antibody in honey bee lysate. Pre-immune serum of anti-VP1P was used as the negative control. The specific bands were indicated as 1-7. Based on mass spectrometry and DWV database analysis, the peptides in Band 1-4, 5, and 6-7 were designated as VP1, VP1+VP2, and VP2+VP3, respectively. a protein marker was shown on the left of the gel.

Table 5.2 Summary of honey bee proteins potentially interacting with VP1.

Peptide sequence	Protein identification	
AVVATPVAK	Cuticular protein1 precursor	Cuticle and cuticle related proteins
IAAAPVAYAAPVAK	Cuticular protein1 precursor	
LAAAPVAYTAPAPTLIH	Cuticular protein1 precursor	
AVVAAPVAK	Cuticular protein2 precursor	
AVAAAPVAATPVAAAPVAVK	Cuticular protein2 precursor	
TIAAAPVAHALPLSYAASAPVISAPIAK	Cuticular protein2 precursor	
STGNLAQIATQSK	cuticular protein CPF1 precursor	
SDDSAHSFVR	pupal cuticle protein G1A	
GFAGQNVISSYTK	pupal cuticle protein G1A	
AAAVAAPAPLLHAAPASLLTR	pupal cuticle protein G1A	
SALIAPAAGYAASITPAAPLLAK	pupal cuticle protein G1A	
YTAPIGTVAPAPLLHATSAEPLIHAAPASFLHAAPAAPLLAK	pupal cuticle protein G1A	
TLIYVLVK	cuticle protein, gibberellin-regulated protein	
AGFAGDDAPR	Actin, actin related protein 1	Actin and actin related proteins
SYELPDGQVITIGNER	Actin, actin related protein 1	
DLYANTVLSGGTTMYPGIADR	Actin, actin related protein 1	
LCYVALDFEQEMATAASSSSLEK	actin related protein 1	
LEADINELEIALDHANK	myosin heavy chain	
TALTDAAGVASLLTTAEAVVAELPK	heat shock protein 60A	Heat shock protein
LSSPLASQSR	70% Identity Liprin-beta-1/2 isoform	
HVPVPVK	tetra-peptide repeat homeobox protein 1	
QIPLPVVQPAVVIEK	tetra-peptide repeat homeobox protein 1	

(Uncharacterized proteins are not listed)

Section 5.4 Discussion

Section 5.4.1 DWV contains a skewed codon usage and adapts to the host with A/T-rich genome

Genome compositions vary among different organisms due to the directional bias toward AT or GC (Lobry and Sueoka, 2002, Sueoka, 1988, Sueoka, 1993). This directional bias could be caused by evolutionary selection, viral RNA polymerase-related copying errors, and host RNA-editing enzymes (Vartanian et al., 2002, Vartanian et al., 1994, Cattaneo et al., 1988). I compared GC contents in the genomes of DWV, honey bee, ectoparasitic mites *V. destructor*, *T. mercedesae*, as well as *D. merlanogaster*, *S. fugiperda*, *L. longipalpis*, and *C. sonorensis*, from which four insect cell lines are derived. Honey bee contains the lowest GC content (32.5%) followed by *C. sonorensis* (33%), from which the *KC* cell line was derived. The genome GC contents in *S. fugiperda* (36.05%), *L. longipalpis* (35.9%) and *D. merlanogaster* (42.1%), are higher than that of honey bee genome (Fig.5.15).

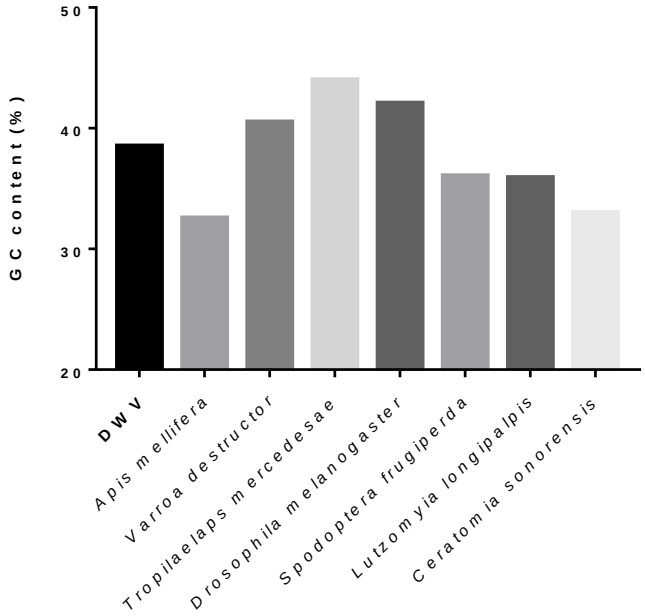

Figure 5.15 Comparison of GC content (%) in DWV and insect's genomes.

The GC content in the genome of DWV (38.5%), *A. mellifera* (32.5%), *V. destructor* (40.5%), *T. mercedesae* (44%), *D. melanogaster* (42.1%), *S. frugiperda* (36.05%), *L. longipalpis* (35.9%) and *C. sonorensis* (33%).

GC content of genome contributes to the codon usage bias, a phenomenon in which synonymous codons occur with different frequencies (Aota and Ikemura, 1986, Chen et al., 2004, Francino and Ochman, 1999, Ikemura and Wada, 1991, Kanaya et al., 2001, Bahir et al., 2009). The codon usage frequency varies in different species, albeit with different intensities (Grantham et al., 1980, Akashi and development, 2001). Viral gene expression can be restricted by codon usage bias (Haas et al., 1996) and enhanced by codon optimization (André et al., 1998). A previous study proved that codon bias of RNA virus, especially for positive-stranded RNA virus, is mainly driven by the genome GC content (Auewarakul, 2005). As mentioned above, the GC content of honey bee genome is relatively low, suggesting DWV adapting to the host with an A/T-rich genome, thus a specific codon usage bias may occur for DWV. I compared the GC content for codon usage at specific position 1, 2, and 3 among DWV, honey bee, *V. destructor*, *T.*

mercedesae, *D. merlanogaster*, *S. fugiperda*, and *C. sonorensis*, (Fig.5.16). The GC content for codon usage in DWV share the most similarities with *C. sonoresis*, from which the *KC* cell line was derived, followed by honey bee. There is an obvious codon usage bias at position 3 for DWV and *C. sonoresis*, which are only 30.15% and 28.62%, respectively (Fig.5.16). My previous result indicated that DWV infection in honey bee primary cells exhibited most similar to in *KC* cells, compared to the other three insects' cells tested, which could be explained by this large difference of codon usage. Due to non-detectable RdRP expression, *KC* cells still shared a different DWV infection mechanism with the one in honey bee. These different viral infection mechanisms may be explained by the lack of critical proteins for viral infection/replication, which present exclusively in honey bee. For both ectoparasitic mites, *V. destructor* and *T. mercedesae*, genome GC contents were evidently higher and the large differences of codon usage in them with in DWV (Fig.5.15 & Fig.5.16), suggesting DWV do not replicate in them, which is consistent with non-detectable replication observed in both mites (Fig.4.3).

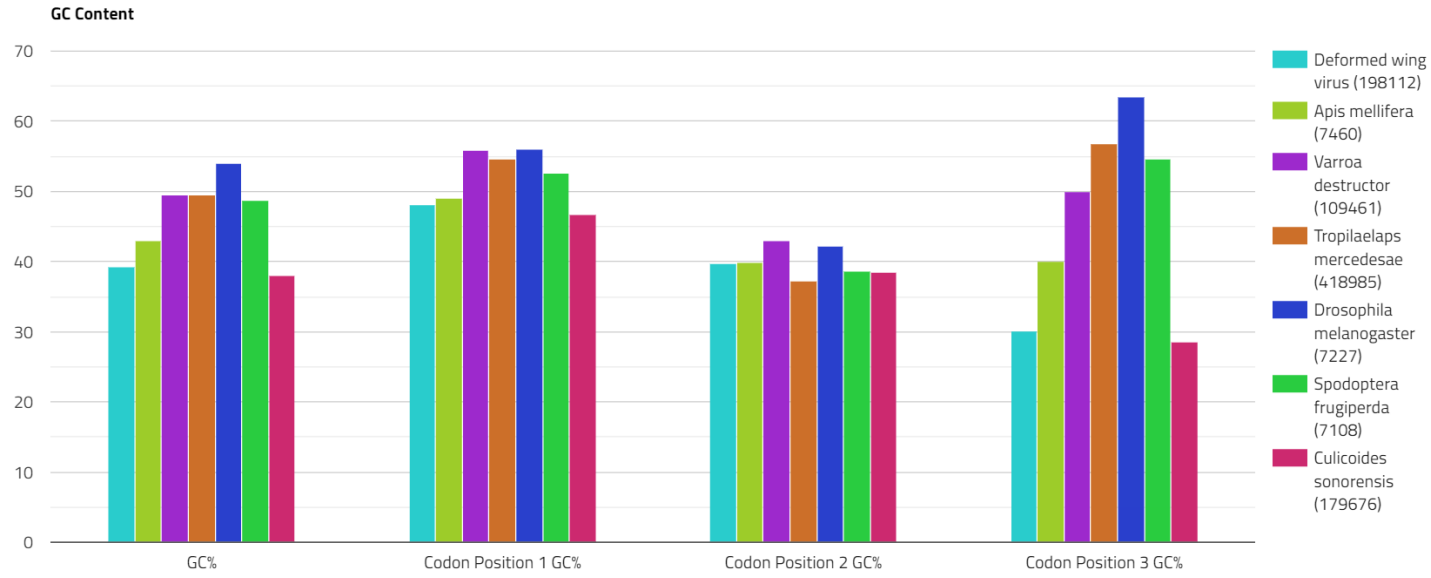

Figure 5.16 The combined GC content (%) for codon usage constructed by TissueCoCoPUTs.
TissueCoCoPUTs (Athey et al., 2017) constructed the graph comparing the GC% content in DWV, *A. mellifera*, *V. destructor* and *T. mercedesae*. The GC% content in total: DWV 39.33%, *A. mellifera* 42.95%, *V. destructor* 49.58%, *T. mercedesae* 50.33%, *D. melanogaster* 53.94%, *S. frugiperda* 48.68%, *C. sonorensis* 37.96%. The GC% content at Position 1: DWV 48.06%, *A. mellifera* 48.97%, *V. destructor* 55.84%, *T. mercedesae* 56.31%, *D. melanogaster* 56.03%, *S. frugiperda* 52.65%, *C. sonorensis* 46.71%. The GC% content at Position 2: DWV 39.77%, *A. mellifera* 39.92%, *V. destructor* 42.98%, *T. mercedesae* 37.05%, *D. melanogaster* 42.26%, *S. frugiperda* 38.71%, *C. sonorensis* 38.55%. The GC% content at Position 3: DWV 30.15%, *A. mellifera* 39.97%, *V. destructor* 49.93%, *T. mercedesae* 57.63%, *D. melanogaster* 63.52%, *S. frugiperda* 54.7%, *C. sonorensis* 28.62%.

I further compared the codon usage frequency between DWV and honey bee or ectoparasitic mites. There is a strong correlation between the codon usage frequency in DWV with the frequency in honey bee ($r = 0.7943$, P value < 0.0001) (Fig.5.17A). The codon usage frequency in *V. destructor* is also associated with the one in DWV, but with a weaker correlation ($r = 0.4996$, P value < 0.0001) (Fig.5.17B). Nevertheless,

no significant correlation between DWV and *T. mercedesae* was identified (r = 0.1974, *P* value = 0.1180) Fig.5.17C).

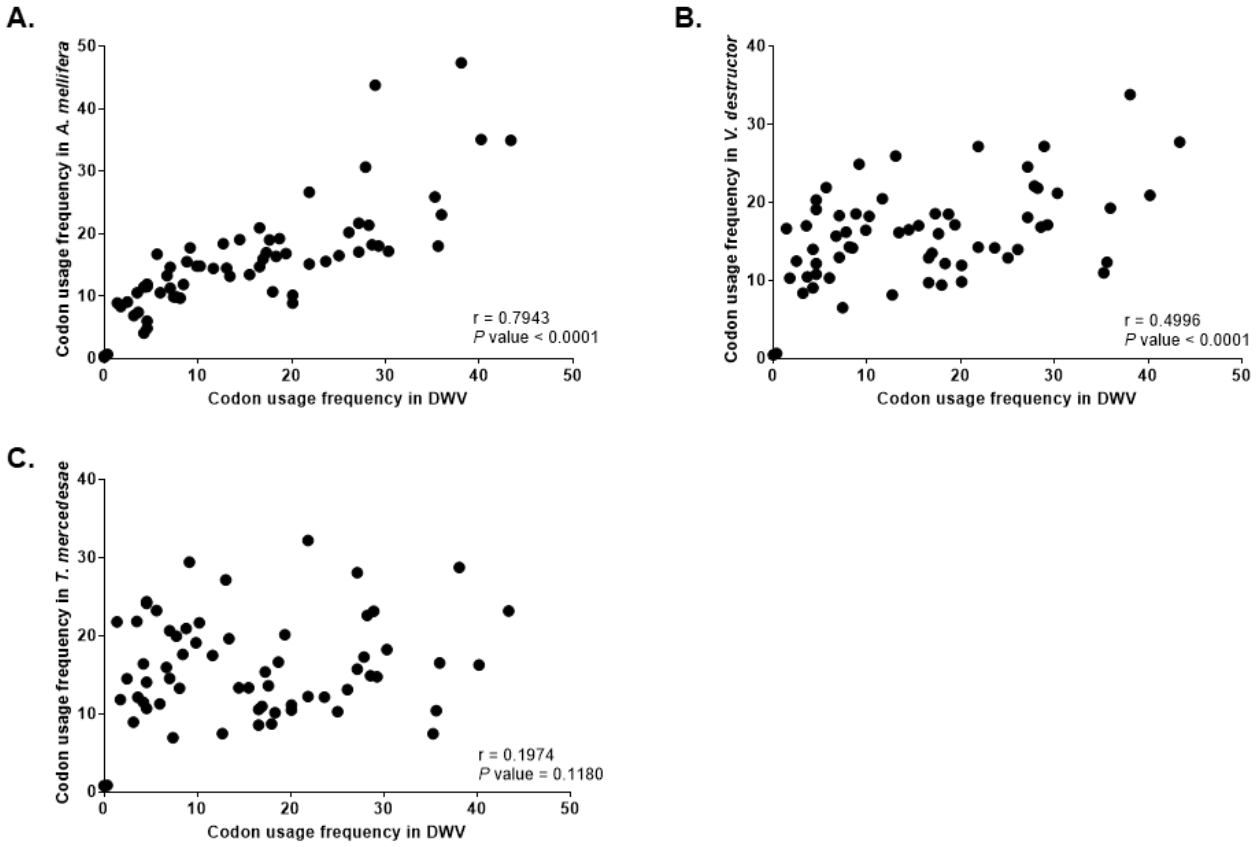

Figure 5.17 Comparisons of the codon usage frequency in DWV and infecting-hosts.

The codon usage frequency in DWV was compared with the frequency in (A) honey bee; (B) *V. destructor*; and (C) *T. mercedesae*. The codon usage frequency was analyzed by CoCoPUTs (Athey et al., 2017). The Pearson correlation values and *P* values are shown.

As a member of positive-strand RNA virus, DWV replication depends on host machinery and utilizes host cellular components (Ahlquist et al., 2003). Therefore, the codon usage of host is expected to affect DWV replication. Compared to *V. destructor* and *T. mercedesae*, codon usage frequency in honey bee shares more similarities with the one in DWV, which is consistent with the active DWV replication observed in honey bee and absence in the two mites. Therefore, the host of DWV is required to have a low GC content of codon usage, especially for the position 3. This co-evolution and adaptation are identified between several viruses and their hosts. Bacterial-infecting viruses strongly adapted to their specific hosts, especially on their GC content (Bahir et al., 2009). The human influenza viruses, including pandemic H1N1, share similar codon usage patterns with their hosts (Wong et al., 2010). The codon usage biases in viruses may provide an advantage for viral protein synthesis, thus promoting virion production and reducing the accessibility to host's immune system (Bahir et al., 2009, Bonhoeffer and Nowak, 1994). However, some viruses use a skewed codon usage which is distinct from that of host cell, to temporally regulate late expression of structural proteins (Shin et al., 2015).

Section 5.4.2 A catalytic role of P-domain for DWV entry and replication

The DWV virion consists of three major structural proteins, VP1, VP2, and VP3, arranged with a pseudo-T3 icosahedral symmetry. The P-domain is protruding at the virion surface. The three-dimensional structure of viral capsid, including P domain, changed under different pH conditions (Skubnik et al., 2017). The localization and flexibility of VP1-P domain suggest a putative receptor-binding site during DWV infection. However, based on my results, P-domain was not a binding site for DWV receptor in honey bee cell. Blocking P domain supressed viral replication in the honey bee pupal cells, and the P domain consists of Asp294, His277, and Ser278, which locate closely and constitute a catalytic triad (Guy Dodson and Wlodawer, 1998, Skubnik et al., 2017). As a result, the P domain may function as a catalytic site to provide the protease, lipase or esterase activity and critical for DWV entry and replication, but not as a binding site for the viral entry. This is supported by the essential role of viral envelope/capsid proteins for determining the viral infectivity and efficiency for host (Bahir et al., 2009). The procapsid (without RNA genome insertion) and RNA-containing infectious capsid share the same conformation; however, the A-particles (putative entry intermediates) and empty capsid (after genome release) undergo a conformational change, which primarily occurred in the P-domain (Fig.5.18) (Martin and Brettell, 2019, Skubnik et al., 2017, Organtini et al., 2017), also supporting the critical role of P-domain on viral infection.

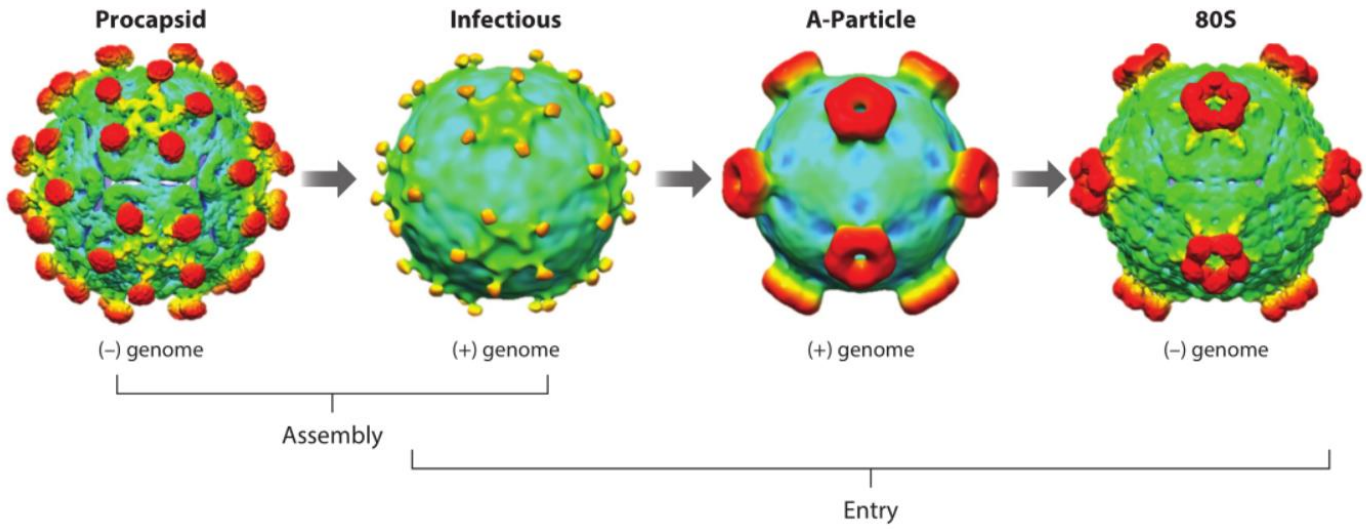

Figure 5.18 Proposed conformational changes of DWV virion during infection.

DWV RNA genome packages into the procapsid genome to produce the infectious virus. Both procapsid and infectious capsid share a same conformation. The capsid transformed into a different form in the A-particles, which is a putative entry intermediate, and the genome release form (80S) (*adapted from* (Martin and Brettell, 2019)).

Section 5.4.3 Honey bee contains critical factors for DWV infection/replication

As my results indicated, DWV replication becomes inefficient in honey bee pupae at late stage of development, which means the critical factors associated with viral infection/replication are reduced during pupal development. The AMP immune effectors, *Hymenoptaecin* and *Defensin-1* mRNAs were induced in honey bee pupae with *T. mercedesae* infestation (Fig.5.12), which are under control of Imd and Toll

immune signalling pathways, respectively (Aronstein et al., 2010, Osta et al., 2004). The induction of Defensin-1 is associated with DWV replication (Fig.5.12), therefore, AMPs may play a role on suppression of DWV infection/replication. AMPs have been reported to target organisms via several mechanisms including disrupting the lipopolysaccharide layer of cell membrane (Jenssen et al., 2006). Previous studies indicate a crucial role of the host membrane on multiple processes for positive-strand RNA viral replication: 1) providing a localization for replication factors' assembly; 2) the membrane surrounds and protects viral replication compartment, allowing replication factors and genomic RNAs to complete replication. This membrane-bounded compartment prevent the accessibility of competing RNA templates, completing processes like translation and host defence responses, such as RNA interference (Ahlquist, 2002, Ahlquist et al., 2003); 3) packaging or retaining replication factors on membranes (Hagiwara et al., 2003, Yamanaka et al., 2000). Several examples indicate viral replication associated with membrane proteins. For example, TMV replication in *Arabidopsis* was inhibited by dual mutation of TOM1 and TOM3, which were host integral membrane proteins (Ahlquist et al., 2003). Therefore, certain down-regulated genes belonging to the GO term of membrane components may potentially contain a role on DWV infection/replication, such as a viral receptor. Nevertheless, further studies are required to verify the specific gene and functions on DWV infection and replication.

Chapter 6 Conclusion

My project aimed to identify the cross-interaction between honey bee, DWV, and ectoparasitic mite *T. mercedesae*. Based on my results, *T. mercedesae* acts as a biological and mechanical vector for DWV transmission to honey bee. It can transmit DWV to honey bee and the wound caused by its feeding activity promotes viral replication in honey bee pupae. Correspondingly, DWV can be transmitted from honey bee to mite via intake of fat body or other tissues through feeding activity, which is suggested by the accumulated DWV in intestinal region of mites. Mite infestation induces *Hymenoptaecin* and *Defensin-1* mRNA in pupae, which are associated with mite feeding activity and DWV replication, respectively. Hymenoptaecin and Defensin-1, as two types of AMPs identified in honey bee, are under control of Toll and Imd immune signalling pathways, respectively. I also identified a positive correlation between DWV copy number in pupae and copy number in infesting mites, which forms two clusters with either high or low copy number in both honey bee pupae and infesting mites. The same DWV type A variant was present in either low or high copy number in both honey bee pupae and infesting *V. destructor* or *T. mercedesae*. These data suggest a previously proposed hypothesis that DWV suppressed the honey bee immune system when DWV copy number reaches a specific threshold, promoting greater replication. DWV replication was only observed in honey bee, not in neither *V. destructor* or *T. mercedesae*, therefore, the high viral load in mites is caused by feeding activity or vertical transmission. Reproductive capability of *T. mercedesae* with high viral load is decreased probably via down-regulation of vitellogenin synthesis. A negative correlation was observed between the amount of *Vitellogenin* mRNA in *T. mercedesae* and *Hymenoptaecin* mRNA in the infesting pupae, suggesting the intake of Hymenoptaecin play a role on down-regulation of vitellogenin synthesis. Therefore, DWV is not completely harmless for the vector *T. mercedesae*, and Hymenoptaecin induced by the mite feeding exerts the negative feedback on the mite reproduction may help establishing an equilibrium between host (honey bee) and parasite (mite). DWV replication/infection occurs inside the host with A/T-rich genome and a skewed codon usage and the accessibility of VP1-P domain on the viral virion is compulsory as well. Some proteins, present in honey bee, especially membrane proteins, probably contain critical role for DWV infection/replication, however, further study required to verify (Fig.6.1).

In order to unravel the underlying the mechanisms of DWV replication in honey bee, further studies are required, including identification of critical components for viral replication and probably exclusively present in honey bee and verification of the function of VP1-P domain on viral replication. Unlocking the key to viral replication would be beneficially for honey bee colony health and maintenance.

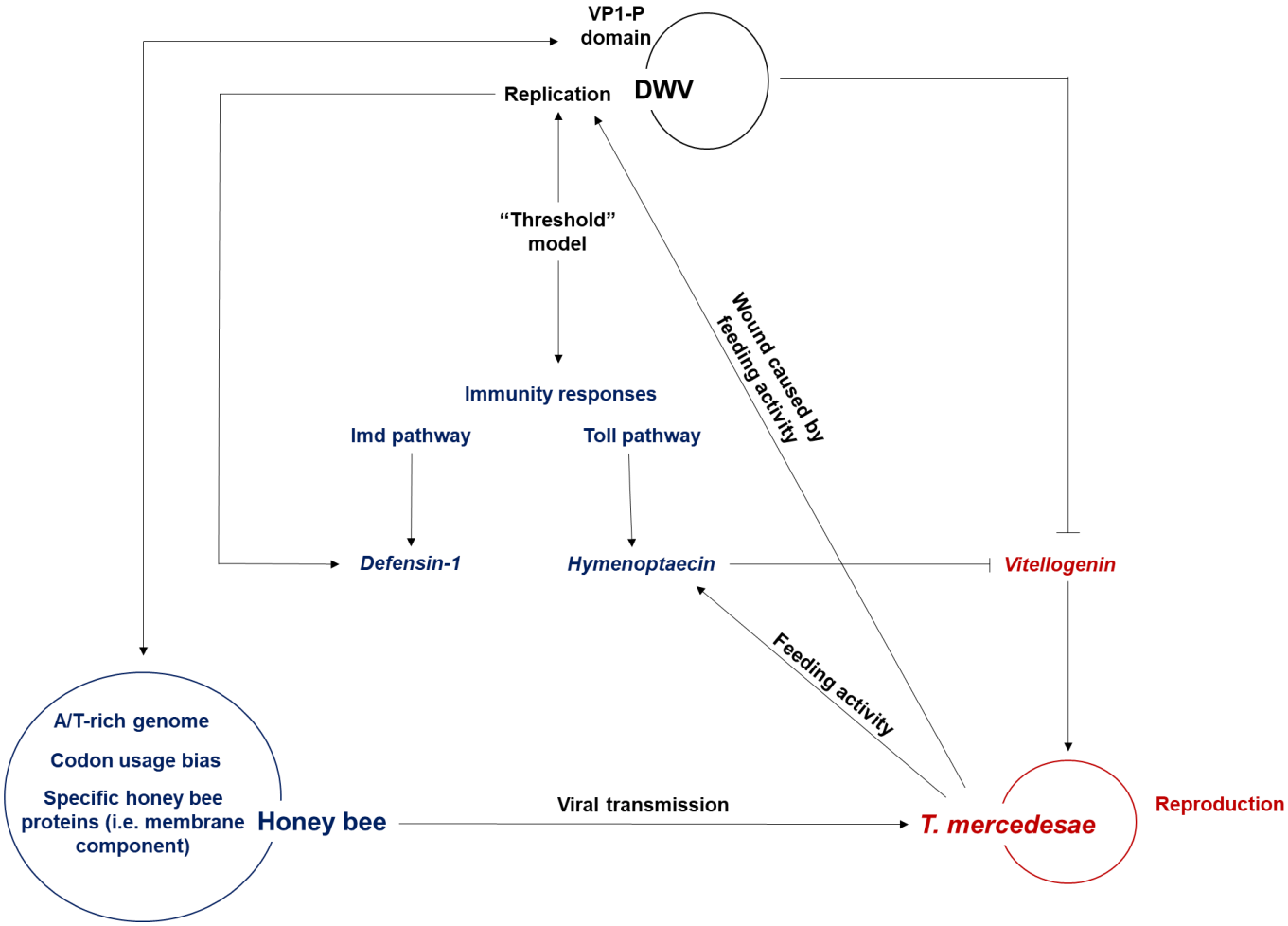

Figure 6.1 The summary of cross-interaction of the triplicate system "Honey bee-DWV-*T. mercedesae*". Description of cross-interactions between honey bee, DWV, and ectoparasitic mite *T. mercedesae*. The components belonging to honey bee, DWV, and *T. mercedesae* are indicated by blue, black, and red colours, respectively.

Supplementary Materials

Primer ID	Nucleotide sequence (5' to 3')
DWV #1	(F) ATTGTGCCAGATTGGACTAC
	(R) AGATGCAATGGAGGATACAG
DWV #2	(F) TTCATTAAAGCCACCTGGAACATC
	(R) TTTCCTCATTAACTGTGTCGTTGA
DWV #3	(F) GATCGCTGAACGTTGTACGC
	(R) ATACCCAAGCACTTGCCTCC
Honey bee *EF-1α* mRNA	(F) TGCAAGAGGCTGTTCCTGGTGA
	(R) CGAAACGCCCCAAAGGCGGA
A. mellifera 18S rRNA	(F) ACCACATCCAAGGAAGGCAG
	(R) ACTCATTCCGATTACGGGGC
V. destructor β-actin mRNA	(F) TCGTACGAGCTTCCCGACGGT
	(R) GGGAGGCAAGGATGGAACCGC
V. destructor 18S rRNA	(F) GTGAAACCGCGAATGGCTC
	(R) TCCGAAGACATGGTTTGCACT
T. mercedesae EF-1α mRNA	(F) ATTCCGGTAAGTCAACCACCAC
	(R) GCTCGGCCTTCAGTTTGTCCAA
T. mercedesae 18S rRNA	(F) CCTTCGGACTTACGGTGACG
	(R) TATGTGGTCGCCGTTTCTCA
ABPV	(F) AATGGGCCTATGGACTTTTCTA
	(R) AAATCTCCTGCAATAACCTTGG
BQCV	(F) GTGGCGGAGATGTATGCGCTTTATC
	(R) CTGACTCTACACACGGTTCGATTAG
CBPV	(F) GACCCCCGTTGGAACGACGC
	(R) CGGACGACGATTGGCGCTCA
IAPV	(F) AAACATCACAGATGCTCAGGGTCGAGACTATATGT
	(R) CTAGGGAGCTACGGAGCGTGATTCGCCTTGTAGCT
KBV	(F) ATGACGATGATGAGTTCAAG
	(R) AATTGCAAGACCTGCATC
SBV	(F) ACCAACCGATTCCTCAGTAG
	(R) CCTTGGAACTCTGCTGTGTA
Hymenoptaecin	(F) CCGACTCGTTTCCGACGAC
	(R) CGTCTCCTGTCATTCCATTC
Defensin-1	(F) GCATTTTGAGAATGAAGAACG
	(R) CAAACTGAGACAGTTAGCAG
Vg-1	(F) ACTGGTCAGCAGCAGTACAC
	(R) CGACGACATTTCGGCGTTAC
Vg-2	(F) ATTAAGGCCTTCGCCAAGATCGACC
	(R) TGAGCGAGGAGCGTGAACTTCGGATC
5'-SacI-VP1	

3’-HindⅢ-VP1	
5’-KpnI-RdRP	
3’-HindⅢ-RdRP	
5’-NdeI-P-domain	TTTCATATGAGGGCTAAGACAGGTTATGCACCATAT
3’-XhoI-P-domain	TTTTCTCGAGCTATTCTGGAATAGCTTCAATAAATTCAAA ATC
5’-NdeI-RdRP	
3’-XhoI-RdRP	
Sf9 16S rRNA	(F) TGATTATGCTACCTTTGTACAGTCA
	(R) AAAGTCTAATCTGCCCACTGAT
Drosophila RP mRNA	(F) GACGCTTCAAGGGACAGTATCTG
	(R) AAACGCGGTTCTGCATGAG
LLL 18S rRNA	(F) GGTGCATGGCCGTTCTTAGT
	(R) ACACACATGGTTTCAGCGTC
KC EF-1α mRNA	(F) ATCCGTGAAGAACGTCTCAAA
	(R) CATGGCTTAACTTCGAGGATG
tagF15	agcctgcgcaccgtggTCCATCAGGTTCTCCAATAACGGA
tag	agcctgcgcaccgtgg
B23	CCACCCAAATGCTAACTCTAAGCG

F: forward primer; R: reverse primer.

References

ADAMS, M. D., CELNIKER, S. E., HOLT, R. A., EVANS, C. A., GOCAYNE, J. D., AMANATIDES, P. G., SCHERER, S. E., LI, P. W., HOSKINS, R. A. & GALLE, R. F. J. S. 2000. The genome sequence of Drosophila melanogaster. 287**,** 2185-2195.

AERTS, A., FRANçOIS, I., CAMMUE, B., THEVISSEN, K. J. C. & SCIENCES, M. L. 2008. The mode of antifungal action of plant, insect and human defensins. 65**,** 2069-2079.

AHLQUIST, P., NOUEIRY, A. O., LEE, W.-M., KUSHNER, D. B. & DYE, B. T. J. J. O. V. 2003. Host factors in positive-strand RNA virus genome replication. 77**,** 8181-8186.

AHLQUIST, P. J. S. 2002. RNA-dependent RNA polymerases, viruses, and RNA silencing. 296**,** 1270-1273.

AIZEN, M. A., GARIBALDI, L. A., CUNNINGHAM, S. A. & KLEIN, A. M. 2008. Long-term global trends in crop yield and production reveal no current pollination shortage but increasing pollinator dependency. *Curr Biol,* 18**,** 1572-5.

AKASHI, H. J. C. O. I. G. & DEVELOPMENT 2001. Gene expression and molecular evolution. 11**,** 660-666.

AKRATANAKUL, P. 1987. *Honeybee diseases and enemies in Asia: a practical guide*, Food & Agriculture Org.

ALBERTI, G. & ZECK-KAPP, G. J. A. Z. 1986. The nutrimentary egg development of the mite, Varroa jacobsoni (Acari, Arachnida), an ectoparasite of honey bees. 67**,** 11-25.

ALLSOPP, M. H., DE LANGE, W. J. & VELDTMAN, R. 2008. Valuing insect pollination services with cost of replacement. *PLoS One,* 3**,** e3128.

ANDERS, S., PYL, P. T. & HUBER, W. J. B. 2015. HTSeq—a Python framework to work with high-throughput sequencing data. 31**,** 166-169.

ANDERSON, D. L., MORGAN, M. J. J. E. & ACAROLOGY, A. 2007. Genetic and morphological variation of bee-parasitic Tropilaelaps mites (Acari: Laelapidae): new and re-defined species. 43**,** 1-24.

ANDERSON, D. L. & ROBERTS, J. M. K. 2013. Standard methods for Tropilaelaps mites research. *Journal of Apicultural Research,* 52**,** 1-16.

ANDRé, S., SEED, B., EBERLE, J., SCHRAUT, W., BüLTMANN, A. & HAAS, J. J. J. O. V. 1998. Increased immune response elicited by DNA vaccination with a synthetic gp120 sequence with optimized codon usage. 72**,** 1497-1503.

AOTA, S.-I. & IKEMURA, T. J. N. A. R. 1986. Diversity in G+ C content at the third position of codons in vertebrate genes and its cause. 14**,** 6345-6355.

ARONSTEIN, K. A., MURRAY, K. D. & SALDIVAR, E. J. B. G. 2010. Transcriptional responses in honey bee larvae infected with chalkbrood fungus. 11**,** 391.

ARRESE, E. L. & SOULAGES, J. L. J. A. R. O. E. 2010. Insect fat body: energy, metabolism, and regulation. 55**,** 207-225.

ATHEY, J., ALEXAKI, A., OSIPOVA, E., ROSTOVTSEV, A., SANTANA-QUINTERO, L. V., KATNENI, U., SIMONYAN, V. & KIMCHI-SARFATY, C. J. B. B. 2017. A new and updated resource for codon usage tables. 18**,** 391.

AUEWARAKUL, P. J. V. R. 2005. Composition bias and genome polarity of RNA viruses. 109**,** 33-37.

BAHAR, A. A. & REN, D. J. P. 2013. Antimicrobial peptides. 6**,** 1543-1575.

BAHIR, I., FROMER, M., PRAT, Y. & LINIAL, M. J. M. S. B. 2009. Viral adaptation to host: a proteome-based analysis of codon usage and amino acid preferences. 5.

BAILEY, L. & BALL, B. V. 1991. *Honey bee pathology,* London, United Kingdom.

BAILEY, L., CARPENTER, J. M. & WOODS, R. D. 1979. Egypt bee virus and Australian isolates of Kashmir bee virus. *Journal of General Virology,* 43**,** 641-647.

BAKONYI, T., GRABENSTEINER, E., KOLODZIEJEK, J., RUSVAI, M., TOPOLSKA, G., RITTER, W. & NOWOTNY, N. 2002. Phylogenetic analysis of acute bee paralysis virus strains. *Appl Environ Microbiol,* 68**,** 6446-50.

BALL, B. association of Varroa jacobsoni with virus diseases of honey bees. Varroa jacobsoni Oud. affecting honey bees: present status and needs: proceedings of a meeting of the EC Experts' Group, Wageningen, 7-9 February 1983/edited by R. Cavalloro, 1983. Rotterdam: Published for the Commission of the European Communities by AA ….

BALL, B. V. 1989. Varroa jacobsoni as a virus vector. *Present status of varroatosis in Europe*

progress in the varroa mite control Office for Official Publications of the European Communities, Luxembourg.

BALL, B. V. 1993. The damaging effects of Varroa jacobsoni infestation. *Living with Varroa, International Bee Research Association, Cardiff, United Kingdom***,** 9-16.

BALL, B. V. & ALLEN, M. F. 1988. The prevalence of pathogens in honey bee (Apis mellifera) colonies infested with the parasitic mite Varroa jacobsoni. *Annals of applied biology,* 113**,** 237-244.

BEHURA, S. K. & SEVERSON, D. W. J. B. R. 2013. Codon usage bias: causative factors, quantification methods and genome-wide patterns: with emphasis on insect genomes. 88**,** 49-61.

BELL-SAKYI, L., DARBY, A., BAYLIS, M., MAKEPEACE, B. L. J. T. & DISEASES, T.-B. 2018. The Tick Cell Biobank: A global resource for in vitro research on ticks, other arthropods and the pathogens they transmit. 9**,** 1364-1371.

BENJEDDOU, M., LEAT, N., ALLSOPP, M. & DAVISON, S. 2001. Detection of acute bee paralysis virus and black queen cell virus from honeybees by reverse transcriptase pcr. *Appl Environ Microbiol,* 67**,** 2384-7.

BERGEM, M., NORBERG, K. & AAMODT, R. M. J. B. D. B. 2006. Long-term maintenance of in vitro cultured honeybee (Apis mellifera) embryonic cells. 6**,** 17.

BONCRISTIANI, H., LI, J., EVANS, J. D., PETTIS, J. & CHEN, Y. J. A. 2011. Scientific note on PCR inhibitors in the compound eyes of honey bees, Apis mellifera. 42**,** 457-460.

BONCRISTIANI, H. F., ROSSI, R. D., CRIADO, M. F., FURTADO, F. M. & ARRUDA, E. 2009. Magnetic purification of biotinylated cDNA removes false priming and ensures strand-specificity of RT-PCR for enteroviral RNAs. *J Virol Methods,* 161**,** 147-53.

BONHOEFFER, S. & NOWAK, M. A. J. P. O. T. N. A. O. S. 1994. Intra-host versus inter-host selection: viral strategies of immune function impairment. 91**,** 8062-8066.

BOWEN-WALKER, P. L., MARTIN, S. J. & GUNN, A. 1999. The Transmission of Deformed Wing Virus between Honeybees (Apis melliferaL.) by the Ectoparasitic MiteVarroa jacobsoniOud. *J Invertebr Pathol,* 73**,** 101-106.

BRETTELL, L. E., MORDECAI, G. J., SCHROEDER, D. C., JONES, I. M., DA SILVA, J. R., VICENTE-RUBIANO, M. & MARTIN, S. J. J. I. 2017. A comparison of deformed wing virus in deformed and asymptomatic honey bees. 8**,** 28.

BRøDSGAARD, C. J., RITTER, W., HANSEN, H. & BRøDSGAARD, H. F. J. A. 2000. Interactions among Varroa jacobsoni mites, acute paralysis virus, and Paenibacillus larvae larvae and their influence on mortality of larval honeybees in vitro. 31**,** 543-554.

BROWN, M. J., DICKS, L. V., PAXTON, R. J., BALDOCK, K. C., BARRON, A. B., CHAUZAT, M. P., FREITAS, B. M., GOULSON, D., JEPSEN, S., KREMEN, C., LI, J., NEUMANN, P., PATTEMORE, D. E., POTTS, S. G., SCHWEIGER, O., SEYMOUR, C. L. & STOUT, J. C. 2016. A horizon scan of future threats and opportunities for pollinators and pollination. *PeerJ,* 4**,** e2249.

BRUNNER, F. S., SCHMID-HEMPEL, P. & BARRIBEAU, S. M. 2014. Protein-poor diet reduces host-specific immune gene expression in Bombus terrestris. *Proc Biol Sci,* 281.

BRUTSCHER, L. M., DAUGHENBAUGH, K. F. & FLENNIKEN, M. L. J. C. O. I. I. S. 2015. Antiviral defense mechanisms in honey bees. 10**,** 71-82.

BUAWANGPONG, N., DE GUZMAN, L., KHONGPHINITBUNJONG, K., FRAKE, A., BURGETT, M. & CHANTAWANNAKUL, P. 2015. Tropilaelaps mercedesae and Varroa destructor: prevalence and reproduction in concurrently infested Apis mellifera colonies. *Apidologie,* 10**,** 1007.

BURDEN, J., GRIFFITHS, C., CORY, J., SMITH, P. & SAIT, S. J. M. E. 2002. Vertical transmission of sublethal granulovirus infection in the Indian meal moth, Plodia interpunctella. 11**,** 547-555.

BURDEN, J. P., NIXON, C. P., HODGKINSON, A. E., POSSEE, R. D., SAIT, S. M., KING, L. A. & HAILS, R. S. 2003. Covert infections as a mechanism for long-term persistence of baculoviruses. *Ecol Lett,* 6**,** 524-531.

BURGETT, M., AKRATANAKUL, P. & MORSE, R. A. 1983. Tropilaelaps clareae: a parasite of honeybees in south-east Asia. *Bee world,* 64**,** 25-28.

BURGETT, M. & AKRATANAKUL, P. J. T. A. B. J. 1985. Tropilaelaps clareae, the little known honey bee brood mite.

CABRERA, A. R., DONOHUE, K. V. & ROE, R. M. J. J. O. I. P. 2009. Regulation of female reproduction in mites: a unifying model for the Acari. 55**,** 1079-1090.

CABRERA CORDON, A., SHIRK, P., DUEHL, A., EVANS, J. & TEAL, P. J. I. M. B. 2013. Variable induction of vitellogenin genes in the varroa mite, V arroa destructor (A nderson & T rueman), by the honeybee, Apis mellifera L, host and its environment. 22**,** 88-103.

CAMPBELL, E. M., BUDGE, G. E., WATKINS, M., BOWMAN, A. S. J. I. B. & BIOLOGY, M. 2016. Transcriptome analysis of the synganglion from the honey bee mite, Varroa destructor and RNAi knockdown of neural peptide targets. 70**,** 116-126.

CAMPHOR, E., HASHMI, A., RITTER, W. & BOWEN, I. J. A. 2005. Seasonal changes in mite (Tropilaelaps clareae) and honeybee (Apis mellifera) populations in Apistan treated and untreated colonies. 40**,** 005.

CARR, A. L., ROE, M. J. P. B. & PHYSIOLOGY 2016. Acarine attractants: chemoreception, bioassay, chemistry and control. 131**,** 60-79.

CARRECK, N. L., BALL, B. V. & MARTIN, S. J. 2010. Honey bee colony collapse and changes in viral prevalence associated with Varroa destructor. *Journal of Apicultural Research,* 49**,** 93-94.

CARRILLO-TRIPP, J., DOLEZAL, A. G., GOBLIRSCH, M. J., MILLER, W. A., TOTH, A. L. & BONNING, B. C. J. S. R. 2016. In vivo and in vitro infection dynamics of honey bee viruses. 6**,** 22265.

CASTEELS-JOSSON, K., ZHANG, W., CAPACI, T., CASTEELS, P. & TEMPST, P. J. J. O. B. C. 1994. Acute transcriptional response of the honeybee peptide-antibiotics gene repertoire and required post-translational conversion of the precursor structures. 269**,** 28569-28575.

CASTEELS, P., AMPE, C., JACOBS, F. & TEMPST, P. J. J. O. B. C. 1993. Functional and chemical characterization of Hymenoptaecin, an antibacterial polypeptide that is infection-inducible in the honeybee (Apis mellifera). 268, 7044-7054.

CASTEELS, P., AMPE, C., JACOBS, F., VAECK, M. & TEMPST, P. J. T. E. J. 1989. Apidaecins: antibacterial peptides from honeybees. 8, 2387-2391.

CASTRESANA, J. 2000. Selection of Conserved Blocks from Multiple Alignments for Their Use in Phylogenetic Analysis. *Mol Biol Evol,* 17, 540-552.

CATTANEO, R., SCHMID, A., ESCHLE, D., BACZKO, K., TER MEULEN, V. & BILLETER, M. A. J. C. 1988. Biased hypermutation and other genetic changes in defective measles viruses in human brain infections. 55, 255-265.

CHAN, M., CHOI, S., CHAN, Q., LI, P., GUARNA, M. & FOSTER, L. J. I. M. B. 2010. Proteome profile and lentiviral transduction of cultured honey bee (Apis mellifera L.) cells. 19, 653-658.

CHANPANITKITCHOTE, P., CHEN, Y., EVANS, J. D., LI, W., LI, J., HAMILTON, M. & CHANTAWANNAKUL, P. 2017. Acute bee paralysis virus occurs in the Asian honey bee Apis cerana and parasitic mite Tropilaelaps mercedesae. *J Invertebr Pathol*.

CHANTAWANNAKUL, P., RAMSEY, S., KHONGPHINITBUNJONG, K. & PHOKASEM, P. J. C. O. I. I. S. 2018. Tropilaelaps mite: an emerging threat to European honey bee. 26, 69-75.

CHEN, S. L., LEE, W., HOTTES, A. K., SHAPIRO, L. & MCADAMS, H. H. J. P. O. T. N. A. O. S. 2004. Codon usage between genomes is constrained by genome-wide mutational processes. 101, 3480-3485.

CHEN, Y., EVANS, J. & FELDLAUFER, M. J. J. O. I. P. 2006a. Horizontal and vertical transmission of viruses in the honey bee, Apis mellifera. 92, 152-159.

CHEN, Y., MCCARTHY, D., ROBINSON, M. & SMYTH, G. K. 2014. edgeR: differential expression analysis of digital gene expression data User's Guide. UsersGuide.

CHEN, Y., PETTIS, J. S. & FELDLAUFER, M. F. 2005a. Detection of multiple viruses in queens of the honey bee Apis mellifera L. *J Invertebr Pathol,* 90, 118-21.

CHEN, Y. P., HIGGINS, J. A. & FELDLAUFER, M. F. 2005b. Quantitative real-time reverse transcription-PCR analysis of deformed wing virus infection in the honeybee (Apis mellifera L.). *Appl Environ Microbiol,* 71, 436-41.

CHEN, Y. P., PETTIS, J. S., COLLINS, A. & FELDLAUFER, M. F. 2006b. Prevalence and transmission of honeybee viruses. *Appl Environ Microbiol,* 72, 606-11.

CHERRY, S., KUNTE, A., WANG, H., COYNE, C., RAWSON, R. B. & PERRIMON, N. J. P. P. 2006. COPI activity coupled with fatty acid biosynthesis is required for viral replication. 2, e102.

CHERRY, S. & PERRIMON, N. J. N. I. 2004. Entry is a rate-limiting step for viral infection in a Drosophila melanogaster model of pathogenesis. 5, 81.

CHRISTOPHIDES, G. K., ZDOBNOV, E., BARILLAS-MURY, C., BIRNEY, E., BLANDIN, S., BLASS, C., BREY, P. T., COLLINS, F. H., DANIELLI, A. & DIMOPOULOS, G. J. S. 2002. Immunity-related genes and gene families in Anopheles gambiae. 298, 159-165.

COTTRELL, T. R. & DOERING, T. L. J. T. I. M. 2003. Silence of the strands: RNA interference in eukaryotic pathogens. 11, 37-43.

CRAILSHEIM, K., BRODSCHNEIDER, R. & NEUMANN, P. The COLOSS puzzle: filling in the gaps. Proceedings of the 4th COLOSS Conference, 2009. 3-4.

DAHLE, B. J. J. O. A. R. 2010. The role of Varroa destructor for honey bee colony losses in Norway. 49, 124-125.

DAINAT, B., KEN, T., BERTHOUD, H. & NEUMANN, P. 2009. The ectoparasitic mite Tropilaelaps mercedesae (Acari, Laelapidae) as a vector of honeybee viruses. *Insectes Sociaux,* 56, 40-43.

DALMON, A., DESBIEZ, C., COULON, M., THOMASSON, M., LE CONTE, Y., ALAUX, C., VALLON, J. & MOURY, B. 2017. Evidence for positive selection and recombination hotspots in Deformed wing virus (DWV). *Scientific reports,* 7, 41045.

DANIHLíK, J., ARONSTEIN, K. & PETŘIVALSKý, M. J. J. O. A. R. 2015. Antimicrobial peptides: a key component of honey bee innate immunity: Physiology, biochemistry, and chemical ecology. 54, 123-136.

DARRIBA, D., TABOADA, G. L., DOALLO, R. & POSADA, D. 2012. jModelTest 2: more models, new heuristics and parallel computing. *Nat Methods,* 9, 772.

DAVARINEJAD, H. 2017. Quantifications of Western Blots with ImageJ.

DE GUZMAN, L., RINDERER, T. E., STELZER, J. A. & ANDERSON, D. J. J. O. A. R. 1998. Congruence of RAPD and mitochondrial DNA markers in assessing Varroa jacobsoni genotypes. 37, 49-51.

DE GUZMAN, L. I., PHOKASEM, P., KHONGPHINITBUNJONG, K., FRAKE, A. M. & CHANTAWANNAKUL, P. 2018. Successful reproduction of unmated Tropilaelaps mercedesae and its implication on mite population growth in Apis mellifera colonies. *J Invertebr Pathol,* 153, 35-37.

DE GUZMAN, L. I., WILLIAMS, G. R., KHONGPHINITBUNJONG, K. & CHANTAWANNAKUL, P. J. J. O. E. E. 2017. Ecology, life history, and management of Tropilaelaps mites. 110**,** 319-332.

DE MIRANDA, J. & FRIES, I. J. J. O. I. P. 2008. Venereal and vertical transmission of deformed wing virus in honeybees (Apis mellifera L.). 98**,** 184-189.

DE MIRANDA, J. R., BAILEY, L., BALL, B. V., BLANCHARD, P., BUDGE, G. E., CHEJANOVSKY, N., CHEN, Y.-P., GAUTHIER, L., GENERSCH, E., DE GRAAF, D. C., RIBlèRE, M., RYABOV, E., DE SMET, L. & VAN DER STEEN, J. J. M. 2015. Standard methods for virus research inApis mellifera. *Journal of Apicultural Research,* 52**,** 1-56.

DE MIRANDA, J. R. & GENERSCH, E. 2010. Deformed wing virus. *J Invertebr Pathol,* 103 Suppl 1**,** S48-61.

DEGRANDI-HOFFMAN, G. & CHEN, Y. J. C. O. I. I. S. 2015. Nutrition, immunity and viral infections in honey bees. 10**,** 170-176.

DELFINADO, M. D. J. J. O. A. R. 1963. Mites of the honeybee in South-East Asia. 2**,** 113-114.

DHANASEKARAN, S., DOHERTY, T. M., KENNETH, J. & METHODS, T. T. S. G. J. J. O. I. 2010. Comparison of different standards for real-time PCR-based absolute quantification. 354**,** 34-39.

DI PRISCO, G., ANNOSCIA, D., MARGIOTTA, M., FERRARA, R., VARRICCHIO, P., ZANNI, V., CAPRIO, E., NAZZI, F. & PENNACCHIO, F. J. P. O. T. N. A. O. S. 2016. A mutualistic symbiosis between a parasitic mite and a pathogenic virus undermines honey bee immunity and health. 113**,** 3203-3208.

DIMMOCK, N. J. & PRIMROSE, S. B. 1994. *Introduction to modern virology. ed*.

DINDA, P., BECK, I., BECK, M. J. C. J. O. P. & PHARMACOLOGY 1977. Some observations on the determination of extracellular fluid volume of jejunal tissue using [3H] inulin and [14C] inulin. 55**,** 389-393.

DITTMANN, F. & STEINER, J. J. J. O. A. R. 1997. Intercellular connection between the lyrate organ and the growing oocyte in Varroa jacobsoni as revealed by Lucifer Yellow dye-coupling. 36**,** 145-149.

DOBIN, A., DAVIS, C. A., SCHLESINGER, F., DRENKOW, J., ZALESKI, C., JHA, S., BATUT, P., CHAISSON, M. & GINGERAS, T. R. J. B. 2013. STAR: ultrafast universal RNA-seq aligner. 29**,** 15-21.

DOMINGO, E. 2002. Quasispecies Theory in Virology. *Journal of Virology,* 76**,** 463-465.

DOMINGO, E. & HOLLAND, J. 1997. RNA virus mutations and fitness for survival. *Annual review of microbiology,* 51**,** 151-178.

DONG, X., ARMSTRONG, S. D., XIA, D., MAKEPEACE, B. L., DARBY, A. C. & KADOWAKI, T. 2017. Draft genome of the honey bee ectoparasitic mite, Tropilaelaps mercedesae, is shaped by the parasitic life history. *Gigascience,* 6**,** 1-17.

DONZé, G., GUERIN, P. M. J. B. E. & SOCIOBIOLOGY 1994. Behavioral attributes and parental care of Varroa mites parasitizing honeybee brood. 34**,** 305-319.

DONZE, G., HERRMANN, M., BACHOFEN, B. & GUERIN, P. R. M. J. E. E. 1996. Effect of mating frequency and brood cell infestation rate on the reproductive success of the honeybee parasite Varroa jacobsoni. 21**,** 17-26.

ELLIS, J. D., EVANS, J. D. & PETTIS, J. 2010. Colony losses, managed colony population decline, and Colony Collapse Disorder in the United States. *Journal of Apicultural Research,* 49**,** 134-136.

ERBAN, T., HARANT, K., HUBALEK, M., VITAMVAS, P., KAMLER, M., POLTRONIERI, P., TYL, J., MARKOVIC, M. & TITERA, D. J. S. R. 2015. In-depth proteomic analysis of Varroa destructor: Detection of DWV-complex, ABPV, VdMLV and honeybee proteins in the mite. 5**,** 1-16.

EVANS, G. O. 1992. Principles of acarology.

EVANS, J. D., SAEGERMAN, C., MULLIN, C., HAUBRUGE, E., NGUYEN, B. K., FRAZIER, M., FRAZIER, J., COX-FOSTER, D., CHEN, Y. & UNDERWOOD, R. J. P. O. 2009. Colony collapse disorder: a descriptive study. 4**,** e6481.

EVANS, J. D. & SCHWARZ, R. S. J. T. I. M. 2011. Bees brought to their knees: microbes affecting honey bee health. 19**,** 614-620.

FERRER-ORTA, C., ARIAS, A., ESCARMIS, C. & VERDAGUER, N. 2006. A comparison of viral RNA-dependent RNA polymerases. *Curr Opin Struct Biol,* 16**,** 27-34.

FIEVET, J., TENTCHEVA, D., GAUTHIER, L., DE MIRANDA, J., COUSSERANS, F., COLIN, M. E. & BERGOIN, M. 2006. Localization of deformed wing virus infection in queen and drone Apis mellifera L. *Virol J,* 3**,** 16.

FORGACH, P., BAKONYI, T., TAPASZTI, Z., NOWOTNY, N. & RUSVAI, M. 2008. Prevalence of pathogenic bee viruses in Hungarian apiaries: situation before joining the European Union. *J Invertebr Pathol,* 98**,** 235-8.

FORSGREN, E., DE MIRANDA, J. R., ISAKSSON, M., WEI, S. & FRIES, I. 2009. Deformed wing virus associated with Tropilaelaps mercedesae infesting European honey bees (Apis mellifera). *Exp Appl Acarol,* 47**,** 87-97.

FRACZEK, R. J., ZOLTOWSKA, K., LIPINSKI, Z. & DMITRYJUK, M. 2013. The mutual influence of proteins from Varroa destructor extracts and from honeybee haemolymph on their proteolytic activity--in vitro study. *Acta Parasitol,* 58**,** 317-23.

FRANCINO, M. P. & OCHMAN, H. J. N. 1999. Isochores result from mutation not selection. 400**,** 30-31.

FRANCIS, R. M., NIELSEN, S. L. & KRYGER, P. 2013. Varroa-virus interaction in collapsing honey bee colonies. *PloS one,* 8**,** e57540.
FUJIYUKI, T., TAKEUCHI, H., ONO, M., OHKA, S., SASAKI, T., NOMOTO, A. & KUBO, T. 2004. Novel insect picorna-like virus identified in the brains of aggressive worker honeybees. *Journal of virology,* 78**,** 1093-1100.
FüRST, M. A., MCMAHON, D. P., OSBORNE, J. L., PAXTON, R. J. & BROWN, M. J. F. 2014. Disease associations between honeybees and bumblebees as a threat to wild pollinators. *Nature,* 506**,** 364.
GALLANT, A. L., EULISS JR, N. H. & BROWNING, Z. J. P. O. 2014. Mapping large-area landscape suitability for honey bees to assess the influence of land-use change on sustainability of national pollination services. 9**,** e99268.
GARRIDO, C. & ROSENKRANZ, P. 2003. The reproductive program of female Varroa destructor mites is triggered by its host, Apis mellifera. *Experimental & applied acarology,* 31**,** 269-273.
GARRIDO, C., ROSENKRANZ, P., STüRMER, M., RüBSAM, R. & BüNING, J. J. A. 2000. Toluidine blue staining as a rapid measure for initiation of oocyte growth and fertility in Varroa jacobsoni Oud. 31**,** 559-566.
GASCUEL, J., MASSON, C., BERMUDEZ, I., BEADLE, D. J. T. & CELL 1994. Morphological analysis of honeybee antennal cells growing in primary cultures. 26**,** 551-558.
GAUTHIER, L., TENTCHEVA, D., TOURNAIRE, M., DAINAT, B., COUSSERANS, F., COLIN, M. E. & BERGOIN, M. J. A. 2007. Viral load estimation in asymptomatic honey bee colonies using the quantitative RT-PCR technique. 38**,** 426-435.
GENERSCH, E. & AUBERT, M. 2010. Emerging and re-emerging viruses of the honey bee (Apis melliferaL.). *Veterinary Research,* 41.
GENERSCH, E. J. T. V. J. 2005. Development of a rapid and sensitive RT-PCR method for the detection of deformed wing virus, a pathogen of the honeybee (Apis mellifera). 169**,** 121-123.
GERTH, M. & HURST, G. D. J. P. 2017. Short reads from honey bee (Apis sp.) sequencing projects reflect microbial associate diversity. 5**,** e3529.
GIAUFFRET, A., QUIOT, J., VAGO, C. & POUTIER, F. J. C. R. H. D. S. D. L. A. D. S. S. D. S. N. 1967. In vitro culture of cells of the bee. 265**,** 800-803.
GIAUFFRET, A. J. I. T. C. 1971. Cell culture of Hymenoptera.
GISDER, S., AUMEIER, P. & GENERSCH, E. 2009. Deformed wing virus: replication and viral load in mites (Varroa destructor). *J Gen Virol,* 90**,** 463-7.
GISDER, S., MOCKEL, N., EISENHARDT, D. & GENERSCH, E. 2018. In vivo evolution of viral virulence: switching of deformed wing virus between hosts results in virulence changes and sequence shifts. *Environ Microbiol,* 20**,** 4612-4628.
GISSELMANN, G., WARNSTEDT, M., GAMERSCHLAG, B., BORMANN, A., MARX, T., NEUHAUS, E. M., STOERTKUHL, K., WETZEL, C. H., HATT, H. J. I. B. & BIOLOGY, M. 2003. Characterization of recombinant and native Ih-channels from Apis mellifera. 33**,** 1123-1134.
GOBLIRSCH, M. J., SPIVAK, M. S. & KURTTI, T. J. J. P. O. 2013. A cell line resource derived from honey bee (Apis mellifera) embryonic tissues. 8**,** e69831.
GODFRAY, H. C., BLACQUIERE, T., FIELD, L. M., HAILS, R. S., POTTS, S. G., RAINE, N. E., VANBERGEN, A. J. & MCLEAN, A. R. 2015. A restatement of recent advances in the natural science evidence base concerning neonicotinoid insecticides and insect pollinators. *Proc Biol Sci,* 282**,** 20151821.
GOULSON, D., NICHOLLS, E., BOTIAS, C. & ROTHERAY, E. L. 2015. Bee declines driven by combined stress from parasites, pesticides, and lack of flowers. *Science,* 347**,** 1255957.
GRANTHAM, R., GAUTIER, C., GOUY, M., MERCIER, R. & PAVE, A. J. N. A. R. 1980. Codon catalog usage and the genome hypothesis. 8**,** 197-197.
GREGORC, A., EVANS, J. D., SCHARF, M. & ELLIS, J. D. J. J. O. I. P. 2012. Gene expression in honey bee (Apis mellifera) larvae exposed to pesticides and Varroa mites (Varroa destructor). 58**,** 1042-1049.
GREGORY, P. G., EVANS, J. D., RINDERER, T. & DE GUZMAN, L. J. J. O. I. S. 2005. Conditional immune-gene suppression of honeybees parasitized by Varroa mites. 5.
GUTIERREZ, D. J. N. N. 2009. Honey bee collapse strikes Japan, up to fifty percent of honey bees gone. 28.
GUY DODSON & WLODAWER, A. 1998. <Catalytic triads and their.pdf>. *Trends in biochemical sciences,* 23**,** 347-352.
HAAS, J., PARK, E.-C. & SEED, B. J. C. B. 1996. Codon usage limitation in the expression of HIV-1 envelope glycoprotein. 6**,** 315-324.
HADDAD, F., QIN, A. X., GIGER, J. M., GUO, H. & BALDWIN, K. M. 2007. Potential pitfalls in the accuracy of analysis of natural sense-antisense RNA pairs by reverse transcription-PCR. *BMC Biotechnol,* 7**,** 21.
HADDAD, N., BATAENEH, A., ALBABA, I., OBEID, D. & ABDULRAHMAN, S. Status of colony losses in the Middle East. Proceedings of the 41st Apimondia Congress, Mointpellier, France, 2009. 36.

HAGIWARA, Y., KOMODA, K., YAMANAKA, T., TAMAI, A., MESHI, T., FUNADA, R., TSUCHIYA, T., NAITO, S. & ISHIKAWA, M. J. T. E. J. 2003. Subcellular localization of host and viral proteins associated with tobamovirus RNA replication. 22**,** 344-353.

HALL, B. G. J. M. B. & EVOLUTION 2013. Building phylogenetic trees from molecular data with MEGA. 30**,** 1229-1235.

HARTIG, S. M. J. C. P. I. M. B. 2013. Basic image analysis and manipulation in ImageJ. 102**,** 14.15. 1-14.15. 12.

HIGHFIELD, A. C., EL NAGAR, A., MACKINDER, L. C., LAURE, M.-L. N., HALL, M. J., MARTIN, S. J. & SCHROEDER, D. C. J. A. E. M. 2009. Deformed wing virus implicated in overwintering honeybee colony losses. 75**,** 7212-7220.

HOFFMANN, J. A., KAFATOS, F. C., JANEWAY, C. A. & EZEKOWITZ, R. J. S. 1999. Phylogenetic perspectives in innate immunity. 284**,** 1313-1318.

HOLLAND, J. J. D., DE LA TORRE, J. & STEINHAUER, D. 1992. RNA virus populations as quasispecies. *Genetic diversity of RNA viruses*. Springer.

HU TAO , WENJUN LIU , BRANDI N. SIMMONS , HELEN K. HARRIS , TIMOTHY, C. COX & MASSIA, M. A. 2010. Purifying natively folded proteins from inclusion bodies using sarkosyl, Triton X-100, and CHAPS. *Bio Techniques,* 48**,** 61-64.

HUNG, A. C., ADAMS, J. R. & SHIMANUKI, H. J. A. B. J. 1995. Bee parasitic mite syndrome.(II). The role of Varroa mite and viruses.

HUNTER, W. B. J. I. V. C. & BIOLOGY-ANIMAL, D. 2010. Medium for development of bee cell cultures (Apis mellifera: Hymenoptera: Apidae). 46**,** 83-86.

IFANTIDIS, M. D., THRASHYVOULOU, A. & PAPPAS, M. 1988. Some aspects of the process of Varroa jacobsoni mite entrance into honey bee (Apis mellifera) brood cells. *Apidologie,* 19**,** 387-396.

IFANTIDIS, M. J. J. O. A. R. 1983. Ontogenesis of the mite Varroa jacobsoni in worker and drone honeybee brood cells. 22**,** 200-206.

IFANTIDIS, M. J. V. J. 1990. Re-examination of some parameters concerning reproduction of the mite. 20-26.

IKEMURA, T. & WADA, K.-N. J. N. A. R. 1991. Evident diversity of codon usage patterns of human genes with respect to chromosome banding patterns and chromosome numbers; relation between nucleotide sequence data and cytogenetic data. 19**,** 4333-4339.

ILYASOV, R., GAIFULLINA, L., SALTYKOVA, E., POSKRYAKOV, A. & NIKOLENKO, A. J. J. O. A. S. 2012. Review of the expression of antimicrobial peptide defensin in honey bees Apis mellifera L. 56**,** 115-124.

IPBES 2016. Summary for policymakers of the assessment report of the Intergovernmental Science-Policy Platform on Biodiversity and Ecosystem Services on pollinators, pollination and food production.

IQBAL, J. & MUELLER, U. 2007. Virus infection causes specific learning deficits in honeybee foragers. *Proc Biol Sci,* 274**,** 1517-21.

ISAWA H, S ASANO, K SAHARA, T IIZUKA & BANDO., H. 1998. Analysis of genetic information of an insect picorna-like virus,infectious flacherie virus of silkworm: evidence for evolutionary relationships among insect, mammalian and plant picorna(-like) viruses. *Arch. Virol.,* 143**,** 127-143.

J. C. BIESMEIJER, S. P. M. R., M. REEMER, R. OHLEMU¨LLER, M. EDWARDS, T. PEETERS, A. P. SCHAFFERS, S. G. POTTS, R. KLEUKERS, C. D. THOMAS, J. SETTELE, W. E. KUNIN 2006. <Parallel declines in pollinators and insect-pollinated plants.pdf>. *Science,* 313**,** 351-354.

J. E. WILSON, M. J. POWELL, S. E. HOOVER & SARNOW., P. 2000. Naturally occurring dicistronic cricket paralysis virus RNA is regulated by two internal ribosome entry sites. *Mol. Cell. Biol.,* 20**,** 4990-4999.

JENSSEN, H., HAMILL, P. & HANCOCK, R. E. J. C. M. R. 2006. Peptide antimicrobial agents. 19**,** 491-511.

JEREMY T. KERR, ALANA PINDAR, PAUL GALPERN, LAURENCE PACKER, SIMON G. POTTS, STUART M. ROBERTS, PIERRE RASMONT, OLIVER SCHWEIGER, SHEILA R. COLLA, LEIF L. RICHARDSON, DAVID L. WAGNER, LAWRENCE F. GALL, DEREK S. SIKES & PANTOJA, A. 2015. Climate change impacts on bumblebees converge. *Science,* 80**,** 177-180.

KANAYA, S., YAMADA, Y., KINOUCHI, M., KUDO, Y. & IKEMURA, T. J. J. O. M. E. 2001. Codon usage and tRNA genes in eukaryotes: correlation of codon usage diversity with translation efficiency and with CG-dinucleotide usage as assessed by multivariate analysis. 53**,** 290-298.

KANBAR, G. & ENGELS, W. J. E. J. O. E. 2004. Number and position of wounds on honey bee (Apis mellifera) pupae infested with a single Varroa mite. 101**,** 323-326.

KANBAR, G. & ENGELS, W. J. P. R. 2003. Ultrastructure and bacterial infection of wounds in honey bee (Apis mellifera) pupae punctured by Varroa mites. 90**,** 349-354.

KATOH, K. & STANDLEY, D. M. 2013. MAFFT multiple sequence alignment software version 7: improvements in performance and usability. *Mol Biol Evol,* 30**,** 772-80.

KAWAKAMI, Y., GOTO, S. G., ITO, K. & NUMATA, H. J. J. O. I. P. 2009. Suppression of ovarian development and vitellogenin

gene expression in the adult diapause of the two-spotted spider mite Tetranychus urticae. 55, 70-77.
KENNEDY, C. M., LONSDORF, E., NEEL, M. C., WILLIAMS, N. M., RICKETTS, T. H., WINFREE, R., BOMMARCO, R., BRITTAIN, C., BURLEY, A. L., CARIVEAU, D., CARVALHEIRO, L. G., CHACOFF, N. P., CUNNINGHAM, S. A., DANFORTH, B. N., DUDENHOFFER, J. H., ELLE, E., GAINES, H. R., GARIBALDI, L. A., GRATTON, C., HOLZSCHUH, A., ISAACS, R., JAVOREK, S. K., JHA, S., KLEIN, A. M., KREWENKA, K., MANDELIK, Y., MAYFIELD, M. M., MORANDIN, L., NEAME, L. A., OTIENO, M., PARK, M., POTTS, S. G., RUNDLOF, M., SAEZ, A., STEFFAN-DEWENTER, I., TAKI, H., VIANA, B. F., WESTPHAL, C., WILSON, J. K., GREENLEAF, S. S. & KREMEN, C. 2013. A global quantitative synthesis of local and landscape effects on wild bee pollinators in agroecosystems. *Ecol Lett,* 16, 584-99.
KHALIL, S. M., DONOHUE, K. V., THOMPSON, D. M., JEFFERS, L. A., ANANTHAPADMANABAN, U., SONENSHINE, D. E., MITCHELL, R. D. & ROE, R. M. J. J. O. I. P. 2011. Full-length sequence, regulation and developmental studies of a second vitellogenin gene from the American dog tick, Dermacentor variabilis. 57, 400-408.
KHONGPHINITBUNJONG, K., DE GUZMAN, L. I., TARVER, M. R., RINDERER, T. E. & CHANTAWANNAKUL, P. J. J. O. A. R. 2015. Interactions of Tropilaelaps mercedesae, honey bee viruses and immune response in Apis mellifera. 54, 40-47.
KHONGPHINITBUNJONG, K., NEUMANN, P., CHANTAWANNAKUL, P. & WILLIAMS, G. R. 2016. The ectoparasitic mite Tropilaelaps mercedesae reduces western honey bee, Apis mellifera, longevity and emergence weight, and promotes Deformed wing virus infections. *Journal of invertebrate pathology,* 137, 38-42.
KIELMANOWICZ, M. G., INBERG, A., LERNER, I. M., GOLANI, Y., BROWN, N., TURNER, C. L., HAYES, G. J. & BALLAM, J. M. J. P. P. 2015. Prospective large-scale field study generates predictive model identifying major contributors to colony losses. 11, e1004816.
KIM, D., LANGMEAD, B. & SALZBERG, S. L. J. N. M. 2015. HISAT: a fast spliced aligner with low memory requirements. 12, 357-360.
KITAGISHI, Y., OKUMURA, N., YOSHIDA, H., NISHIMURA, Y., TAKAHASHI, J.-I., MATSUDA, S. J. I. V. C. & BIOLOGY-ANIMAL, D. 2011. Long-term cultivation of in vitro Apis mellifera cells by gene transfer of human c-myc proto-oncogene. 47, 451-453.
KITPRASERT, C. 1984. Biology and systematics of the parasitic bee mite, Tropilaelaps clareae Delfinado and Baker (Acarina: Laelapidae).
KLEIN, A.-M., VAISSIèRE, B. E., CANE, J. H., STEFFAN-DEWENTER, I., CUNNINGHAM, S. A., KREMEN, C. & TSCHARNTKE, T. 2007. Importance of pollinators in changing landscapes for world crops. *Proceedings of the Royal Society B: Biological Sciences,* 274, 303-313.
KOENIGER, N. & MUZAFFAR, N. J. J. O. A. R. 1988. Lifespan of the parasitic honeybee mite, Tropilaelaps clareae, on Apis cerana, dorsata and mellifera. 27, 207-212.
KREIßL, S. & BICKER, G. J. J. O. N. 1992. Dissociated neurons of the pupal honeybee brain in cell culture. 21, 545-556.
KUENEN, L. & CALDERONE, N. J. J. O. I. B. 1997. Transfers ofvarroa mites from newly emerged bees: Preferences for age- and function-specific adult bees (Hymenoptera: Apidae). 10, 213-228.
KUKAN, B. J. J. O. I. P. 1999. Vertical transmission of nucleopolyhedrovirus in insects. 74, 103-111.
KUKIELKA, D., ESPERóN, F., HIGES, M. & SáNCHEZ-VIZCAíNO, J. M. J. J. O. V. M. 2008. A sensitive one-step real-time RT-PCR method for detection of deformed wing virus and black queen cell virus in honeybee Apis mellifera. 147, 275-281.
KUSTER, R. D., BONCRISTIANI, H. F. & RUEPPELL, O. J. J. O. E. B. 2014. Immunogene and viral transcript dynamics during parasitic Varroa destructor mite infection of developing honey bee (Apis mellifera) pupae. 217, 1710-1718.
L. BAILEY, BRENDA V. BALL & PERRY, J. N. 1981. The prevalence of viruses of honey bees in Britain. *Ann. appl. Biol.,* 97, 109-118.
LAI, M. M. C. 1992. RNA recombination in animal and plant viruses. *Microbiol Rev,* 56, 61-79.
LAIGO, F. & MORSE, R. 1968. The mite Tropilaelaps clareae in Apis dorsata colonies in the Philippines. *Bee World,* 49, 116-118.
LAMP, B., URL, A., SEITZ, K., EICHHORN, J., RIEDEL, C., SINN, L. J., INDIK, S., KOGLBERGER, H. & RUMENAPF, T. 2016. Construction and Rescue of a Molecular Clone of Deformed Wing Virus (DWV). *PLoS One,* 11, e0164639.
LANZI, G., DE MIRANDA, J. R., BONIOTTI, M. B., CAMERON, C. E., LAVAZZA, A., CAPUCCI, L., CAMAZINE, S. M. & ROSSI, C. 2006. Molecular and biological characterization of deformed wing virus of honeybees (Apis mellifera L.). *Journal of virology,* 80, 4998-5009.
LAUGHTON, A. M., BOOTS, M. & SIVA-JOTHY, M. T. J. J. O. I. P. 2011. The ontogeny of immunity in the honey bee, Apis mellifera L. following an immune challenge. 57, 1023-1032.
LAURING, A. S. & ANDINO, R. 2010. Quasispecies theory and the behavior of RNA viruses. *PLoS Pathog,* 6, e1001005.
LE CONTE, Y., ELLIS, M. & RITTER, W. J. A. 2010. Varroa mites and honey bee health: can Varroa explain part of the colony

losses? 41, 353-363.
LE GALL, O., CHRISTIAN, P., FAUQUET, C. M., KING, A. M., KNOWLES, N. J., NAKASHIMA, N., STANWAY, G. & GORBALENYA, A. E. 2008. Picornavirales, a proposed order of positive-sense single-stranded RNA viruses with a pseudo-T = 3 virion architecture. *Arch Virol,* 153, 715-27.
LI, H., HANDSAKER, B., WYSOKER, A., FENNELL, T., RUAN, J., HOMER, N., MARTH, G., ABECASIS, G. & DURBIN, R. J. B. 2009. The sequence alignment/map format and SAMtools. 25, 2078-2079.
LIAO, M., ZHOU, J., GONG, H., BOLDBAATAR, D., SHIRAFUJI, R., BATTUR, B., NISHIKAWA, Y. & FUJISAKI, K. 2009. Hemalin, a thrombin inhibitor isolated from a midgut cDNA library from the hard tick Haemaphysalis longicornis. *Journal of insect physiology,* 55, 165-174.
LOBRY, J. R. & SUEOKA, N. J. G. B. 2002. Asymmetric directional mutation pressures in bacteria. 3, research0058. 1.
LUO, Q. H., ZHOU, T., DAI, P. L., SONG, H. L., WU, Y. Y., WANG, Q. J. E. & ACAROLOGY, A. 2011. Prevalence, intensity and associated factor analysis of Tropilaelapsmercedesae infesting Apismellifera in China. 55, 135-146.
MARTIN, S. J. 1994. Ontogenesis of the mite Varroa jacobsoni Oud. in worker brood of the honeybee Apis mellifera L. under natural conditions. *Experimental applied acarology,* 18, 87-100.
MARTIN, S. J., BALL, B. V. & CARRECK, N. L. J. J. O. A. R. 2013. The role of deformed wing virus in the initial collapse of varroa infested honey bee colonies in the UK. 52, 251-258.
MARTIN, S. J. & BRETTELL, L. E. J. A. R. O. V. 2019. Deformed wing virus in Honeybees and Other Insects. 6, 49-69.
MARTIN, S. J., HIGHFIELD, A. C., BRETTELL, L., VILLALOBOS, E. M., BUDGE, G. E., POWELL, M., NIKAIDO, S. & SCHROEDER, D. C. 2012. Global honey bee viral landscape altered by a parasitic mite. *Science,* 336, 1304-1306.
MARTIN, S. J. E. & ACAROLOGY, A. 1995. Ontogenesis of the mite Varroa jacobsoni Oud. in drone brood of the honeybee Apis mellifera L. under natural conditions. 19, 199-210.
MARTIN, S. J. J. J. O. A. E. 2001. The role of Varroa and viral pathogens in the collapse of honeybee colonies: a modelling approach. *Journal of Applied Ecology,* 38, 1082-1093.
MARXER, M., VOLLENWEIDER, V. & SCHMID-HEMPEL, P. J. P. T. O. T. R. S. B. B. S. 2016. Insect antimicrobial peptides act synergistically to inhibit a trypanosome parasite. 371, 20150302.
MAZZEI, M., CARROZZA, M. L., LUISI, E., FORZAN, M., GIUSTI, M., SAGONA, S., TOLARI, F. & FELICIOLI, A. J. P. O. 2014. Infectivity of DWV associated to flower pollen: experimental evidence of a horizontal transmission route. 9.
MCDERMAID, A., MONIER, B., ZHAO, J., LIU, B. & MA, Q. J. B. I. B. 2019. Interpretation of differential gene expression results of RNA-seq data: review and integration. 20, 2044-2054.
MCMAHON, D. P., FURST, M. A., CASPAR, J., THEODOROU, P., BROWN, M. J. F. & PAXTON, R. J. 2015. A sting in the spit: widespread cross-infection of multiple RNA viruses across wild and managed bees. *J Anim Ecol,* 84, 615-624.
MCMAHON, D. P., NATSOPOULOU, M. E., DOUBLET, V., FüRST, M., WEGING, S., BROWN, M. J., GOGOL-DöRING, A. & PAXTON, R. J. Elevated virulence of an emerging viral genotype as a driver of honeybee loss. Proc. R. Soc. B, 2016. The Royal Society, 20160811.
MOCKEL, N., GISDER, S. & GENERSCH, E. 2011. Horizontal transmission of deformed wing virus: pathological consequences in adult bees (Apis mellifera) depend on the transmission route. *J Gen Virol,* 92, 370-7.
MONDET, F., DE MIRANDA, J. R., KRETZSCHMAR, A., LE CONTE, Y. & MERCER, A. R. J. P. P. 2014. On the front line: quantitative virus dynamics in honeybee (Apis mellifera L.) colonies along a new expansion front of the parasite Varroa destructor. 10, e1004323.
MOORE, J., JIRONKIN, A., CHANDLER, D., BURROUGHS, N., EVANS, D. J. & RYABOV, E. V. 2011. Recombinants between Deformed wing virus and Varroa destructor virus-1 may prevail in Varroa destructor-infested honeybee colonies. *Journal of General Virology,* 92, 156-161.
MOORE, N. & ELEY, S. 2017. Picornaviridae: Picornaviruses of Inverterbrates. *Atlas of Invertebrate Viruses.* CRC Press.
MORALES-HOJAS, R., HINSLEY, M., ARMEAN, I. M., SILK, R., HARRUP, L. E., GONZALEZ-URIARTE, A., VERONESI, E., CAMPBELL, L., NAYDUCH, D. & SASKI, C. J. B. G. 2018. The genome of the biting midge Culicoides sonorensis and gene expression analyses of vector competence for bluetongue virus. 19, 624.
MORDECAI, G. J., BRETTELL, L. E., MARTIN, S. J., DIXON, D., JONES, I. M. & SCHROEDER, D. C. 2016a. Superinfection exclusion and the long-term survival of honey bees in Varroa-infested colonies. *The ISME journal,* 10, 1182-1191.
MORDECAI, G. J., BRETTELL, L. E., PACHORI, P., VILLALOBOS, E. M., MARTIN, S. J., JONES, I. M. & SCHROEDER, D. C. J. S. R. 2016b. Moku virus; a new Iflavirus found in wasps, honey bees and Varroa. 6, 34983.
MORDECAI, G. J., WILFERT, L., MARTIN, S. J., JONES, I. M. & SCHROEDER, D. C. 2016c. Diversity in a honey bee pathogen: first report of a third master variant of the Deformed Wing Virus quasispecies. *The ISME journal,* 10, 1264-1273.
MORSE, R. & FLOTTUM, K. J. O. A. R. C. 1997. Honey Bee Pests Predators and Diseases Medina.
MORSE, R. A. & LAIGO, F. 1969. *Apis dorsata in the Philippines (including an annotated bibliography)*, Philippine

Association of Entomologists.
MOTULSKY, H. J. G. S. I., SAN DIEGO, CA 2003. Prism 4 statistics guide—statistical analyses for laboratory and clinical researchers. 122-126.
MüLLER, U. 2019. Sustainable agriculture through protection of wild bee health: Investigation of transmission risk of the honey bee pathogen Nosema ceranae. *Doctoral dissertation*.
MUNDERLOH, U. G., KURTTI, T. J. J. E. & ACAROLOGY, A. 1989. Formulation of medium for tick cell culture. 7**,** 219-229.
MUTA, T. & IWANAGA, S. 1996. The role of hemolymph coagulation in innate immunity. *Curr Opin Immunol,* 8**,** 41-7.
NAGY, P. D. & POGANY, J. J. N. R. M. 2012. The dependence of viral RNA replication on co-opted host factors. 10**,** 137.
NANDAKUMAR, S., MA, H. & KHAN, A. S. J. G. A. 2017. Whole-genome sequence of the Spodoptera frugiperda Sf9 insect cell line. 5**,** e00829-17.
NANNELLI, R. J. E. D. R. 1985. Ulteriori conoscenze sulla morfologia e lo sviluppo, della larva e delle ninfe di Varroa jacobsoni Oud (Mesostigmata: Varroidae). 67**,** 287-303.
NATSOPOULOU, M. E., MCMAHON, D. P., DOUBLET, V., FREY, E., ROSENKRANZ, P. & PAXTON, R. J. 2017. The virulent, emerging genotype B of Deformed wing virus is closely linked to overwinter honeybee worker loss. *Sci Rep,* 7**,** 5242.
NAVAJAS, M., MIGEON, A., ALAUX, C., MARTIN-MAGNIETTE, M., ROBINSON, G., EVANS, J., CROS-ARTEIL, S., CRAUSER, D. & LE CONTE, Y. 2008. Differential gene expression of the honey bee Apis mellifera associated with Varroa destructor infection. *BMC Genomics,* 9**,** 301.
NAZZI, F., BROWN, S. P., ANNOSCIA, D., DEL PICCOLO, F., DI PRISCO, G., VARRICCHIO, P., DELLA VEDOVA, G., CATTONARO, F., CAPRIO, E. & PENNACCHIO, F. J. P. P. 2012. Synergistic parasite-pathogen interactions mediated by host immunity can drive the collapse of honeybee colonies. 8**,** e1002735.
NEEDHAM, G. R., PAGE JR, R., DELFINADO-BAKER, M. & BOWMAN, C. 1988. Africanized honey bees and bee mites.
NEGI, J., KUMAR, N. R. J. J. O. A. & SCIENCE, N. 2014. Changes in protein profile and RNA content of Apis mellifera worker pupa on parasitization with Tropilaelaps clareae. 6**,** 693-695.
NEUMANN, P. & CARRECK, N. L. 2010. Honey bee colony losses. *Journal of Apicultural Research,* 49**,** 1-6.
NEUMANN, P., YANEZ, O., FRIES, I. & DE MIRANDA, J. R. 2012. Varroa invasion and virus adaptation. *Trends Parasitol,* 28**,** 353-4.
NGUYEN, L. T., HANEY, E. F. & VOGEL, H. J. J. T. I. B. 2011. The expanding scope of antimicrobial peptide structures and their modes of action. 29**,** 464-472.
NORDSTRöM, S. 2003. Distribution of deformed wing virus within honey bee (Apis mellifera) brood cells infested with the ectoparasitic mite Varroa destructor. *Experimental applied acarology,* 29**,** 293-302.
ONGUS, J. R., PETERS, D., BONMATIN, J.-M., BENGSCH, E., VLAK, J. M. & VAN OERS, M. M. 2004. Complete sequence of a picorna-like virus of the genus Iflavirus replicating in the mite Varroa destructor. *Journal of General Virology,* 85**,** 3747-3755.
ORGANTINI, L. J., SHINGLER, K. L., ASHLEY, R. E., CAPALDI, E. A., DURRANI, K., DRYDEN, K. A., MAKHOV, A. M., CONWAY, J. F., PIZZORNO, M. C. & HAFENSTEIN, S. J. J. O. V. 2017. Honey bee deformed wing virus structures reveal that conformational changes accompany genome release. 91**,** e01795-16.
OSHLACK, A., ROBINSON, M. D. & YOUNG, M. D. J. G. B. 2010. From RNA-seq reads to differential expression results. 11**,** 220.
OSTA, M. A., CHRISTOPHIDES, G. K., VLACHOU, D. & KAFATOS, F. C. J. J. O. E. B. 2004. Innate immunity in the malaria vector Anopheles gambiae: comparative and functional genomics. 207**,** 2551-2563.
OTVOS JR, L. J. J. O. P. S. A. O. P. O. T. E. P. S. 2005. Antibacterial peptides and proteins with multiple cellular targets. 11**,** 697-706.
PAUL, A. V. 2002. Possible Unifying Mechanism of Picornavirus genome replication. *Molecular biology of picornavirus***,** 227-246.
PETTIS, J. S., ROSE, R., LICHTENBERG, E. M., CHANTAWANNAKUL, P., BUAWANGPONG, N., SOMANA, W., SUKUMALANAND, P. & VANENGELSDORP, D. J. J. O. E. E. 2013. A rapid survey technique for Tropilaelaps mite (Mesostigmata: Laelapidae) detection. 106**,** 1535-1544.
PEYREFITTE, C. N., PASTORINO, B., BESSAUD, M., TOLOU, H. J. & COUISSINIER-PARIS, P. J. J. O. V. M. 2003. Evidence for in vitro falsely-primed cDNAs that prevent specific detection of virus negative strand RNAs in dengue-infected cells: improvement by tagged RT-PCR. 113**,** 19-28.
PFAFFL, M. W. 2007. Relative quantification. *Real-time PCR.* Taylor & Francis.
PHILIPPE BLANCHARD, MAGALI RIBIèRE, OLIVIER CELLE, PERRINE LALLEMAND, FRANK SCHURR, VIOLAINE OLIVIER, ANNE LAURE ISCACHE & FAUCON, J. P. 2007. Evaluation of a real-time two-step RT-PCR assay for quantitation of Chronic bee paralysis virus (CBPV) genome in experimentally-infected bee tissue and in life stages of a

symptomatic colony. *Journal of Virological Methods,* 141**,** 7-13.
PHOKASEM, P., DE GUZMAN, L. I., KHONGPHINITBUNJONG, K., FRAKE, A. M. & CHANTAWANNAKUL, P. 2019. Feeding by Tropilaelaps mercedesae on pre- and post-capped brood increases damage to Apis mellifera colonies. *Sci Rep,* 9**,** 13044.
POSADA-FLOREZ, F., CHILDERS, A. K., HEERMAN, M. C., EGEKWU, N. I., COOK, S. C., CHEN, Y., EVANS, J. D. & RYABOV, E. V. J. B. 2019. Deformed wing virus type A, a major honey bee pathogen, is vectored by the mite Varroa destructor in a non-propagative manner. 660985.
POSTLETHWAIT, J. H. & GIORGI, F. 1985. Vitellogenesis in insects. *Oogenesis*. Springer.
POTTS, S. G., BIESMEIJER, J. C., KREMEN, C., NEUMANN, P., SCHWEIGER, O. & KUNIN, W. E. 2010a. Global pollinator declines: trends, impacts and drivers. *Trends Ecol Evol,* 25**,** 345-53.
POTTS, S. G., ROBERTS, S. P. M., DEAN, R., MARRIS, G., BROWN, M. A., JONES, R., NEUMANN, P. & SETTELE, J. 2010b. Declines of managed honey bees and beekeepers in Europe. *Journal of Apicultural Research,* 49**,** 15-22.
QU, N., JIANG, J., SUN, L., LAI, C., SUN, L. & WU, X. J. B. 2008. Proteomic characterization of royal jelly proteins in Chinese (Apis cerana cerana) and European (Apis mellifera) honeybees. 73**,** 676.
RAFFIQUE, M. K., MAHMOOD, R., ASLAM, M. & SARWAR, G. J. P. J. O. Z. 2012. Control of Tropilaelaps clareae mite by using formic acid and thymol in honey bee Apis mellifera L. colonies. 44.
RAHNAMAEIAN, M. J. P. S. & BEHAVIOR 2011. Antimicrobial peptides: modes of mechanism, modulation of defense responses. 6**,** 1325-1332.
RAMSEY, S. D., OCHOA, R., BAUCHAN, G., GULBRONSON, C., MOWERY, J. D., COHEN, A., LIM, D., JOKLIK, J., CICERO, J. M., ELLIS, J. D., HAWTHORNE, D. & VANENGELSDORP, D. 2019. Varroa destructor feeds primarily on honey bee fat body tissue and not hemolymph. *Proc Natl Acad Sci U S A,* 116**,** 1792-1801.
REHM, S.-M. & RITTER, W. J. A. 1989. Sequence of the sexes in the offspring of Varroa jacobsoni and the resulting consequences for the calculation of the developmental period. 20**,** 339-343.
RENZI, M. T., RODRíGUEZ-GASOL, N., MEDRZYCKI, P., PORRINI, C., MARTINI, A., BURGIO, G., MAINI, S. & SGOLASTRA, F. 2016. Combined effect of pollen quality and thiamethoxam on hypopharyngeal gland development and protein content in Apis mellifera. *Apidologie,* 47**,** 779-788.
RIBIèRE, M., BALL, B. V. & AUBERT, M. 2008. *Natural history and geographical distribution of honey bee viruses,* European Communities, Luxembourg.
RINDERER, T. E., OLDROYD, B. P., LEKPRAYOON, C., WONGSIRI, S., BOONTHAI, C. & THAPA, R. J. J. O. A. R. 1994. Extended survival of the parasitic honey bee mite Tropilaelaps clareae on adult workers of Apis mellifera and Apis dorsata. 33**,** 171-174.
RITTER, W., SCHNEIDER-RITTER, U. J. A. H. B. & BEE MITES/EDITORS, G. R. N. 1988. Differences in biology and means of controlling Varroa jacobsoni and Tropilaelaps clareae, two novel parasitic mites of Apis mellifera.
RONQUIST, F. & HUELSENBECK, J. P. 2003. MrBayes 3: Bayesian phylogenetic inference under mixed models. *Bioinformatics,* 19**,** 1572-4.
ROSENKRANZ, P., AUMEIER, P. & ZIEGELMANN, B. 2010. Biology and control of Varroa destructor. *J Invertebr Pathol,* 103 Suppl 1**,** S96-119.
ROY, S., SAHA, T. T., ZOU, Z. & RAIKHEL, A. S. 2017. Regulatory Pathways Controlling Female Insect Reproduction. *Annu Rev Entomol*.
RUTTNER, F. 1980. Das Eindringen von Varroa jacobsoni nach Europa im Rückblick.
RYABOV, E. V., WOOD, G. R., FANNON, J. M., MOORE, J. D., BULL, J. C., CHANDLER, D., MEAD, A., BURROUGHS, N. & EVANS, D. J. 2014. A virulent strain of deformed wing virus (DWV) of honeybees (Apis mellifera) prevails after Varroa destructor-mediated, or in vitro, transmission. *PLoS pathogens,* 10**,** e1004230.
SADOV, A. J. P. 1976. Study of female Varroa. 8**,** 15-16.
SANCHEZ-BAYO, F., GOULSON, D., PENNACCHIO, F., NAZZI, F., GOKA, K. & DESNEUX, N. 2016. Are bee diseases linked to pesticides? - A brief review. *Environ Int,* 89-90**,** 7-11.
SANTILLAN-GALICIA, M. T., CARZANIGA, R., BALL, B. V. & ALDERSON, P. G. J. J. O. G. V. 2008. Immunolocalization of deformed wing virus particles within the mite Varroa destructor. 89**,** 1685-1689.
SATO, K.-I. 2012. *Embryogenesis*, BoD–Books on Demand.
SCHNEIDER, I. J. D. 1972. Cell lines derived from late embryonic stages of Drosophila melanogaster. 27**,** 353-365.
SCHONING, C., GISDER, S., GEISELHARDT, S., KRETSCHMANN, I., BIENEFELD, K., HILKER, M. & GENERSCH, E. 2012. Evidence for damage-dependent hygienic behaviour towards Varroa destructor-parasitised brood in the western honey bee, Apis mellifera. *J Exp Biol,* 215**,** 264-71.
SCHROEDER, D. C. & MARTIN, S. J. 2012. Deformed wing virus: The main suspect in unexplained honeybee deaths worldwide. *Virulence,* 3**,** 589-591.

SEARLE, B. C. J. P. 2010. Scaffold: a bioinformatic tool for validating MS/MS-based proteomic studies. 10**,** 1265-1269.
SHAH, K. S., EVANS, E. C. & PIZZORNO, M. C. J. V. J. 2009. Localization of deformed wing virus (DWV) in the brains of the honeybee, Apis mellifera Linnaeus. 6**,** 182.
SHEN, M., YANG, X., COX-FOSTER, D. & CUI, L. 2005. The role of varroa mites in infections of Kashmir bee virus (KBV) and deformed wing virus (DWV) in honey bees. *Virology,* 342**,** 141-9.
SHIN, Y. C., BISCHOF, G. F., LAUER, W. A. & DESROSIERS, R. C. J. P. O. T. N. A. O. S. 2015. Importance of codon usage for the temporal regulation of viral gene expression. 112**,** 14030-14035.
SINGH, R., LEVITT, A. L., RAJOTTE, E. G., HOLMES, E. C., OSTIGUY, N., LIPKIN, W. I., DEPAMPHILIS, C. W., TOTH, A. L. & COX-FOSTER, D. L. J. P. O. 2010. RNA viruses in hymenopteran pollinators: evidence of inter-taxa virus transmission via pollen and potential impact on non-Apis hymenopteran species. 5**,** e14357.
SKUBNIK, K., NOVACEK, J., FUZIK, T., PRIDAL, A., PAXTON, R. J. & PLEVKA, P. 2017. Structure of deformed wing virus, a major honey bee pathogen. *Proc Natl Acad Sci U S A,* 114**,** 3210-3215.
SMIRNOV, A. M. 1978. Research results obtained in USSR concerning aetiology, pathogenesis, epizootiology, diagnosis and control of Varroa disease in bees. *Apiacta. An international technical magazine of apicultural and economic information*.
SMITH, K. M., LOH, E. H., ROSTAL, M. K., ZAMBRANA-TORRELIO, C. M., MENDIOLA, L. & DASZAK, P. 2013. Pathogens, pests, and economics: drivers of honey bee colony declines and losses. *Ecohealth,* 10**,** 434-45.
SOROKER, V., HETZRONI, A., YACOBSON, B., VOET, H., SLABEZKI, S., EFRAT, H. & CHEJANOVSKY, N. Colony losses in Israel: incidence of viral infection and beehive populations. Proceedings of the 41st Apimondia Congress, Mointpellier, France, 2009. 38.
STANLEY, M. J. A. B. P. H. 1968. Initial results of honeybee tissue culture. 11**,** 45-55.
STEFFAN-DEWENTER, I., POTTS, S. G. & PACKER, L. 2005. Pollinator diversity and crop pollination services are at risk. *Trends Ecol Evol,* 20**,** 651-2; author reply 652-3.
STEINER, J., DIEHL, P. A., VLIMANT, M. J. E. & ACAROLOGY, A. 1995. Vitellogenesis in Varroa jacobsoni, a parasite of honey bees. 19**,** 411-422.
STEINER, J., DITTMANN, F., ROSENKRANZ, P., ENGELS, W. J. I. R. & DEVELOPMENT 1994. The first gonocycle of the parasitic mite (Varroa juobsoni) in relation to preimaginal development of its host, the honey bee (Apis mellifra carnicar). 25**,** 175-183.
STEINHAUER, D. A., DOMINGO, E. & HOLLAND, J. J. J. G. 1992. Lack of evidence for proofreading mechanisms associated with an RNA virus polymerase. 122**,** 281-288.
STEINHAUER, N. A., RENNICH, K., WILSON, M. E., CARON, D. M., LENGERICH, E. J., PETTIS, J. S., ROSE, R., SKINNER, J. A., TARPY, D. R., WILKES, J. T. & VANENGELSDORP, D. 2014. A national survey of managed honey bee 2012–2013 annual colony losses in the USA: results from the Bee Informed Partnership. *Journal of Apicultural Research,* 53**,** 1-18.
STEPHEN MARTIN, ANN HOGARTH, JOHN VAN BREDA & PERRETT, J. 1998. A scientific note on Varroa jacobsoni Oudemans and the collapse of Apis mellifera L. colonies in the United Kingdom. *Apidologie,* 29**,** 369-370.
STEWART FRANKEL, REGINAL SOHN & LEINWAND, L. 1990. The use of sarkosyl in generating soluble protein after bacterial expression. *Proc Natl Acad Sci U S A,* 88**,** 1192-1196.
STOUT, J. C. & MORALES, C. L. 2009. Ecological impacts of invasive alien species on bees. *Apidologie,* 40**,** 388-409.
SUEOKA, N. J. J. O. M. E. 1993. Directional mutation pressure, mutator mutations, and dynamics of molecular evolution. 37**,** 137.
SUEOKA, N. J. P. O. T. N. A. O. S. 1988. Directional mutation pressure and neutral molecular evolution. 85**,** 2653-2657.
SUGURU, F., JIRO, I., MINEKO, F., TOMOKO, Y., TAKUJI, K. & KUMPEI, K. J. J. B. C. 1990. A potent antibacterial protein in royal jelly. 265**,** 11333-11337.
SWEVERS, L., RAIKHEL, A., SAPPINGTON, T., SHIRK, P. & LATROU, K. 2005. Vitellogenesis and post-vitellogenic maturation of the insect ovarian follicle.
TANTILLO, G., BOTTARO, M., DI PINTO, A., MARTELLA, V., DI PINTO, P. & TERIO, V. 2015. Virus Infections of Honeybees Apis Mellifera. *Ital J Food Saf,* 4**,** 5364.
TENTCHEVA, D., GAUTHIER, L., BAGNY, L., FIEVET, J., DAINAT, B., COUSSERANS, F., COLIN, M. E. & BERGOIN, M. 2006. Comparative analysis of deformed wing virus (DWV) RNA inApis melliferaandVarroa destructor. *Apidologie,* 37**,** 41-50.
TENTCHEVA, D., GAUTHIER, L., JOUVE, S., CANABADY-ROCHELLE, L., DAINAT, B., COUSSERANS, F., COLIN, M. E., BALL, B. V. & BERGOIN, M. J. A. 2004a. Polymerase Chain Reaction detection of deformed wing virus (DWV) in Apis mellifera and Varroa destructor. 35**,** 431-439.
TENTCHEVA, D., GAUTHIER, L., ZAPPULLA, N., DAINAT, B., COUSSERANS, F., COLIN, M. E. & BERGOIN, M. 2004b.

Prevalence and seasonal variations of six bee viruses in Apis mellifera L. and Varroa destructor mite populations in France. *Appl Environ Microbiol,* 70**,** 7185-91.

TEWARSON, N. C. J. I. J. O. I. R. 1982a. Immunocytochemical localization of host (Apis mellifera) proteins in growing oocytes of a hemophagous mite (Varroa jacobsoni) by the unlabeled antibody—enzyme (PAP) method. 5**,** 345-348.

TEWARSON, N. J. A. 1982b. Resorption of undigested proteins and their incorporation into the eggs of Varroa jacobsoni [honey-bees, Apis mellifera].

THOMPSON, D. M., KHALIL, S. M., JEFFERS, L. A., ANANTHAPADMANABAN, U., SONENSHINE, D. E., MITCHELL, R. D., OSGOOD, C. J., APPERSON, C. S. & ROE, R. M. J. J. O. I. P. 2005. In vivo role of 20-hydroxyecdysone in the regulation of the vitellogenin mRNA and egg development in the American dog tick, Dermacentor variabilis (Say). 51**,** 1105-1116.

THOMPSON, D. M., KHALIL, S. M., JEFFERS, L. A., SONENSHINE, D. E., MITCHELL, R. D., OSGOOD, C. J., ROE, R. M. J. I. B. & BIOLOGY, M. 2007. Sequence and the developmental and tissue-specific regulation of the first complete vitellogenin messenger RNA from ticks responsible for heme sequestration. 37**,** 363-374.

TIAN, C., GAO, B., FANG, Q., YE, G. & ZHU, S. J. B. G. 2010. Antimicrobial peptide-like genes in Nasonia vitripennis: a genomic perspective. 11**,** 187.

TUFAIL, M., LEE, J., HATAKEYAMA, M., OISHI, K., TAKEDA, M. J. A. O. I. B. & AMERICA, P. P. I. C. W. T. E. S. O. 2000. Cloning of vitellogenin cDNA of the American cockroach, Periplaneta americana (Dictyoptera), and its structural and expression analyses. 45**,** 37-46.

TUFAIL, M. & TAKEDA, M. J. J. O. I. P. 2008. Molecular characteristics of insect vitellogenins. 54**,** 1447-1458.

VAN ENGELSDORP, D., HAYES, J., JR., UNDERWOOD, R. M. & PETTIS, J. 2008. A survey of honey bee colony losses in the U.S., fall 2007 to spring 2008. *PLoS One,* 3**,** e4071.

VANENGELSDORP, D., CARON, D., HAYES, J., UNDERWOOD, R., HENSON, M., RENNICH, K., SPLEEN, A., ANDREE, M., SNYDER, R., LEE, K., ROCCASECCA, K., WILSON, M., WILKES, J., LENGERICH, E. & PETTIS, J. 2012. A national survey of managed honey bee 2010–11 winter colony losses in the USA: results from the Bee Informed Partnership. *Journal of Apicultural Research,* 51**,** 115-124.

VANENGELSDORP, D., HAYES JR, J., UNDERWOOD, R. M., CARON, D. & PETTIS, J. 2011. A survey of managed honey bee colony losses in the USA, fall 2009 to winter 2010. *Journal of Apicultural Research,* 50**,** 1-10.

VANENGELSDORP, D. & MEIXNER, M. D. 2010. A historical review of managed honey bee populations in Europe and the United States and the factors that may affect them. *Journal of Invertebrate Pathology,* 103**,** S80-S95.

VARTANIAN, J.-P., HENRY, M. & WAIN-HOBSON, S. J. J. O. G. V. 2002. Sustained G→ A hypermutation during reverse transcription of an entire human immunodeficiency virus type 1 strain Vau group O genome. 83**,** 801-805.

VARTANIAN, J.-P., MEYERHANS, A., SALA, M. & WAIN-HOBSON, S. J. P. O. T. N. A. O. S. 1994. G--> A hypermutation of the human immunodeficiency virus type 1 genome: evidence for dCTP pool imbalance during reverse transcription. 91**,** 3092-3096.

VAUGHN, J., GOODWIN, R., TOMPKINS, G. & MCCAWLEY, P. J. I. V. 1977. The establishment of two cell lines from the insectspodoptera frugiperda (lepidoptera; noctuidae). 13**,** 213-217.

VERONESI, E., ANTONY, F., GUBBINS, S., GOLDING, N., BLACKWELL, A., MERTENS, P. P., BROWNLIE, J., DARPEL, K. E., MELLOR, P. S. & CARPENTER, S. J. P. O. 2013. Measurement of the infection and dissemination of bluetongue virus in Culicoides biting midges using a semi-quantitative rt-PCR assay and isolation of infectious virus. 8**,** e70800.

VILCINSKAS, A. 2010. Coevolution between pathogen-derived proteinases and proteinase inhibitors of host insects. *Virulence,* 1**,** 206-214.

WANG, X. 2004. Sequence analysis and genomic organization of a new insect picorna-like virus, Ectropis obliqua picorna-like virus, isolated from Ectropis obliqua. *Journal of General Virology,* 85**,** 1145-1151.

WECHSLER, S., MCHOLLAND, L. & WILSON, W. J. J. O. I. P. 1991. A RNA virus in cells from Culicoides variipennis. 57**,** 200-205.

WILFERT, L., LONG, G., LEGGETT, H., SCHMID-HEMPEL, P., BUTLIN, R., MARTIN, S. & BOOTS, M. 2016. Deformed wing virus is a recent global epidemic in honeybees driven by Varroa mites. *Science,* 351**,** 594-597.

WILLIAMS, G. R., TARPY, D. R., VANENGELSDORP, D., CHAUZAT, M. P., COX-FOSTER, D. L., DELAPLANE, K. S., NEUMANN, P., PETTIS, J. S., ROGERS, R. E. & SHUTLER, D. 2010. Colony collapse disorder in context. *Bioessays,* 32**,** 845-846.

WILSON-RICH, N., DRES, S. T. & STARKS, P. T. J. J. O. I. P. 2008. The ontogeny of immunity: development of innate immune strength in the honey bee (Apis mellifera). 54**,** 1392-1399.

WONG, E. H., SMITH, D. K., RABADAN, R., PEIRIS, M. & POON, L. L. J. B. E. B. 2010. Codon usage bias and the evolution of influenza A viruses. Codon Usage Biases of Influenza Virus. 10**,** 253.

WOYKE, J. J. A. 1984. Survival and prophylactic control of Tropilaelaps clareae infesting Apis mellifera colonies in Afghanistan. 15, 421-434.
WOYKE, J. J. E. & ACAROLOGY, A. 1994. Mating behavior of the parasitic honeybee mite Tropilaelaps clareae. 18, 723-733.
WOYKE, J. J. J. O. A. R. 1987a. Length of stay of the parasitic mite Tropilaelaps clareae outside sealed honeybee brood cells as a basis for its effective control. 26, 104-109.
WOYKE, J. J. J. O. A. R. 1987b. Length of successive stages in the development of the mite Tropilaelaps clareae in relation to honeybee brood age. 26, 110-114.
WOYKE, J. J. T. A. B. J. 1985. Tropilaelaps clareae, a serious pest of Apis mellifera in the tropics, but not dangerous for apiculture in temperate zones.
WU, C. Y., LO, C. F., HUANG, C. J., YU, H. T. & WANG, C. H. 2002. The complete genome sequence of Perina nuda picorna-like virus, an insect-infecting RNA virus with a genome organization similar to that of the mammalian picornaviruses. *Virology,* 294, 312-23.
WU, Y., DONG, X. & KADOWAKI, T. J. F. I. M. 2017. Characterization of the copy number and variants of deformed wing virus (DWV) in the pairs of honey bee pupa and infesting Varroa destructor or Tropilaelaps mercedesae. 8, 1558.
WU, Y., LIU, Q., WEISS, B., KALTENPOTH, M. & KADOWAKI, T. 2020. Honey Bee Suppresses the Parasitic Mite Vitellogenin by Antimicrobial Peptide. 11.
XU, P., SHI, M. & CHEN, X.-X. J. P. O. 2009. Antimicrobial peptide evolution in the Asiatic honey bee Apis cerana. 4.
YAMANAKA, T., OHTA, T., TAKAHASHI, M., MESHI, T., SCHMIDT, R., DEAN, C., NAITO, S. & ISHIKAWA, M. J. P. O. T. N. A. O. S. 2000. TOM1, an Arabidopsis gene required for efficient multiplication of a tobamovirus, encodes a putative transmembrane protein. 97, 10107-10112.
YANG, D., BIRAGYN, A., HOOVER, D. M., LUBKOWSKI, J. & OPPENHEIM, J. J. J. A. R. I. 2004. Multiple roles of antimicrobial defensins, cathelicidins, and eosinophil-derived neurotoxin in host defense. 22, 181-215.
YANG, X. & COX-FOSTER, D. L. J. P. O. T. N. A. O. S. 2005. Impact of an ectoparasite on the immunity and pathology of an invertebrate: evidence for host immunosuppression and viral amplification. 102, 7470-7475.
YUE, C. & GENERSCH, E. 2005. RT-PCR analysis of Deformed wing virus in honeybees (Apis mellifera) and mites (Varroa destructor). *J Gen Virol,* 86, 3419-24.
YUE, C., SCHRODER, M., BIENEFELD, K. & GENERSCH, E. 2006. Detection of viral sequences in semen of honeybees (Apis mellifera): evidence for vertical transmission of viruses through drones. *J Invertebr Pathol,* 92, 105-8.
YUE, C., SCHRODER, M., GISDER, S. & GENERSCH, E. 2007. Vertical-transmission routes for deformed wing virus of honeybees (Apis mellifera). *Journal of General Virology,* 88, 2329-2336.
ZEIL, J., DI PASQUALE, G., SALIGNON, M., LE CONTE, Y., BELZUNCES, L. P., DECOURTYE, A., KRETZSCHMAR, A., SUCHAIL, S., BRUNET, J.-L. & ALAUX, C. 2013. Influence of Pollen Nutrition on Honey Bee Health: Do Pollen Quality and Diversity Matter? *PLoS ONE,* 8.
ZHANG, Q., ONGUS, J. R., BOOT, W. J., CALIS, J., BONMATIN, J.-M., BENGSCH, E. & PETERS, D. J. J. O. I. P. 2007. Detection and localisation of picorna-like virus particles in tissues of Varroa destructor, an ectoparasite of the honey bee, Apis mellifera. 96, 97-105.
ZIONI, N., SOROKER, V. & CHEJANOVSKY, N. 2011. Replication of Varroa destructor virus 1 (VDV-1) and a Varroa destructor virus 1-deformed wing virus recombinant (VDV-1-DWV) in the head of the honey bee. *Virology,* 417, 106-12.
ZOU, Z., LOPEZ, D. L., KANOST, M. R., EVANS, J. D. & JIANG, H. 2006. Comparative analysis of serine protease-related genes in the honey bee genome: possible involvement in embryonic development and innate immunity. *Insect Mol Biol,* 15, 603-14.